KINETICS AND MECHANISM OF INTERACTION OF DRUGS WITH METAL IONS

ABSTRACT
THESIS

SUBMITTED FOR THE AWARD OF THE DEGREE OF

Doctor of Philosophy

IN

CHEMISTRY

BY

AFTAB ASLAM PARWAZ KHAN

DEPARTMENT OF CHEMISTRY
ALIGARH MUSLIM UNIVERSITY
ALIGARH (INDIA)

2010

ABSTRACT

This thesis describes the kinetics and mechanism of oxidation of some drugs in different media. The reactions have been followed spectrophotometrically. The study of oxidation of drugs is of immense importance both from mechanistic and synthetic point of view. It has a bearing on the chemical processes of life also.

The introductory chapter reports the kinetics and mechanism of oxidation of Levofloxacin (LF) by $KMnO_4$ in alkaline medium at a constant ionic strength (0.10 mol dm^{-3}). It is a first order reaction, but fractional order in both LF and alkali. Decrease in the dielectric constant of the medium results in a decrease in the rate of reaction. The effects of added products and ionic strength have also been investigated. The main products identified were hydroxylated LF and Mn(VI). A mechanism involving free radical is proposed. In a composite equilibrium step, LF binds to MnO_4^- Pto form a complex that subsequently decomposes to the products. Investigations of the reaction at different temperatures allowed the determination of the activation parameters with respect to the slow step of the proposed mechanism.

Second chapter deals with the effect of cationic-cetyltrimethylammonium bromide, (CTAB) and anionic surfactant sodium dodecyl sulphate, (SDS) on the rate of oxidation of D-penicillamine by alkaline hexacyanoferrate(III) has been

studied by spectrophotometrically at different temperatures. The effect of CTAB and SDS on the rate of reaction has been studied even below the critical miceller concentration (CMC) of the surfactants indicating binding of the substrate with the surfactants. On the basis of the kinetic results, the mechanism of the reaction has been proposed. The kinetic data have been rationalized in terms of Manger and Portnoy's model for micellar inhibition and binding parameters (viz. binding constants, partition coefficient, free energy transfer from water to micelle, etc.) as well as activation parameters.

Two simple and sensitive kinetic methods for the determination of Ampicillin (AMP), are described. The first method is based on kinetic investigation of the oxidation reaction of the drug with alkaline potassium permanganate at room temperature at fixed time of 25 min. The absorbance of the colored manganate ions is measured at 610 nm. The second method is based on the reaction of AMP with 1-chloro-2,4-dinitrobenzene (CDNB) in the presence of 0.1 mol/L sodium bicarbonate. Spectrophotometric measurement was done by recording the absorbance at 490 nm for a fixed time of 60 min. All variables affecting the development of the color were investigated and the conditions were optimized. Plots of absorbance against concentration in both procedures were rectilinear over the ranges 5–30 and 50–260 μgmL^{-1}, with mean recoveries of 99.75 and 99.91, respectively. The proposed methods were successfully applied for the determination of AMP in bulk powder and in dosage form. The

determination of AMP by the fixed concentration method is feasible with the calibration equations obtained, but the fixed time method proves to be more applicable.

Chapter four includes the kinetics of oxidation of L-Glutamic acid by quinoliniumdichromatre in perchloric acid medium. The rate of the reaction was found to increase with increasing concentrations of the L-Glutamic acid, perchloric acid and ionic strength. The reactions are first order with respect to both QDC and L-Glutamic acid. Added products, had insignificant effect on the reaction rate. The activation parameters have been evaluated and lend further support to the proposed mechanism. The thermodynamic quantities were also determined and discussed.

Chapter five deals with the the kinetics and mechanism of substitution of cyanide ion in hexacyanoferrate(II) by EDTA catalysed by mercury(II), It has been studied spectrophotometrically at 365 nm in potassium hydrogen phthalate buffer of pH = 5.0 and ionic strength, I = 0.1M, maintained by (KNO_3) at 25^0C. Effect of the pH and concentration of the EDTA, $[Fe(CN)^{4-}_6]$ on the rate of reaction has been studied. The kinetics and mechanism of the reaction has been shown through dissociative mechanism. The catalytic activity of mercury(II) has also been studied as a function of its concentration. The maximum reaction product was detected at pH = 5 after which a decline in absorption occurs

followed by precipitation. It is an inexpensive method to identify and remove the cyanide ion in solution even at very low concentration of the order of 10^{-4}M.

Kinetics and mechanism of oxidation of captopril (CPL) by hexacyanoferrate(III) in alkaline medium has been studied spectrophotometrically. The reaction showed first order kinetics in hexacyanoferrate(III) and alkali concentrations and, an order of less than unity in CPL concentration. The rate of reaction increases with increase in alkali concentration. Increasing ionic strength increases the rate but the dielectric constant of the medium has no significant. A mechanism involving the formation of a complex between CPL and hexacyanoferrate(III) has been proposed. The reaction constants involved in the mechanism are evaluated. There is a good agreement between the observed and calculated rate constants under different experimental conditions. Investigations at different temperatures allowed the determination of the activation parameters with respect to the slow step of the proposed mechanism.

KINETICS AND MECHANISM OF INTERACTION OF DRUGS WITH METAL IONS

THESIS

SUBMITTED FOR THE AWARD OF THE DEGREE OF

Doctor of Philosophy

IN

CHEMISTRY

BY

AFTAB ASLAM PARWAZ KHAN

DEPARTMENT OF CHEMISTRY
ALIGARH MUSLIM UNIVERSITY
ALIGARH (INDIA)

2010

DEPARTMENT OF CHEMISTRY
FACULTY OF SCIENCE
ALIGARH MUSLIM UNIVERSITY, ALIGARH – 202002
(INDIA)

Prof. K. S. Siddiqi

☎ Off. : 0571-2703515 Ext. 3361
Resi. : 0571-2401664
Mobile No. : 09837284930
E-mail : ks_siddiqi@ yahoo.co.in

Date:.....

Certificate

This is to certify that the work incorporated in this thesis entitled, ***"Kinetics and Mechanism of Interaction of Drugs with metal ions"*** *is the original contribution of* ***Mr. Aftab Aslam Parwaz Khan,*** *carried out under my guidance is suitable for submission for the award of Ph.D. degree in Chemistry of Aligarh Muslim University, Aligarh.*

K. S. Siddiqi

(Prof. K. S. Siddiqi)

Dedicated To my Family

CONTENTS

Acknowledgements

THESIS

Acknowledgement

I surrender myself to ***THE ALMIGHTY ALLAH*** *whose benign benediction has given me required strength, insight and zeal for fulfillments of my ardent desire throughout this work.*

I couldn't find words to express my heartfelt gratitude to my supervisor ***Prof.K.S.Siddiqi,*** *Chairman, Department of Chemistry A.M.U., for his constant encouragement, guidance, keen interest, expert supervision, critical and valuable advice throughout the course of this work. Infact, without his continuous encouragement and help, this study would not have been completed. 'Thanks a lot, Sir...Without you I would not have got an opportunity to write this acknowledgement'.*

I also offer my sincere thanks to all my teachers who have been helpful to me throughout my stay in the Department.

I consider myself extremely fortunate to have such wonderful and encouraging parents, ***Er. Shafiullah Khan*** *and* ***Mrs. Amina Khatoon*** *who have taught me to believe in myself and follow my dreams. I express my heartful gratitude to my other family members whose constant encouragement, support, inspiration and blessings have been a motivating force behind the completion of this work.*

This thesis is a cumulative effort of many people who are very precious and indispensable part of my life. I am thankful to Shams Tabrez, Lamabam Peter , Mashhood Ras, Shams Shahnawaz, Shahnawaz Khan, Shams Usmani, Shahid,Belal, Tarique, Irshad, Qaisar, Ashraf, Shahabudin, Junaid, Shahnawaz Abbas ,Javed Siddiqui, Hamid, Gauhar, Fahad, Mashiurrehman, Owais, Atif and Asad who gave their helping hands and shared my moments of joy and sorrows equally.

I could not have completed this work without the unbelievable support and help rendered by Shahab A.A.Naami, Ayaz, Jamal, Raju ,Yusuf, Ahmad, Bashar,

Asim, Shahid, Ziya, Zaki, Qasim, Ajmal, Greesh, Muddassir, Moheman, Abuzar, Hamid Fatima , Mariya, Sadia, Anila, Ruchi, Sana, Shaista, Faraha, Saima, Aiman and Seema. There is no better team around and I will never be able to thank you enough.

Finally, a note of thanks to each and every person who was directly or indirectly involved in this research work. 'Thanks a lot to everyone....for making me reache this landmark of my life'.

Dated : .....

Place : *Aligarh*

(Aftab Aslam Parwaz Khan)

PUBLICATIONS

PAPERS PUBLISHED/ACCEPTED/COMMUNICATED

1. *Kinetics and mechanistic investigation of the oxidation of antibacterial agent Levofloxacin by permanganate ion in alkaline medium*
   Aftab Aslam Parwaz Khan, *Ayaz Mohd, Shaista Bano, Ahmad Husain and K.S.Siddiqi Trans Met. Chem. 35,117-123, 2010* ***(Springer)***

2. *Kinetics and Mechanism of Oxidation of D-penicillamine by Potassium Hexacyanoferrate(III) Ions in Aqueous Solution in the Presence of Sodium Dodecyl Sulphate and Cetyltrimethylammonium Bromdie*
   Aftab Aslam Parwaz Khan, *Ayaz Mohd, Shaista Bano, K.S.Siddiqi*
   J. Dis. Sci. Tech.(2010) –Accepted ***(Taylor & Francis)***

3. *Resonance Rayleigh Scattering Spectra, Non-linear Scattering Spectra of selected Cephalosporins -Cd(II) Chelate with Titan Yellow and their Analytical Applications*
   Shaista Bano, Ayaz Mohd, ***Aftab Aslam Parwaz Khan*** *and K.S. Siddiqi*
   J. Dis. Sci. Tech.(2010) –Accepted ***(Taylor & Francis)***

4. *Binding constant: Fluorescence quenching of ciprofloxacin with Fe (III) and Zn (II)*
   K. S. Siddiqi, Ayaz Mohd, ***Aftab Aslam Parwaz Khan****, and Shaista Bano*
   Asian. J. Chem. 22,1957-1965,2010

5. *Development of spectrofluorimetric methods for the determination of levosulpiride in pharmaceutical formulation*
   Shaista Bano, Ayaz Mohd, ***Aftab Aslam Parwaz Khan*** *and K. S. Siddiqi*
   Journal of Analytical Chemistry. (2010) –Accepted ***(Springer)***

6. *Interaction and Fluorescence Quenching Study of Levofloxacin with Divalent Toxic Metal Ions*
   Ayaz Mohd, ***Aftab Aslam Parwaz Khan*** *and Shaista Bano and K.S. Siddiqi*
   (Eurasian Journal of Analytical Chemistry) (2010)-Accepted

7. *Spectroscopic and Substitution Kinetic Studies of Hexacyanoferrate(II) Complexes by EDTA catalysed with Mercury(II)*
   K. S. Siddiqi, ***Aftab Aslam Parwaz Khan****, Ayaz Mohd, and Shaista Bano*
   E - Journal of Chem. 6(S1), S103-110, 2009

8. *Spectrophotometric investigation of oxidation of Cefpodoxime Proxetil by permanganate in alkaline medium : A kinetic study*
   Aftab Aslam Parwaz Khan, *Ayaz Mohd, Shaista Bano, K.S. Siddiqi*
   J. Korean Chem. Soc.53,709-716, 2009

9. *Interaction of CFP with Metal ions: Complex Formation of CFP with Metal ion by Absorption and Fluorescence Spectrophotometery*
   K. S. Siddiqi, Ayaz Mohd, ***Aftab Aslam Parwaz Khan,*** *and Shaista Bano*
   J. Korean Chem. Soc. 53, 152-158, 2009

10. *Fluorescence enhancement of levosulpiride upon coordination with transition metal ions and spectrophotometric determination of complex formation*
    K. S. Siddiqi, Shaista Bano, Ayaz Mohd, and ***Aftab Aslam Parwaz Khan,*** *Analytical Letters, 42, 2192 - 2205, 2009.* ***(Taylor & Francis)***

11. *Binding interaction of captopril with metal ions: A fluorescence quenching study*
    K. S. Siddiqi, Shaista Bano, Ayaz Mohd, and ***Aftab Aslam Parwaz Khan,*** *Chinese Journal of Chemistry.27,1755-1761,(2009)* ***(Willey Inter Sciences)***

12. *Spectrophotometric interaction of the Oxidation of Captopril by Hexacyanoferrate(III) in Aqueous Alkaline Medium: A Kinetic and Mechanistic Approach*
    Aftab Aslam Parwaz Khan, *Ayaz Mohd, Shaista Bano and K.S.Siddiqi*
    J. Dis. Sci. Tech.(2010) –Communicated ***(Taylor & Francis)***

13. *Kineitcs and Mechanism of deamination and decarboxylation of 2-aminopentanedioic acid by quinoliniumdichromatre (QDC) in aqueous perchloric acid*
    Aftab Aslam Parwaz Khan, *Ayaz Mohd, Shaista Bano and K.S.Siddiqi*
    Industrial & Engineering Chemistry Research (2010) – Communicated ***(ACS)***

14. *The determination of Ampicillin in Pharmaceutical Preparations by potassium permanganate ion and 1-chloro-2,4-dinitrobenzene*
    Aftab Aslam Parwaz Khan, *Ayaz Mohd, Shaista Bano and K.S.Siddiqi*
    Spectrochimica Acta Part A: Molecular Spectroscopy (2010) – Communicated
    (Elsevier)

Abstract

THESIS

ABSTRACT

This thesis describes the kinetics and mechanism of oxidation of some drugs in different media. The reactions have been followed spectrophotometrically. The study of oxidation of drugs is of immense importance both from mechanistic and synthetic point of view. It has a bearing on the chemical processes of life also.

The introductory chapter reports the kinetics and mechanism of oxidation of Levofloxacin (LF) by $KMnO_4$ in alkaline medium at a constant ionic strength (0.10 mol dm^{-3}). It is a first order reaction, but fractional order in both LF and alkali. Decrease in the dielectric constant of the medium results in a decrease in the rate of reaction. The effects of added products and ionic strength have also been investigated. The main products identified were hydroxylated LF and Mn(VI). A mechanism involving free radical is proposed. In a composite equilibrium step, LF binds to MnO_4^- Pto form a complex that subsequently decomposes to the products. Investigations of the reaction at different temperatures allowed the determination of the activation parameters with respect to the slow step of the proposed mechanism.

Second chapter deals with the effect of cationic-cetyltrimethylammonium bromide, (CTAB) and anionic surfactant sodium dodecyl sulphate, (SDS) on the rate of oxidation of D-penicillamine by alkaline hexacyanoferrate(III) has been

studied by spectrophotometrically at different temperatures. The effect of CTAB and SDS on the rate of reaction has been studied even below the critical miceller concentration (CMC) of the surfactants indicating binding of the substrate with the surfactants. On the basis of the kinetic results, the mechanism of the reaction has been proposed. The kinetic data have been rationalized in terms of Manger and Portnoy's model for micellar inhibition and binding parameters (viz. binding constants, partition coefficient, free energy transfer from water to micelle, etc.) as well as activation parameters.

Two simple and sensitive kinetic methods for the determination of Ampicillin (AMP), are described. The first method is based on kinetic investigation of the oxidation reaction of the drug with alkaline potassium permanganate at room temperature at fixed time of 25 min. The absorbance of the colored manganate ions is measured at 610 nm. The second method is based on the reaction of AMP with 1-chloro-2,4-dinitrobenzene (CDNB) in the presence of 0.1 mol/L sodium bicarbonate. Spectrophotometric measurement was done by recording the absorbance at 490 nm for a fixed time of 60 min. All variables affecting the development of the color were investigated and the conditions were optimized. Plots of absorbance against concentration in both procedures were rectilinear over the ranges 5–30 and 50–260 μgmL^{-1}, with mean recoveries of 99.75 and 99.91, respectively. The proposed methods were successfully applied for the determination of AMP in bulk powder and in dosage form. The

determination of AMP by the fixed concentration method is feasible with the calibration equations obtained, but the fixed time method proves to be more applicable.

Chapter four includes the kinetics of oxidation of L-Glutamic acid by quinoliniumdichromatre in perchloric acid medium. The rate of the reaction was found to increase with increasing concentrations of the L-Glutamic acid, perchloric acid and ionic strength. The reactions are first order with respect to both QDC and L-Glutamic acid. Added products, had insignificant effect on the reaction rate. The activation parameters have been evaluated and lend further support to the proposed mechanism. The thermodynamic quantities were also determined and discussed.

Chapter five deals with the the kinetics and mechanism of substitution of cyanide ion in hexacyanoferrate(II) by EDTA catalysed by mercury(II), It has been studied spectrophotometrically at 365 nm in potassium hydrogen phthalate buffer of pH = 5.0 and ionic strength, I = 0.1M, maintained by (KNO_3) at 25^0C. Effect of the pH and concentration of the EDTA, $[Fe(CN)^{4-}_6]$ on the rate of reaction has been studied. The kinetics and mechanism of the reaction has been shown through dissociative mechanism. The catalytic activity of mercury(II) has also been studied as a function of its concentration. The maximum reaction product was detected at pH = 5 after which a decline in absorption occurs

followed by precipitation. It is an inexpensive method to identify and remove the cyanide ion in solution even at very low concentration of the order of $10^{-4}M$.

Kinetics and mechanism of oxidation of captopril (CPL) by hexacyanoferrate(III) in alkaline medium has been studied spectrophotometrically. The reaction showed first order kinetics in hexacyanoferrate(III) and alkali concentrations and, an order of less than unity in CPL concentration. The rate of reaction increases with increase in alkali concentration. Increasing ionic strength increases the rate but the dielectric constant of the medium has no significant. A mechanism involving the formation of a complex between CPL and hexacyanoferrate(III) has been proposed. The reaction constants involved in the mechanism are evaluated. There is a good agreement between the observed and calculated rate constants under different experimental conditions. Investigations at different temperatures allowed the determination of the activation parameters with respect to the slow step of the proposed mechanism.

Chapter- 1

Kinetics and Mechanism of Oxidation of Levofloxacin by Permanganate in Alkaline medium

INTRODUCTION

Potassium permanganate is widely used as an oxidizing agent where the reactions are governed by the pH of the medium. Of all the oxidation states (+2 to +7) of manganese +7 is the most potent state in both acid and alkaline media. Permanganate ion finds extensive application in organic synthesis [1-2] and, in catalysis [3-5]. Kinetic studies are important source of mechanistic information of the reaction as demonstrated by the results referring to unsaturated acids both in aqueous [6] and non-aqueous media [7]. The mechanism of oxidation depends on the nature of the substrate and pH of the system [8]. In strongly alkaline medium, the stable reduction product [9-11] of MnO_4^- is MnO_4^{2-}, although MnO_2 appears only after the complete consumption of MnO_4^-. No mechanistic information is available to distinguish between a direct one-electron reduction of Mn(VII) to Mn(VI) and a mechanism, in which a hypomanganate ion is formed in a two-electron reduction followed by its rapid oxidation [12-13].

Levofloxacin, (−)-(S)-9-fluoro-2,3-dihydro-3-methyl-10- (4-methyl- 1-piperazinyl) -7-oxo-7H pyrido[1,2,3-de]-1,4-benzoxazine-6-carboxylic acid hemihydrate (Fig.1) is one of the commonly used fluoroquinolone antimicrobials, being active S-isomer, was isolated from the racemic ofloxacin. Levofloxacin possesses a broad spectrum of activity against Gram-positive and Gram-negative bacteria [14]. It is also active against *Chlamydia pneumoniae* and *Mycoplasma pneumoniae* [15]. Because of its effective antibacterial activity and low frequency of adverse effect on oral administration, levofloxacin is widely used in the treatment of infectious diseases, such as community-acquired pneumonia and acute exacerbation of chronic bronchitis [16]. The antibacterial action of the quinolones is not linearly proportional to their concentration and optimum concentration must be maintained to prevent the replication of surviving bacteria [17]. The intrinsic fluorescence of fluoroquinolones is used for their determination in biological samples after their preliminary extraction with organic solvents [18]. A method was proposed for determining these antibiotics in biological fluids using a mixed-ligand complex formed by terbium and triphenyl phosphine oxide [19]. The interaction of fluoroquinolones with metal ions has attracted considerable interest not only for the development of analytical techniques but also to provide information about the mechanism of action of the pharmaceutical preparation [20]. Since the metal ions cause fluorescence quenching of the drug

spectrofluorimetric method for quantitative determination of the quinolone type drugs has been developed [21]. Although titrimetric [22] spectrophotometeric [23], electrochemical [24], electrophoretic [25] and chromatographic [26] techniques are already in use they are time consuming. The accumulation of fluoroquinolone antibiotics in aquatic environments even in low concentrations, may cause threat to the ecosystem and human health by inducing multiplication of drug resistant bacteria as a result of long-term exposure. Chemical oxidation of pollutants in drinking and waste water by permanganate ion has been widely used. The present study is an attempt to explore the mechanistic pathway of oxidation of levofloxacin by permanganate ion in alkaline medium.

EXPERIMENTAL

Analytical reagent grade chemicals were used. Double distilled water was used throughout the work. The solution of Levofloxacin (Sigma-Aldrich, India) was prepared in distilled water. The potassium permanganate (Ranbaxy Fine Chem. Ltd, India) solution was prepared and standardized against oxalic acid[27]. Potassium permanganate solution was prepared as described by Carrington and Symons [28]. KOH and KNO_3 (Merck Ltd., Mumbai, India) were employed to maintain the alkalinity and ionic strength, respectively. The absorption spectra were obtained with Elico-SL-169 double beam UV–vis

spectrophotometer. All potentiometric measurements were carried out with Elico-LI-120 pH meter.IR spectra of the product was scanned with Nicolet 5700-FT-IR spectrometer (Thermo, U.S.A.).

Kinetic measurements and procedure

The oxidation of Levofloxacin by permanganate ion was followed under pseudo- first order conditions where its concentration was greater than that of manganese (VII), unless otherwise stated. The reaction was initiated by mixing previously thermostated solutions of MnO_4^- and Levofloxacin which also contained required quantities of KOH and KNO_3 to maintain alkalinity and ionic strength, respectively. The course of the reaction was followed by monitoring the change in absorbance of MnO_4^- at its absorption maximum of 526 nm. It was already verified that there was no interference from other reagents in the range of absorption under consideration. Application of Beer's Law was verified, giving $\varepsilon = 2083 \pm 50$ dm^3 mol^{-1} cm^{-1} [9]. The first order rate constant K_{obs} was evaluated from a plot of log [permanganate] versus time. It was linear up to 75% of the reaction (Fig.2). Fresh solutions were used while conducting the experiments. Regression analysis of experimental data to obtain the regression coefficient, r and the standard deviation S of points from the regression line was done using a Microsoft Excel-2007.

RESULTS AND DISCUSSION

The order of the reaction was determined form a plot of logk_{obs} versus log (concentration) of drug and, OH^- separately keeping other factors constant. Keeping the concentration of LF (1.0×10^{-3} mol dm^{-3}), alkali (2.0×10^{-3} mol dm^{-3}) and ionic strength constant (0.10 mol dm^{-3}) the permanganate concentration was varied in the range of 4.0×10^{-5} to 6.0×10^{-4} mol dm^{-3}. All kinetic runs exhibited identical characteristics. The linearity of plots of log (absorbance) versus time, for different concentrations of permanganate indicates order in Mn(VII) concentration as uniform (Fig.2). It was also confirmed by the constant values of pseudo first order rate constants, k_{obs}, for different Mn(VII) concentrations (Table 2). The LF concentration was varied (4.0×10^{-4} to 6.0×10^{-3} mol dm^{-3}) keeping permanganate concentration and ionic strength constant. The k_{obs} increased with increaseing concentration of LF (Fig. 4). At low concentration of LF, the reaction was first order and, at high concentration, the reaction was independent of its concentration. Keeping all other factors constant the alkali concentration was varied (1.0×10^{-3} to 1.0×10^{-2} mol dm^{-3}). The rate constant increases with increasing concentration (Fig. 5), of alkali indicating a fractional-order dependence of the rate on alkali concentration.

Stoichiometry and product analysis

Different set of reaction mixtures containing LF and an excess of MnO^{4-} with constant OH^- and KNO_3 concentration were kept in closed vessels under nitrogen atmosphere. After 2 hours, the Mn(VII) concentration was assayed by measuring the absorbance at 526 nm. The results indicated a 1:2 stoichiometry, as given in Scheme 1.

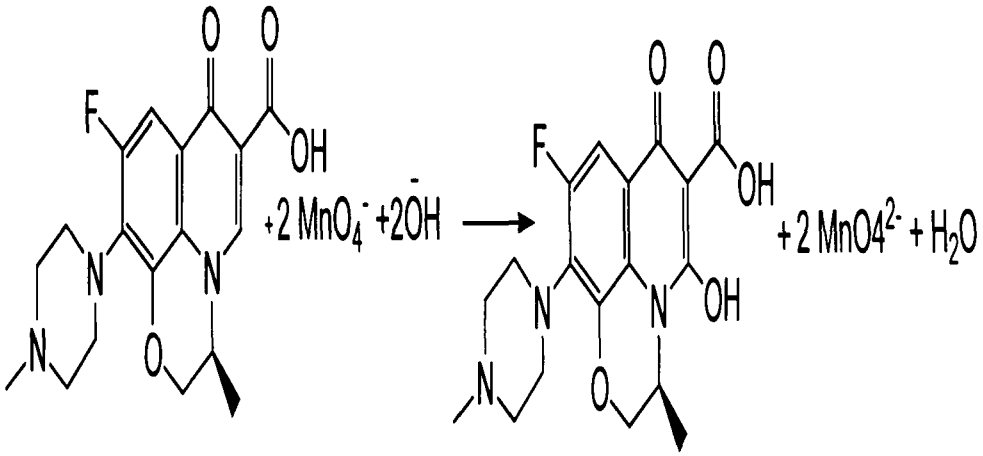

Scheme 1.

The main reaction product, Mn(VI) and 9-fluoro-2,3-dihydro-3-methyl-5-hydroxy-10-(4-methyl-1-piperazinyl)-7-oxo-7Hpyrido[1,2,3-de]-1,4 benzoxazine-6 carboxylic acid was isolated and identified by TLC and FT-IR spectrum. The ν(C=O) of free LF at 1,722 cm^{-1} was shifted to 1,626 cm^{-1} when complexed with metal ions (Fig.6) suggesting coordination through the carboxylate group.

This is known that when there is a difference of over 200 cm-1 between symmetric and antisymmetric (CO) streaching frequency of the carboxylate

group it is boded as a bidentate group while a difference of 100-200 cm^{-1} in the same region it refers to a the bonding of carboxylate group in a monodentate fashion[29-30].

In a our case, we have observed a difference of 144cm^{-1} (Table 1) between the antisymmetric and symmetric ν(C=O) it is therefore ascertained that it is acting as monodentate group. The relative positions of the asymmetric and symmetric stretching vibrations are given in (Table 1) gives a separation >100 cm^{-1}, suggesting monodentate bonding for the carboxylate group.

Effect of ionic strength, dielectric constant and temperature

The effect of ionic strength was studied by varying the potassium nitrate concentration between 0.01 to 0.10 mol dm^{-3} keeping all other parameters constant. The effect of the dielectric constant (D) was studied by varying the t-butanol–water content (v/v) keeping all other conditions constant. The rate of reaction increases with increasing t-butanol volume. The plot of log k_{obs} versus 1/D was linear with positive slope (Fig.7). The kinetics was also studied at four different temperatures with varying concentrations of LF and alkali, keeping other conditions constant. The rate constant was found to increase with increase in temperature. The rate of the slow step was obtained from the slopes and intercepts of 1/kobs versus 1/[LF] and 1/kobs versus 1/[OH^-] plots at four different temperatures (20-37°C). The activation energy corresponding to these

rate constants was evaluated from the Arrhenius plot of log k versus 1/T from which other activation parameters were obtained (Table 3).

Test for free radicals

In order to test for the interference by the free radicals, the acrylonitrile was added to the reaction mixture and then left for 24 hours under nitrogen atmosphere. Subsequent of methanol resulted in the precipitation of a polymer, suggesting the involvement of free radicals in the reaction. The blank experiment of reacting permanganate and LF alone with acrylonitrile did not induce polymerization under the same conditions. Initially added acrylonitrile decreased the rate of reaction [31]

The reduction product of Mn(VII), i.e., Mn(VI) is stable at pH 12, and no further reduction is observed [10]. However, on prolonged standing, the green Mn(VI) is reduced to Mn(IV) under our experimental conditions. Permanganate ion in alkaline medium exhibits various oxidation states, such as Mn(VII), Mn(V) and Mn(VI). During the course of the reaction, colour changes from violet Mn(VII) to dark green Mn(VI) through blue Mn(IV). Fig. 3 clearly shows five peaks in the spectrum of which three peaks are prominent. The concentration of MnO^{4-} decreases at 526 nm as a result of the Mn(VII), while increases formation of Mn(VI) at 610 and 460 nm. As the reaction proceeds, a yellow turbidity slowly develops and, after keeping for a long time

the solution decolourises and forms a brown precipitate. This suggests that the initial products might have undergone further oxidation resulting in a lower oxidation state of manganese. It appears that the alkali combines with permanganate to give $[MnO4.OH]^{2-}$ [32-33]. In the second step, $[MnO4.OH]^{2-}$ combines with LF to form an intermediate complex. The variable order with respect to LF most probably results from the complex formation between oxidant and LF prior to the slow step. A plot of 1/kobs versus 1/[LF] (Fig.4) shows an intercept which is in confirmity with the complex formation. Further evidence was obtained from the UV–vis spectra of reaction mixtures. Two isosbestic points were observed for this reaction (Fig. 3), indicating an attainment of equilibrium before the slow step [34-35]. In our proposed mechanism, one electron is transferred from LF to Mn(VII). The cleavage of this complex (C) is regarded as the slowest step, leading to the formation of an LF radical intermediate and Mn(VI). The radical intermediate further reacts with another Mn(VII) species, $[MnO_4.OH]^{2-}$, to give the, Mn(VI) and alcohol (Scheme 2). The effect of the ionic strength and dielectric constant on the rate is consistent with the involvement of a neutral molecule in the reaction.

The proposed structure of the complex (C) is given below.

2-

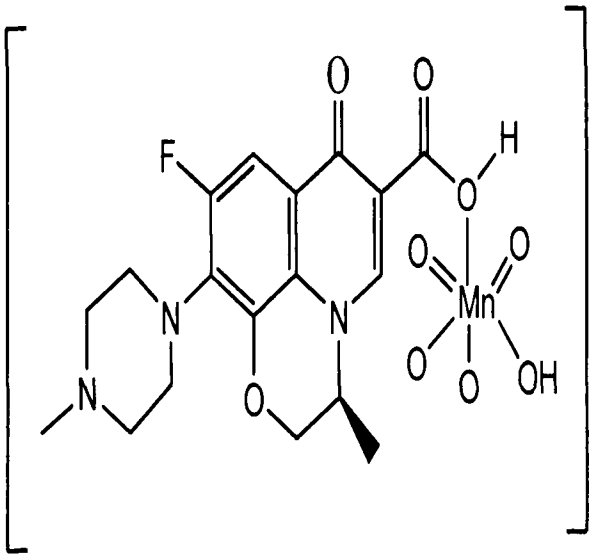

Complex (C)

From Scheme 2, the rate law (Eq. 7) can be derived as follows:

$$\text{Rate} = \frac{-d[MnO_4^-]}{dt} = kK_1K_2[MnO_4^-]_f[LF]_f[OH^-]_f \quad (1)$$

The total $[MnO_4^-]$ can be written as

$$\text{Rate} = \frac{-d[MnO_4^-]}{dt} = kK_1K_2[MnO_4^-]_f[LF]_f[OH^-]_f$$

$$[MnO_4^-]_t = [MnO_4^-]_f + [MnO_4.OH]^{2-} + [\text{Complex}]$$

$$= [MnO_4^-]_f + [MnO_4^-][OH^-] + K_1K_2[MnO_4^-][LF][OH^-]$$

$$= [MnO_4^-]_f (1 + K_1[OH^-] + K_1K_2[LF][OH^-])$$

$$[MnO_4^-]_f = \frac{[MnO_4^-]_t}{1 + K_1[OH^-] + K_1K_2[LF][OH^-]} \qquad (2)$$

where "t" and "f" stand for total and free concentration of [OH $^-$]. Similarly, total [OH $^-$] can be calculated as

$$[OH^-]_t = [OH^-]_f + [MnO_4.OH]^{2-} + [\text{Complex}]$$

$$[OH^-]_f = \frac{[OH^-]_t}{1 + K_1[MnO_4^-] + K_1K_2[LF][MnO_4^-]} \qquad (3)$$

In view of the low concentrations of MnO_4^- and LF, the terms $K_1[MnO_4^-]$ and $K_1K_2[MnO_4^-]$ [LF] in Eq.3 can be neglected

Thus,

$$[OH^-]_f = [OH^-]_t \qquad (4)$$

Similarly,

$$[LF]_f = [LF]_t \qquad (5)$$

Substituting Eq. 2, 4, and 5 in Eq. 1 we get

$$\text{Rate} = \frac{kK_1K_2[MnO_4^-][LF][OH^-]}{1+ K_1[OH^-] + K_1K_2[LF][OH^-]} \qquad (6)$$

Or

$$\frac{\text{Rate}}{[MnO_4^-]} = k_{obs} = \frac{kK_1K_2[LF][OH^-]}{1+ K_1[OH^-] + K_1K_2[LF][OH^-]} \qquad (7)$$

Equation 7 confirms all the observed orders with respect to different species, which can be verified by rearranging then to equation 8.

$$\frac{1}{k_{obs}} = \frac{1}{kK_1K_2[LF][OH^-]} + \frac{1}{kK_2[LF]} + \frac{1}{k} \qquad (8)$$

The other conditions being constant, plots of 1/kobs versus 1/[LF] and 1/kobs versus 1/[OH^-] are linear (Figs. 4 and 5). The slopes and intercepts of such plots yield *K1, K2* and k (Table 3). The rate constants were calculated from these values and, there is a reasonable agreement between the calculated and

the experimental [36] values (Table 2). The thermodynamic quantities for the first and second equilibrium steps of Scheme 2 can be evaluated. The [LF] and [OH^-] (Table 1) were varied at four different temperatures. Van't Hoff's plots of $\log K_1$ versus 1/T and $\log K_2$ versus 1/T gave the values of enthalpy, $\Delta H^{\#}$, entropy, $\Delta S^{\#}$ and free energy of reaction, ΔG, calculated for the first and second equilibrium steps (Table 3). A comparison of the latter (from K_2) with those obtained for the slow step of the reaction shows that they mainly refer to the rate-limiting step, supporting the fact that the reaction before the rate determining step is fairly fast and involves low activation energy [37-38]. The moderate values of $\Delta H^{\#}$ and $\Delta S^{\#}$ were both favorable for electron transfer process. The $\Delta S^{\#}$ value is within the expected range for radical reactions and has been ascribed to the nature of electron pairing and unpairing processes and, the loss of degrees of freedom formerly available to the reactants upon the formation of a rigid transition state [39]. The negative value of $\Delta S^{\#}$ indicates that complex (C) is more ordered than the reactants [40-41]. The enthalpy of activation and a relatively low value of the entropy and a higher rate constant of the slow step indicate that the oxidation most probably occurs via inner-sphere mechanism [42-43]. A detailed mechanistic interpretation is given in scheme 3.

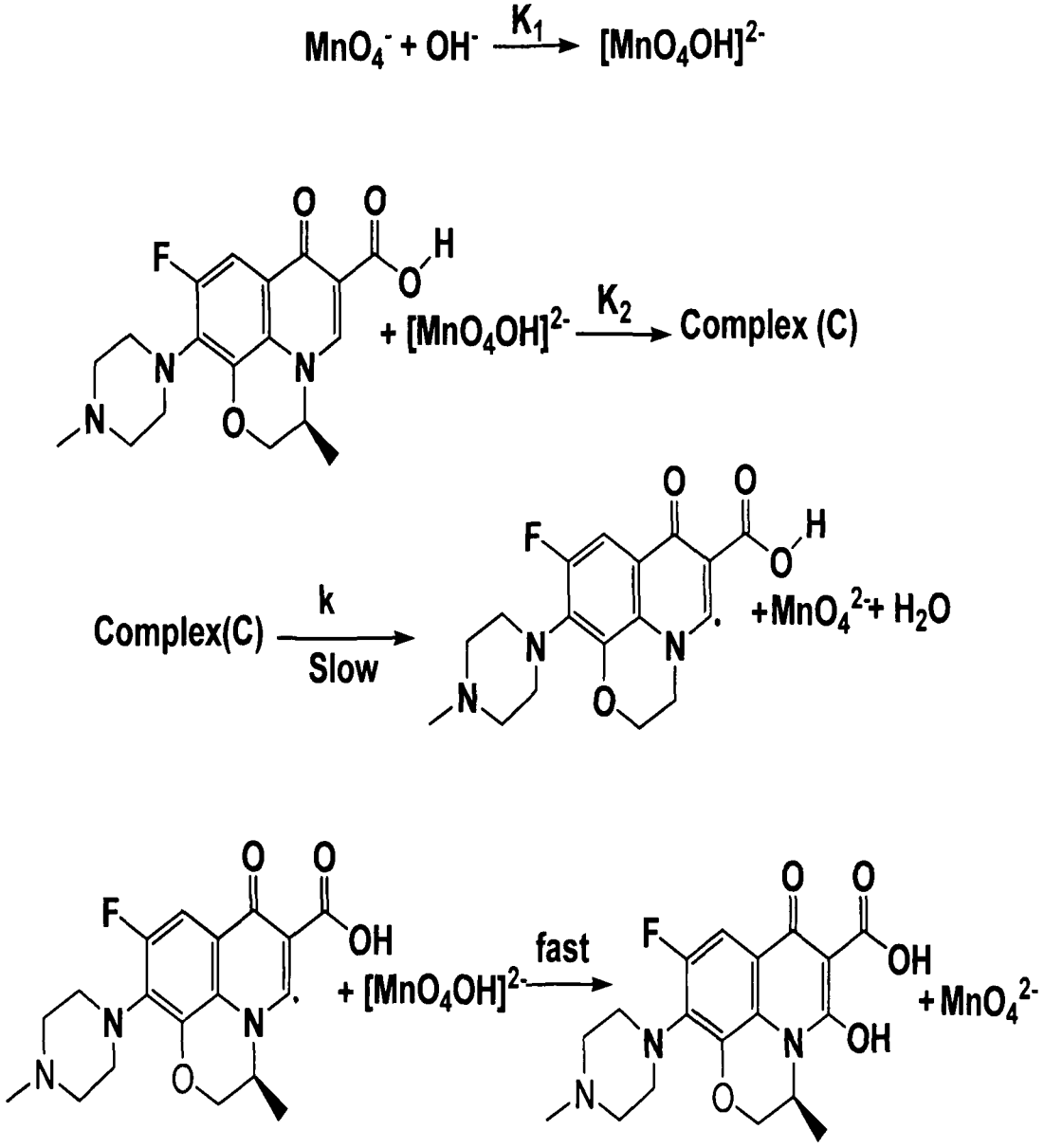

Scheme 2. Mechanism for the Oxidation of Levofloxacin by Alkaline MnO_4^-.

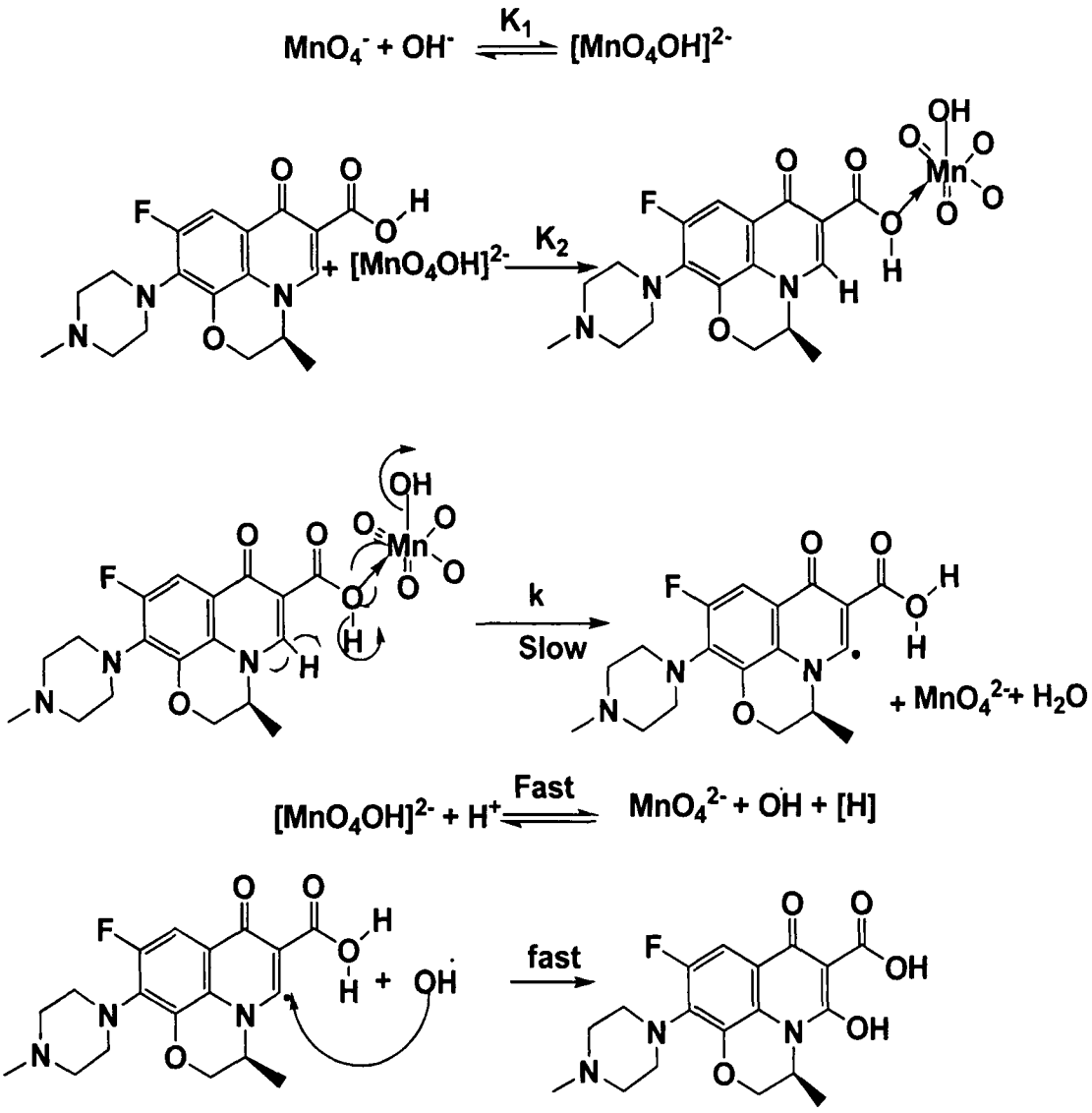

Scheme 3. Detailed Mechanistic of Oxidation of Levofloxacin by Permanganate in Alkaline medium.

CONCLUSION

It is noteworthy that the oxidant species [MnO^{4-}] required for completion of reaction at pH 12, gets disturbed below this pH and produces Mn(IV) product, which slowly develops yellow turbidity. In this reaction, the role of pH is crucial. The rate constant of the slowest step and other equilibrium constants involved in the mechanism were evaluated and, activation parameters with respect to the slowest step were computed. The proposed mechanism is consistent with the product and kinetic parameters.

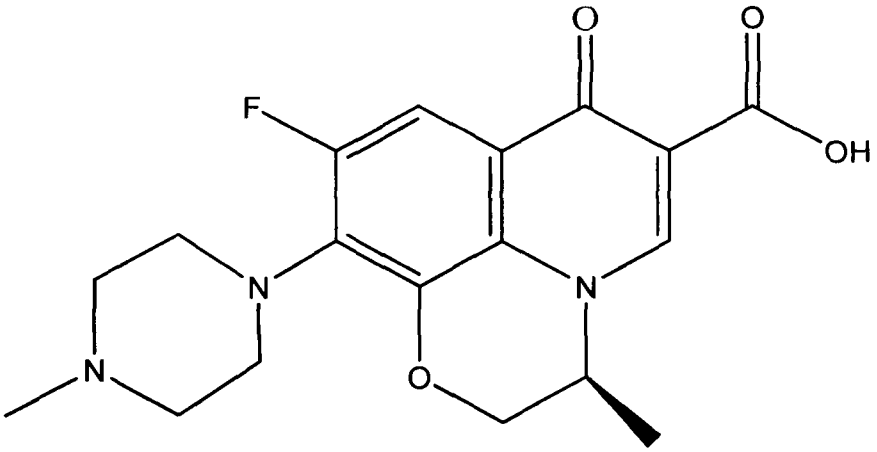

Fig.1 Structure of Levoflaxacin

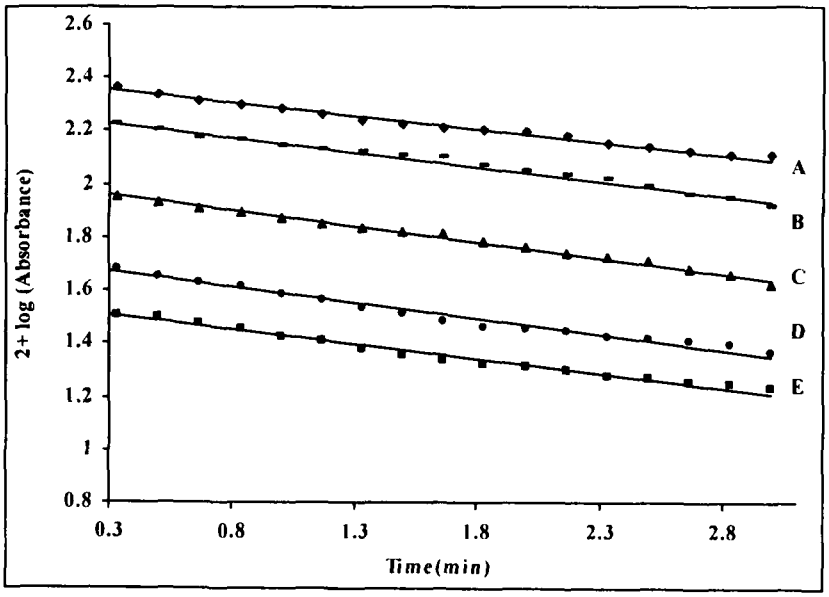

Fig.2 First order plots of the oxidation of levofloxacin by permanganate in aqueous alkaline medium. [LF] = 1×10^{-3}, [OH$^-$] = 2×10^{-3}, I = 0.10/mol dm^{-3}. [MnO_4^-]$\times10^4$ mol dm^{-3} = (A) 0.4, (B) 0.8, (C) 1.0, (D) 2.0, (E) 3.0.

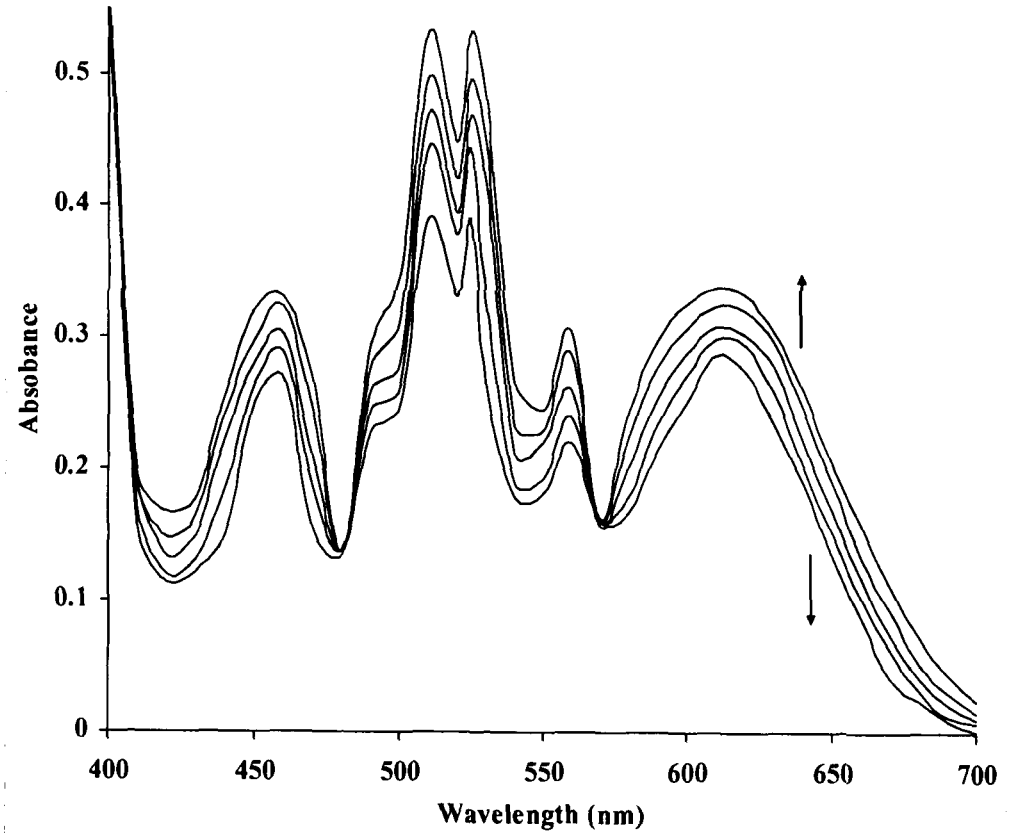

Fig.3 Spectral changes during the oxidation of levofloxacin (LF) by MnO_4^- in alkailine medium at 25 °C: $[MnO_4^-] = 1\times 10^{-4}$, $[LF] = 1\times10^{-3}$, $[OH^-] = 2\times10^{-3}$, $I = 0.10/mol\ dm^{-3}$.

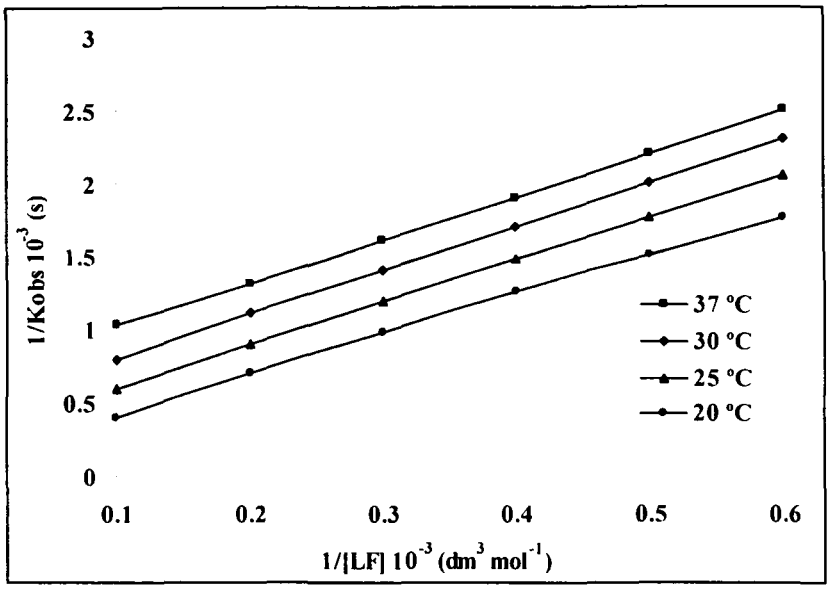

Fig.4 Plots of 1/kobs vs 1/[LF] at four different temperatures

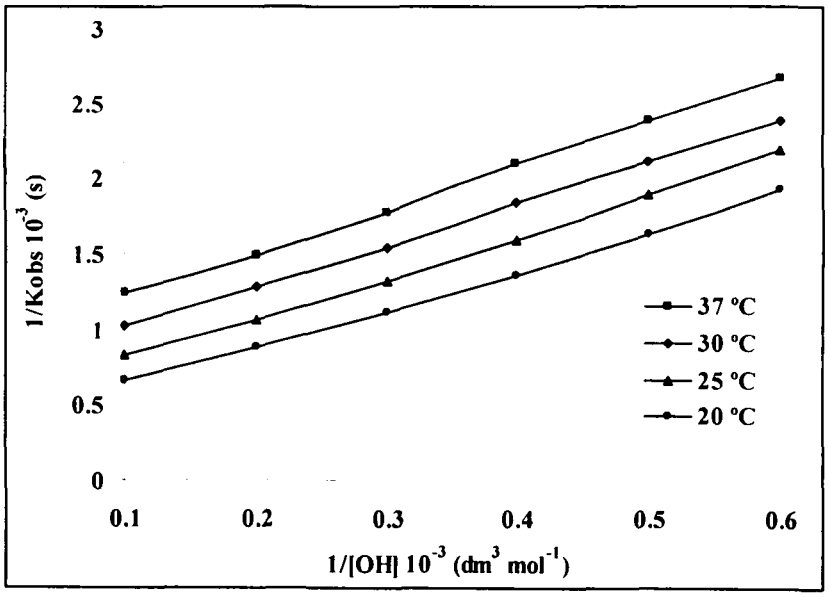

Fig.5 Plots of 1/kobs vs 1/[OH⁻] at four different temperatures

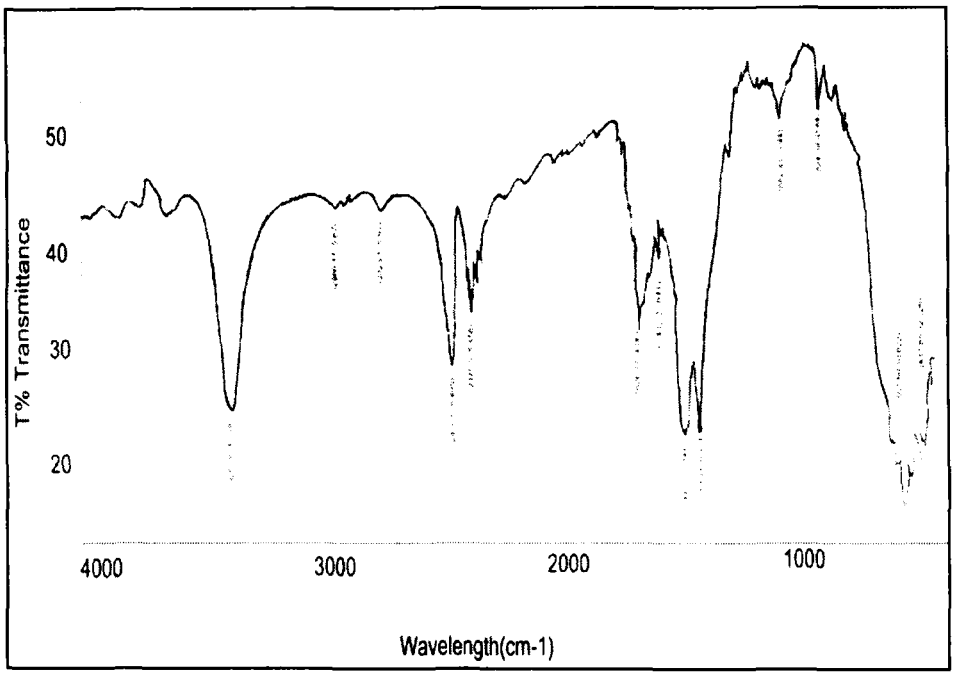

Fig.6 FT-IR spectrum of oxidation product of levofloxacin

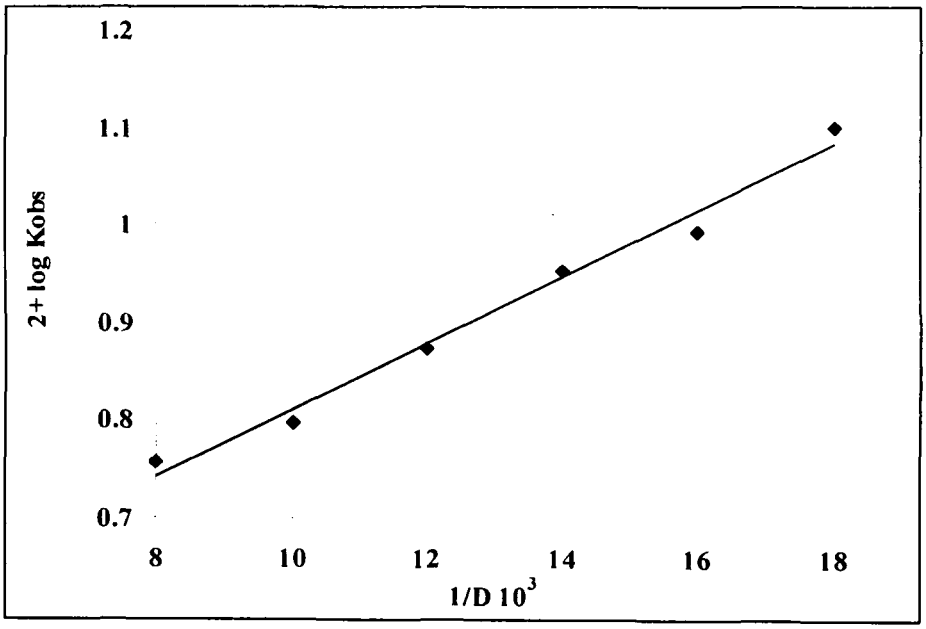

Fig.7 Effect of dielectric constant on the oxidation of levofloxacin by alkaline MnO_4^- at 25.0 °C.

Table1. FT-IR frequencies (cm^{-1}) of levofloxacin and its oxidation product

Compound	*v(OH)*	*v(C=O)*	v_{asym} *(COO)*	v_{sym}*(COO*
Levofloxacin	3411	1722	1622	1462
Oxidation Product	3305	1626	1586	1442

Table 2. Effects of [LF], [MnO^{4-}], and [OH^-] on the oxidation of levofloxacin by permanganate at 25^{0}C and ionic strength I = 0.10/mol dm^{-3}.

$10^4\times$ [MnO_4^-] (mol dm^{-3})	$10^3\times$ [LF] (mol dm^{-3})	$10^3\times$ [OH^-] (mol dm^{-3})	$k_{cal} \times 10^{-3}$ (s^{-1})	$k_{obs} \times 10^{-3}$ (s^{-1})
Variation of [MnO_4^-]				
0.4	3.0	2.0	4.12	4.10
0.8	3.0	2.0	4.12	4.10
1.0	3.0	2.0	4.12	4.10
2.0	3.0	2.0	4.12	4.10
3.0	3.0	2.0	4.12	4.10
Variation of [LF]				
3.0	0.4	2.0	3.67	3.65
3.0	0.6	2.0	3.76	3.74
3.0	0.8	2.0	3.12	4.10
3.0	1.0	2.0	4.28	4.25
3.0	4.0	2.0	5.38	5.35
3.0	6.0	2.0	5.41	5.40
Variation of [OH^-]				
3.0	3.0	0.4	2.19	2.18
3.0	3.0	0.8	2.39	2.38
3.0	3.0	1.0	2.84	2.82
3.0	3.0	2.0	3.32	3.30
3.0	3.0	4.0	3.61	3.60
3.0	3.0	6.0	4.43	4.41

Table 3. Activation and thermodynamic parameters for the oxidation of levofloxacin by alkaline permanganate with respect to the slow step of the reaction scheme 2

Effect of temperature with respect to slow step of the Scheme 1		
Temperature (K)		**k $\times 10^3$ (s^{-1})**
293 298 303 310		10.6 11.8 12.2 13.5
Activation parameters		*Values*
Ea (kJ mol^{-1}) *$\Delta H^{\pm}$ (kJ mol^{-1})* *$\Delta S^{\pm}$(J K^{-1} mol^{-1})* *$\Delta G^{\pm}$ (kJ mol^{-1})*		14.9 11.9 -143.2 63.05
(c) *Equilibrium Constants K_1 and K_2 at Different Temperatures.*		
Temp. (K)	*$K_1 \times 10^{-2} dm^6$ mol^{-2}*	*$K_2 \times 10^{-3}$ dm^3 mol^{-1}*
293 298 303 310	5.44 7.59 9.62 12.43	6.17 6.69 5.32 4.34
(d) Thermodynamic Parameters	*K_1 values*	*K_2 values*
$\Delta H^{\pm}$ (kJ mol^{-1}) *$\Delta S^{\pm}$(J K^{-1} mol^{-1})* *$\Delta G^{\pm}$ (kJ mol*	58.1 123.5 -8.7	-78.6 -89.7 -8.35

REFERENCE

[1]. A. Shaabani, F.Tavasoli-Rad and D.G. Lee: Synth. *Commun. Synth. Comm,.* 35, 571**(2005)**

[2]. S. Caron, R.W. Dugger, S.G. Ruggeri, J.A. Ragan and D.H. Brown Ripin: *Chem. Rev.,* 106, 2943**(2006)**

[3]. D. G. Lee, In W.S. Trahanovsky: (ed) Oxidation in Organic Chemistry, Part D. Academic Press, New York, p 147**(1982)**

[4]. L.I.Simandi, In S. Patai and Z. Rappoport (eds) The Chemistry of Functional Groups. *Wiley, Chichester Suppl.* C**(1983)**

[5]. D.G. Lee, E.J. Lee and K.C .Brown: Phase Transfer Catalysis, New Chemistry, Catalysis and Applications, ACS Symposium Series, vol. 326. American Chemical Society, Washington**(1987)**

[6]. A.J. Fatiadi: *Synthesis* 106,85**(1987)**

[7]. J.F. Perez-Benito and D.G. Lee:*J. Org. Chem.,* 52,3239**(1987)**

[8]. R. Stewart, K.A. Gardner, L.L. Kuehnert and J.M. Mayer: *Inorg. Chem.*, 36,2069**(1997)**

[9]. L.I. Simandi, M. Jaky, C.R. Savage and Z.A .Schelly : *J. Am. Chem. Soc.*, 107,4220**(1985)**

[10].P.L .Timmanagoudar, G.A. Hiremath and S.T. Nandibewoo: *Trans.Met.Chem.*,22,193**(1997)**

[11].S. Nadimpalli, R. Rallabandi and L.S.A. Dikshitulu : *Trans. Met. Chem.*, 18,510**(1993)**

[12].R.G. Panari, R.B .Chougale and S.T. Nandibewoor: *Pol. J. Chem.,* 72,99**(1998)**

[13]. A.Bohn, M. Adam, H.H Mauermann, S.S Stein and K.K Mullen: *Tetrahedron Lett,.* 33,2795**(1992)**

[14]. D. Croisier, M. Etienne, E. Bergoin, P.E. Charles, C. Lequeu, L. Piroth, H. Portier and P. Chavanet : *Antimicrob Agents Chemother.*, 48,1699**(2004)**

[15]. P.M .Roblin and M.R. Hammerschlag: *Antimicrob Agents Chemother.*, 47,1447**(2003)**

[16]. Jr. R.C. Owens and P.G. Ambrose: *Med. Clin. North. Am.*, 84,1447**(2000)**

[17]. M. V.Shulgina, N.I .Fadeeva, T. N. Bolshakova, I. B. Levshin and R.G. Glushkov: J. *Parm. Chem.*, 33,343**(1999)**

[18]. T.B .Waggoner and M.C .Bowman: *J. Assoc. Anal. Chem.*, 70,813**(1987)**

[19]. C.J. Veiopoulou, P.C. Ioannou and *E.S.* Liaidou: *J. Pharm. Biomed. Ana.,l* 15,1839**(1997)**

[20]. I. Turel, P.A. Golobi, A. Klazar, B. Pihlar, P. Buglyo, E. Tolib, D. Rehder and K. J. Sepiv: *J. Inorg. Biochem.*, 95,199**(2003)**

[21]. E. Kilic, F. Koseoglu, M.A Akay : *J .Pharm. Biomed. Anal.*,12,347**(1994)**

[22]. S. Mostafa, M. Elsadek, *E.* Awadalla: *J. Pharm. Biomed. Anal.*, 27,133**(2002)**

[23]. Z. Liu, Huang and R. Cai: *Analyst.*, 125,1477**(2000)**

[24]. M.A.G. Trindade, P.A.C .Cunha, T.A.de Arauja , G.M.dasilva and V.S.Ferreira: Ecl.Quim, Sao Paulo., 31, 31**(2006)**

[25]. C. Fierens, S. Hillaert and W.V. Bossche: *J. Pharm. Biomed. Anal.*, 76,220**(2000)**

[26]. J. Novakovic, K. Nesmark, H. Nova and K. Filka: *J. Pharm. Biomed. Anal.*, 25,957**(2001)**

[27]. G.H .Jeffery, J. Bassett, J. Mendham and R.C. Denny: Vogel's Textbook of Quantitative Chemical Analysis, 5th ed edn.Longman, EssexEssex, p 370**(1996)**

[28]. A. Carrington and M.C.R. Symons: *J. Chem. Soc.,* 3373**(1956)**

[29]. B. Macias, M.V. Villa, I. Rubio, A. Castineiras and J. Borras: *J. Inorg. Biochem,* 84,163**(2001)**

[30]. B. Macias, M.V. Villa, M. Saste, A .Castineiras and *J* .Borras: *J. Pharm. Sci.,* 91,2416**(2002)**

[31]. S. Bhattacharya and P. Benerjee: *Bull. Chem. Soc.,* 69,3475**(1996)**

[32]. R.G. Panari, R.B. Chougale and S.T. Nandibewoor: *J. Phys. Org.*,11,1 **(1998)**

[33].K.A. Thabaj, S.D. Kulkarni, S.A. Chimatadar and S.T. Nandibewoor: *Polyhedron,*26,4877**(2007)**

[34]. R. Chang: Physical Chemistry with Applications to Biological Systems. MacMillan Publishing Co. Inc, New York, p 536**(1981)**

[35]. D.N .Sathyanarayana: Electronic Absorption Spectroscopy and Related Techniques. Universities Press (India) Ltd, Hyderabad, p 12**(2001)**

[36]. D.C. Bilehal, R.M .Kulkarni and S.T. Nandibewoor: *Z. Phys. Chem.,* 1(2003)

[37]. K.S. Rangappa, M.P. Raghavendra, D.S. Mahadevappa and D. Channegouda: *J. Org. Chem.*, 63,531**(1998)**

[38]. D.C. Bilehal, R.M. Kulkarni and S.T. Nandibewoor: *Can. J. Chem.*, 79,1926 **(2001)**

[39]. C. Walling: Free Radicals in Solution. Academic Press, New York, p 38**(1957)**

[40]. K.S. Rangappa, N. Anitha and N.M. Madegouda: *Synth.. React..Inorg. Met. Org. Chem.*, 31,1499**(2001)**

[41]. Z.D. Bugarcic, S.T. Nandibewoor, M.S.A. Hamza, F. Heimemann and R . V.Eldik: *Dalton Trans.,* 2984**(2006)**

[42]. K.W. Hicks : *J. Inorg. Nucl. Chem.*, 38,1381**(1976)**

[43]. S.A. Farokhi and S.T. Nandibewoor : *Tetrahedron* ,59,7595**(2003)**

Chapter-2

Kinetics and Mechanism of Oxidation of D-penicillamine by Potassium Hexacyanoferrate(III) Ions in Aqueous Solution in the Presence of Sodium Dodecyl Sulphate and Cetyltrimethylammonium Bromide

INTRODUCTION

D penicillamine (D-PENSH) and 3-mercapto-D-valine are degradation product of β-lactam antibiotics. D-PENSH is used in the treatment of Wilson's disease to sequester copper from the brain [1]. It has also been used for the treatment of cystiuria, heavy metal poisoning and rheumatoid arthritis [2]. Several methods have been reported for its analysis including colorimetry [3–11], fluorimetry [12], chromatography [13–21], flow injection analysis [22–24], electrophoresis [25–27], potentiometry [28–29], voltammetry [30–33] and NMR spectrometry [34–35].

Rates of enzymatic, organic and inorganic reactions have been investigated in the presence of micelles formed by a variety of surfactants after undergoing both thermal and photochemical reactions [36]. Most kinetic studies of micellar effects upon electron-transfer reactions have been made

utilizing charged micelles as reaction medium, where both hydrophobic and electrostatic interactions have been found [37]. The rate of bimolecular reaction between organic substrates and inorganic ions are affected by the medium of chemical reaction and properties of the micellar surface. They are also dependent on how strongly organic substrates and reactive ions bind to micellar surfaces [38]. Hexacyanoferrate(III) is a one electron oxidant with a redox potential of + 0.36V [41], which has been used extensively to study the oxidation of many organic substrates [39–43].

In this work the oxidation of D-PENSH by hexacyanoferrate(III) in aqueous solution has been studied in detail in presence of cationic surfactants, cetyltrimethylammonium bromide (CTAB) and anionic surfactant, sodium dodecyl sulphate (SDS). The effect of CTAB and SDS on the rate of reaction has been observed even below the critical miceller concentration (CMC) of the surfactants indicating binding of the substrate with the surfactants. On the basis of the kinetic results, the mechanism of the reaction has been proposed. The kinetic data have been rationalized in terms of Manger and Portnoy's [44] model for micellar inhibition, binding parameters (viz. binding constants, partition coefficient, free energy transfer from water to micelle, etc.) and activation parameters.

EXPERIMENTAL

Materials

Stock solution of potassium hexacyanoferrate(III) (BDH), D-PENSH and the surfactants, SDS, and CTAB (Merck Ltd, Mumbai, India) were prepared just before the experiment to avoid ageing. Hexacyanoferrate(II) solution was prepared by dissolving a known amount of $K_4[Fe(CN)_6]$ in water. NaOH and $NaClO_4$ (Merck Ltd, Mumbai, India) were used to maintain alkalinity and ionic strength respectively.

Procedure

Appropriate quantities of solutions of hexacyanoferrate(III), NaOH and surfactant were transferred in a 50 cm^3 glass vessel. The reaction was initiated by adding a suitable amount of D-penicillamine and placed separately on a water bath maintained at adesired temperature. The rate of reaction was measured by monitoring the absorbance by hexacynoferrate(III) as a function of time at 420 nm. Molar absorption coefficient of hexacynoferrate(III) was found to be1060±50 $dm^3mol^{-1}cm^{-1}$.

Critical Micelle Concentration

CMC of the surfactant (CTAB and SDS) solution was determined from the curve of specific conductivity versus surfactant concentration and, the break point of nearly two straight lines was taken as an indication of micelle formation [45–46] (Table 4).

Stoichiometry of the Reaction

The reaction mixtures containing an excess of $[Fe(CN)_6^{3-}]$ over [D-PENSH] were kept separately in presence and absence of alkali and in presence of each surfactant at 25°C for 24 h. The amount of unreacted $[Fe(CN)_6^{3-}]$ in reaction mixture was determined spectrophotometrically. The reaction may be represented by the following scheme 1.

$$2\text{D-PENSH} + 2\ Fe(CN)_6^{3-} + 2\ OH^-$$

$$\downarrow$$

$$\text{D-PENS—SNEP-D} + 2\ Fe(CN)_6^{4-} + H_2O$$

Scheme 1

Evaluation of rate constant

The reaction was studied at different concentrations of the reactants. The log (absorbance) versus time plots (Fig. 1) were linear upto 80% of the reaction which suggests a first-order dependence of the rate in hexacyanoferrate(III). Thus, the pseudo first-order rate constant k_ψ in hexacyanoferrate(III) was evaluated from the slopes of these plots. The results were reproducible within ±5% in repeat kinetic runs.

RESULTS AND DISCUSSION

In the absence of the surfactants the reactions showed a first order dependence of the rate with respect to each alkali, oxidant and substrate concentration. The observed rate constant k_ψ in the presence of surfactant at different initials concentration of [hexacyanoferrate(III)] were almost identical (Table 1). The plot of k_ψ versus [substrate] was found to be linear (Fig. 2) in the absence of the surfactant, while in the presence of surfactant the rate constant deviates from linearity at higher concentrations of the substrate, suggesting that in the presence of surfactant the order of reaction in substrate decreases at higher [substrate]. The plot of $1/k_\psi$ versus 1/[substrate] in the presence of the surfactant (Fig. 3) was also found to be linear with a positive intercept, which further confirmed the suggested Michaelis–Menten type kinetic behavior.

The effect of alkali on the rate of oxidation at fixed ionic strength were identical both in the absence and presence of surfactants. The plot of k_ψ versus

[OH^-] (Fig. 4) was linear with positive slope, suggesting a first-order dependence of rate with respect to [OH^-].

It is noteworthy that even the addition of hexacyanoferrate(II) (0.002 mol dm^{-3}) and sodium perchlorate (0.04 mol dm^{-3}) had negligible effect on rate of oxidation of D-PENSH in the presence of surfactants.

The effect of each surfactant on the rate of reaction has been studied over a wide concentration range of surfactant at four temperatures. The rate constant of surfactant shows that k_ψ decreases on increasing surfactant concentration (Figs. 5 and 6) and attains constancy at higher concentration. The retarding effect of CTAB and SDS has been observed below CMC of surfactant (9.4×10^{-4} mol dm^{-3} in case of CTAB and 7.8×10^{-3} mol dm^{-3} in case of SDS).

The activation parameters (*E*a, $\Delta H^{\#}$ and $\Delta S^{\#}$) have been evaluated in the presence and absence of the surfactant using Arrhenius and Eyring equations (Table 2). The large values of *E*a and $\Delta H^{\#}$ in the presence of surfactants are consistent with the accepted view that the slow reaction (in the presence of surfactant) would require a higher *E*a or $\Delta H^{\#}$. The entropy of activation is less negative in presence and absence of the surfactant. A negative value of $\Delta S^{\#}$ indicates that the activated complex in the transition state has a more ordered structure than the reactants in the ground state [47]. A positive change in entropy of activation in the presence of the surfactant, (less negative $\Delta S^{\#}$)

suggests that the reactants become relatively more rigid, which is not surprising, in view of the binding of the reactants to the surfactant. Change in the free energy ($\Delta G^{\circ} \approx 55.5 \pm 1.0$ kJ/mol) suggests the same mechanism of reaction both in the absence and presence of surfactants.

On the basis of kinetic results, the mechanism of reaction in the absence of surfactant may be proposed (Scheme 2).

$$\text{D-PENSH} + OH^- \xrightarrow{K_1} \text{D-PENS}^- + H_2O$$

$$\text{D-PENS}^- + Fe(CN)_6^{3-} \underset{}{\overset{K_2}{\rightleftharpoons}} \text{D-PENS}^{\bullet} + Fe(CN)_6^{4-} \qquad \text{Slow}$$

$$\text{D-PENS}^{\bullet} + \text{D-PENS}^{\bullet} \xrightarrow{K_3} \text{D-PENS—SNEP-D} \qquad \text{Fast}$$

$$\text{D-PENS}^- + \text{Surfactant} \underset{}{\overset{K_s}{\rightleftharpoons}} \text{Product} \quad (X)$$

Scheme 2

The formation of D-PENS$^-$ in alkaline medium and the existence of its free radical in the presence of one or two electron abstracting oxidant is reported [47].

According to Scheme 2, the rate of disappearance of [$Fe(CN)_6^{3-}$] may be shown as,

$$-\frac{d[Fe(CN)_6^{3-}]}{dt} = K_2[\text{D-PENS}^-][Fe(CN)_6^{3-}] \quad (1)$$

And

$$[\text{D-PENS}^-] = K_1[\text{D-PENSH}][OH^-] \quad (2)$$

K_1 also includes water molecule. On substituting the value of [D-PENS$^-$] in Eq. (1), the rate law becomes,

$$-\frac{d[Fe(CN)_6^{3-}]}{dt} = K_1[\text{D-PENSH}][OH^-][Fe(CN)_6^{3-}] \quad (3)$$

The rate law (3) is in agreement with the first-order dependence of rate with respect to hexacyanoferrate(III), [OH$^-$] and substrate concentration in the absence of the surfactants. A positive salt effect in the absence of surfactant is also in favour of the rate determining step involving interaction between similarly charged species. In the presence of the surfactants, an inhibition effect on the rate of reaction and kinetic results suggests the binding of substrate with the surfactants (Scheme 2) .

The total concentration of D-PENSH is given as

$$[\text{D-PENSH}]_T = [\text{D-PENSH}] + [\text{D-PENS}^-] + [X^-] \quad (4)$$

where $[\text{D-PENS}^-] = K_1[\text{D-PENSH}][OH^-]$, and

$$[X] = Ks[\text{D-PENS}^-][\text{Surfactant}] = K_1 Ks[\text{D-PENSH}][OH^-][\text{Surfactant}]$$

On substituting the value of [D-PENS$^-$] and [X] in Eq. (4), the value of [D-PENSH] in terms of $[\text{D-PENSH}]_T$ may be obtained as,

$$[\text{D-PENSH}] = \frac{[\text{D-PENSH}]_T}{1 + K_1[OH^-]\{1 + Ks[\text{Surfactant}]\}} \quad (5)$$

Therefore, the rate law (3) in terms of $[\text{D-PENSH}]_T$ may be written as,

$$-\frac{d[Fe(CN)_6^{3-}]}{dt} = \frac{K_1\,[\text{D-PENSH}]_T\,[OH^-]\,[Fe(CN)_6^{3-}]}{1 + K_1[OH^-]\{1 + Ks[\text{Surfactant}]\}} \quad (6)$$

The rate law (6) is in agreement with the observed experimental results in the presence of surfactants, i.e. first-order dependence of the rate with respect to hexacyanoferrate(III) and D-PENSH concentration; fractional order dependence of the rate with respect to [OH$^-$] and retarding effect of surfactants on the rate of reaction. To evaluate the binding constants between the substrate

and surfactants (Scheme 3), the kinetic data have been analysed in terms of Mangar and Portnoy's [48] model reported for micellar catalysis/inhibition. According to this model the substrate 'S' is distributed between the aqueous and micellar pseudo phase (Scheme 3.)

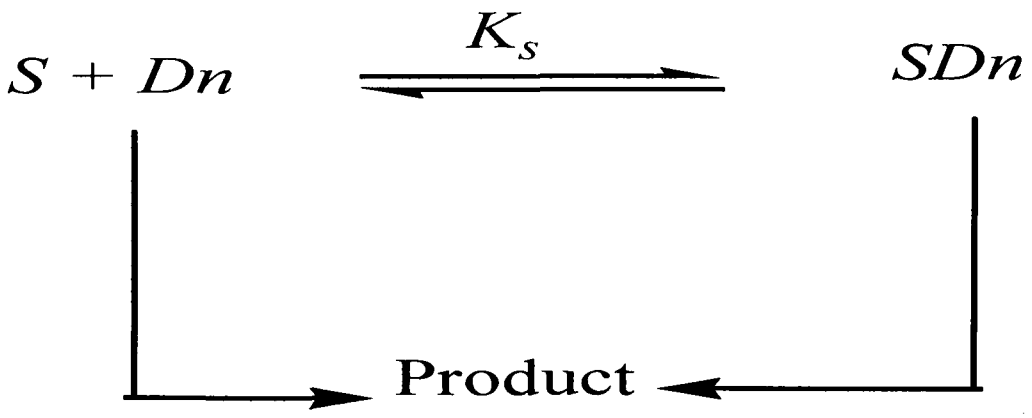

Scheme 3

The observed rate constant k_ψ may be given as

$$K\psi = \frac{k_0 + kmKs\{[D] - CMC\}}{1 + Ks\{[D] - CMC\}} \qquad (7)$$

where k_ω, k_m, k_ψ are rate constants in aqueous phase, micellar media and observed rate constant, respectively. K_s is the binding constant of substrate with surfactant. *D*n, *S*, and *SD*n represent micellar surfactant, free substrate, and associated substrate, respectively.

The above equation may be rearranged in the form

$$\frac{1}{k_\omega - k_\psi} \quad \frac{1}{k_\omega - k_m} + \frac{1}{(k_\omega - k_m)K_s\{[D] - CMC\}} \qquad (8)$$

This equation (8) has been found to be most appropriate for continuous binding in different reactions. The applicability of Mangar and Portnoy's [44] model can be tested by the plot of $1/(k_\omega - k_\psi)$ versus $1/\{[D]-CMC\}$. The k_m and K_s may also be evaluated with the help of intercept and slope of the plot. In the present investigation the binding of CTAB and SDS has been observed at the concentrations which are below their CMC. The validity of the equation in this case has been tested by plotting $1/(k_\omega - k_\psi)$ against $1/\{[D]-CMC\}$ (Figs. 7 and 8) and showed the applicability of the Mangar and Portnoy's model in the system. The k_m and K_s have also been evaluated. The K_s of the substrate with surfactant can also be correlated to the partition coefficient, P i.e. [substrate]micelle / [substrate]water ratio [49–52], by the following relation.

$$K_S = P\bar{V}$$

where $\bar{V}$ is the partial molar volume [53] of surfactant monomer. The standard transfer free energy [54–55] per mole $\Delta\mu^\circ$ of a solute from water to micelle is also related to binding constant, K_s by the following equation.

$$\Delta\mu^\circ = -RTln(55.5)Ks$$

The effect of organized structure on the rate of chemical reaction has been attributed to the hydrophobic and electrostatic interactions (Table 3). The electrostatic surface potential at the miceller surface can attract or repel the reaction species and hydrophobic interactions can bring about incorporation into micelle even if the reagent bears the same charge. Thus, the rate and the mechanism of chemical reactions may be affected by electrostatic or hydrophobic interactions. The results of the present investigation can be explained on the basis of both the electrostatic and hydrophobic forces.

The observed kinetic data, retardation of the rate with an increase in surfactant concentration and negative values of k_m in the case of CTAB and SDS indicate that the reaction between negatively charged D-PENSH and hexacyanoferrate (III) proceeds in the aqueous phase, not in the miceller phase. When surfactant is present in the reaction mixture, it binds the substrate by hydrophobic interactions causing a decrease in the concentration of the

substrate in aqueous phase and, thus a retarding effect of the surfactant on the rate of reaction was observed. High value of K_s and P in case of CTAB clearly indicates that the D-PENSH is more solubilized or bind with CTAB. In case of CTAB, the electrostatic attraction between D-PENS$^-$ and positively charged surfactant in alkaline medium may favor the binding of surfactant with substrate in addition to hydrophobic interactions. Thus, CTAB binds the substrates leaving a small fraction in aqueous phase. In case of SDS, the electrostatic repulsion between negatively charged substrate and anionic surfactant opposes the binding between the surfactant and the substrate. Thus, the hydrophobic interaction favored the binding while electrostatic repulsions opposed it. Consequently, the binding between the surfactant and the substrate may be less (and hence a less retarding effect of the surfactant on the rate) in case of SDS. This is supported by the low values of K_s and P of SDS in comparison with CTAB. The K_s and P decrease with increasing temperature in both CTAB and SDS. It suggest that the binding is an exothermic process. The transfer of free energy change per mole from water to micelle ($\Delta\mu^\circ$) are also in accordance with the above results.

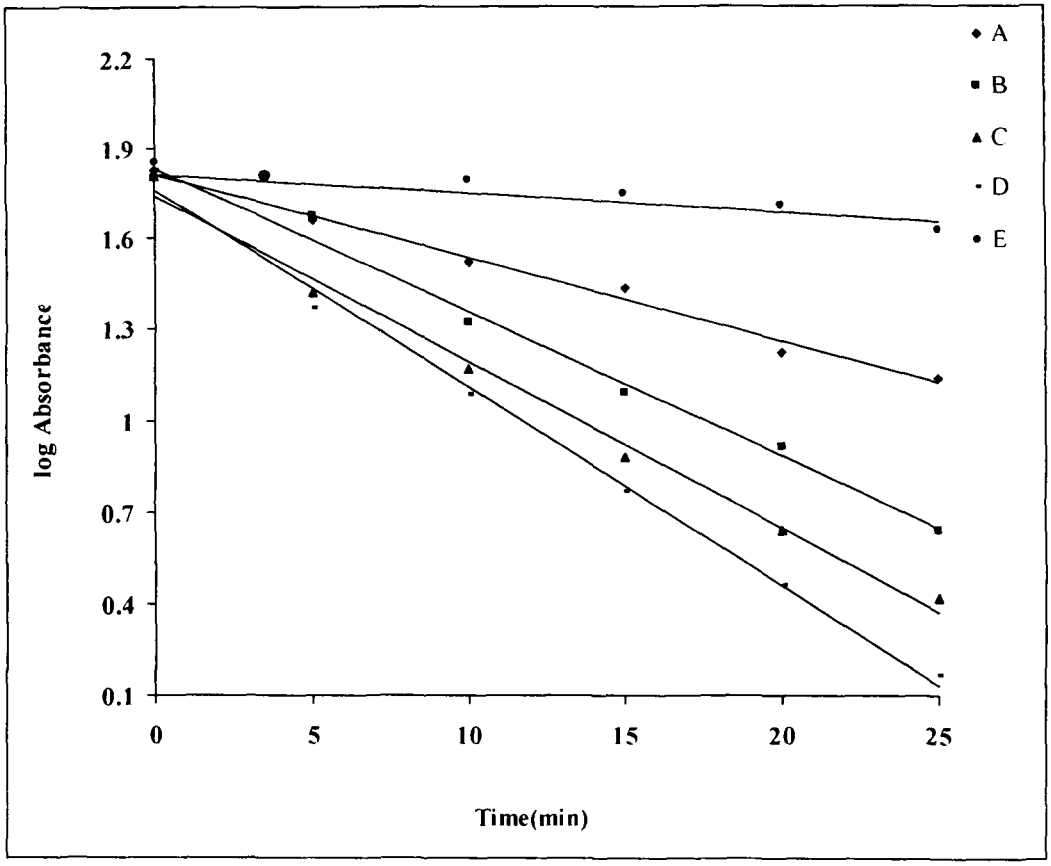

Fig.1 Plots of absorbance versus times (min) at 25°C,$[Fe(CN)_6^{3-}]$ = 10.0 $\times 10^{-4}$ mol dm^{-3}, [substrate] = 12.0 $\times$ 10^{-3} mol dm^{-3}, [CTAB] = 5.5 $\times$ 10^{-4} mol dm^{-3}, $[OH^-]$= A= 2×10^{-3} B = 2×10^{-3} C = 2×10^{-3} D = 2×10^{-3} and E = 2×10^{-3} mol dm^{-3} respectively, I = 0.8 $\times$ 10^{-2} mol dm^{-3}

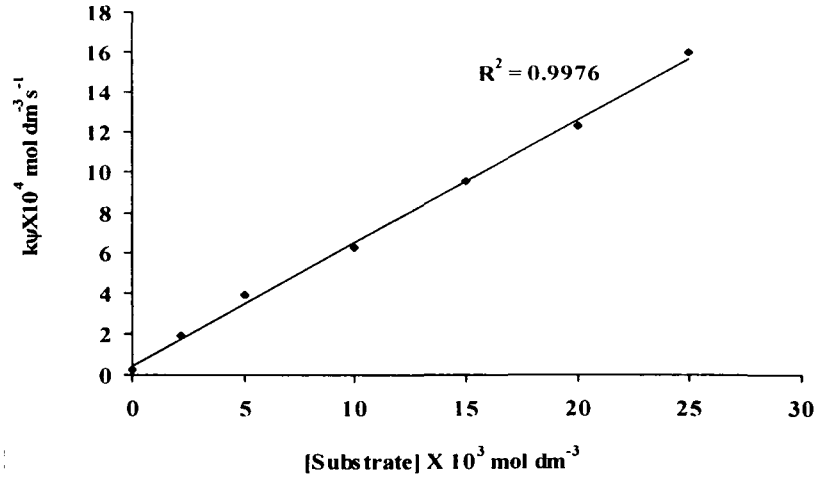

Fig.2 Plot of k_ψ versus [D-PENSH] at 25° C. $[Fe(CN)_6^{3-}]$ = 10.0 ×10^{-4} mol dm^{-3}, $[OH^-]$ = 2×10^{-3} mol dm^{-3} respectively, I = 0.8 × 10^{-2} mol dm^{-3}

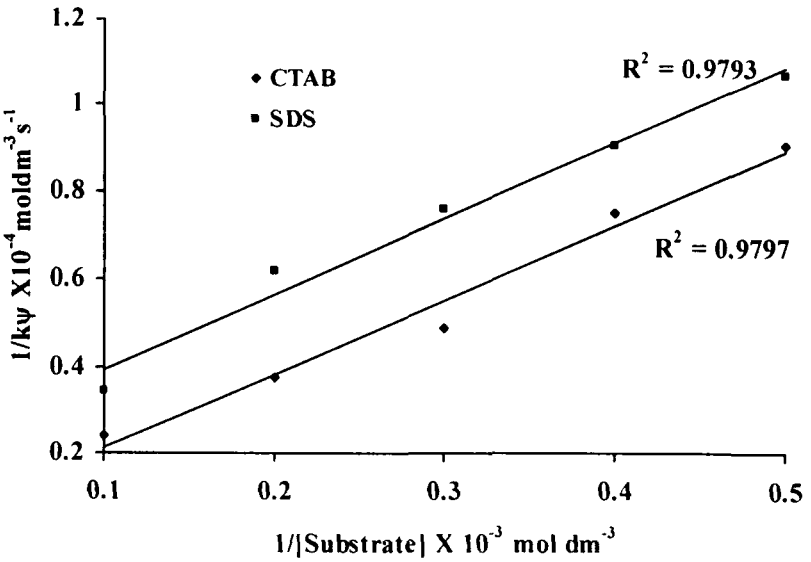

Fig.3 Plots of 1/kψ versus 1/[substrate] at 25°C. $[Fe(CN)_6^{3-}]$ = 10.0 × 10^{-4} mol dm^{-3}, [OH−] = 2.0 × 10^{-3} mol dm^{-3}, [CTAB] = 5.5 × 10^{-4} mol dm−3, [SDS] = 13.86 × 10^{-3} mol dm^{-3}, respectively. I = 0.8 × 10^{-2} mol dm^{-3}

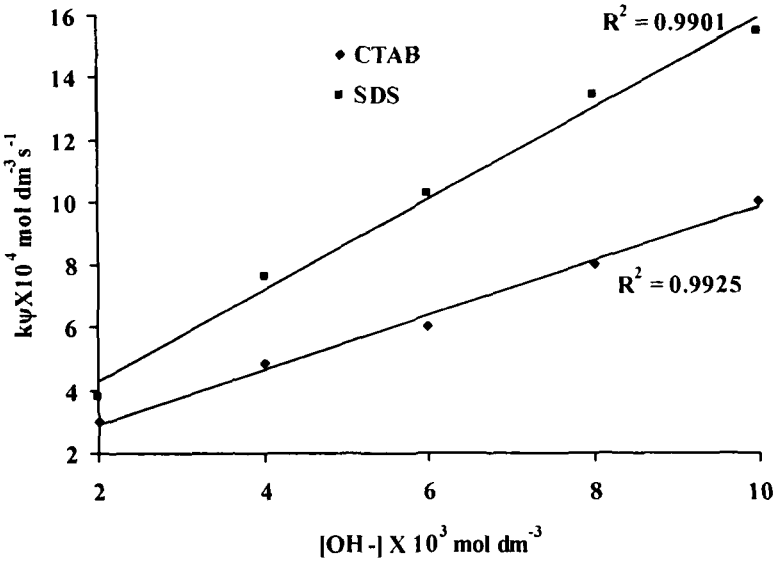

Fig.4 Plots of k_ψ versus [OH⁻] at 25°C. [Substrate] = 10.0 × 10−3 mol dm−3. [Fe(CN)3−6] = 10.0×10−3 mol dm−3, [CTAB] = 5.0 × 10^{-4} moldm−3. and [SDS] = 13.86 × 10^{-3} mol dm^{-3}, respectively.

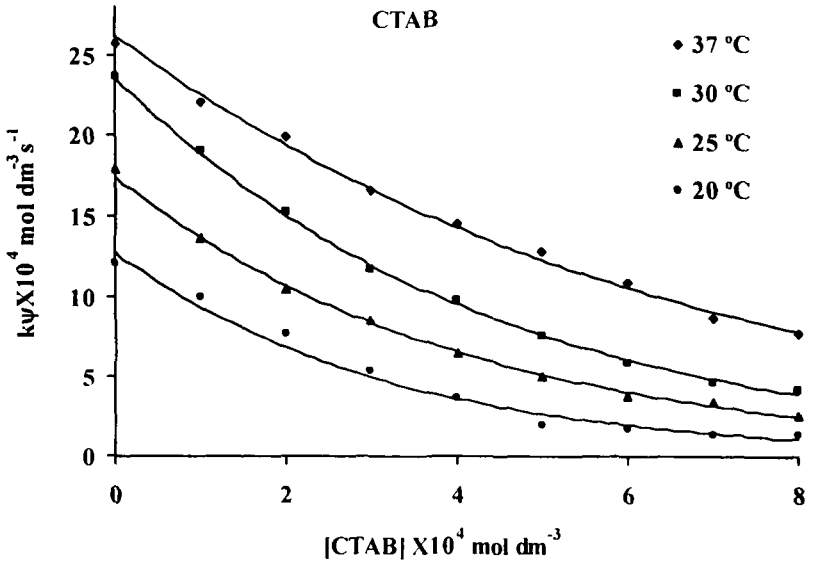

Fig.5 Plots of k_ψ versus [surfactant] at various temperatures. $[Fe(CN)_6^{3-}]$ =10.0×10^{-3} mol dm^{-3}, [D-PENSH] = 12.0×10^{-3} mol dm^{-3}, [OH−] = 2.0× 10^{-3} mol dm^{-3}.

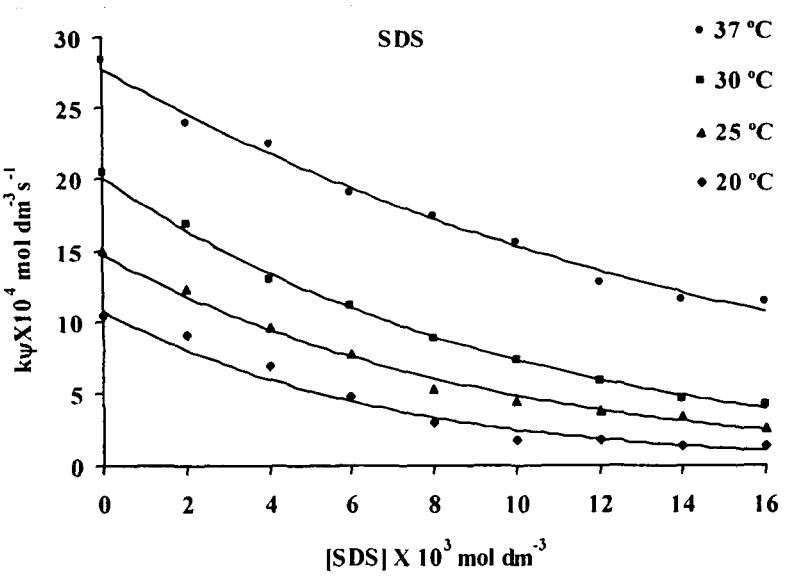

Fig.6 Plots of k_ψ versus [surfactant] at various temperatures. $[Fe(CN)_6^{3-}]$ $=10.0\times10^{-3}$ mol dm^{-3}, [D-PENSH] = 12.0×10^{-3} mol dm^{-3}, [OH−] = 2.0×10^{-3} mol dm^{-3}.

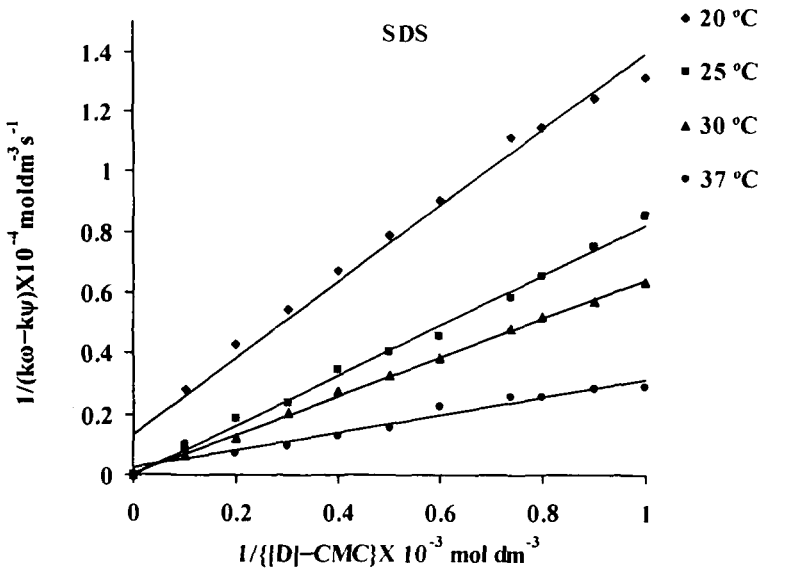

Fig.7 Plots of $1/(k_\omega - k_\psi)$ versus 1/{[D]-CMC} at different temperatures; $[[Fe(CN)_6^{3-}]$ =10.0×10^{-3} mol dm^{-3}, [D-PENSH] = 12.0×10^{-3} mol dm^{-3}, [OH−] = 2.0×10^{-3} mol dm^{-3}.

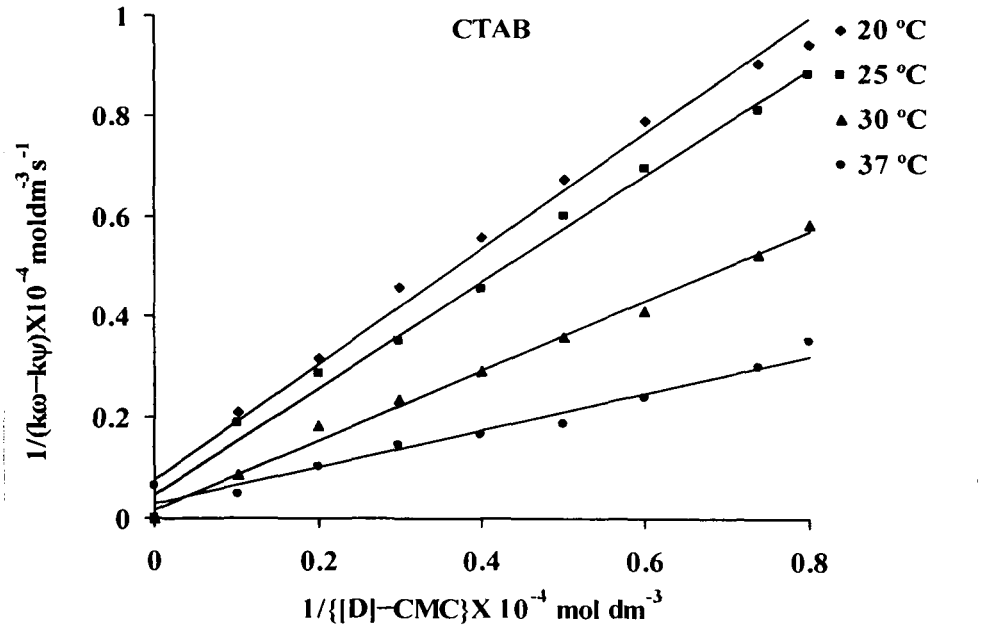

Fig.8 Plots of $1/(k_\omega - k_\psi)$ versus $1/\{[D]-CMC\}$ at different temperatures; $[Fe(CN)_6^{3-}] = 10.0\times10^{-3}$ mol dm^{-3}, [D-PENSH] = 12.0×10^{-3} mol dm^{-3}, $[OH^-] = 2.0\times10^{-3}$ mol dm^{-3}.

Table 1. Effect of [hexacyanoferrate(III)] on the rate constant at 25°C, [D-PENSH] = 12.0×10^{-3} mol dm^{-3}, [CTAB] = $.55\times10^{-4}$ mol dm^{-3}, [SDS] = 12.25×10^{-2} mol dm^{-3} and [OH$^-$] = 2.0×10^{-3} mol dm^{-3}

$[Fe(CN)_6^{3-}]\ 10^4$ (mol dm^{-3})	$k_\psi \times10^4$ (mol dm^{-3}s^{-1})	
	[CTAB]	[SDS]
6.0	8.7	3.2
8.0	8.1	3.1
10.0	8.6	3.0
12.0	8.6	3.0
14.0	8.6	3.0

Table 2. Activation parameters for the oxidation of D-PENSH in absence and presence of surfactants

Surfactant	*Ea (kJ mol^{-1})*	*$\Delta H^{\#}$ (kJ mol^{-1})*	*$-\Delta S^{\#}$ (JK^{-1} mol^{-1})*	*$\Delta G^{\#}$ (kJ mol^{-1})*
Absent	71.4	69.5	123.6	54.9
CTAB	73.6	70.4	116.3	56.3
SDS	91.5	88.2	69.4	55.6

Table 3. Binding Constants (Ks) and Rate Constants in Micellar Media (km) Partition Coefficients (P), Partial molar volume and Free-Energy Transfer from Water to Micelle ($-\Delta\mu^o$) at Different Temperatures

Temperature	CTAB					SDS				
	$km\ 10^4$ (mol $dm^{-3}\ s^{-1}$)	$Ks\ 10^2$	P	V	$-\Delta\mu^o$(kJ mol^{-1})	$km\ 10^4$ (mol $dm^{-3}\ s^{-1}$)	$Ks\ 10^2$	P	V	$-\Delta\mu^o$(kJ mol^{-1})
20°C	9.2	302	1142	26.44	101.4	11.2	2.31	8.8	26.25	66.6
25°C	4.4	255	857	29.75	98.7	7.6	2.14	4.4	48.63	64.8
30°C	2.1	223	571	39.06	96.0	4.3	1.57	1.8	88.70	62.2
35°C	1.3	126	285	44.21	90.4	2.6	1.13	1.4	84.96	58.9

Table 4. Critical micelle concentration value of CTAB and SDS surfactant in the presence of [Fe(CN)3−6] =10.0×10^{-3} mol dm^{-3}, [D-PENSH] = 12.0×10^{-3} mol dm^{-3}

Surfactant	*CMC* mol dm^{-3}
CTAB	9.4×10^{-4}
SDS	7.8×10^{-3}

REFERENCES

[1]. Martindale, The Extra Pharmacopoeia, 28th ed. (James E.F. Reynolds), Pharmaceutical Press, London, **(1982)**

[2]. I.L. Bonta, M.J. Parnhman, L.E. Vincent and P.C. Bragt: Antirheumatic drugs: present deadlock and new vistas, Prog. Med. Chem.,17,203 **(1980)**

[3]. P.B. Issopoulos and S.E. Salta: Farm. 52 (II) . 113 **(1997)**

[4]. H.F. Askal, G.A. Saleh, O.H. Abdelmageed and I.H. Rafaat: Saudi Pharm. J. 2, 84 **(1994).**

[5]. P.B. Issopoulos and P.T. Economou: Anal. Chim. Acta. 257,203 **(1992)**

[6]. A.Besada: Anal. Lett. 21, 435**(1988)**

[7]. A.Besada and N.B. Tadros: Mikrochim. Acta. 2, 225 **(1987)**

[8]. A. Besada, N.B. Tadros and Y.A. Gawargious: Anal. Lett. 20, 809 **(1987)**

[9]. N. Buyuktimkin and yuktimkin: Pharmazie 40,581**(1985)**

[10]. M.A. Raggi, V. Vacrini and A.M. Di-Pietra, Pharm: Acta.Helv. 58,94**(1983)**

[11]. M.A. Raggi, V. Vacrini and A.M. Di-Pietra: J. Pharm. Sci. 71,1384 **(1982)**

[12]. S.Y. Byeon, J.K. Choi, G.S. Yoo and Yakche :Hakhoechi. 20, 73 **(1990)**

[13]. J. Russell, J.A. Mckeown, C. Hensman, W.E. Smith and J.Reglinski: J. Pharm. Biomed. Anal. 15,1757**(1997)**

[14]. Z. Nhang, W.R.G. Baeyens, X. Zhang, Y. Zhao and G.Van-Der-Weken: Ana. Chim. Acta. 347, 325 **(1997)**

[15]. K. Nakashima, T. Ishimaru, N. Kuroda and S. Akiyama: Biomed. Chromatogr. 9, 90**(1995)**

[16]. G. Bringmann, D. Feineis and C. Hesselmann: Anal. Lett. 25,497 **(1992)**

[17]. K. Nakashima, M. Muraoka, S. Nakatsuji, S. Akiyama and Rinsho:Kagaku. 17 ,51**(1988)**

[18]. E. Busker, K. Guenther and J. Martens: J. Chromatogr. 350,179 **(1985)**

[19]. S. Biffar, V. Greely and D. Tibbetts: J. Chromatogr. 318,404 **(1985)**

[20]. I.C. Shaw, A.E.M. McLean and C.H. Boult: J. Chromatogr.Biomed. Appl. 26,206**(1983)**

[21]. J.O. Miners, I. Fearnley, K.J. Smith, D.J. Birkett, P.M.Brooks and M.W. Whitehouse:J. Chromatogr. Biomed.Appl. 26, 89**(1983)**

[22]. T. Perez-Ruiz, C. Martinez-Lozano, V. Tomas and C.Sidrach-de-Cardona: J. Pharm. Biomed. Anal. 15, 33 **(1996)**

[23]. M.S. Garcia, C. Sanchez-Pedreno, M.I. Albero and V. Rodenas: J. Pharm. Biomed. Anal. 11, 633 **(1993)**

[24]. P. Vinas, J.A. Sanchez–Prieto and M. Hernandez–Cordoba: Microchem. J. 41, 2 **(1990)**

[25]. B.B. Tewari: J. Chromatogr. 793, 220 **(1998)**

[26]. B.B. Tewari: Biomed. Chromatogr. 10, 221 **(1996)**

[27]. A.Chen and G.M. Pollack: J. Chromatogr. Biomed. Appl.681,363 **(1996)**

[28]. T. Jovanovic, Z. Koricanacz and B. Stankovic: Pharmazie 46, 293 **(1991)**

[29]. J. Motonaka, S. Ikeda, N. Tanaka and Bunseki: Kagaku.31,669 **(1982)**

[30]. A.Ion, F.G. Banica, A.G. Fogg and H. Kozlowski: Electroanalysis. 8, 40 **(1996)**

[31]. U. Forsman: J. Electroanal. Chem. Interfacial. Electrochem.152, 241 **(1983)**

[32]. U. Forsman and A. Karlsson: Anal. Chim. Acta. 128, 135 **(1981)**

[33]. A.G. Fogg and N.M. Fayad: Anal. Chim. Acta. 113, 91 **(1980)**

[34]. S.E. Ibrahim and A.A. Al–Badr: Spectrosc. Lett. 13, 471**(1980)**

[35]. J. Nelson: J. Assoc. Off. Anal. Chem. 64, 1174 **(1981)**

[36]. A .Rodrigues, M.M.Graciani and M.L. Moya: Langmuir 12,4090 **(1996)**

[37]. A.I. Carbone, F.P.Cavasino and C. J. Sbriziolo: Chem. Soc. Faraday Trans. 1. 84, 207 **(1988)**

[38]. M.A.B. Marin, F. Nome, D. Zanette and C.Zucco: J. Phys. Chem. 99, 10879 **(1995)**

[39]. R.C. Acharya, N.K. Saran, S.R. Rao and M.N.Das: Int. J. Chemi. Kinet. 14, 143 **(1982)**

[40].K.B.Wibweg, H.Mattz and M. Okane: Inorg. Chem. 7, 831 **(1986)**

[41]. S.M. Zourab, E.M. Ezzo, H.J. Aila and J.K.J. Salem: J. Dispers. Sci. Technol. 24, 67**(2003)**

[42]. R. Mehrota and R.C. Kapoor: J. Chem. Soc., Dalton Trans 2. 998, 1003 **(1984)**

[43]. N. Kambo and S.K. Upadhyay: J. Dispers. Sci. Technol. 27,6 **(2006)**

[44].F.M. Manger and C.E. Portnoy:Am. Chem. Soc. 89, 4698 **(1967)**

[45].P. Mukherjee, K. J. Mysele, Critical Micelle Concentration of aqueous Solution, NSRDS-NBS 36,Suprintedent of Documents,Washington,DC **(1971)**

[46]. I.A. Khan, M. Bano,and Kabir-ud-Din: J. Dispers. Sci. Technol.31, 177 **(2010)**

[47]. A A P Khan ,A Mohd ,S Bano and K S Siddiqi . J.Korean Chem. Soc.53, 709**(2009)**

[48]. T.J.Wallace, A. Schriesheim, H. Hurwitz and M.B. Glaser: J. Ind. Eng. Chem.Process Des. Dev. 3 , 237 **(1964)**

[49].G.P. Panigrahi and S.K. Mishra: Indian J. Chem. 32(A) ,956 **(1993)**

[50]. I.V. Berezin, K. Martinek and Y.K.Yatsimirskii: Rus. Chem. Rev. (Eng. Trans.) 42, 787**(1973)**

[51].H.L. Hodge and M.A. de Arayo:Inorg. Chem. 83, 3236 **(1982)**

[52]. A.A. Bhalekar and J.B.F. Engberts: J. Am. Chem. Soc. 100, 5914 **(1978)**

[53]. M.R.K. Sherwani, R. Sharma, A. Gangwal and R. Bhutra: Indian J. Chem. 42(A), 2527**(2003)**

[54].C.A. Bunton and L. Sepulveda: J. Phys. Chem. 83, 680 **(1979)**

[55].C. Hirose and L. Sepulveda: J. Phys. Chem. 85,3689 **(1981)**

Chapter-3

The determination of Ampicillin in Pharmaceutical Preparations by potassium permanganate and 1-chloro-2,4-dinitrobenzene

INTRODUCTION

Ampicillin, AMP (6R)-6-(a-phenyl-D-glycylamino) penicillanic acid (Fig 1) is a semisynthetic penicillin [1] . It is prepared from the benzylpenicillin or penicillin-G [2], which is prepared by a biosynthetic process using various strains of Penicillium notatum and Penicillium chrysogenum [3] Penicillin-G was the first antibiotic to be used in the chemotherapy. It is a bacterio static drug of choice for the treatment of infections caused by most of the Gram-positive and Gram-negative bacteria [4-5]. AMP is acidic in nature, and it acts by inhibiting the protein synthesis [6] of the bacterial cell wall. The basic ampicillin is 6-aminopenicillanic acid, which consists of a thiazolidine ring linked to β-lactam ring. The side chain determines the antibacterial and pharmacological characteristics of this compound [7]. Several procedures reported for the determination of ampicillin in pure form, pharmaceutical formulations and biological fluids include spectrophotometric [8-11], polarographic [12-13], flow injection analysis [14] and HPLC [15-16]. The

complexes of ampicillin with different metal ions have also been studied [17–19].

Kinetic-based methods of pharmaceutical analysis are not widely applied although they do not suffer any interference from additives which probably affects other methods.

In the present work, we are reporting a spectrophotometric method for the determination of AMP by measuring the absorbance at 610 nm after its oxidation by alkaline $KMnO_4$ or, at 490 nm after addition of CDNB in the presence of borate buffer. All variables affecting the development of the color were investigated and the conditions were optimized. The determination of AMP by the fixed concentration method is effective with the calibration equations obtained, but the fixed time method proves to be more sensitive.

EXPERIMENTAL

Apparatus

A Shimadzu UV-visible 1601 spectrophotometer, Elico-LI 120 pH meter and a water bath shaker NSW 133, India were used.

Materials

Ampiciline (Sigma, India) $KMnO_4$, NaOH, HCl and CDNB, (Merck Ltd, Mumbai, India) were used. Pharmaceutical preparations were purchased from commercial sources in the local market. Double distilled, de-ionized water was used throughout. Stock solutions of the compounds were wrapped with carbon paper to protect them from light.

Preparation of standard Solution

The stock solution of AMP (1×10^{-2}M) was prepared in 1×10^{-2}M M HCl and stored at 4°*C*.

Procedure A

AMP equivalent to 5–30 μg mL^{-1} (solution A) was transferred into a series of 50 mL volumetric flasks. To each flask 1 mL of 0.5 mol L^{-1} NaOH and 2 mL of 5×10^{-3} mol L^{-1} $KMnO_4$ was added and made up with water, and left to stand for 25 min. The absorbance of the resulting solution was measured at 610 nm at 5-min intervals at ambient temperature (25°C) against a blank solution prepared simultaneously. To obtain the standard calibration curve, a plot of absorbance against the concentration of drug was made.

Procedure B

Aliquots equivalent to 50–260 μg mL^{-1} AMP (solution B) were transfer into a series of 10-mL volumetric flask. To each flask 2 mL of 3.5×10^{-3} mol L^{-1} CDNB and 0.2 mol L^{-1} borate buffer was mixed and made up to the mark with distilled water, and left to stand for 60 min. The absorbance of the reaction mixture was measured at 490 nm at 10-min intervals at ambient temperature (25 °C) against a blank solution. To obtain the standard calibration curve, a plot of absorbance against the concentration of AMP was made.

Procedures for formulations

The drug equivalent to 500 mg of AMP was transferred into a 100 ml volumetric flask containing about 75 ml of distilled water. It was shaken thoroughly for about 15–20 min, filtered through a Whatman filter paper No. 40 and made up to the mark with distilled water. 25 ml of the filtrate was diluted to 100 ml and a suitable aliquot was analyzed .

RESULTS AND DISCUSSION

Optimization of the reactions conditions:

Method A (oxidation with $KMnO_4$)

The reaction between AMP and $KMnO_4$ in alkaline solution yields a green color as a result of the formation of manganate ion, which absorbs at 610

nm (Fig. 2). The maximum intensity of the color is attained after 25 min, and remains stable for at least 1 h. The reaction was investigated under various conditions of reagent concentration and alkalinity.

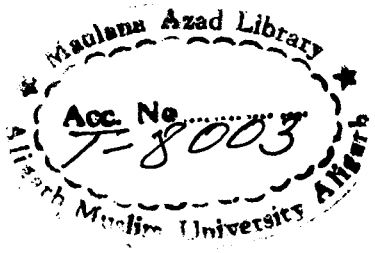

The influence of $KMnO_4$ on the absorbance

An increase in the rate of reaction is directly proportional to the concentration of $KMnO_4$. The absorbance was studied in the range 1×10^{-4} to 1×10^{-3} mol L^{-1} keeping all other parameters constant. It was found that 7.5×10^{-4} mol L^{-1} $KMnO_4$ is the optimum concentration for the absorbance of AMP as shown in (Fig 3). The effect of the colour development was investigated by adding different volumes (0.1–2.0 ml of 7.5×10^{-4} mol L^{-1}) of $KMnO_4$ to the drug. The maximum absorbance of the green colour was attained with 1.8 ml of the reagent, and then remained constant even when higher volumes were added (Fig. 4) and hence 2 ml of the reagent was used throughout the experiment.

The influence of the NaOH

The absorbance of MnO_4^{2-} was also examined as function of volume (0.2-2.0ml) of 0.5 mol L^{-1} NaOH at 25^0C. The optimum absorbance was obtained with 0.9 ml NaOH, after which increase in volume of NaOH did not make any change in absorbance. 1 ml of 0.5mol L^{-1} NaOH was, therefore, used throughout the experiment (Fig.5).

Method B (complexation with CDNB)

The reaction of AMP with CDNB in slightly alkaline borate buffer produces an orange-yellow color with maximum absorbance at 477 nm (Fig. 6). This bathochromic shift from 370 nm CDNB to 490 nm may be attributed to the formation of a charge transfer complex through n–π^* interaction, where the electron donor is the amine moiety and the π-acceptor is the CDNB moiety of the drug [20]. The possibility of the reaction of AMP with CDNB was investigated under various conditions. It was found that the reaction proceeds in alkaline medium at room temperature. The colored adduct remains stable for about 1.5 hours. The extent of formation of this species depends on the concentration of reactants, alkalinity, temperature and pH.

The influence of the CDNB

The effect of CDNB concentration on the absorbance of yellow colored Meisenheimer complex was studied in the range 1×10^{-4} - 4×10^{-3} mol L^{-1}. It was found that 3.5×10^{-3} mol L^{-1} CDNB is the optimum concentration for the absorbance of AMP (Fig.7). Therefore, the optimum concentration of 3.5×10^{-3} mol L^{-1} of CDNB was chosen for further work.

The influence of pH

Maximum absorbance was obtained at pH 7.8 after which the absorbance of the reaction product began to decrease gradually until pH 9.5., The optimum pH was, therefore, kept at 7.8 (Fig. 8). Other buffers having the same pH such as phosphate buffer and hexamine buffer were tried and compared with 0.2 mol L^{-1} of borate buffer. The borate buffer was found to be superior to other buffers of the same pH since it gave the highest absorbance.

Calibration Graphs

After optimizing the reaction conditions, the fixed time was applied to the determination of AMP in pure form over the concentration ranges 5-30 μg/mL and, 50-260 μg/mL for both methods. (Fig. 9,10).

Analysis of the data gave the following regression equations:

A = 0.1606 + 0.01054C (r = 0.9906) Method A

A = 0.3068 + 0.001126C (r = 0.9919) Method B

Kinetic study of the reactions

The rate of the reaction was studied at room temperature and was found to be dependent on the concentration of AMP.

The rates were followed with:

1. In the range 5–30 μg mL^{-1}, keeping KMnO4 and NaOH constant at high concentration as described in the general procedures, applying method A; and

2. In the range 50–260 μg mL^{-1}, keeping other reactants, and CDNB constant at high concentration as described in the general procedures, applying method B.

It is clear from the plots (Figs. 11 and 12) that the rate is proportional to the concentration of AMP and obeys the equation:

$$\textbf{Rate} = \textbf{K'[AMP]}^{\textbf{n}} \qquad \textbf{(1)}$$

where K' is the pseudo first-order rate constant and n is the order of the reaction. The rate may be estimated by the variable-time method measured as $\Delta A/\Delta t$, where A is the absorbance and t is the time in seconds [21]. Taking logarithms of rates and concentration as shown in Table 2, Eq. (1) is transformed into:

$$\textbf{log (rate)} = \textbf{log } \Delta\textbf{A } /\Delta \textbf{ t} = \textbf{log K'} + \textbf{n log [AMP]} \qquad \textbf{(2)}$$

Regression of log (rate) versus log (AMP) gave the regression equations:

$$\textbf{log (rate)} = -\textbf{0.9172} + \textbf{0.9923 log C}$$

$$\textbf{r} = \textbf{0.9936 Method A}$$

$$\textbf{log (rate)} = -\textbf{0.6790} + \textbf{0.8808 log C}$$

$$\textbf{r} = \textbf{0.9914 Method B}$$

Hence K'= 0.121S^{-1} or 0.209S^{-1}, applying methods A or B, respectively,and the reactions can be approximated to first order (n≈1) with respect to AMP concentration

Evaluation of the Kinetic Methods

Under the optimized experimental conditions the concentration of AMP was determined using an excess of $KMnO_4$ and NaOH with respect to AMP, applying method A; and an excess concentration of CDNB with respect to the initial concentration of AMP applying method B. However, the rate is directly proportional to the concentration of drug in a pseudo-first rate equation as follows:

$$\textbf{Rate} = \textbf{K'[drug]} \qquad \textbf{(3)}$$

where K' is the pseudo-order rate constant. Several experiments were then carried out to obtain the drug concentration from the rate data according to Eq. (3). The rate constant, fixed- concentration and fixed time methods [22-23] were tried and the most suitable analytical method was selected taking into account the applicability, the sensitivity, the correlation coefficient (r) and the intercept.

Rate-constant method

Graphs of log (absorbance) versus time over a large concentration range of AMP (1.4×10^{-5} to 8.4×10^{-5} mol L^{-1}, and 1.5×10^{-4} to 7.5×10^{-4} mol L^{-1}) were plotted by method A or B, respectively. The pseudo-first order rate constants

corresponding to different AMP concentrations were then calculated from the slopes multiplied by –2.303 (Table 3).

Regression of (C) versus K' gave the equations:

$$K' = -4.5 \times 10^{-3} + 76.96\ C\ (r = 0.9831)\ \textbf{Method A}$$

$$K' = -4.1 \times 10^{-3} + 0.5119\ C\ (r = 0.8739)\ \textbf{Method B}$$

The value of r is indicative of poor linearity, probably because of inconsistency of K'.

Fixed-concentration method

Rate of reaction was recorded for different concentrations of AMP (5.6×10^{-5} to 8.4×10^{-5} mol L^{-1}, and 4.5×10^{-4} to 7.5×10^{-4}) mol L^{-1}. A pre-selected value of the absorbance was fixed and the time was measured in seconds. The reciprocal of time ($1/t$) versus the initial concentration of AMP was plotted (Table 4). The following equations for calibration graphs were obtained by linear regression:

$$\textbf{1/t} = -4.5 \times 10^{-3} + 76.97\ \textbf{C (r = 0.9831) for Method A}$$

$$\textbf{1/t} = -4.1 \times 10^{-3} + 1.862\ \textbf{C (r = 0.9962) for Method B}$$

Fixed-time method

The absorbance was measured at a preselected fixed time. Calibration graph of absorbance versus initial concentration of AMP was established at fixed time of 5, 10, 15, 20 and 25 min applying method A and, 10, 20, 30, 40, 50 and 60 min applying method B with the regression equation shown in Table1.

It is clear that the slope increases with time and the most acceptable values of the correlation coefficient (r) and the intercept were obtained for a fixed times interval for measurement (Table 5).

Mechanism of the Reaction

The stoichiometry of the reaction was studied adopting the limiting logarithmic method [24]. The ratio of the reaction between log Abs versus log [AMP], log [$KMnO_4$] and log [CDNB] were calculated by dividing the slope of $KMnO_4$ and CDNB by the slope of the drug curve. The ratio of AMP to KMnO4 and that for AMP to CDNB was found to be1:2 and 1:1 respectively The proposed pathway of the reaction is given below.

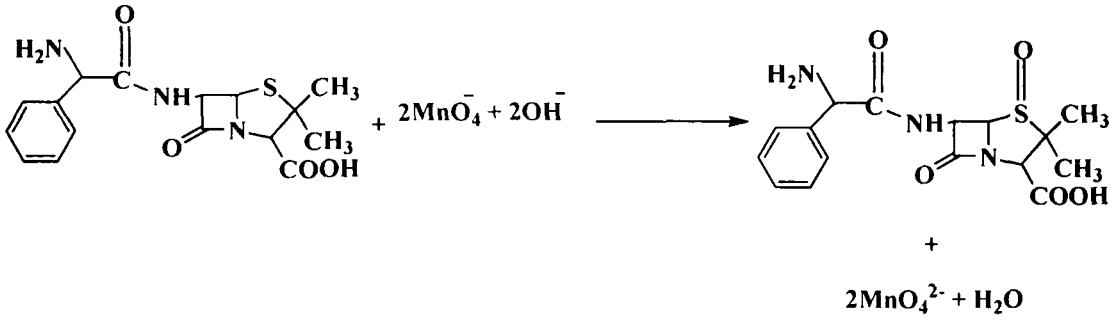

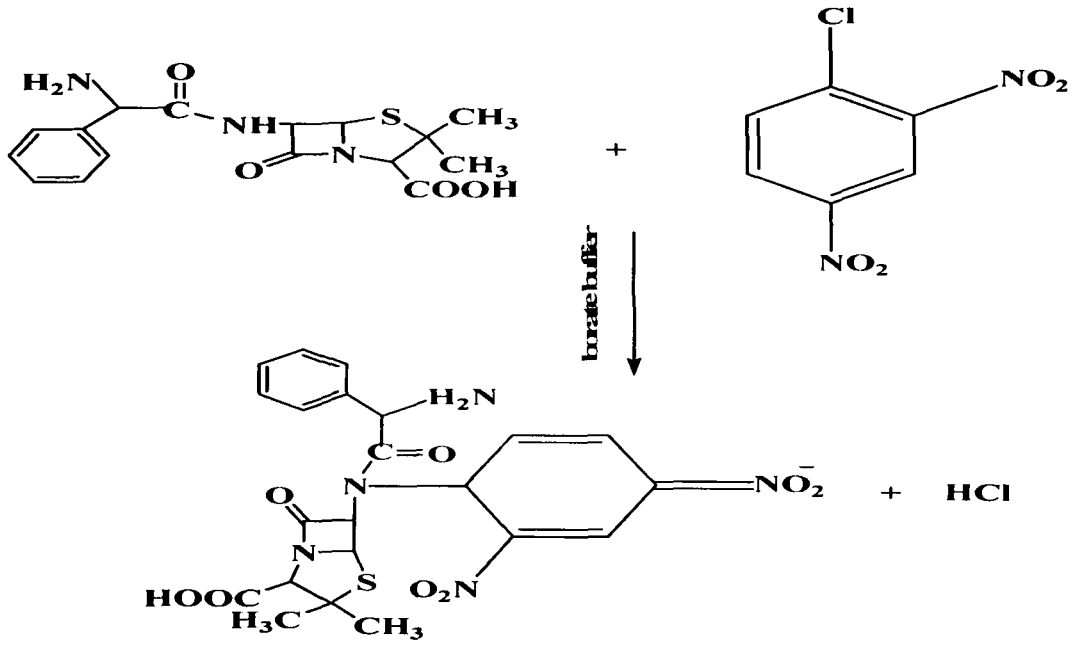

VALIDATION OF THE PROPOSED METHOD

Accuracy and Precision of the Proposed Methods

Accuracy *and* precision was checked according to USP validation guidelines [25] at three concentration levels within the specified range. Six

replicate measurements were recorded at each concentration level. The results are summarized in Table 6

Limit of detection (LOD)

LOD was calculated from standard deviation of response and the slope of calibration curve. The limit of detection was expressed as :

$$\mathbf{LOD = 3\,\sigma / S}$$

where σ is the standard deviation of intercept, S is the slope of calibration curve (Table 5). In our work, reasonably good results were obtained where the calculated drug concentration by LOD equations were actually detected in these experiments.

Limit of quantitation (LOQ)

LOQ was calculated based on standard deviation of intercept and slope of calibration curve. In this method, the limit of quantification is expressed as :

$$\mathbf{LOQ = 10\,\sigma / S}$$

The results were (Table 5) indicate good sensitivity of the proposed method. The calculated LOQ values were further validated by laboratory experiments. In our work, good results were obtained where the calculated drug concentration by LOQ equations were actually quantified in these experiments.

Application to pharmaceutical dosage forms

The rate constant and fixed time methods have been applied for the determination of AMP in commercial pharmaceutical dosage forms. The concentration of investigated AMP was computed from its regression equations. The results of proposed methods were statistically compared with those of reported methods [26-28]. The mean recovery values were 99.7533 and 99.91 respectively , which ensures that there is no interference of other active compounds present in the drug. The calculated and theoretical values of both the proposed and the reported methods had 95% confidence level. This indicates good precision and accuracy in the analysis of AMP in pharmaceutical dosage forms.

CONCLUSION

Different methods were established to determine AMP concentration kinetically. The reaction rate, rate constant and fixed time methods were applied. Applying the fixed time method, it is clear that the slope increased with time and the most acceptable values of correlation coefficients (r) and intercepts were obtained. The proposed method is sensitive enough to enable determination of trace amounts of drug. Since our method is selective it avoids interference of colored and turbid background of samples.

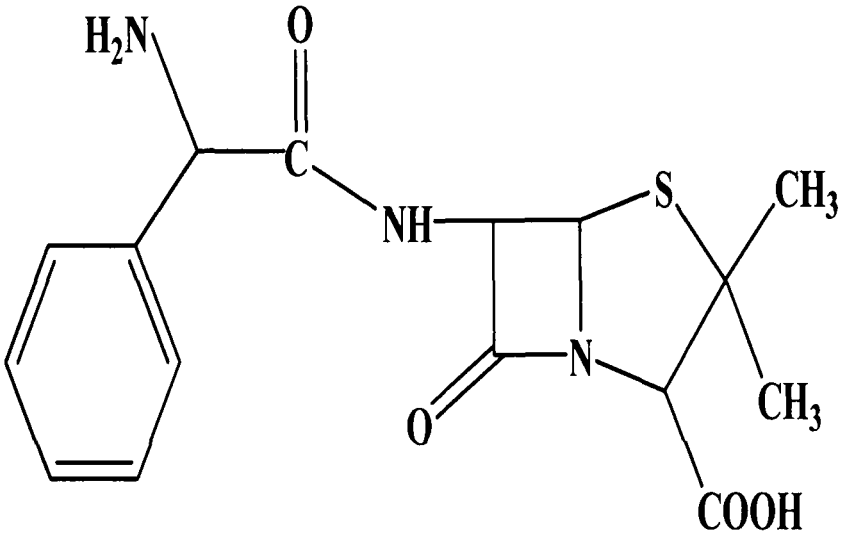

Fig.1 Structure of AMP

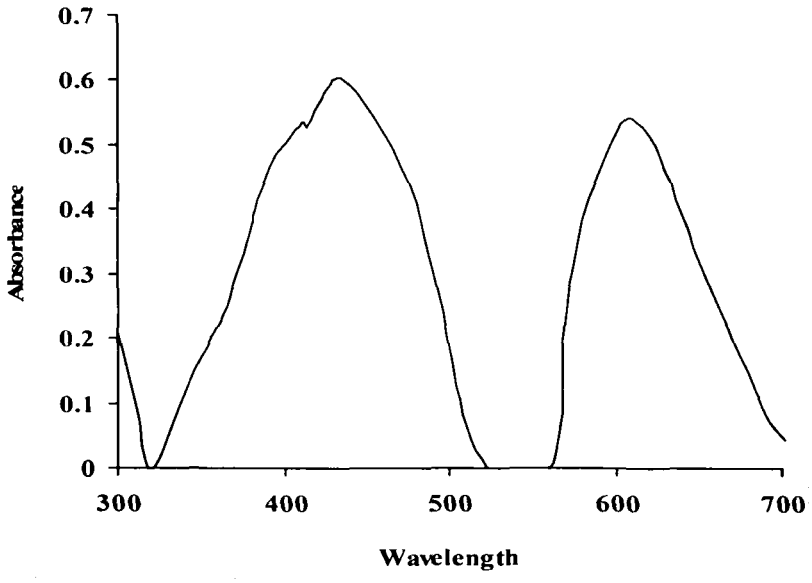

Fig.2 Absorption spectrum of AMP (25μgmL^{-1}) after reaction with $KMnO_4$: (a) oxidation product, (b) manganate ion (Method A)

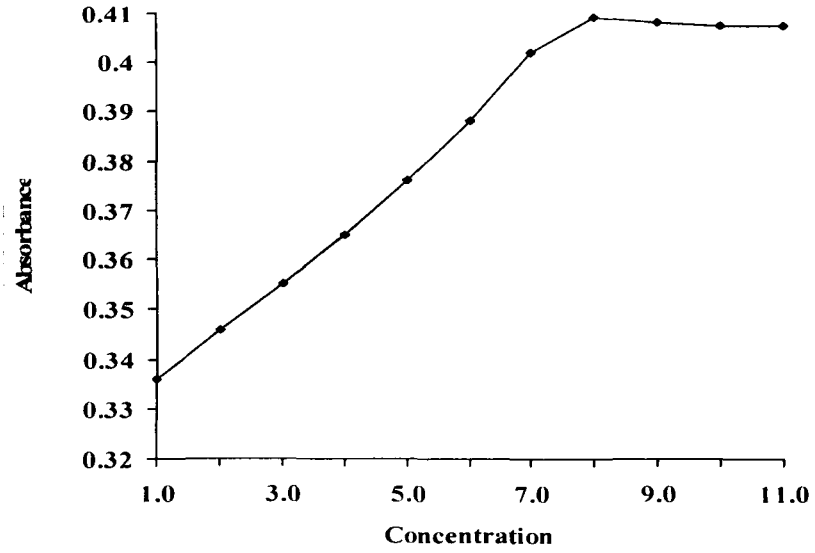

Fig.3 Effect of the concentration (1×10^{-4} to 1×10^{-3} mol L^{-1}) of $KMnO_4$ on absorbance produced by its reaction with AMP (25 μgmL^{-1} ; 1 ml of 0.5 mol L^{-1} NaOH)

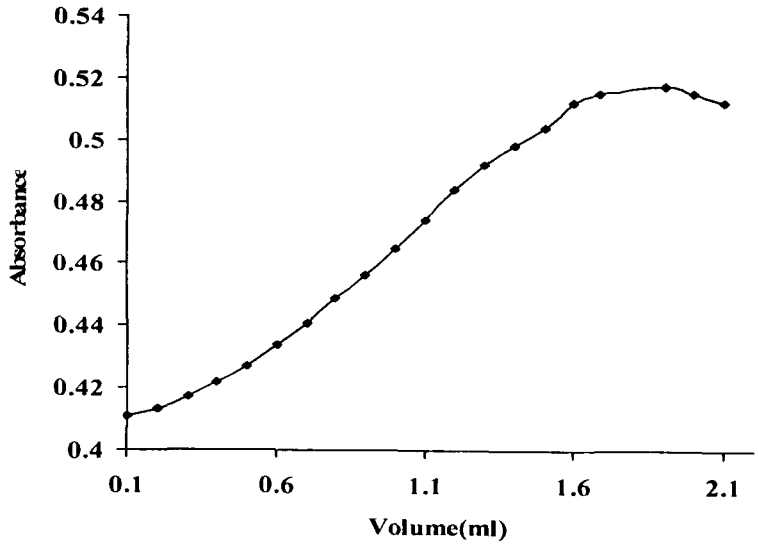

Fig.4 Effect of the volume of $KMnO_4$ 2 mol L^{-1} on the intensity of the colour produced by its reaction with AMP (25 μgmL^{-1} ; 1 ml of 0.5 mol L^{-1} NaOH)

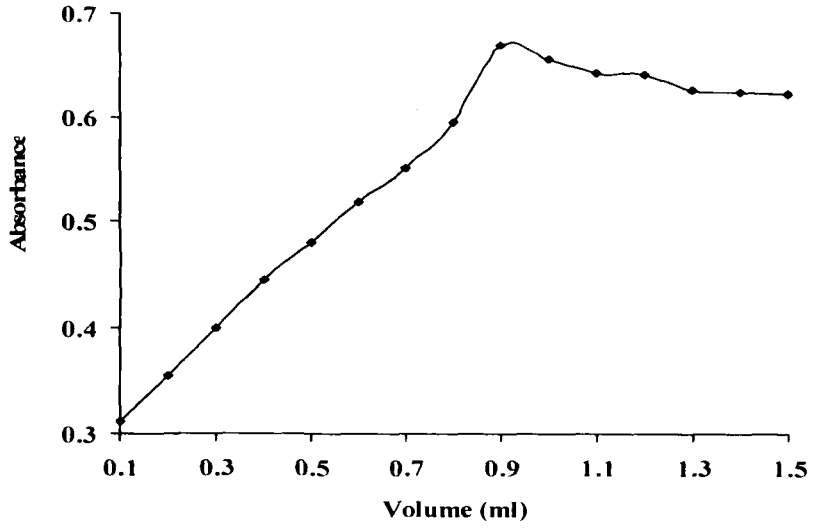

Fig.5 Effect of the volume of NaOH (0.5 mol L^{-1}) on the intensity of the colour produced by the reaction of AMP (25 μgmL^{-1}); with $KMnO_4$ (2 ml of 7.5 mol L^{-1})

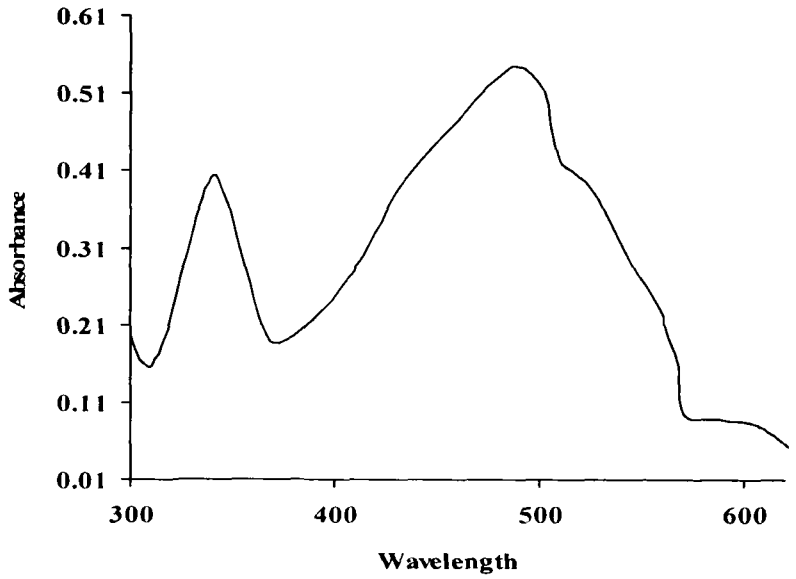

Fig. 6 Absorption spectrum of AMP (250 μgmL^{-1}) after its reaction with CDNB at pH 7.8 (Method B)

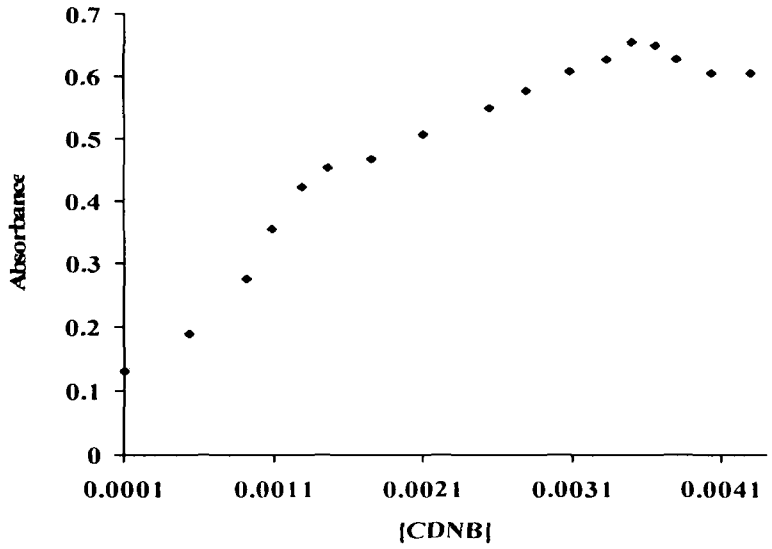

Fig.7 Effect of the concentration (1×10^{-4} - 4×10^{-3} mol L^{-1}) of CDNB on the absorbance of the reaction product of AMP (250 μgmL^{-1}) in 0.2 mol L^{-1} borate buffer.

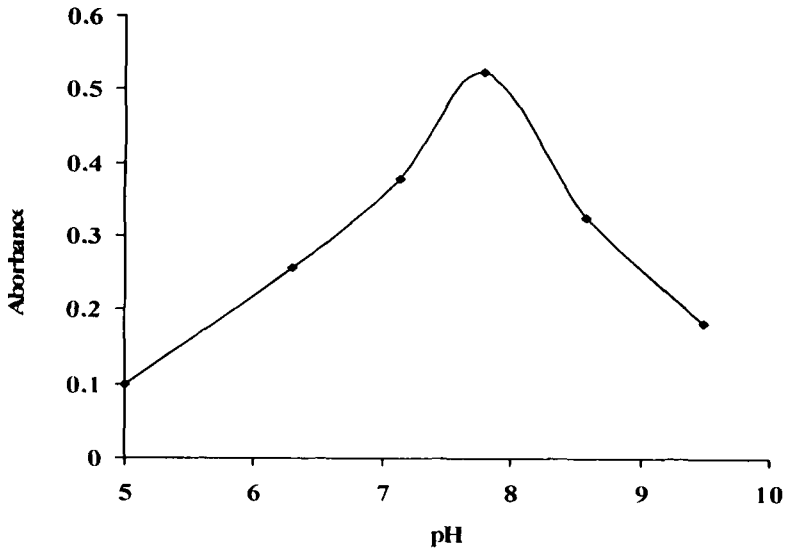

Fig.8 Effect of the pH of CDNB (3.5×10^{-3} mol L^{-1}) on the absorbance of the product keeping AMP Constant (250 μgmL^{-1}).

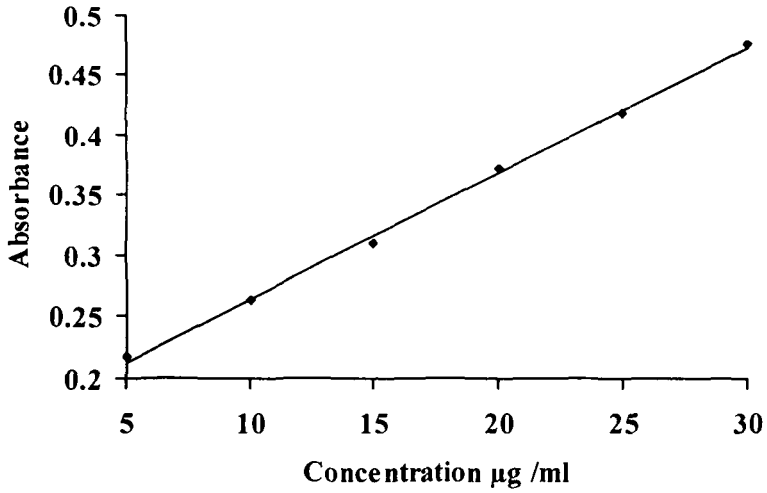

Fig.9 Spectrophotometric calibration curve for Method A

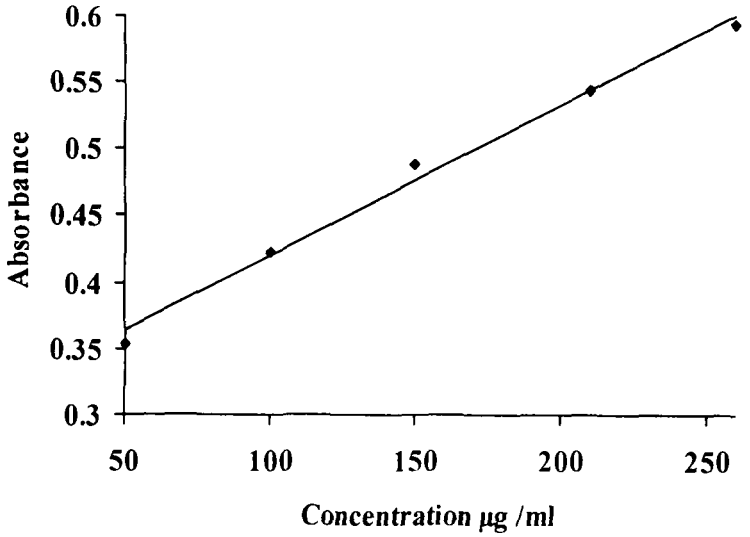

Fig.10 Spectrophotometric calibration curve for Method B

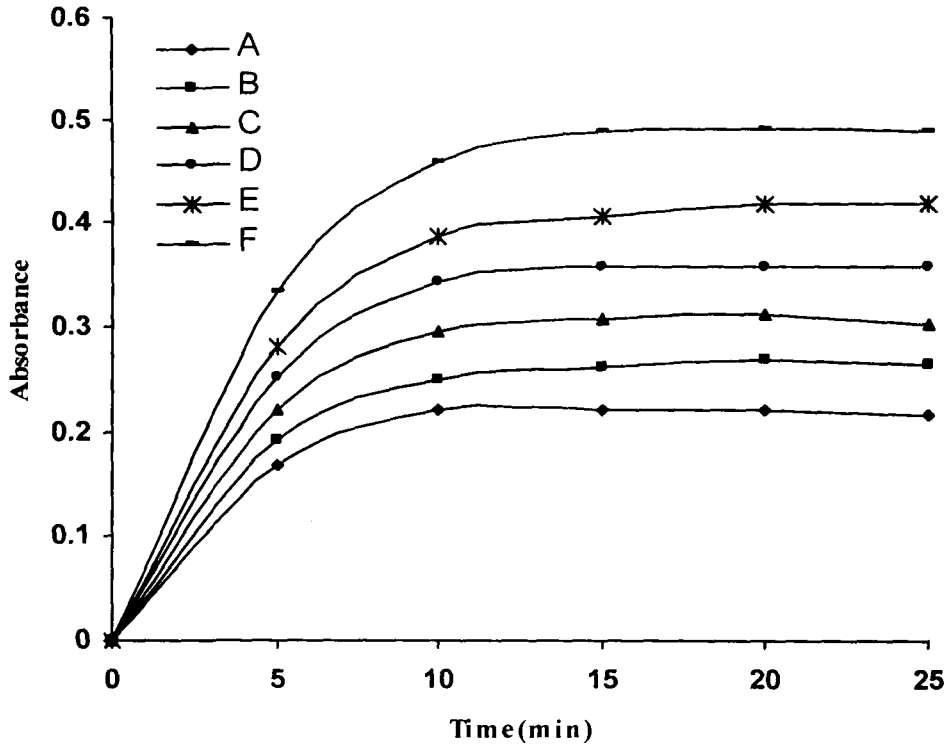

Fig.11 Absorbance vs. time plots for the reaction of AMP in alkaline $KMnO_4$ (Method A) showing the dependence of the reaction on AMP concentration. Concentration of AMP: (1) 1.4×10^{-5}, (2) 2.8×10^{-5}, (3) 4.2×10^{-5}, (4) 5.6×10^{-5}, (5) 7.0×10^{-5}, (6) 8.4×10^{-5} mol L^{-1}

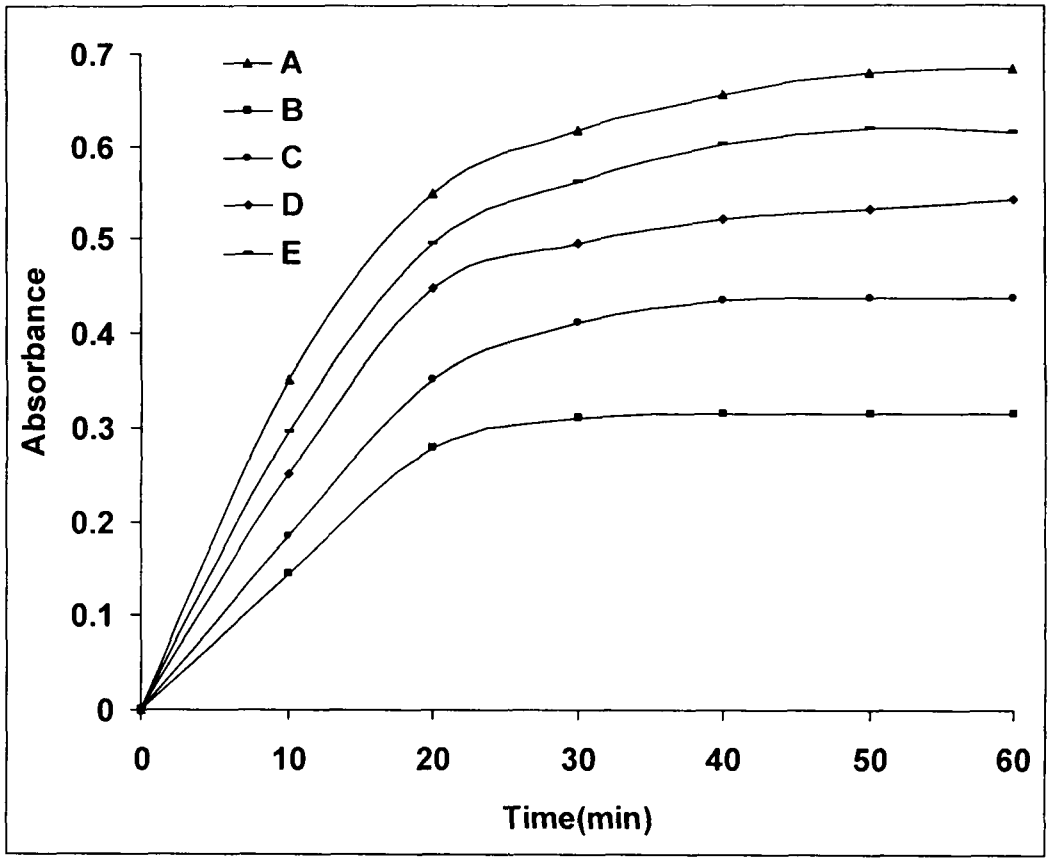

Fig.12 Absorbance vs. time plots for the reaction of AMP and CDNB (Method B) showing the dependence of the reaction on AMP concentration. Concentration of AMP: (A) 1.5×10^{-4}, (B) 3×10^{-4}, (C) 4.5×10^{-4}, (D) 6×10^{-4}, (E) 7.5×10^{-4} mol L^{-1}

Table1. Calibration equations at different fixed times for AMP in the ranges 5 -30 μgmL^{-1} and 50 -260 μgmL^{-1} applying methods A and B, respectively

Time(min.)	Regression Equation	Correlation coefficient (r)
Method A (oxidation with KMnO4)		
5	A= -.05554 + .04126 C	0.9912
10	A= -.04602 + .04406 C	0.9945
15	A= -.02212 + .05130 C	0.9975
20	A= -.00122 + .0286 C	0.9932
25	A= -.00015 + .0311 C	0.9982
Method B (Reaction with CDNB)		
10	A= -.04041 + .03805 C	0.9968
20	A= -.02110 + .04102 C	0.9959
30	A= -.0076 + .0032 C	0.9982
40	A= -.00078 + .0032 C	0.9991
50	A= -3.05×10^{-3} + .03826 C	0.9989
60	A= 2.12×10^{-3} + .03932 C	0.9994

Table 2. Logarithms of the rates for different concentrations of AMP

Log ΔA/Δt	**Log [AMP], (mol L^{-1})**
Method A (oxidation with KMnO4)	
-3.942	-4.854
-3.690	-4.553
-3.491	-4.376
-3.360	-4.244
-3.281	-4.155
-3.150	-4.075
Method B (Reaction with CDNB)	
-4.066	-3.824
-3.750	-3.523
-3.552	-3.251
-3.500	-3.222
-3.452	-3.125

Table 3. Values of K' calculated from slopes of log A versus t graphs multiplied by -2.303, for different concentrations of AMP.

K' **(s^{-1})**	**Log [AMP], (mol L^{-1})**
Method A (oxidation with KMnO4)	
-9.4773×10^{-4}	1.4×10^{-5}
-7.9414×10^{-4}	2.8×10^{-5}
-5.6421×10^{-4}	4.2×10^{-5}
-4.9483×10^{-4}	5.6×10^{-5}
-5.3669×10^{-4}	7.0×10^{-5}
-4.8899×10^{-4}	8.4×10^{-5}
Method B (Reaction with CDNB)	
-4.9344×10^{-4}	1.5×10^{-4}
-4.6647×10^{-4}	3.0×10^{-4}
-3.7702×10^{-4}	4.5×10^{-4}
-1.5545×10^{-4}	6.0×10^{-4}
-1.0255×10^{-4}	7.5×10^{-4}

Table 4. Values of reciprocal of time taken at fixed absorbance (0.4 and 0.3) for different rates of various concentrations of AMP

1/*t* (s^{-1})	**Log [AMP], (mol L^{-1})**
Method A (oxidation with KMnO4)	
1.11×10^{-3}	5.6×10^{-5}
8.40×10^{-4}	7.0×10^{-5}
6.70×10^{-4}	8.4×10^{-5}
Method B (Reaction with CDNB)	
3.34×10^{-4}	4.5×10^{-4}
3.03×10^{-4}	6.0×10^{-4}
2.78×10^{-4}	7.5×10^{-4}

Table 5. Analytical parameters for fixed time method for spectrophotometric determination of AMP in pure form

Parameters	Method A	Method A
Optical characteristics:		
λmax, nm	610	490
Linearity range (μgmL^{-1})	5-30	50-260
Regression equation:		
intercept (a)	0.086321	0.099403
Standard deviation of intercept (Sa)	0.681385	0.581394
slope (b)	0.013807	0.002215
Standard deviation of slope (Sb)	0.00201	0.000445
Correlation coefficient(r)	0.9977	0.9919
LOD(μgmL^{-1})	0.162	0.866
LOQ(μgmL^{-1})	0.493	0.2625

Table 6. Evaluation of precision for determination of AMP

Amount Taken (µg ml–1)	Amount Found (µg ml–1)	% Recovery ± S.D.	± RSD[a](%)	SAE[b]
Method A				
10	9.96	99.86	0.520	0.02
20	19.2	99.34	0.478	0.04
30	30.05	100.06	0.368	0.05
Method B				
55	54.95	99.97	0.432	0.02
150	150.02	100.04	0.428	0.03
260	259.05	99.72	0.424	0.06

REFERENCES

[1]. G. Goodman: The Pharmacological Basis of Therapeutics, Vol. II, 8th edn, Pergamon Press, New York, 1076 **(1991)**

[2]. G. Wilson: Text Book of Organic Medicinal and Pharmaceutical Chemistry,8th edn, J.R. Lipponcot Company, Philadelphia, 237**(1982)**

[3]. Driver Bentley, Text Book Pharmaceutical Chemistry, 8th edn, Oxford University Press, London, p. 793 **(1969)**

[4]. R. S. Satoskar and S. D. Bhandarkar: Pharmacology and Pharmacotherapeutics, Vol. II, 11th edn, Popular Prakashan, Bombay, 561 **(1990)**

[5]. H. P. Rang, M. N. Dale and J. M. Ritter: Pharmacology, 3rd edn, Chuchill Livingstone Publications, 725 **(1996)**

[6]. R.S.Satoskar and S. D. Bhandarkar: Pharmacology and Pharmacotherapeutics, 11th edn, Popular Prakashan, Bombay, 2, 549 **(1990)**

[7]. H. P. Rang, M. N. Dale and J. M. Ritter: Pharmacology, 4th edn, Chuchill Livingstone Publications, 691 **(1998)**

[8]. H.F. Askal, G.A. Saleh and N.M. Omer: Utility of certain pi-acceptors for the spectrophotometric determination of some penicillins, Analyst 116, 387 **(1991)**

[9]. H.A. Al-Khamees, F.S. ElShafie, M.E. Hagga, M.E. Alawady and E.A. Gad-Kareim: Sci. Pharm. 63, 191 **(1995)**

[10]. S.Y. Sun, W. Chen, Z.X. Pan, M.S. Zhang, J. Qu and P.F. Li: Fenxi Shinyanshi. 15, 39 **(1996)**

[11]. C.S.P. Sastry, S.G. Rao, P.Y. Naidu and K.R. Srinivas:Talanta 45, 1227**(1998)**

[12]. F. Belal, M.S. Rizk and M. Eid: J. Pharm. Biomed. Anal. 17, 275 **(1998)**

[13]. G.O. El-Sayed, A.S. Amin, Y.M. Issa and DC: Anal. Lett. 27, 2515 **(1994)**

[14]. M.C. Garcia, M.I. Alberto and V. Rodenas: J. Pharm. Biomed. Anal. 12,1585 **(1994)**

[15]. E. Verdon and P. Couedor: Anal. Chem. 82 ,1083 **(1999)**

[16]. M. Ishida, K. Kobayashi, N. Awata and F. Sakamoto: J. Chromatogr. 727, 245 **(1999)**

[17].G. Mukherjee and T. Ghosh: J. Inorg. Biochem. 59,827 **(1995)**

[18].V.G. Alekseev and I.S. Samuilova: Russ. J. Inorg. Chem. 53, 327 **(2008)**

[19]. S.J. Lyle and S.S. Yassin: Anal. Chim. Acta. 274, 225 **(1993)**

[20]. A. Amin, G. Ragab and H. Saleh: J. Pharm. Biomed. Anal. 30,1347 **(2002)**

[21]. A. Weisberger, S. Friess and E. Lewis :Techniques of organic **(1953).**

[22]. Chemistry, part 1, Interscience New York Yatsimirskii, K. B. *Kinetic Methods of Analysis*; Pergamon Press:Oxford, vol 3 **(1966)**

[23]. H. A. Laitinen and W. E. Harris: *Chemical Analysis*, 2nd Ed.; McGraw-Hill: New York, **(1975).**

[24]. J. Rose:*Advanced Physicochemical Experiments*, Pitman, London, UK, 67,**(1964).**

[25]. The United States Pharmacopoeia XXV and NF XX, American Pharmaceutical Association , Washington, DC **(2002).**

[26]. G.A. Saleh, H. Askal, I. Darwish and A. El-Shorbagi: Anal. Sciences 19, 281**(2003)**

[27]. M.M. Ayad, A.A. Shalaby, H.E. Abdellatef and H.M. Elsaid: J. Pharm. Biomed. Anal. 18, 975 **(1999)**

[28].G.A. Saleh, H. Askal, M.F. Radwan and M.A. Omar: Talanta 54, 1205 **(2001)**

Chapter-4

Kineitcs and Mechanism of deamination and decarboxylation of 2-aminopentanedioic acid by quinoliniumdichromatre (QDC) in aqueous perchloric acid

INTRODUCTION

Oxidation of amino acids is of great importance both from chemical view point and from its bearing on the mechanism of amino acid metabolism. Amino acids not only act as building blocks in protein synthesis but also play a significant role in the metabolism. They are subjected to many reactions and can supply precursors for many endogenous substances like hemoglobin in blood. They can undergo many kinds of reactions, depending on whether a particular amino acid contains a polar or non-polar subtituent. 2-Aminopentanedioic acid / L-Glutamic acid (glu-e) is one of the most abundant amino acids, especially high in cereal proteins and can be oxidized by different oxidants [1-4]. A salt of glu-e is used in the production of monosodium glutamate and nutritional supplements. L-glutamate itself can be used as medicine and promotes oxidation process. It combines with ammonia as a drug-free glutamine. It is mainly used for the treatment of hepatic coma and severe liver dysfunction, but the response is not satisfactory. Racemic

glutamate is used for the production of drugs. Physiologically, it plays a role in the metabolism of amino groups and is the precursor of neurotransmitter, gamma-aminobutyric acid, L-glutamic acid. Being acidic in nature it is important in determining 3-D conformation of proteins.

It is well established that the reduction of chromium(VI) to chromium(III) with a variety of organic and inorganic reductants can occur by a multiplicity of mechanisms which depend on the nature of the reducing agent [5]. The existence of different species of chromium(VI) in acid solutions, unstable oxidation states [chromium(IV) and chromium(V)] and the tendency of chromium(III) to form a variety of complexes, all combine to give systems of considerable complexity [6]. Attempts have been made to confirm the intermediacy of chromium(IV) and chromium(V) by use of competitive experiments [7–8] In acid solution, the reported reduction potential of the Cr(VI)/Cr(III) couple is 1.33V [9]. The reagent, quinoliniumdichromate (QDC) is a versatile oxidant that deserves further investigation and some kinetic studies of the oxidation of inorganic substrates by QDC are available [10]. A number of reports on the mechanism of oxidation of several substrates by quinolinium dichromate are available which is shown to oxidize primary and secondary alcohols to the corresponding aldehydes [11-12], cyclic alcohols to cyclic ketones [13], bicyclic alcohols [14] and benzyl alcohol [15]. The α-hydroxyacids [16] and α-ketoacids [17] are oxidized with QDC and their

reactions are studied kinetically. QDC oxidizes cinnamic and crotonic acids smoothly in N,N-dimethylformamide in the presence of an acid to give aldehydes [18-27].

Since there are no reports on the kinetics of oxidation of 2-aminopentanedioic acid by QDC we are reporting the kinetics of its oxidation by QDC in perchloric acid, in order to identify the chromium(VI) intermediate and to propose a suitable mechanism. The activation parameters and thermodynamic quantities have been determined and discussed.

EXPERIMENTAL

Stock solutions of L-glutamic acid (Merck, Mumbai,India). quinolinium dichromate (QDC) (Sigma-Aldrich) were prepared in double distilled water and standardized iodometrically [12]. $HClO_4$ and $NaClO_4$ were employed to maintain the required acidity and ionic strength, respectively.

Kinetic Studies

The reaction was initiated by mixing the previously thermostated solutions of Glu-e and QDC, which also contained the required amount of perchloric acid, sodium perchlorate and double distilled water. The reaction was followed spectrophotometrically at 360 nm . The spectral changes during

the reaction under standard conditions at room temperature are given in Fig.1. Application of Beer's law under the reaction conditions was verified between 1.0×10^{-4} and 1.0×10^{-3} mol dm^{-3} of QDC and the extinction coefficient was found to be ε = 1,246 ± 12 $dm^3mol^{-1}cm^{-1}$. The pH of the reaction mixture in the beginning and in the end remained constant. The kinetic runs were followed for more than 80% completion of the reaction and first order kinetics was observed. The pseudo-first order rate constants, k_{obs} obtained from the slope of the plots of log(absorbance) versus time were linear (Fig.2). The k_{obs} were reproducible within ±5% and are the average of at least three independent kinetic runs (Table 1).

RESULTS AND DISCUSSION

Reaction Orders

The order of reaction was determined from a plot of log k_{obs} versus log(concentration) of QDC (2.0×10^{-4} to 2.0×10^{-3} mol dm^{-3}) at constant concentration of glu-e (2.0×10^{-2} mol dm^{-3}, $HClO_4$ =3.0 mol dm^{-3}) and ionic strength, I = 2.80 mol dm^{-3}, and was found to be unity. Negligible variation in k_{obs} occurs with varying concentration of QDC (Table 1). The plot of log [a/(a-x)] versus time for different concentrations of QDC is linear and uniform (Fig.2). The Glu-e concentration was varied in the range of (5×10^{-3} to 5 × 10^{-}

^{2} mol dm^{-3}) at constant concentration of QDC. $HClO_4$ and ionic strength was found to be uniform (Table 1).

Product Analysis

Different sets of reaction mixtures containing glu-e, an excess of QDC with constant ionic strength and acidity were left to stand for 12 h in an inert atmosphere at 25°C. The succinic semialdehyde produced was also identified from FT-IR spectrum. The ν(C=O) appears at 1696 cm^{-1} (Fig.3) which is the characteristic band of aldehyde. It does not undergo further oxidation. Ammonia was identified by Nessler's reagent [29]. The CO_2 liberated was qualitatively detected [30] by passing the gas into lime water. The results indicated that two moles of $QHCrO_4$ (in term of Cr (VI)) consumed four mole of glu-e (Scheme 1.)

$$4\,COOHCH_2CH_2CHNH_2COOH + 2\,QHCrO_4 + 2\,H^+ \longrightarrow 4\,COOHCH_2CH_2CHO + 2CrO_2^- + 4CO_2 + 4NH_3 + 4\,H^+ + 2Q$$

Scheme.1

Effect of Temperature

The rate of reaction was measured at different temperature with varying concentration of perchloric acid and keeping other conditions constant. The rate constant, k obtained from the intercept of the plots of 1/kobs versus 1/glu-e was found to increase with temperature .The values of rate constant of glu-e at 293 K 298 K 303 K and 308 K, was found to be 6.50 s^{-1}, 7.36 s^{-1}, 11.32 and 13.28 s^{-1}, respectively. The energy of activation corresponding to these constants was evaluated from a plot of log k versus 1/T (Table 2).

Effect of perchloric acid Concentration

The effect of acidity on the rate of reaction was studied by varying the concentration of the perchlroric acid (2.5-4.5mol dm^{-3}). The k_{obs} was found to be directly proportional to the concentration of the acid (Table 1).

Effect of Ionic Strength and Dielectric Constant

When the ionic strength was varyied the rate constant was found to be proportional to the ionic concentration. The plot of log k_{obs} versus I was linear with positive slope (Fig.5) ($r > 0.9985$, $\sigma < 0.0836$). The effect of relative permittivity (D) on the rate constant was studied by varying the acetic acid content (v/v). Attempt to measure the relative permittivity was unsuccessful. However, they were computed from the values of pure liquids [31]. The rate

constant was found to increase with increase in the dielectric constant of the medium. A plot of log k_{obs} versus $1/D$ was linear with negative slope (Fig.6) ($r > 0.9614$, $\sigma < 0.0791$).

The QDC reacts with two moles of $HClO_4$ to give H_2CrO_4 [32-33]. It H_2CrO_4 reacts with glu-e forming a complex, which is reduced to an intermediate chromium(IV) and a product of glu-e. Subsequently, another molecule of acid chromate reacts with one molecule of glu-e producing another chromium(IV) intermediate, and a product of glu-e. In a further fast step, one molecule of chromium(IV) reacts with one more molecule of glu-e giving chromium(III) and final product of succinic semialdehyde (Scheme 2).

The results indicate the formation of a complex between glu-e and chromium(VI) in presence of perchloric acid. The formation of this complex was proved kinetically by Michaelis–Menten plot, i.e., a non-zero intercept of the plot of $1/k_{obs}$ versus 1/[glu-e] (Fig.4). The colour indicates the formation of Cr(VI)-species and appearance of Cr(III)-species with the isosbestic point at λ=530 nm.

$$QDC + 2H^+ \underset{}{\overset{K_1}{\rightleftharpoons}} H_2CrO_4 + Q\,(\text{Quinoline})$$

$$H_2CrO_4 + COOHCH_2CH_2CHNH_2COOH \overset{K_2}{\rightleftharpoons} \text{Complex}$$

$$\text{Complex} \xrightarrow[\text{Slow}]{k} COOHCH_2CH_2CHO + \underset{Cr(IV)}{H_2CrO_3} + CO_2 + NH_3$$

$$H_2CrO_4 + COOHCH_2CH_2CHNH_2COOH \xrightarrow{\text{Fast}} COOHCH_2CH_2CHO + \underset{Cr(IV)}{H_2CrO_3} + CO_2 + NH_3$$

$$H_2CrO_3 + COOHCH_2CH_2CHNH_2COOH \xrightarrow{\text{Fast}} COOHCH_2CH_2CHO + \underset{Cr(III)}{CrO_2^-} + CO_2 + NH_3 + 2H^+$$

Scheme 2

Appearance of isosbestic point indicates very low concentration of the probable intermediates like Cr(V) , Cr(IV) [34] and their gradual decay to [Cr(III)] . The characteristic of electronic spectrum of Cr(III)-species lies in the range 320–600 nm. The original absorption maxima, (560 and 430 nm) was replaced by a single peak at 360 nm due to the formation of chromium(VI). Similar results have also been obtained by the oxidation of 2-propanol from chromium(VI) in aqueous acetic acid and, oxidation of thallium(I) by QDC in aqueous acetic acid-chloride media [35-36].

$$\text{Rate} = k\ \text{Complex C}$$

$$\text{Rate} = -\frac{d[QDC]}{dt} = kK_1K_2[\text{Glu-e}]_f\,[QDC]_f\,[H^+]_f^{\,2} \quad (1)$$

The total concentration of QDC is given by,

$$[QDC]_t = [QDC]_f + [H_2CrO_4] + [\text{Complex C}]$$

$$[QDC]_t = [QDC]_f + K_1[QDC]_f\,[H^+]_f^{\,2} + K_1K_2[\text{Glu-e}]_f\,[QDC]_f\,[H^+]_f^{\,2}$$

$$= [QDC]_f + \{\,1 + K_1\,[H^+]_f^{\,2} + K_1K_2[\text{Glu-e}]_f\,[H^+]_f^{\,2}\,\}$$

Therefore

$$[QDC]_f = \frac{[QDC]_t}{1+ K_1 [H^+]_f^2 + K_1K_2[Glu\text{-}e]_f [H^+]_f^2} \qquad (2)$$

where 't' and 'f' stand for total and free concentration of QDC.

$$[Glu\text{-}e]_t = [Glu\text{-}e]_f + [Complex\ C]$$

$$= [Glu\text{-}e]_f + K_1K_2[Glu\text{-}e]_f [QDC]_f [H^+]_f^2$$

$$= [Glu\text{-}e]_f \{ 1+ K_1K_2[QDC]_f [H^+]_f^2 \}$$

Therefore,

$$[Glu\text{-}e]_t = \frac{[Glu\text{-}e]_f}{1+ K_1K_2[QDC]_f [H^+]_f^2} \qquad (3)$$

In view of the low concentration of QDC used in the experiment (Eq. 3) the term $K_1K_2\,[QDC]_f\,[H^+]_f^2$ can be neglected in comparison to unity.

Hence,

$$[Glu\text{-}e]_t = [Glu\text{-}e]_f \qquad (4)$$

and

$$[H^+]_t^2 = [H^+]_f^2 + [H_2CrO_4] + [Complex\ C]$$

$$= [H^+]_f^2 + K_1[QDC]_f[H^+]_f^2 + K_1K_2[Glu\text{-}e]_f\,[QDC]_f\,[H^+]_f^2$$

$$= [H^+]_f^2 \{\ 1 + K_1\,QDC]_f + K_1K_2\,[Glu\text{-}e]_f\,[QDC]_f\}$$

$$[H^+]_f^2 = \frac{[H^+]_t^2}{1 + K_1\,[QDC]_f + K_1K_2[Glu\text{-}e]_f\,[QDC]_f} \qquad (5)$$

Similarly,

$$[H^+]_t^2 = [H^+]_f^2 \qquad (6)$$

Substituting Eqs. 2,4, and 6 in Eq. 1, we get Eq. 7, which explains all the experimentally observed orders with respect to different species of reaction.

$$\text{Rate} = -\frac{d[QDC]}{dt} = \frac{kK_1K_2[\text{Glu-e}][QDC][H^+]^2}{1+K_1[H^+]^2 + K_1K_2[\text{Glu-e}][H^+]^2} \quad (7)$$

Or

$$\frac{\text{Rate}}{[QDC]} = K_{obs} = \frac{kK_1K_2[\text{Glu-e}][H^+]^2}{1+K_1[H^+]^2 + K_1K_2[\text{Glu-e}][H^+]^2} \quad (8)$$

The rate law (8) can be rearranged to Eq. 9, which is suitable for verification.

$$\frac{1}{K_{obs}} = \frac{1}{kK_1K_2[\text{Glu-e}][H^+]^2} + \frac{1}{K_1K_2[\text{Glu-e}]} + \frac{1}{k} \quad (9)$$

According to Eq. 8, plots of 1/kobs versus 1/[glu-e] and 1/kobs versus $1/[H^+]^2$ should be linear (Fig. 4). The slopes and intercepts of such plots determine the values of K_1, K_2, k and the thermodynamic quantities for the first and second equilibrium steps of Scheme 2 (Table 2).

For example at 35 °C:

(i)From the plot of 1/kobs versus 1/[glu-e]

$(\text{Intercept})_1 = 1 / k$

Therefore , k =1/(Intercept)1= $1.328\times 10^{-2}sec^{-1}$

$$(Slope)_1 = 1/kK_1K_2[H^+]^2 + 1/k$$

(ii) From the plot of 1/kobs versus $1/[H^+]^2$

$$(Intercept)_2 = 91.37 = 1/kK_1K_2[Glu\text{-}e] + 1/k$$

From $(Intercept)_1$, the value of $k = 1.328\times 10^{-2}sec^{-1}$

Hence,

$91.37 = 1/1.328\times 10^{-2}\times K_2 \times 2.0\ 10^{-2} + 1 / 1.328\times 10^{-2}$

$1+ K_2(2.0\times10^{-2}) = 91.37 \times 1.328\times 10^{-2} K_2\times2.0\ 10^{-2}$

$1+.02\ K_2 = .0242678\ K_2$

$K_2 = 234.31 dm^3mol^{-1}$

$(Slope)_2 = 812.2 = 1/kK_1K_2[Glu\text{-}e]$

$$812.2 = 1/ 1.328\times 10^{-2} \times 234.31 dm^3mol^{-1} \times 2.0\ 10^{-2}\times K_1$$

$K_1 = 1.978\times 10^{-2}\ dm^6mol^{-2}$

At 35°C:

$K_1 = 1.978\times 10^{-2}\ dm^6mol^{-2}$

$K_2 = 234.31 dm^3mol^{-1}$

$k = 1.328\times 10^{-2}sec^{-1}$

Similarly k, K_1 and K_2 were calculated at different temperatures (Table 2). Van't Hoff plots were made (log K_1 versus 1/T and log K_2 versus 1/T). The ΔH, ΔS and ΔG were calculated for the first and second equilibrium steps (Scheme 2). A comparison of these values (Table 2) with those obtained for the

slow step refer to the rate limiting step, supporting the fact that the reaction before the rate determining step is fairly fast and involves a high activation energy [37-39]. An increase in the volume of acetic acid leads to an increase in the reaction rate. A plot of $\log k_{obs}$ versus 1/D was linear with positive slope which is contrary to the convention. Perhaps the effect is countered substantially by the formation of active species to a greater extent in a low dielectric constant medium leading to the net increase in the rate [40]. The mechanism is also supported by moderate values of ΔH and ΔS . The negative ΔS value indicates that the complex (C) is more ordered than the reactants [41]. The observed modest enthalpy of activation and a higher rate constant for the slow step indicates that the oxidation, presumably occurs via an inner-sphere mechanism. This conclusion is supported by observations [42-44] made earlier.

CONCLUSION

The reaction between Glu-e and QDC is very slow in low perchloric acid concentration at room temperature.The oxidant, chromium(VI) exists in acid medium as H_2CrO_4, which takes part in the chemical reaction. The rate constant of slow step and other equilibrium constants involved in the mechanism are evaluated and activation parameters with respect to slow step of reaction were computed. The overall mechanistic sequence described here, is consistent with the products formed.

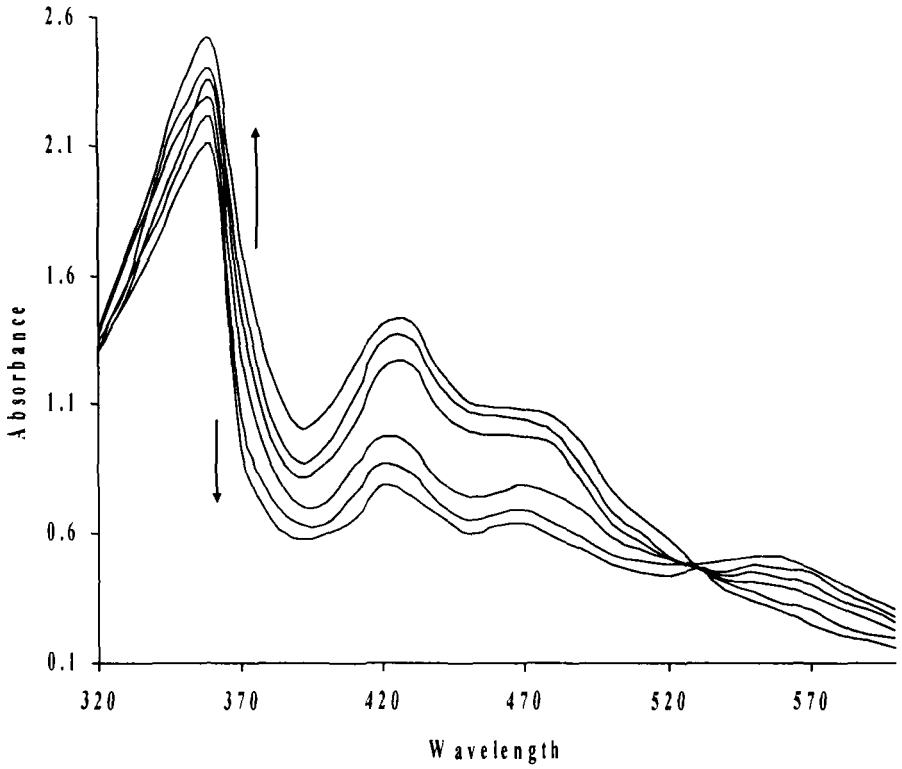

Fig.1 Spectral changes during the oxidation of Glu-e by QDC in aqueous perchloric acid at 25°C; QDC = 8.0 × 10^{-2}/mol dm^{-3}, [Glu-e] = 2.0 × 10^{-2}/mol dm^{-3}, [HClO4] = 3.0, and I =2.80/mol dm^{-3} (scanning time interval 1.0 min)

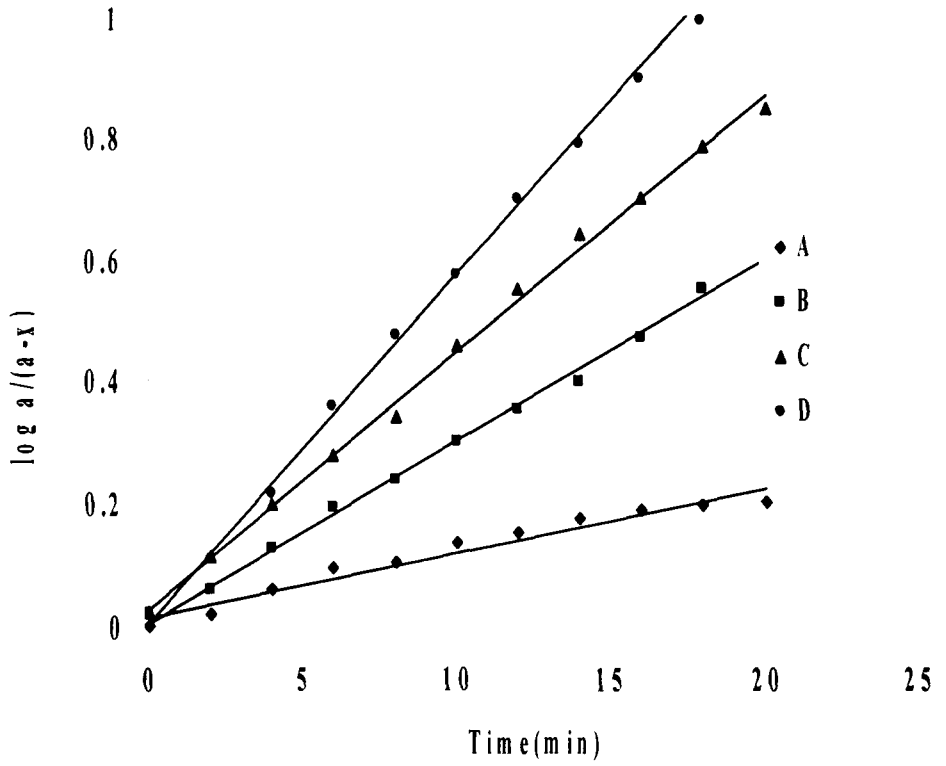

Fig.2 Plot of log a/(a-x) versus time in aqueous perchloric acid at 25 °C, Glu-e = 2.0 × 10^{-2}, [$HClO_4$] = 3.0, I = 2.80 mol dm^{-3} and QDC = (A) 2.0 (B) 6.0, (C) 8.0, and (D) 10.0 mol dm^{-3}

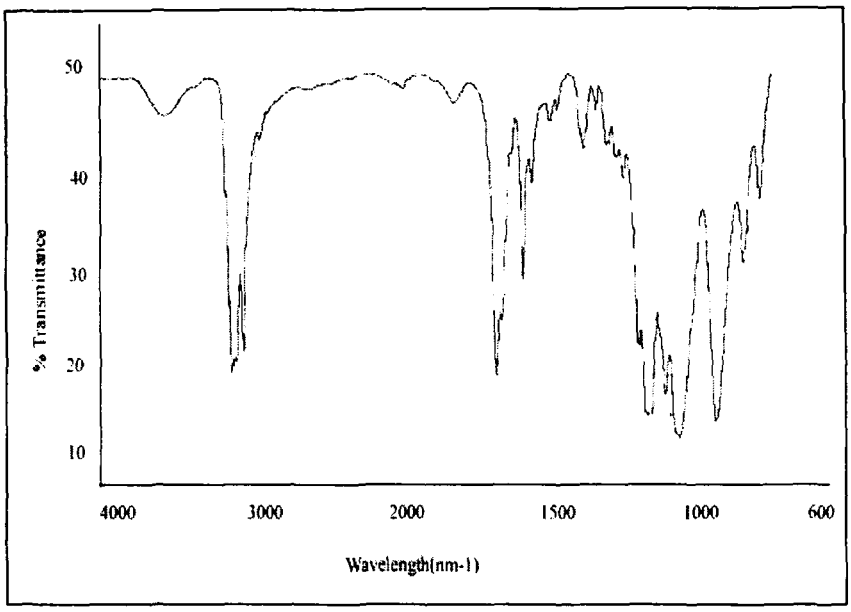

Fig.3 FT-IR spectrum of the product of oxidation of Glu-e by QDC

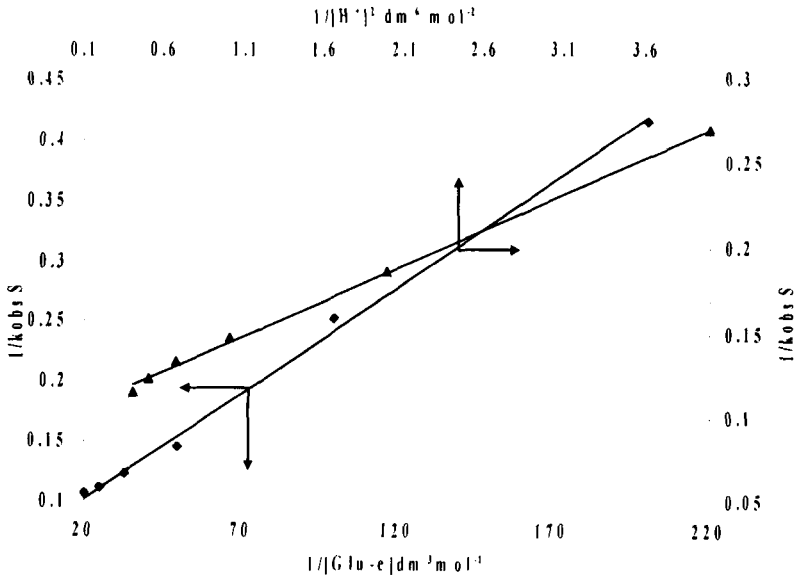

Fig.4 Verification of rate law (7) in the form of Eq.9 (Table 1)

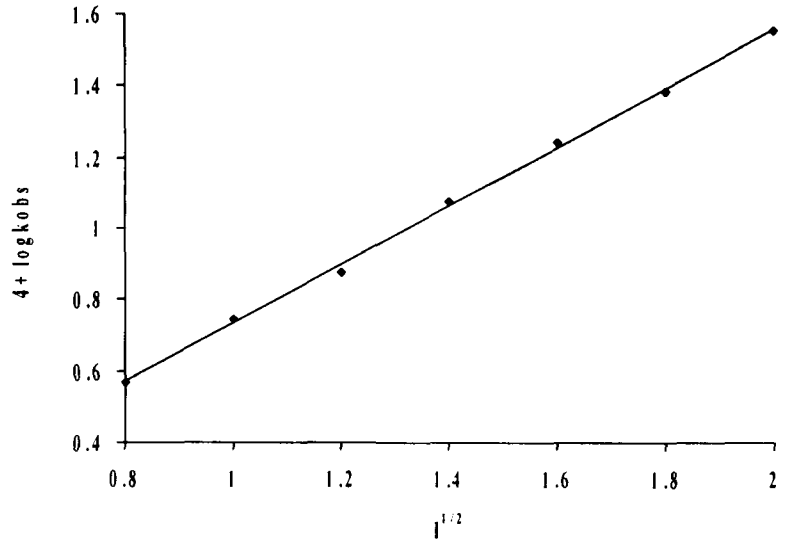

Fig.5 Effect of ionic strength on the oxidation of Glu-e by QDC in aqueous perchloric acid medium at 25°C

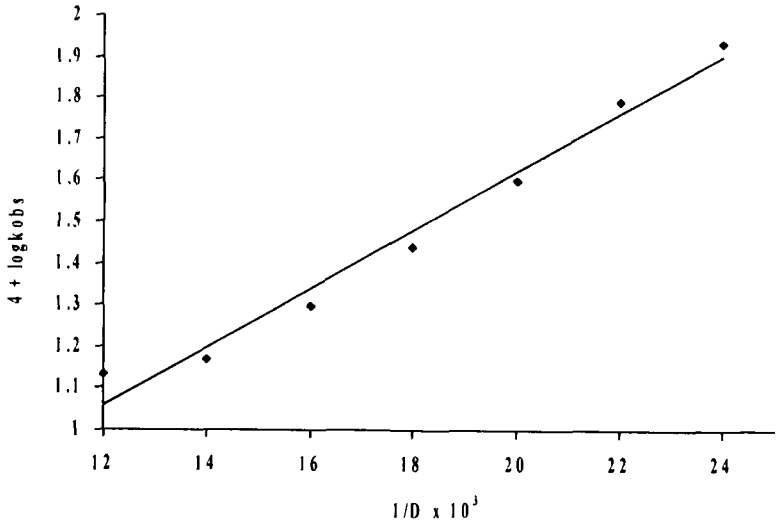

Fig.6 Effect of dielectric constant on the oxidation of Glu-e by QDC in aqueous perchloric acid medium at 25°C

Table1. Effect of variation of QDC, Glu-e, and perchloric acid on the oxidation of glu-e by QDC in perchloric acid medium at I = 2.80 mol dm^{-3} and at 25°C (Scheme.2)

[QDC] × 10^4 (mol dm^{-3})	[Glu-e] × 10^2 (mol dm^{-3})	[$HClO_4$] (mol dm^{-3})	k_{obs} × 10^{-3} (s^{-1})	k_{cal} × 10^{-3} (s^{-1})
Variation of [QDC]				
2.0	2.0	3.00	6.24	6.35
6.0	2.0	3.00	6.31	6.35
8.0	2.0	3.00	6.19	6.35
10.0	2.0	3.00	5.98	6.35
16.0	2.0	3.00	6.36	6.35
20.0	2.0	3.00	6.34	6.35
Variation of [Glu-e]				
8.0	0.5	3.00	2.41	2.43
8.0	1.0	3.00	3.96	3.56
8.0	2.0	3.00	6.87	7.36
8.0	3.0	3.00	8.15	8.18
8.0	4.0	3.00	8.96	8.93
8.0	5.0	3.00	9.30	9.31
Variation of [$HClO_4$]				
8.0	2.0	1.50	3.71	3.71
8.0	2.0	2.50	5.36	5.36
8.0	2.0	3.00	6.78	6.78
8.0	2.0	3.50	7.47	7.47
8.0	2.0	4.00	8.16	8.16
8.0	2.0	4.50	8.73	8.73

Table 2. Activation parameters and thermodynamic quantities of the oxidation of glu-e by QDC in aqueous perchloric acid medium.

Temperature (K)	$k \times 10^3$ (s^{-1})	log k	$1/T \times 10^3$
(a) Effect of temperature with respect to slow step of the Scheme 1			
293 298 303 308	6.500 7.360 11.32 13.28	0.716 0.866 1.053 1.120	3.413 3.356 3.300 3.246
Parameters			Values
(b) Activation parameters			
Ea (kJ mol^{-1}) $\Delta H^{\pm}$ (kJ mol^{-1}) $\Delta S^{\pm}$(J K^{-1} mol^{-1}) $\Delta G^{\pm}$ (kJ mol^{-1})	58.2 51.7 -62.3 59.1		
(c) Temp. (K) mol^{-1}	$K_1 \times 10^2 dm^6$ mol^{-2}		$K_2 \times 10^{-2}$ dm^3
293 298 303 308	6.34 4.66 3.12 1.97		1.32 1.45 1.63 2.34
(d) Thermodynamic Parameters	using K_1 values		using K_2 values
$\Delta H^{\pm}$ (kJ mol^{-1}) $\Delta S^{\pm}$(J K^{-1} mol^{-1}) $\Delta G^{\pm}$ (kJ mol	-71.2 -251 -1.70		21.3 119 -14.1

REFERENCE

[1]. P. Swamy and N. Vaz: Proc. Indian Acad. Sci., (Chem. Sci.) 113, 325 **(2001)**

[2]. A.L. Harihar, R.G. Panari and S.T. Nandibewoor: Oxdn. Comm., 22, 308 **(1999)**

[3]. B.S. Sherigar, I.K. Bhatt, I.Pinto and N.M. Madegouda:Int. J. Chem. Kinet., 27,675. **(1995)**

[4]. S. Nahar, S. Jain, C.M. Gangawal and P.D. Sharma: J. Indian Chem. Soc., 72,863 **(1995)**

[5]. M. Mitewa and P.R. Bontchev: Coord. Chem. Rev., 61,241**(1985)**

[6]. J.K. Beattie and G.P. Haight: Jr., Progr. Inorg. Chem.,17,93 **(1972)**

[7]. K.B. Wiberg and W.H. Richardson: J. Am. Chem. Soc., 84,2800 **(1962)**

[8]. G.P. Haight, Jr., T.J. Huang and B.Z. Shakhashiri: J. Inorg. Nucl. Chem., 33, 2169 **(1971)**

[9]. J.F. Perez-Benito and C. Arias: Can. J. Chem., 71,649 **(1993)**

[10]. Jr.M.C. Day and J. Selbin:Theoretical inorganic chemistry. Reinhold Publishing Corporation, New York, p 226 **(1964)**

[11]. S. A. Chimatadar, T. Basavaraj and S.T. Nandibewoor: Polyhedron, 25, 2976 **(2006)**

[12]. K. Balasubramanian and V. Prathibha:Ind. J. Chem., 25B 326 **(1986)**

[13]. S. Meenakshisundaram and M. Amutha: Bull. Pol. Acad. Sci. Chem., 49,165 **(2001)**

[14]. I.Nongkynrih and K. M. Mahanti: Bull. Chem.Soc. Jpn., 69, 1403 **(1996)**

[15]. I.Nongkynrih and K. M. Mahanti: Bull. Chem. Soc. Jpn., 68, 3325 **(1995)**

[16]. S. Kabilan, R. Girija, R. J. C. Reis and A. P. M. Segurado: J.Chem. Soc. Perkin Trans. 2., 6 1151 **(2002)**

[17]. K. Aruna, P. Manikyamba and V. E. Sundaram: Coll. Czech. Chem. Comm., 58,1624 **(1993)**

[18]. S. Das, G. S. Chaubey and M. K. Mahanti, Kinetics and Catalysis.,43,794 **(2002)**

[19]. I.Nongkynrih and K. M. Mahanti: Bull. Chem.Soc. Jpn., 67, 2320 **(1994)**

[20]. K. Aruna and P. Manikyamba: Indian J. Chem. Sect. A.: Inorg., Bio-Inorg., Phys., Theor. Anal. Chem., 34, 822**(1995)**

[21]. G. S. Chaubey, S. Das and M. K. Mahanti: Can. J. Chem. /Rev. Can. Chim., 81 204 **(2003)**

[22]. G. S. Chaubey, S. Das and M. K. Mahanti:Kinetics and Catalysis, 43, 789 **(2002)**

[23]. G. S. Chaubey, S. Das and M. K. Mahanti:Bull. Chem. Soc. Jpn., 75, 2215 **(2002)**

[24]. K. Aruna and P. Manikyamba: Int. J. Chem. Kinet., 29, 437 **(1997)**

[25]. E. Karim and M. K. Mahanti :Pol. J. Chem., 66, 1471 **(1992)**

[26]. J. Raha, G. C. Sarma and M. K. Mahati: Bull. Soc. Chim.Fr., 4, 487**(1991)**

[27]. A.S. Chimatadar, S.B. Koujalagi and S.T. Nandibewoor: Trans. Met. Chem., 27,704 **(2002)**

[28]. I.Nongkynrih and M. K. Mahanti: J.Org.Chem., 58, 4925 **(1993)**

[29]. L. J. Ballamy: The IR Spectra of Complex Molecules, Methuen and Co, London, 2nd Ed. p. 425 **(1958)**

[30]. G. H. Jeffery, J. Bassett, J. Mendham and R. C. Denney, Vogel's Text Book of Quantitative Chemical Analysis, ELBS Longman, Essex, UK, 5th Ed. p. 371.**(1996)**

[31]. K. Dass and M. J. Dass: Chem. Soc. Dalton Trans., 589 **(1994)**

[32]. E. David and R. Lide: Handbook of Chemistry and Physics, CRC Press Inc., London, 73rd ed. pp.8 **(1993)**

[33]. F. Feigl:Spot Tests in Organic Analysis, Elsevier, New York, p. 212 **(1975)**

[34]. J. Y. Tong and E. L. King: J Am Chem Soc.,75, 6180 **(1953)**

[35]. V. Daier , S . Siganorella, M. Rizzotto, M. I. Frascaroli, C. Palopolic, C. Broudino, J.M. Salas-peregrin and L.F. Sala :Can .J. Chem., 77,57 **(1999)**

[36]. M. Rahaman, and J. Rocek: J Am Chem Soc., 93, 5462 **(1971)**

[37]. A.S. Chimatadar, S.B. Koujalagi and S.T. Nandibewoor:Trans.Met.., 27,81 **(2004)**

[38]. K.S. Rangappa, M.P. Ragavendra, D.S. Mahadevappa and D. Channegouda: J Org Chem., 63,421 **(1966)**

[39]. E. A. M. Hughes:Physical Chemistry, Pergamon Press, New York, 2nd ed. pp. 1333 **(1961)**

[40]. E. S. Amis: Solvent Efeect on Reaction Rate and Mechanism Academic Press, New York, **(1966)**

[41]. V. C. Seregar, C. V. Hiremath and S. T. Nandibewoor, Transition Met Chem.,31,541 **(2006)**

[42]. Weissberger: Investigation of Rates and Mechanism of Reactions in Techniques of Chemistry, Wiley Interscience Publication, New York , 4th ed. p. 421 **(1974)**

[43]. M. Martinez, M.A. Pitarque and R.V. Eldik, J Chem Soc Dalton Trans., 2665 **(1996)**

[44]. A .P. Khan , A . Mohd . S. Bano . A. Husain and K. S. Siddiqi : 35.117(2010)

[45]. D. Bilehal, R. Kulkarni and S.T.Nandibewoor: J. Mol. Cat. A. Chem., 232.21**(2005)**

Chapter-5

Kinetics of Substitution of Hexacyanoferrate(II) by EDTA catalysed with Mercury(II)

INTRODUCTION

During the last decade, many novel methods for the determination of mercury(II) have been developed [1–6]. It has been demonstrated that of all the heavy metals mercury(II) easily forms bond to cyanide and slowly removes it from hexacyanoferrate(II). Kinetics and mechanism of ligand replacement in low spin Fe(II) complex has been done, although it is limited to the study of pentacyano(L)ferrate(II) complex[1-7]. Few studies have been done in aqueous electrolyte and micellar media to acquire an in depth knowledge of the mechanism [8-9]. The kinetics of oxidation of the hexacyanoferrate(II) complex by various reagents in acidic and basic media have been studied and, all these investigations have been applied to specific analytical problems [10-13]. $K_4[Fe(CN)_6^{4-}]$ hardly undergoes exchange reaction as CN^- itself is a very strong ligand although slow exchange of labelled CN^- group or aminopyridine is slow but under the action of u.v. light reversible aquation occurs leading to the formation of $[Fe(CN)_5H_2O]^{3-}$[14]. However, only monosubstituted $[Fe(CN)_5L]^{3-}$ has been obtained either through photochemical or dissociation reaction or by metal catalysed substitution reaction[15].

$$[Fe(CN)_6^{4-}]+H_2O \longrightarrow [Fe(CN)_5H_2O]^{3-}+CN^- \quad (1)$$

Hexacyanoferrate(II) reacts with EDTA according to the following equation

$$[Fe(CN)_5H_2O]^{3-} + EDTA \longrightarrow [Fe(CN)_5EDTA]^{3-} + H_2O \quad (2)$$

$$CN^- + H_2O \longrightarrow HCN + OH^- \quad (3)$$

Mercury(II) readily forms complex with cyanide ion but decomposes in uv light.

$$Hg^{2+} + [Fe(CN)_6^{4-}] + H_2O \longrightarrow [Fe(CN)_5H_2O]^{3-} + HgCN^+ \quad (4)$$

$$HgCN^+ + H^+ \longrightarrow HCN + Hg^{2+} \quad (5)$$

In the present work we have studied the kinetics of substitution of CN^- by EDTA, catalysed by Hg^{2+}. A probable mechanism has been proposed. Any attempt to study the substitution of CN^- by phenanthroline, pyridine, hydrazine and piperazine resulted in precipitation even in low concentration.

EXPERIMENTAL

Double distilled, de-ionized water was used throughout.The chemicals used were of analytical grade. Stock solutions of the compounds were wrapped with carbon paper to protect them from photodecomposition. The mercury(II) and hexacyanoferrate(II) solutions were diluted just before use. The desired pH= 5 of the reaction mixture was maintained by KHP-NaOH buffer [16]. The ionic strength was maintained at 0.1 M by adding appropriate amount of KNO_3

Procedure

A mixture of 2.0 ml of each EDTA, phthalate buffer of pH = 5.0 and mercury(II) chloride were mixed in a flask thermally equilibrated for about 30 minutes at 25^0C and left to stand for 10 min to ensure completion of reaction. Finally, 2.0ml of $[Fe(CN)_6]^{4-}$ was added to this mixture and the wavelength of maximum absorption (365 nm) was determined (Fig.1).

RRSULTS AND DISCUSSION

Effect of pH

The reaction was studied first by fixed time kinetic method in the pH range 1-13. (measured at t =5 and 10 minutes after mixing the reagents) Fig.2 shows plots of absorbance versus pH of the reaction mixture. It was found that, the absorbance increases with increasing pH and attains a maximum between pH 5.0 and 5.5. However, above this pH the absorption decreases which is due to the deficiency of protons. The rate is reduced at low pH due to the formation of various protonated forms of $[Fe(CN)_6]^{4-}$ which are less reactive than $[Fe(CN)_6^{4-}]$ itself [17].

Effect of EDTA

The complex formation with EDTA is influenced by a change in pH of the solution which is either perhaps due to ionization of the metal complex at low pH or hydrolysis of the metal ion at higher pH. The effect of EDTA was examined as a function of its concentration at 5 pH. A plot of initial rate versus EDTA shows slow change in rate constant (Fig. 3) in varied 2×10^{-5} to 7×10^{-5} M and finally decreases at still higher concentrations. A fixed concentration of 4×10^{-4} M was thus selected as optimum.

Effect of $[Fe(CN)_6]^{4-}$ on the initial rate

The initial rate were evaluated as a function of $[Fe(CN)_6^{4-}]$ by changing its concentration from 5×10^{-4} to 2×10^{-2} M, keeping all other parameters constant. The plot of log Vi versus log $[Fe(CN)_6^{4-}]$ (Fig 4) indicates variable

order of dependence in $[Fe(CN)_6^{4-}]$ is exhibited ranging from first order to higher concentration but certainly not tending towards zero order.

Effect of $[Hg^{2+}]$ on initial rate

The concentration of mercury(II) was varied between ($1x10^{-5}$ to $2x10^{-3}$M) and those of the $[Fe(CN)_6^{4-}]$ and EDTA were kept constant. The pH and temperature were maintained at 5 and, 25^0C respectively (Fig. 5). The large variation in $[Hg^{2+}]$ was selected in order to test the linearity between initial rate and $[Hg^{2+}]$ for its analytical application. A plot of the absorbance measured at an interval of one min versus $[Hg^{2+}]$ as a function of pH (Fig. 5) indicates that the rate increases linearly until the ratio of the $[Fe(CN)_6^{4-}]$ and $[Hg^{2+}]$ reaches 1:1.When the concentration of $[Hg^{2+}]$ exceeds that of $[Fe(CN)_6^{4-}]$ the absorption begins to diminish and follows a non –linear pattern. The intercept computed from the initial linear portion of the fig.5 provides the rate due to the uncatalyzed path. However, decline in the rate of reaction at higher $[Hg^{2+}]$ is probably due to the formation of a binary adduct, $[Fe(CN)_6^{4-}.\ 2HgCl_2]$. In a separate experiment it was observed that a white precipitate is formed immediately after mixing $[Fe(CN)_6^{4-}]$ with $[Hg^{2+}]$ in1:2 molar ratio which rapidly turned blue, confirming the formation of a binuclear complex. A similar observation has also been made by Beck [18].

Effect of temperature and ionic strength

The rate of the $[Hg^{2+}]$ catalyzed ligand exchange between $[Fe(CN)_6^{4-}]$ and EDTA was studied as a function of temperature in the range 20-30^{0}C. The higher temperature was avoided due to the possibility of decomposition of $[Fe(CN)_5EDTA]^{3-}$. The Arrhenius equation was used to determine the activation energy (Ea) for the catalyzed reaction. The enthalpy ($\Delta H^{\neq}$) and entropy of activation ($\Delta S^{\neq}$) were calculated using Eyring equation. The values of activation parameters were found to be Ea = 78.2 KJ mol^{-1}, $\Delta S^{\neq}$ = -48.67 $K^{-1}J\ mole^{-1}$ and $\Delta H^{\neq}$ = -52.5 KJ $mole^{-1}$.The effect of ionic strength on the initial rate of reaction was also studied by varying the ionic strength between 0.015 and 0.2 M range. The higher ionic strength was avoided due to the limited solubility of (KNO_3). When KCl was used to maintain the ionic strength the rate was found to decrease considerably. This is probably due to a subsequent decrease in $[Hg^{2+}]$ or $[HgCl^{+}]$ along with the ion-pair formation between $[Fe(CN)_6^{4-}]$ and $[Hg^{2+}]$ [19].

The following scheme for the mercury(II) catalyzed ligand exchange between $[Fe(CN)_6^{4-}]$ and EDTA has been proposed:

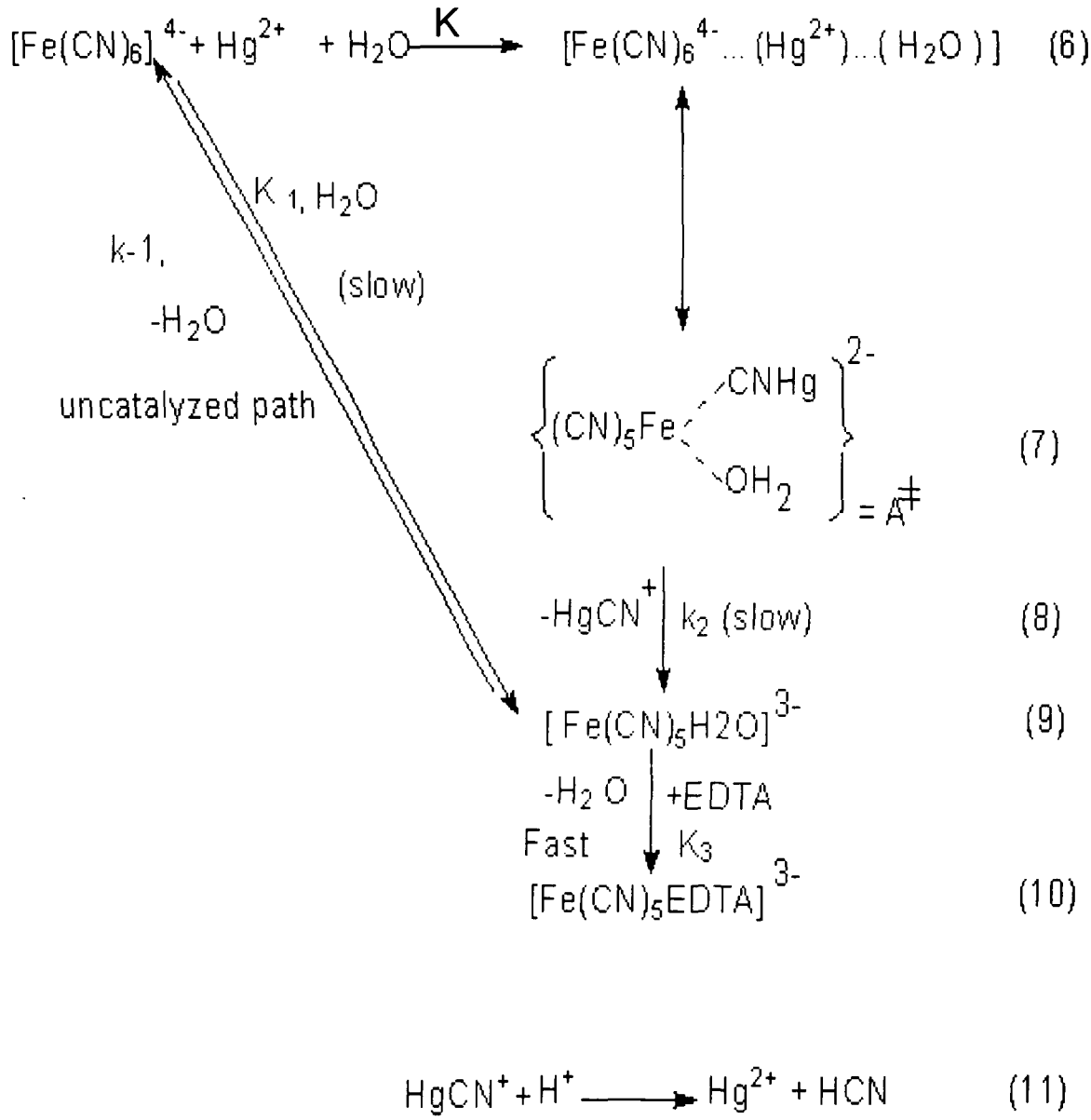

Formation of the complex, $[Fe(CN)_5EDTA]^{3-}$ through the catalyzed path can be written as:

$$d[Fe(CN)_5EDTA]^{3-}/dt = K_2[A^{\neq}] \quad (12)$$

while that for the uncatalyzed path the

$$rate = k'[Fe(CN)_6^{4-}] \quad (13)$$

where, k′ is a composite rate constant involving a concentration term. If the rate determining step is taken to be the composition of the activated complex ($A^{\neq}$), the activity of the mercury(II) at low concentration can be easily explained by the above mechanism. The overall rate for uncatalyzed reaction can be expressed through equation (13) using a non limiting concentration of EDTA .

$$Rate = d[Fe(CN)_5EDTA]^{3-}/dt = k'[Fe(CN)_6^{4-}] + \frac{k_2K[Fe(CN)_6^{4-}][Hg^{2+}][H_2O]}{1+K[Fe(CN)_6^{4-}]} \quad (14)$$

The second term in the above equation refers to the rate of the catalyzed reaction and explains the variable order dependence in $[Fe(CN)_6^{4-}]$. K is defined as the equilibrium constant for the association of the mercury(II) with water and $[Fe(CN)_6^{4-}]$. Since water is in a large excess, the equation (14) is reduced to equation (15)

$$Rate = k'[Fe(CN)_6^{4-}] + k'_2K[Hg^{2+}][Fe(CN)_6^{4-}] \quad (15)$$

Now equation (15) yields the observed rate constant (k_{obs}) as expressed by equation (16)

$$k_{obs}=k'+k'_2K[Hg^{2+}] \quad (16)$$

where, $k'_2 = k_2 + [H_2O]$.

A plot of the initial rate versus $[Hg^{2+}]$ at low $[Fe(CN)_6^{4-}]$ is given in fig.6.

In case of higher $[Fe(CN)_6^{4-}]$, equation (14) takes the form of equation (17).

$$\text{Rate} = k' [Fe(CN)_6^{4-}] + k_2'[Hg^{2+}] \quad (17)$$

The value of the initial rate (V_i) as a function of $[Hg^{2+}]$ at low $[Fe(CN)_6^{4-}]$ is listed in table 1.The k' and k_2' have been calculated from fig.6 of initial rate versus $[Hg^{2+}]$ using equation (17) at specified experimental condition. The rate constant k' and k_2 are found to be 4.17×10^{-3} S^{-1} and 2.50 S^{-1} respectively, at I = 0.1M, pH = 5, temp = 25 ^{0}C. The value of k_1' and k_2 so obtained are substituted in equation (17) to evaluate the equilibrium constant K at various $[Hg^{2+}]$ at low $[Fe(CN)_6^{4-}]$. The K (Table 1) and the average value of log K (2.80) in our case is comparable with that reported by Beck for $[Fe(CN)_6^{4-}.Hg(CN)_2]$ complex (log = 2.38) [17]. Although the values of k_2 have been calculated employing high $[Fe(CN)_6^{4-}]$ using equation (17) it can be obtained even at low $[Fe(CN)_6^{4-}]$ using equation (18).

$$k_2 = \frac{\text{Rate} - k'[Fe(CN)_6^{4-}]}{K[Fe(CN)_6^{4-}][Hg^{2+}][H_2O]} \quad (18)$$

However, the values calculated from this equation are almost identical. The ionic

behavior of $[Hg^{2+}]$ may be represented by the following reactions.

$$Hg^{2+} + Cl^- \underset{}{\overset{k_1}{\rightleftharpoons}} HgCl^+$$

$$HgCl^+ + Cl^- \underset{}{\overset{k_2}{\rightleftharpoons}} HgCl_2$$

It has been shown that when $Hg(NO_3)_2$ reacts with $[Fe(CN)_6^{4-}]$ in solution the resultant was $Hg_2[Fe(CN)_6^{4-}]$ [20], which has also been verified from the absorption spectra of both the reacting components and the eventual product. This is quite obvious because the $[Hg^{2+}]$ is more electropositive than K^+ ion. The activation energy calculated for this reaction is lower than those reported [21-22] for the replacement of CN^- in nearly similar reaction systems. The entropy of activation is negative which is obvious if the virtual solvations of the activated complex and its highly charged dissociation products are considered. Thus, the activation parameters provide further support to the proposed mechanism.

CONCLUSION

In the present work we have studied the kinetics of substitution of CN^- by EDTA catalyzed by $[Hg^{2+}]$. A probable mechanism of the reaction has been

proposed. The results presented here clearly demonstrate that the chelating agent EDTA was used for the neutralization of CN^- in complex formation which is more effective and inexpensive. The values of thermodynamic parameters are Ea = 78.2 KJ mol^{-1}, $\Delta S^{\neq}$ = -48.67 JK^{-1} $mole^{-1}$ and $\Delta H^{\neq}$ = -52.5 KJ mole-1. The negative value of the parameters show the exothermic nature of reaction.

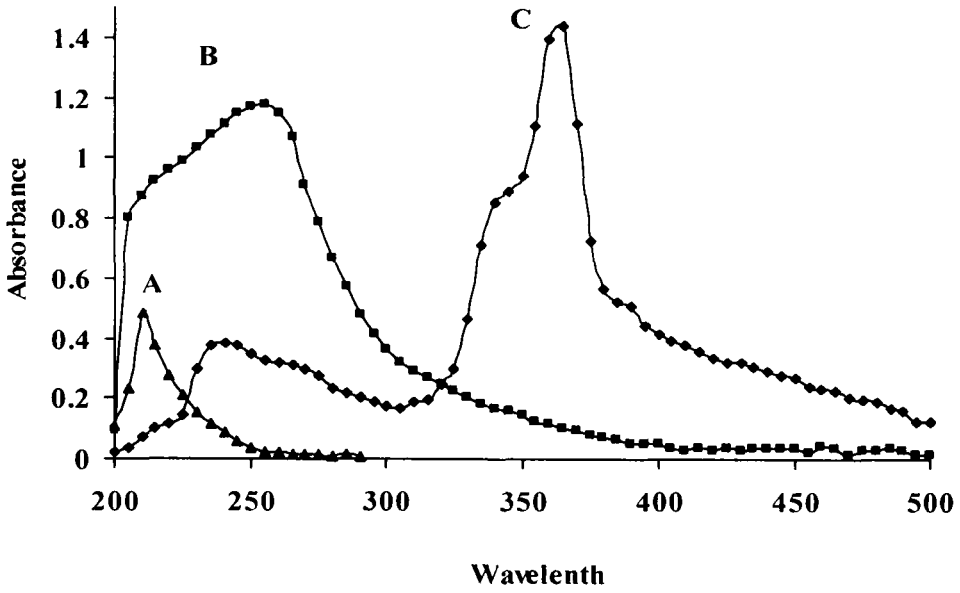

Fig.1 Absorption spectra of reactants and products: (A) [EDTA] = $1X10^{-3}M$; (B)$[Fe(CN)_6]^{4-}$ =$5X10^{-4}$ M (C) $[Fe(CN)_6]^{4}$ ($4X10^{-4}$ M) +[EDTA]($4X10^{-3}$M) + $[Hg^{2+}]$($3X10^{-5}$ M)at pH = 5.0

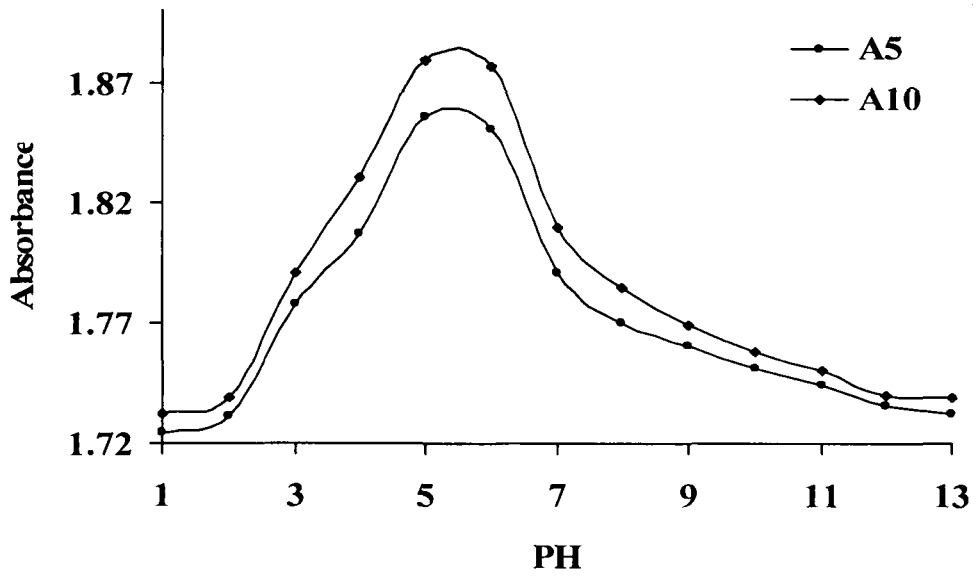

Fig.2 Effect of pH on Hg^{2+} catalysed substitution of CN^- in hexacyanoferrate(II) by EDTA , $[Fe(CN)_6^{4-}] = 5X10^{-3}M$, EDTA = $X10^{-5}M$, $[Hg^{2+}] = 3X10^{-5}$ M , Temp = 25^0C and I = 0.1M (KNO_3).

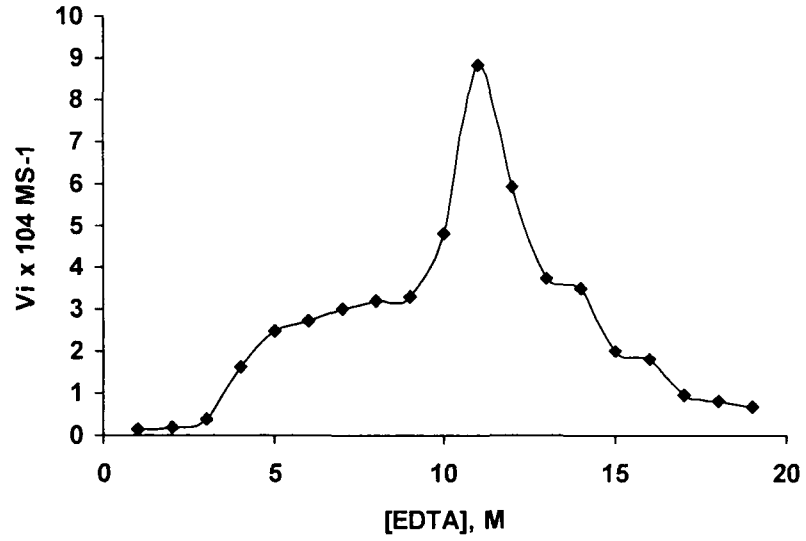

Fig.3 Effect of EDTA on initial rate, $[Fe(CN)_6^{4-}]$ = 3.5X10^{-2} M, $[Hg^{2+}]$ = 3x10^{-5} M, pH = 5, Temp =25^{0}C and I = 0.1M (KNO_3)

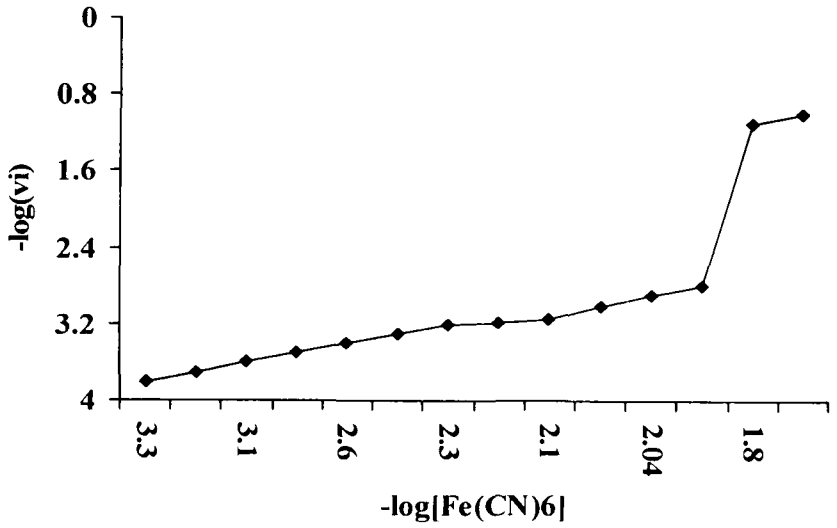

Fig.4 Dependence of the initial rate on $[Fe(CN)_6^{4-}]$ in presence of $[Hg^{2+}]$ [EDTA] 3x10^{-4}M, $[Hg^{2+}]$ = 3x10^{-5} M, pH 5.0, temp = 25^{0}C and 0.2 M (KNO_3).

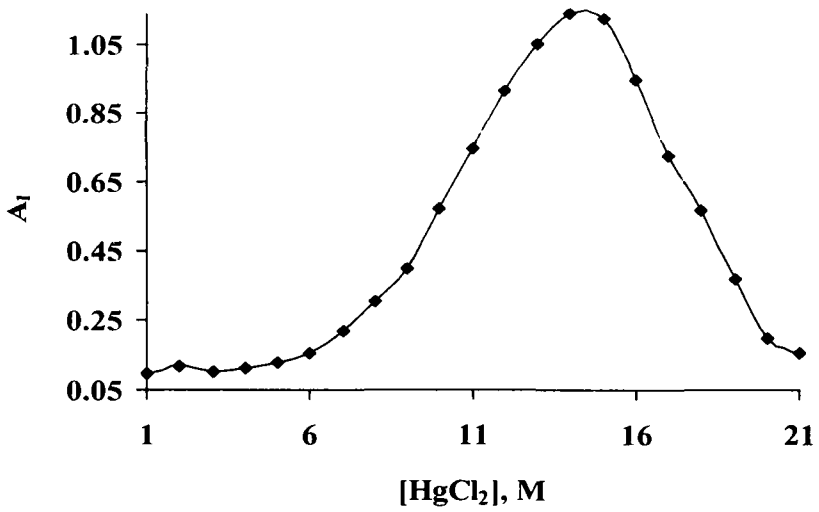

Fig.5 Dependence of the initial rate of substitution of CN^- in $[Fe(CN)_6^{4-}]$ by EDTA on $[HgCl_2]$, $[Fe(CN)_6^{4-}] = 3.5x10^{-3}$ M, [EDTA] = $3x10^{-4}$ M, pH = 5 , temp = 25^0C and I = 0.1 M (KNO_3).

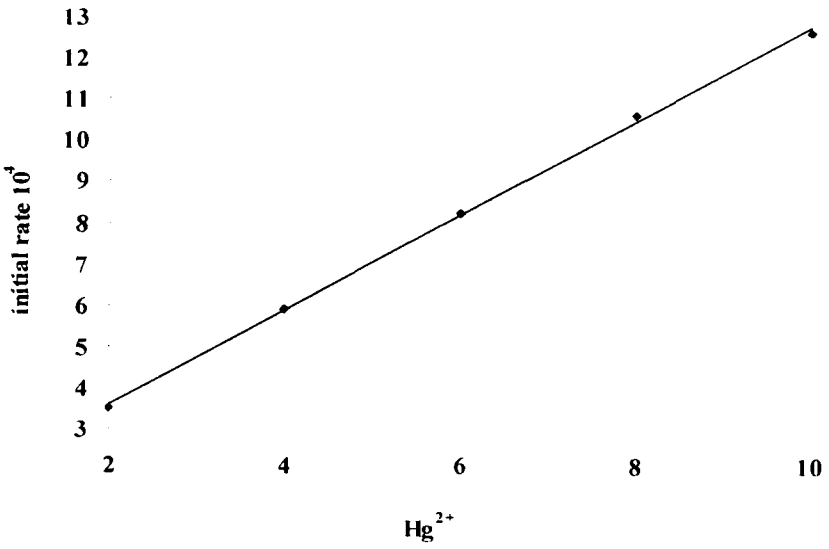

Fig.6 Effect of variation of $[Hg^{2+}]$ on initial rate (Vi) at high concentration of $[Fe(CN)_6^{4-}]$ under the condition $[Fe(CN)_6^{4-}] = 8\times10^{-4}$ M , [EDTA]= 5×10^{-4} M, pH = 5 , temp. = 25^0C, I = 0.1 M (KNO_3).

Table1. Calculation of K by varying $[Hg^{2+}]$ at constant $[Fe(CN)_6^{4-}]$. $[Fe(CN)_6^{4-}] = 8x10^{-4}$ M, $[Hg^{2+}] = 5X10^{4-}$ M, pH = 5, temp= 25^0C and I = 0.1 M (KNO_3).

$[Hg^{2+}] \times 10^{-4}$ (M)	Vi x 10^4	K(calcd.)
2	3.5	709.07
4	5.9	660.02
6	7.9	610.60
8	10.6	625.80
10	12.6	601.80
	Average log k = 2.80	

REFERENCES

[1]. E.A. Abu-Gharib, R. Ali, M..J. Blandamer and J. Burgess: Trans. Met. Chem., 12, 371(**1987**)

[2]. G. Stochel and R.V.Eldik: Inorg. Chim. Acta. (and refs. therein).,155, 95 (**1989**)

[3]. S.D.S.S. Borges, A.L. Coelho, I.S. Moreira and M.A.B.D. Araujo: Polyhedron, 13, 1015 (**1994**)

[4]. S. Alshehri: Trans. Met. Chem., 22, 553(**1997**)

[5]. I. Maciejowska, Z..Stasicka, G. Stochel and R.V.Eldik: J.Chem.Soc., 3643 (**1999**)

[6]. G. Fernandez, M.G.M. Del, A. Rodriguz, M.Munoz and M.L. Moya: React Kinet. Cat. Lett., 70, 389 (**2000**)

[7]. E.M.Sabo, R.E. Shepherd, M.S. Rau and M.G. Elliott: Inorg. Chem. , 26, 2897 (**1987**)

[8]. M.D. Fernando, J. Refael, G.H. Carlos and S. Francisco: New J. Chem. , 23, 1203 (**1999**)

[9]. G. Fernandez, M.G.M. Del, A. Rodriguz, M. Munoz and M.L Moya: J. Colloid Interf. Sci., 47,225 (**2000**)

[10]. R. He and J. Wang: Xiyou Jinshu Cailiao Yu Gongcheng., 28, 60(1999) Chem. Abstr., 130, 275849g. (**1999**)

[11]. A. Zmikic, D. Cvrtila, D. Pavlovic, I.Murati, W. Reynolds and S. J. Asperger :Chem. Soc., Dalton Trans.,1284 (**1973**)

[12].Y.L. Feng, H.Narasaki, L.C.Tian, S.M. Wu and H.Y. Chen: Anal. Sci., 15, 915 (**1999**)

[13]. S.Prasad : *J.Anal.Chem.*60,581(**2005**)

[14].T. Alam and Kamaluddin:Bull. Chem. Soc. Jpn., 72, 1697(**1999**)

[15]. A.G. Sharpe: The Chemistry of Cyano Complexes of Transition Metals, Academic Press, London, p. 1081, 1262**(1976)**

[16].R.C. Weast: CRC Handbook of Chemistry and Physics, The Chemical Rubber Co., Ohio, 49th edit., D-79**(1969)**

[17].W.A. Eaton, P. George and G.H. Hanaria: J. Phys. Chem. , 71, 2016 **(1967)**

[18]. M.T. Beck, and A. Fourteen: Magic Number of Coordination Chemistry, Proc. XX ICCC, Calcutta, India **(1979)** In Coordination Chemistry-20, Pergamon Press, Oxford, p. 31**(1979)**

[19]. M. Kimura, S. Yuko, K. Shinobu and T.Keiichi: Bull.Chem. Soc., 72, 1293 **(1999)**

[20].B. Athos, D. M. Domenico and C. Agatino: Talanta,22,197 **(1975)**

[21].B.R. Reddy and S. Raman:Indian J. Chem., 23A, 616 **(1984)**

[22]. S. Raman, Indian J. Chem. 19, 907**(1980)**

Chapter- 6

Spectrophotometric interaction of the Oxidation of Captopril by Hexacyanoferrate(III) in Alkaline Medium: A Kinetic and Mechanistic Approach

INTRODUCTION

Captopril,(*2S*)-1-[(*2S*)-2-methyl-3-sulfanylpropanoyl]pyrrolidine-2-carboxylic acid (CPL) (Fig. 1) is a well-known prescribed for the treatment of hypertension and heart failure [1-2]. It inhibits the active sites of a zinc glycoprotein, the angiotensin I converting enzyme (ACE), blocking the conversion of angiotensin I to angiotensin II, whose levels are elevated in patients with hypertension. CPL has three different potential donor groups (S_{thiol}, $O_{acid,}$ and O_{amide}) which may bind metal ions. It has been shown that the ratio of the metal:drug in the complex varies with change in pH of the mediam. The drug forms 1:1 acidic and 1:2 complex in nearly basic media respectively [3]. There exists an equilibrium between cis and trans isomers of the drug, however, the trans isomer is the active form when bound to the enzyme [4]. On the other hand the sulfhydryl group in the drug acts as a free radical scavenger [5-6]. Several methods have been reported, for the analysis of CPL in

pharmaceutical preparation. It has also been assayed spectrofluorimetrically after reacting with fluorogenic reagents [7-8]

The chemistry of hexacyanoferrate(III) in alkaline medium is well understood, in particular its capacity to oxidise inorganic and organic compounds [9-17]. Since there is no report on the oxidation of CPL by hexacyanoferrate(III) in alkaline medium, we have under taken this work to investigate the redox chemistry of hexacyanoferrate(III) in this medium and arrive at a suitable mechanistic pathway for the process.

EXPERIMENTAL

Reagents and Materials

Reagent grade chemicals and double-distilled water were used throughout. An aqueous solution of $K_3[Fe(CN)_6]$ (BDH) in water and was standardized iodometrically [18]. CPL (Across organics), NaOH, (Merck Ltd, India), NaCl and HCl (Ranbaxy fine chem. Ltd, India) were used as received.

Kinetic Measurements

A mixture of $[Fe(CN)_6]^{3-}$, and [CPL] containing required amounts of NaOH, and NaCl was thermostated. The progress of the reaction was followed

by a decrease in absorbance maximum, 420 nm, of $[Fe(CN)_6]^{3-}$ as a function of time. The spectrophotometer was attached to a desktop computer with the required program to evaluate the kinetic data. The Beer's law (420 nm) was obeyed in concentration range (8.0×10^{-5} to 8.0×10^{-4} mol dm^{-3}) (ε = 1060 + 1.5% dm^3 mol^{-1} cm^{-1}). The pseudo-first-order rate constant k_{obs} was calculated from the slopes of log absorbance versus time plot and, was reproducible within (5%).The plots were linear up to 80% completion of reaction (Fig.2).

RESULTS AND DISCUSSION

Effect of CPL Concentration

The effect of the CPL concentration on the rate of its oxidation was investigated by alkaline $[Fe(CN)_6^{3-}]$, pH (7.8) and ionic strength (0.50 mol dm^{-3}) was investigated at 25^0C. The concentration of $[Fe(CN)_6^{3-}]$ were kept constant and, that of CPL was varied (1.0×10^{-4} -1.0×10^{-3} mol dm^{-3}). It was found that the k_{obs} increases with increasing concentration of CPL (Table 1).

Effect of NaOH Concentration

Keeping all other conditions constant, $[OH^-]$ was varied (0.05 to 0.40 mol dm^{-3}).It was noticed that with increasing $[OH^-]$ the rate of reaction was also increases (Table 1).

Effect of [Hexacyanoferrate(III)]

The effect of $[Fe(CN)_6]^{3-}$ concentration (8.0×10^{-5}-8.0×10^{-4} mol dm^{-3})was found to be unity as the plot of log $[Fe(CN)_6^{3-}]$ versus time was linear with non- variation in slopes for different $[Fe(CN)_6]^{3-}$ (Table 1).

Polymerization Study

The oxidation of organic compounds by $[Fe(CN)_6]^{3-}$ is expected to occur the free radical generated by CPL. The formation of free radical during the reaction was ascertained by an initial addition of monomer, acrylonitrile followed by dilution with methanol, which resulted in a copious precipitation.

Reaction Orders

The order of the reaction was determined from a plot of the slope of log k_{obs} vs log of drug (concentration). The CPL concentration was varied (1.0×10^{-4} -1.0×10^{-3} mol dm^{-3}) a plot of log (absorbance) vs time was linear up to 80% completion of the reaction as (Fig 2.). It indicates a unit order dependence on $[Fe(CN)_6]^{3-}$ concentration. It was also confirmed by varying $[Fe(CN)_6]^{3-}$ concentration which did not result in any change in the pseudo-first-order rate

constants, k_{obs} (Table 1). The k_{obs} increases with increasing in concentration of CPL (Table 1). The effect of alkali on the reaction was studied in the range of 0.05 to 0.4 mol dm^{-3} at constant concentrations of CPL, $[Fe(CN)_6]^{3-}$ and ionic strength. The rate constant increases with increasing alkali concentration and, the order was found to be less than unity.

Stoichiometry of the reaction

Five set of reaction mixture containing CPL,OH^- and $[Fe(CN)_6]^{3-}$ were taken .The mixture was left to stand for 24 h at 25°C and then absorbance was measured. The λmax (420nm) was determined (Fig. 3). The stoichiometry of the reaction was studied adopting the limiting logarithmic method [19]. The ratio of the reaction between log Abs versus log [CPL] and log $[Fe(CN)_6]^{3-}$ were calculated by dividing the slope of $[Fe(CN)_6]^{3-}$ by the slope of the CPL curve. It was found that, the ratio was 1:3 .The proposed pathway as shown in eq.1.

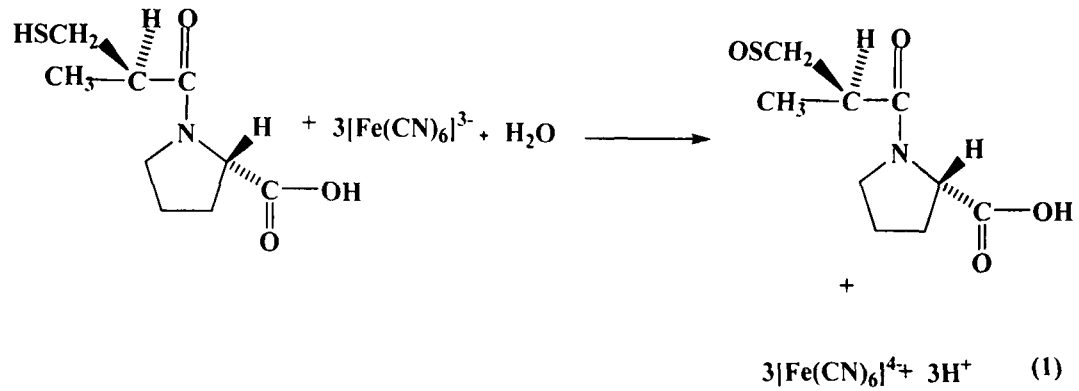

(1)

Evaluation of Ea, $\Delta H^{\#}$, $\Delta G^{\#}$ and $\Delta S^{\#}$

The oxidation of CPL by $[Fe(CN)_6]^{3-}$ was investigated constant pH and ionic strength at four temperatures (Table 2). *E*a was calculated from the Arrhenius plot of log k_{obs} vs $1/T$, (81.0 ±.02 kJ.mol^{-1}) indicate positive higher activation energy showes the rate increases at higher temperature. Other thermodynamic parameters were calculated applying Eyring equation

$$\text{Log K/T} = [\text{ log kb/h} + \text{S/2.302R}] - \Delta\text{H/ 2.303R1/T}$$

$\Delta H^{\#}$ was evaluated from the slope (-ΔH/ 2.303R1/T) and $\Delta S^{\neq}$ from the intercept [log kb/h + S/2.302R] of the compiled Eyring plot. The Gibbs free energy of activation was determined by $\Delta G^{\neq}$ = -2.303 RTlogK at room temperature (Table.2).

Effect of Ionic Strength and Dielectric Constant

The ionic strength was varied (0.1 and 0.9 mol dm^{-3}) by the addition of sodium chloride keeping the concentrations of other components constant. The apparent first-order rate constant showed a nearly ten-fold increase (Table 3). A plot of log k_{obs} versus I was linear with a unit positive slope (Fig 4).

The dielectric constant (*D*) of the medium was varied by varying the *tert*-butyl alcohol / H_2O percentage (v/v). Since the *D* for various percentage compositions was not available in literature, they were computed by using their *D* in pure state. The plot of log k_{obs} versus 1/*D* was found to be linear with positive slope (Fig 4) and showed that as *D* decreases the k_{obs} increased (Table 3).

Keeping all other conditions constant the concentrations of the oxidant HCF(III), substrate (CPL) and alkali was varied. The reaction fallowed the first-order. Based on the experimental results, a mechanism can be proposed for which all the observed orders for each constituent such as [oxidant], substrate and [OH^-] may be well accommodated. Oxidation of CPL by HCF(III) in NaOH medium is a non-complementary reaction with oxidant undergoing six equivalent changes.

The substrate with HCF(III) formed complex C in alkali medium decomposes in slow step to a free radical. further reacts with one mol of HCF(III) in aqueous medium to give an intermediate product of CPL and HCF(II). The intermediate product of CPL reacts with one mol of HCF(III) in fast steps to give the product, (*2S*)-1-[(*2S*)-2-methyl-3-sulfinyl propanoyl] pyrrolidine-2-carboxylic acid and HCF(II). Another two mole of free radical of CPL in fast step to form the final products, (2S,2-S)-1,1-

[disulphanediylbis[(2S)-2-ethyl-1-oxopropane-3,1-diyl]-bis[pyrrolidine-2-carboxylic] acid (captopril-disulphide) satisfying the stoichiometry. The results can be accommodated by Scheme 1.

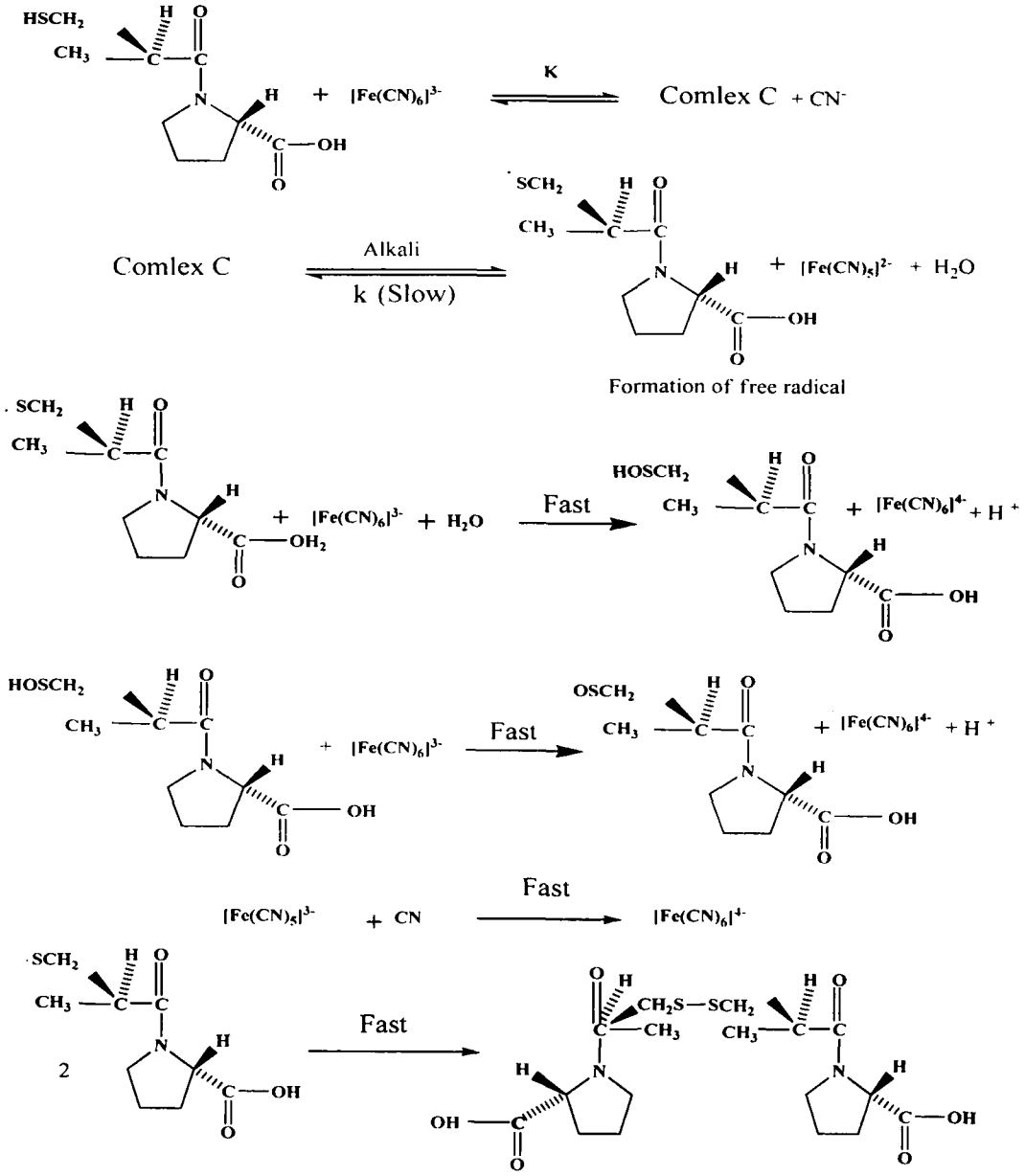

SCHEME. 1

The probable structure of the complex is

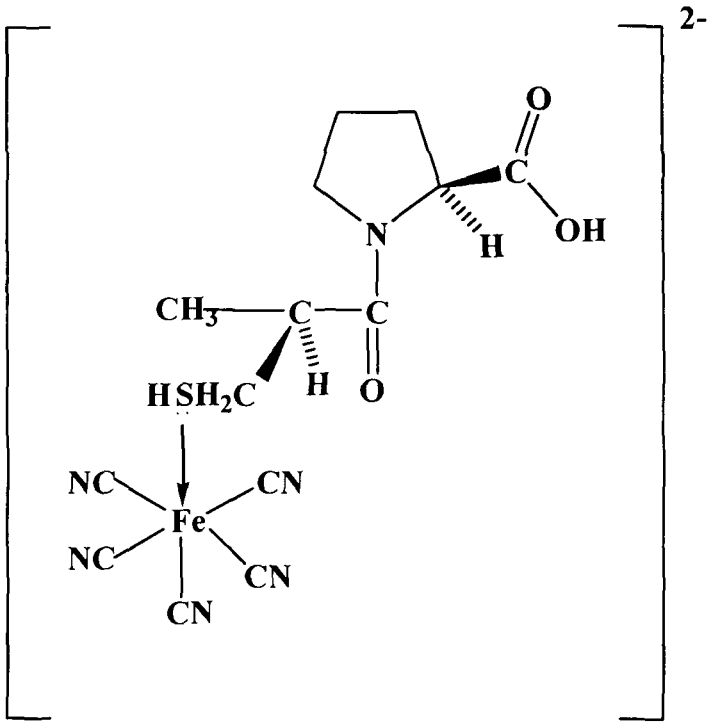

Complex (C)

The results can be verified by Spectrophotometric measurements of the complex c (A hypsochromic shift, of complex C ca. 10 nm from 350 to 360 nm is observed together with hyperchromicity at 360 nm). Analogous effects upon complex formation between a substrate and an oxidant have been observed in other investigations [20]. Further, the formation of complex is also proved kinetically by the non-zero intercept of the plot of $1/k_{obs}$ vs $1/[OH^-]$ and $1/k_{obs}$ vs 1/[CPL] (Fig. 5). The modest enthalpy of activation, relatively low entropy of activation, and higher rate constant for the slow step, indicate that the

oxidation presumably occurs by the use of an inner-sphere mechanism [21]. Scheme 1 is in accordance with the generally accepted principle of non-complementary oxidation taking place in sequence of one electron step.

The rate law for the mechanism (Scheme 1) may be derived as-

$$\text{Rate} = \frac{d[Fe(CN)_6^{3-}]}{dt} = \frac{k K [Fe(CN)_6^{3-}][CPL][OH^-]}{(1+ K[Fe(CN)_6^{3-}])(1+ K[CPL])} \quad (2)$$

$$\text{Rate} = \frac{k K [Fe(CN)_6^{3-}][CPL][OH^-]}{1+ K[CPL] + K[Fe(CN)_6^{3-}](1+ K[CPL])} \quad (3)$$

or

$$\textbf{Rate} = \frac{\boldsymbol{k K [Fe(CN)_6^{3-}][CPL][OH^-]}}{\boldsymbol{1+ K[CPL] + K[Fe(CN)_6^{3-}]+ K[CPL]K[Fe(CN)_6^{3-}]}} \quad \textbf{(4)}$$

or

$$\textbf{Rate} = \frac{\boldsymbol{k K [Fe(CN)_6^{3-}][CPL][OH^-]}}{\boldsymbol{1+ K[CPL] + K [Fe(CN)_6^{3-}]+ K^2[CPL] [Fe(CN)_6^{3-}]}} \quad \textbf{(5)}$$

Since the terms $K[Fe(CN)_6^{3-}]$ and $K^2[CPL]\ [Fe(CN)_6^{3-}]$ in the denominator in Eq. (5) are negligible compared to unity in view of the low concentration of $[Fe(CN)_6^{3-}]$.

The Eq. (5) becomes

$$\text{Rate} = \frac{k\,K\,[Fe(CN)_6^{3-}][CPL]\,[OH^-]}{1+K[CPL]} \qquad (6)$$

$$\frac{\text{Rate}}{[Fe(CN)_6^{3-}]} = k_{obs} = \frac{k\,K[CPL]\,[OH^-]}{1+K[CPL]} \qquad (7)$$

The rate law (7) can be rearranged to (Eq 8.)

$$\frac{1}{k_{obs}} = \frac{1}{kK[CPL]\,[OH^-]} + \frac{1}{k} \qquad (8)$$

According to Eq. (8), the plots of $1/k_{obs}$ vs $1/[OH^-]$ and $1/k_{obs}$ vs 1/[CPL] should be linear, (Fig.5).The slope and intercept of such plot the reaction constants, K and k were calculated as 10.2×10^{-2} dm^3mol^{-1}, 2.67×10^3 dm^3 mol^{-1} s^{-1}, respectively. Using these values rate constants under different experimental conditions were calculated and compared with experimental data (Table 1). There is a reasonable agreement between them. The effect of increasing ionic strength on the rate explains qualitatively the reaction between two negatively charged ions, as seen in complex C (scheme 1). The negative value of the entropy of activation indicates that the complex is more ordered than the

reactants [22]. The observed modest activation energy and large entropy of activation supports a transition state in the reaction.

CONCLUSION

In summary, the commercially more valuable CPL can be oxidized by hexacyanoferrate(III) in alkaline medium. The rate constant of the slow step and other equilibrium constants involved in the mechanism are evaluated and activation parameters with respect to the slow step of reaction were computed.

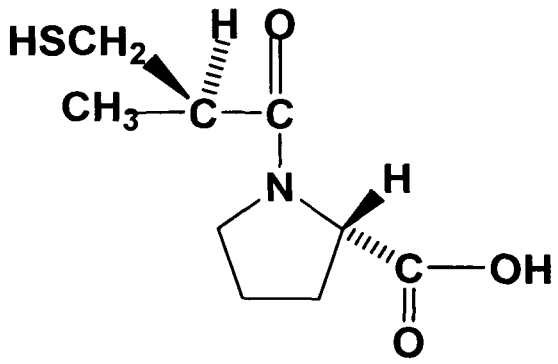

Fig.1 Structure of captopril

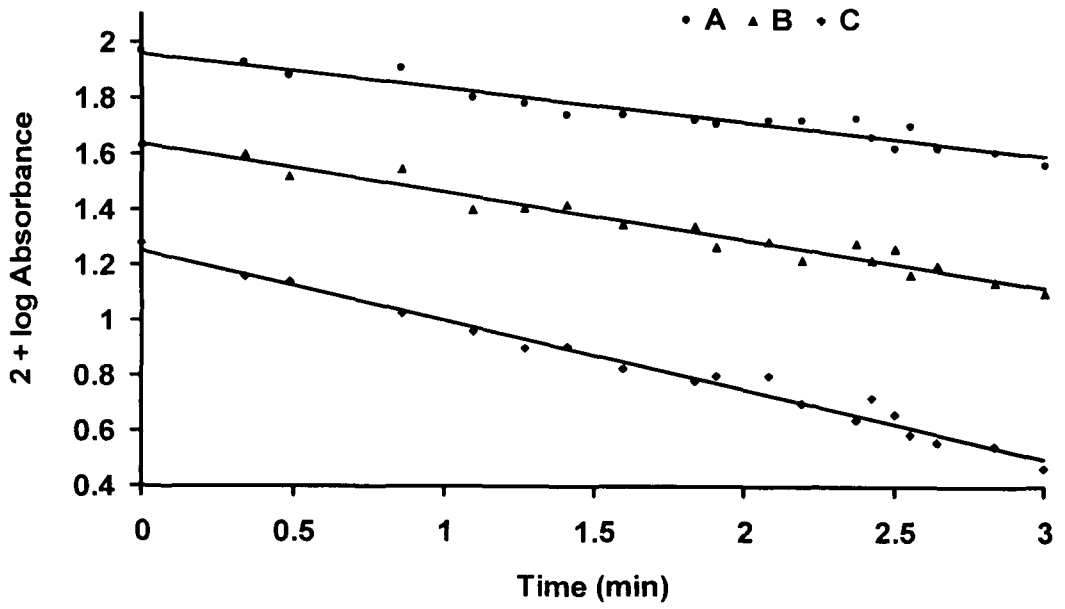

Fig.2 First-order plots for the oxidation of CPL by Hexacyanoferrate(III) in an aqueous alkaline medium at 25°C: [CPL] = 4.0 × 10^{-3} mol dm^{-3}; [OH^-] = 0.10 mol dm^{-3} and I = 0.5 mol dm^{-3}; [$Fe(CN)_6]^{3-}$ × 10^{-4} mol dm^{-3} (A) 1.0, (B) 3.0 and (C)5.0.

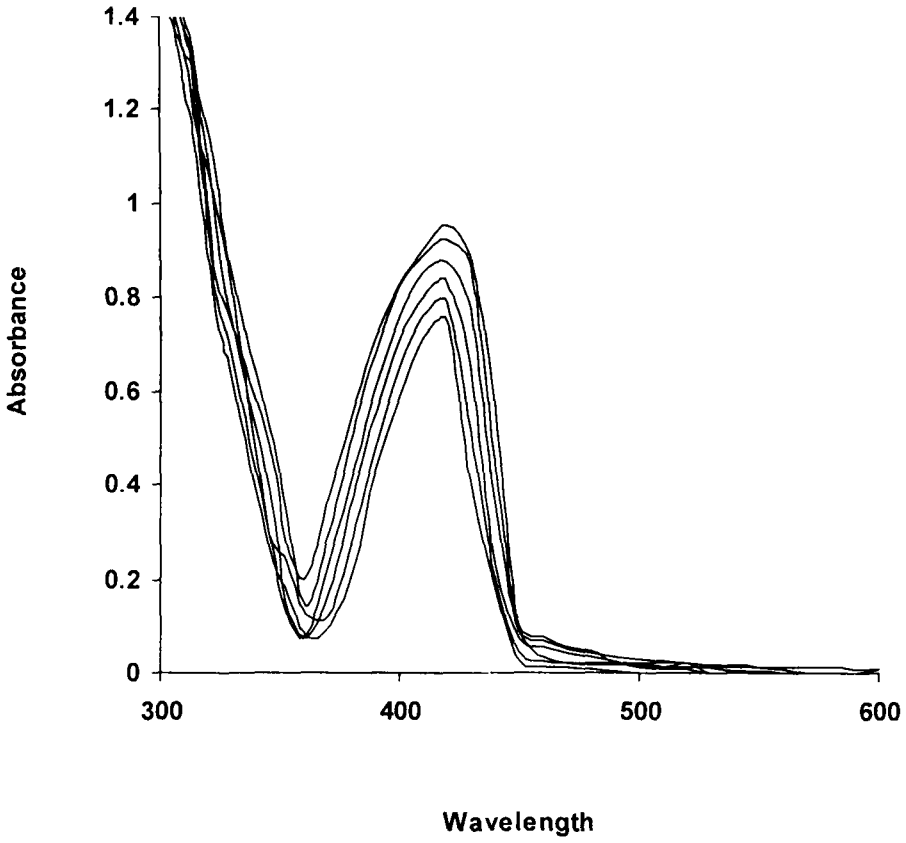

Fig.3 Spectral scan of the reaction mixture of $[Fe(CN)_6]^{3-}$, and CPL $[Fe(CN)_6]^{3-} = 4.0 \times 10^{-4}$ mol dm^{-3}, [CPL]= 4.0×10^{-3} mol dm^{-3}, Ionic Strength = 0.5 mol dm^{-3} (NaCl), and $[OH^-] = 0.10$ mol dm^{-3} at 25°C (scan after 1min)

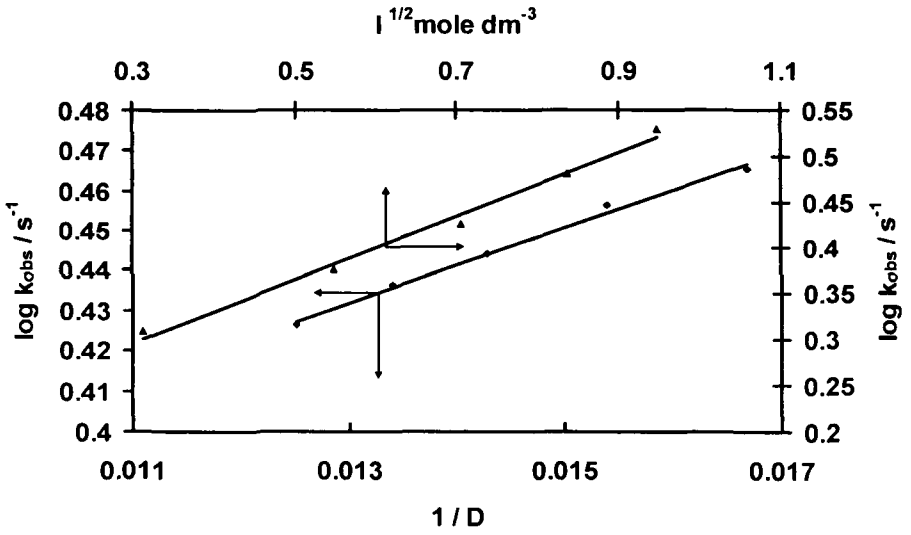

Fig. 4 Effect of ionic strength and dielectric constant on the oxidation of CPL by hexacyanoferrate(III) in alkaline medium at 25°C.

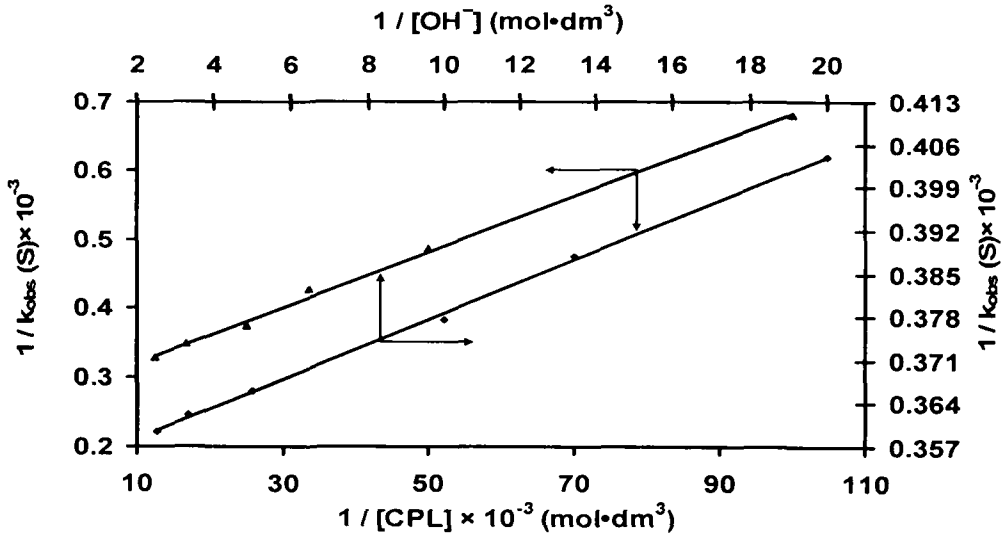

Fig.5 Verification of rate law eq 3 at a different [OH⁻] and [CPL] on oxidation of CPL by Hexacyanoferrate(III) in an aqueous alkaline medium at 25°C.

Table 1. Effect of Variations of $[Fe(CN)_6^{3-}]$, [CPL], and $[OH^-]$ on the Oxidation of CPL by $[Fe(CN)_6^{3-}]$ at 30 ◦C, I = 0.80 mol·dm^{-3}

$[Fe(CN)_6^{3-}] \times 10^4$	[CPL] × 10^3	$[OH^-]$(mol·dm^3)	$k_{obs} \times 10^3$ (s^{-1})	
			Observed	Calculated
Variation $[Fe(CN)_6^{3-}]$(mol·dm^3)				
0.8	4.0	0.10	2.61	2.67
1.0	4.0	0.10	2.66	2.67
2.0	4.0	0.10	2.65	2.67
4.0	4.0	0.10	2.67	2.67
6.0	4.0	0.10	2.69	2.67
8.0	4.0	0.10	2.65	2.67
Variation [CPL] (mol·dm^3)				
4.0	1.0	0.10	1.46	1.47
4.0	2.0	0.10	1.95	1.99
4.0	3.0	0.10	2.31	2.35
4.0	4.0	0.10	2.64	2.67
4.0	6.0	0.10	2.87	2.88
4.0	8.0	0.10	3.00	3.04
Variation $[OH^-]$(mol·dm^3)				
4.0	4.0	0.050	2.46	2.47
4.0	4.0	0.075	2.55	2.58
4.0	4.0	0.10	2.67	2.67
4.0	4.0	0.20	2.76	2.73
4.0	4.0	0.30	2.75	2.76
4.0	4.0	0.40	2.77	2.79

Table 2. Activation and thermodynamic parameters for the oxidation of CPL by hexacyanoferrate(III) in aqueous alkaline medium with respect to the slow step of Scheme 1.

(a) Effect of temperature:	
Temp. (K)	$k \times 10^3$ *(dm^3 mol^{-1} s^{-1})*
298	2.67
303	2.83
308	2.96
313	3.00
(b) Activation parameters:	
Ea (kJ·mol^{-1})	81.0±.02
$\Delta G^{\#}$ *(kJ·mol^{-1})*	76.5 ±.02
$\Delta H^{\#}$ *(kJ·mol^{-1})*	37± 10
$\Delta S^{\#}$ *(J·K^{-1} mol^{-1})*	-73.4 ±.02

Table 3. Effect of Ionic Strength and Dielectric Constant on the Oxidation of CPL by Hexacyanoferrate(III) in alkali medium at 25 °C.

ionic strength I		*dielectric constant D*	
D) 80.0		*I) 0.5 mol dm^{-3}*	
I	$k_{obs} \times 10^3$	*D*	$k_{obs} \times 10^3$
0.1 mol dm^{-3}	2.04	80.0	2.67
0.3 mol dm^{-3}	2.38	75.0	2.73
0.5 mol dm^{-3}	2.67	70.0	2.78
0.7mol dm^{-3}	3.03	65.0	2.89
0.9mol dm^{-3}	3.39	60.0	2.92

Note: $[Fe(CN)_6^{3-}] = 4.0 \times 10\text{-}4$, [CPL] = 4.0 × 10-3 and $[OH^-]$ = 0.1/ mol dm-3

REFERENCES

[1]. J. E. F. Reynolds: (Ed.), 31st Edition, Martindale, The Extra Pharmacopoeia, *The Pharmaceutical Press*, London, 821**(1996)**

[2]. N.E.Enany, F. Belal and M.Rizk: *Int. J of Biomedical Sci*, vol 4, No2, June **(2008)**

[3]. M. A. Hughes, G. L. Smith and D. R.Williams: *Inorg. chim. Acta,* 107, 247 **(1985)**

[4]. S. Cavalu, S. C. Pinzaru and V.Chis: *Romanian J. Biophys.17,* 195**(2007)**

[5]. K. Nakagawa, A. Ueno, Y. Nishikawa and Z. Yakugaku: *The pharmaceutical society of Japan. 126,* 37**(2006)**

[6]. M. Tamba and A.Torreggiani:*Free Radical Res.* 32, 199 **(2000)**

[7]. C. Chassaing, J. Gronin, C. S. Wilcox and I.W. Wainer: *J Chromatogr B: Biomed Appl.* 735, 219**(1999)**

[8]. K. S. Siddiqi, S. Bano, A. Mohd and A. A. Parwaz Khan: *Chinease Journal of Chemistry,* 27.1 **(2009)**

[9]. E. P Kelson and P. P. Phengsy: *Int. J. Chem. Kinet.* 32, 760**(2000)**

[10]. A. I. Vovk, I. V. Muraveva, V. P. Kukhar and V. F. Baklan: *Russ. J. Gen. Chem.* 70, 1108 **(2000)**

[11]. P. T. Speakman, and W. A. Waters: *J. Chem. Soc.* 40 **(1955)**

[12]. T. P. Jose, S. T. Nandibewoor and S. M. Tuwar: *J. Sol. Chem.* 35, 47**(2006)**

[13]. V. Singh, N. Singh, M. P. Saxena and B. B. L: *Indian J. Chem.*, 8, 529 **(1970)**

[14]. J. M. Leal, B.Garcia and P. L.Domingo: *Coord. Chem. Rev.*, 173, 79**(1998)**

[15]. S. M . Tuwar, S. T. Nandibewoor and J. R. Raju: *Trans. Met. Chem.* 16, 335 **(1991)**

[16]. T. P. Jose, M. A. Angadi, M. S. Salunke and S. M. Tuwar: *J. Mol. Struct.* 892, 121**(2008)**

[17]. K. Sharanabasamma, M. A. Angadi, M. S. Salunke, and S. M. Tuwar: *Ind. Eng. Chem. Res.* 48, 10381**(2009)**

[18]. J. Mendham, R. C. Denney, J. D. Barnes and M. J. K, Thomas: *Vogel's Text Book of QuantitatiVe Chemical Analysis*, 6th ed.; Pearson Education: Delhi, India, p 466 **(2003)**

[19]. H. E. Bent and C. L. French: J.Am.Chem.Soc.63,568 **(1941).**

[20]. J.M. Lancaster, R. S. J. Murray: Chem Soc A,2755**(1971)**

[21]. K.S.Rangappa,M.P.Raghavendra, D. S. Mahadevappa and D. J. Channegouda: *Org. Chem. 63*, 531**(1998)**

[22]. R. M. Mulla. Hiremath, C. Gurubasavaraj, S.T.Nandibewoor: Monatshefte für Chemie / Chem. Month.14,1489 **(2004)**

Reprints of Publication

TRANSITION METAL CHEMISTRY

An International Journal

5

2006

Springer

Transition Met Chem (2010) 35:117–123
DOI 10.1007/s11243-009-9303-z

Kinetic and mechanistic investigation of the oxidation of the antibacterial agent levofloxacin by permanganate in alkaline medium

Aftab Aslam Parwaz Khan · Ayaz Mohd · Shaista Bano · Ahmad Husain · K. S. Siddiqi

Received: 25 June 2009 / Accepted: 25 October 2009 / Published online: 12 November 2009

Abstract The kinetics and mechanism of oxidation of levofloxacin (LF) by manganese(VII) in alkaline medium at constant ionic strength was studied spectrophotometrically. The reaction exhibits 2:1 Mn:LF stoichiometry and is first order in permanganate but fractional order in both LF and alkali. Decrease in the dielectric constant of the medium results in a decrease in the rate of reaction. The effects of added products and ionic strength have also been investigated. The main products identified were hydroxylated LF and Mn(VI). A mechanism involving free radicals is proposed. In a composite equilibrium step, levofloxacin binds to MnO_4^- to form a complex that subsequently decomposes to the products. Investigations of the reaction at different temperatures allowed the determination of the activation parameters with respect to the slow step of the proposed mechanism.

Introduction

Potassium permanganate is widely used as an oxidizing agent as well as in analytical chemistry. These reactions are governed by the pH of the medium. Of all the oxidation states of manganese from +2 to +7, permanganate, manganese(VII), is the most potent oxidant in acid as well as in alkaline media. Permanganate oxidation finds extensive applications in organic synthesis [1, 2], especially since the advent of phase transfer catalysis [3–5]. Kinetic studies are important sources of mechanistic information on such reactions, as demonstrated by the results referring to unsaturated acids both in aqueous [3–6] and in non-aqueous media [7]. The mechanism of oxidation depends on the nature of the substrate and pH of the system [8]. In strongly alkaline medium, the stable reduction product [9–11] of permanganate is manganate ion, MnO_4^{2-}. MnO_2 appears only after long time, i.e., after the complete consumption of MnO_4^-. No mechanistic information is available to distinguish between a direct one-electron reduction to Mn(VI) and a mechanism in which a hypomanganate ion is formed in a two-electron reduction followed by its rapid re-oxidation [12, 13].

Levofloxacin (LF), (−)-(S)-9-fluoro-2,3-dihydro-3-methyl-10-(4-methyl-1-piperazinyl)-7-oxo-7H pyrido [1,2,3-de]-1,4-benzoxazine-6-carboxylic acid hemihydrate, is one of the commonly used fluoroquinolone antimicrobials, being the active S-isomer isolated from racemic ofloxacin. Levofloxacin possesses a broad spectrum of activity against various bacteria, including Gram-positive and Gram-negative microorganisms [14]. It is also active against the causes of atypical respiratory infection such as *Chlamydia pneumoniae* and *Mycoplasma pneumoniae* [15]. Because of its effective antibacterial activity and low frequency of adverse effects on oral administration, levofloxacin has been widely used for the treatment of infectious diseases, such as community-acquired pneumonia and acute exacerbation of chronic bronchitis [16]. The antibacterial action of the quinolones is not linearly proportional to their concentration, and the optimum concentration must be maintained to prevent the surviving bacteria from regrowing [17]. The intrinsic fluorescence of fluoroquinolones is used for their determination in biological samples after their preliminary extraction with organic solvents [18]. A method was proposed for determining these antibiotics in biological fluids using a mixed-ligand complex formed by terbium and triphenylphosphine oxide [19]. The interaction

A. A. P. Khan · A. Mohd · S. Bano · A. Husain · K. S. Siddiqi (✉)
Department of Chemistry, Aligarh Muslim University, Aligarh, UP 202002, India
e-mail: ks_siddiqi@yahoo.co.in; aizi_pasha@yahoo.com

of fluoroquinolones with metal ions has attracted considerable interest not only for the development of analytical techniques, but also to provide information about the mechanism of action of the pharmaceutical preparation [20]. Since the metal ions cause fluorescence quenching of the drug, spectrofluorimetric methods for the quantitative determination of the quinolone type drugs have been developed [21] besides titrimetric [22], spectrophotometric [23], electrochemical [24], electrophoretic [25] and chromatographic [26] techniques. The accumulation of fluoroquinolone antibiotics in aquatic environments, even in low concentrations, may cause threats to the ecosystem and human health by inducing multiplication of drug resistant bacteria as a result of long-term exposure. Chemical oxidation of pollutants in drinking and waste water by permanganate ion has been widely used. The present study is an attempt to explore the mechanism of oxidation of levofloxacin by permanganate in alkaline medium on the basis of kinetic parameters.

Experimental

All chemicals used were of analytical reagent grade, and double distilled water was used throughout the work. A solution of levofloxacin (Sigma-Aldrich) was prepared by dissolving a known amount of its hydrochloride salt in distilled water. The permanganate (Ranbaxy Fine Chem. Ltd, India) solution was prepared and standardized against oxalic acid by a standard procedure [27]. Potassium manganate solution was prepared as described by Carrington and Symons [28]. KOH (Merck Ltd.) and KNO_3 (Merck Ltd.) were employed to maintain the pH and ionic strength, respectively.

The absorption spectra were obtained with an Elico-SL-169 double beam UV–vis spectrophotometer. All potentiometric measurements were carried out with an Elico-LI-120 pH meter, and the products were analyzed using a Nicolet 5700-FT-IR spectrometer (Thermo, USA).

Kinetic measurements and procedure

The oxidation of LF by permanganate was followed under pseudo first-order conditions where LF was greater than manganese(VII) at 25 °C. The reaction was initiated by mixing thermally equilibrated solutions of MnO_4^- and LF that also contained the required quantities of KOH and KNO_3 to maintain alkalinity and ionic strength, respectively. The reaction was monitored by the decrease in absorbance of MnO_4^- at its absorption maximum of 526 nm. It was verified that there is no interference from other reagents at this wavelength. Beer's Law was obeyed in this concentration range, and ε was found to be 2083 ± 50 dm^3 mol^{-1} cm^{-1} (compared to the literature, ε = 2200 [9]). The first-order rate constants k_{obs} were evaluated from plots of log [permanganate] versus time. The plots in all cases were linear up to 75% of the reaction (Fig. 1), and k_{obs} values were reproducible at 526 nm, notwithstanding the increasing absorbance of Mn(VI) at 610 nm during the course of the reaction (Fig. 3). The effect of dissolved oxygen on the rate of reaction was checked by following the reaction in nitrogen atmosphere. No significant difference between the results obtained under nitrogen and in the presence of air was observed. In view of the all-pervading contamination of basic solutions by carbonate, the effect of carbonate on the reaction was also studied. Added carbonate had no effect on the reaction rate. Nevertheless, fresh solutions were used during the experiments. Regression analysis of the experimental data to obtain the regression coefficient r and the standard deviation S was performed using Microsoft Excel 2007.

Results

The reaction orders were determined using the slopes of log k_{obs} versus log (concentration) plots by varying the concentration of the reductant and OH^- while keeping other factors constant. With fixed concentrations of LF, 1.0 × 10^{-3} mol dm^{-3}, and alkali, 2.0 × 10^{-3} mol dm^{-3}, at constant ionic strength, 0.10 mol dm^{-3}, the permanganate concentration was varied in the range of 4.0 × 10^{-5} to 6.0 × 10^{-4} mol dm^{-3}. All kinetic runs exhibited identical characteristics. The linearity of plots of log (absorbance) versus time, for different concentrations of permanganate, indicates that the order in Mn(VII) is uniform (Fig. 1). This was also confirmed by the constant values of the pseudo first-order rate constants, k_{obs}, for different Mn(VII)

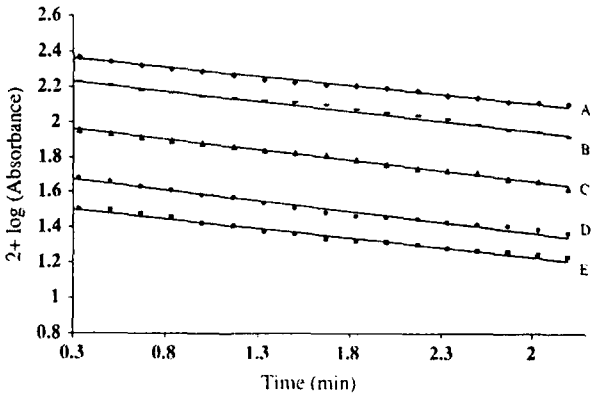

Fig. 1 First-order plots of the oxidation of levofloxacin by permanganate in aqueous alkaline medium. [LF] = 1 × 10^{-3}, [OH^-] = 2 × 10^{-3} and I = 0.10/mol dm^{-3}. [MnO_4^-]×10^4 mol dm^{-3} = (A) 0.4, (B) 0.8, (C) 1.0, (D) 2.0 and (E) 3.0

Table 1 Effects of [LF], [MnO_4^-] and [OH^-] on the oxidation of levofloxacin by permanganate in aqueous alkaline medium at 25 °C and ionic strength I=0.10/mol dm^{-3}

$10^4 \times [MnO_4^-]$ mol dm^{-3}	$10^3 \times$ [LF] mol dm^{-3}	$10^3 \times [OH^-]$ mol dm^{-3}	$k_{cal} \times 10^3$ (S^{-1})	$k_{obs} \times 10^3$ (S^{-1})
0.4	3.0	2.0	4.12	4.10
0.8	3.0	2.0	4.12	4.10
1.0	3.0	2.0	4.12	4.10
2.0	3.0	2.0	4.12	4.10
3.0	3.0	2.0	4.12	4.10
3.0	0.4	2.0	3.67	3.65
3.0	0.6	2.0	3.76	3.74
3.0	0.8	2.0	3.12	4.10
3.0	1.0	2.0	4.28	4.25
3.0	4.0	2.0	5.38	5.35
3.0	6.0	2.0	5.41	5.40
3.0	3.0	0.4	2.19	2.18
3.0	3.0	0.8	2.39	2.38
3.0	3.0	1.0	2.84	2.82
3.0	3.0	2.0	3.32	3.30
3.0	3.0	4.0	3.61	3.60
3.0	3.0	6.0	4.43	4.41

concentrations (Table 1). The LF concentration was varied in the range of 4.0×10^{-4} to 6.0×10^{-3} mol dm^{-3} at constant alkali and permanganate concentrations and constant ionic strength of 0.10 mol dm^{-3} at 25 °C. The k_{obs} values increased with increase in LF over the concentration range shown in (Fig. 4). At low concentration of LF, the reaction was first order in LF and at high concentration of LF, the reaction was independent of LF. The effect of alkali on the reaction was studied at constant concentrations of LF and permanganate and a constant ionic strength of 0.10 mol dm^{-3} at 25 °C. The alkali concentration was varied in the range of 1.0×10^{-3} to 1.0×10^{-2} mol dm^{-3}. The rate constant increased with increase in alkali concentration (Fig. 5), indicating a fractional-order dependence of the rate on alkali concentration.

Stoichiometry and product analysis

Different reaction mixtures containing LF and an excess of MnO_4^- with constant OH^- and KNO_3 concentration were kept in closed vessels under nitrogen atmosphere at room temperature. After 2 hours, the Mn(VII) concentration was assayed by measuring the absorbance at 526 nm. The results indicated a 1:2 stoichiometry, as given in Scheme 1.

Table 2 FT-IR frequencies (cm^{-1})

Compound	ν(OH)	ν(C=O)	ν_{asym} (COO)	ν_{sym}(COO)
Levofloxacin	3411	1722	1622	1462
Oxidation Product	3305	1626	1586	1442

The main reaction products, Mn(VI) and 9-fluoro-2,3-dihydro-3-methyl-5-hydroxy-10-(4-methyl-1-piperazinyl)-7-oxo-7H pyrido [1,2,3-de]-1,4-benzoxazine-6 carboxylic acid, were isolated and identified with the help of TLC and characterized by FT-IR. The FT-IR spectra of LF and its complexes are similar. The (C=O) band appears at 1,722 cm^{-1} in the spectrum of LF; the complexes show this band at ca. 1,626 cm^{-1}, suggesting that the coordination of the ligand occurs through the carboxylate oxygen atom. A carboxylate ligand can bind to the metal atom as a monodentate ligand, giving changes in the relative positions of the antisymmetric and symmetric stretching vibrations with the aim of deducing the coordination mode [29, 30]. The FT-IR spectra of the complex (Table 2) give a separation >100 cm^{-1}, suggesting monodentate bonding for the carboxylate group.

Effects of ionic strength, dielectric constant and temperature

The effect of ionic strength was studied by varying the potassium nitrate concentration from 0.01 to 0.10 mol dm^{-3} at constant concentrations of permanganate, LF and alkali. Increasing ionic strength had no effect on the rate constant. The effect of the dielectric constant (D) was studied by varying the t-butanol–water content (v/v) in the reaction mixture with all other conditions held constant. The rate of reaction increases with increasing t-butanol volume. The plot of log k_{obs} versus $1/D$ was linear with positive slope (Fig. 2).

The kinetics was also studied at four different temperatures with varying concentrations of LF and alkali, keeping other conditions constant. The rate constants were found to increase with increase in temperature. The rate of the slow step was obtained from the slopes and intercepts of $1/k_{obs}$ versus 1/[LF] and $1/k_{obs}$ versus 1/[OH^-] plots at four different temperatures (25–37 °C). The activation energy corresponding to these rate constants was evaluated

Scheme 1 Formation of hydroxylated LF and Mn(VI)

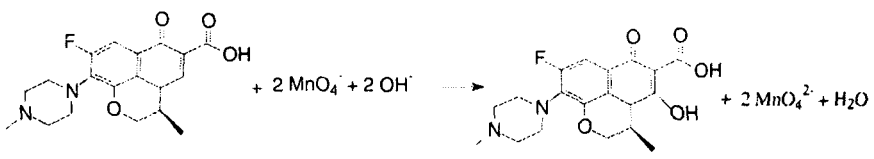

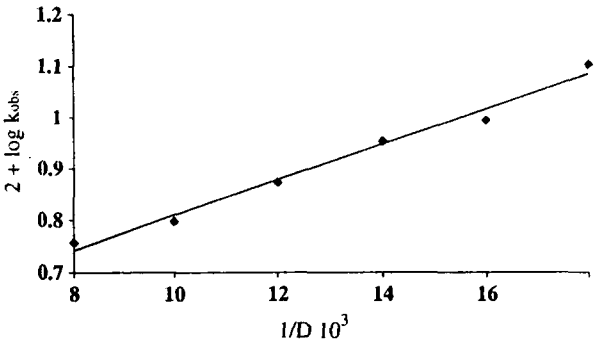

Fig. 2 Effect of dielectric constant on the oxidation of levofloxacin by alkaline MnO_4^- at 25 °C

from the Arrhenius plot of log k versus $1/T$ from which other activation parameters were also obtained (Table 3).

Test for free radicals

To test for the involvement of free radicals, acrylonitrile was added to the reaction mixture, which was then kept for 24 h under nitrogen. Addition of methanol, resulted in the precipitation of a polymer, suggesting the involvement of free radicals in the reaction. The blank experiment of reacting either permanganate and LF alone with acrylonitrile did not induce polymerization under the same conditions. Initially added acrylonitrile decreased the rate of reaction [31].

Table 3 Activation and thermodynamic parameters for the oxidation of LF by alkaline permanganate with respect to the slow step of the reaction Scheme 2

Temperature(K)	10^3k (S^{-1})	
Effect of Temperature with respect to the slow step of Scheme 2.		
293	10.6	
298	11.8	
303	12.2	
310	13.5	
	Value	
Activation parameter		
Ea (kJmole^{-1})	14.9	
ΔH (kJmole^{-1})	11.9	
ΔS ± (Jk^{-1}mole^{-1})	−143.2	
ΔG ± (kJmole^{-1})	63.10	
Effect of temperature (K)	$10^{-2}K_2$ (dm^3 mol^{-1})	$10^{-3}K_2$ (dm^3 mol^{-1})
Equilibrium constants K_1 and K_2 at different temperatures		
293	5.44	6.17
298	7.59	6.69
303	9.62	5.32
310	12.43	4.34
	K_1 values	K_2 values
Thermodynamic parameters		
ΔH (kJmole^{-1})	58.1	−78.6
ΔS ± (Jk^{-1}mole^{-1})	123.5	−89.7
ΔG ± (kJmole^{-1})	−8.7	−8.35

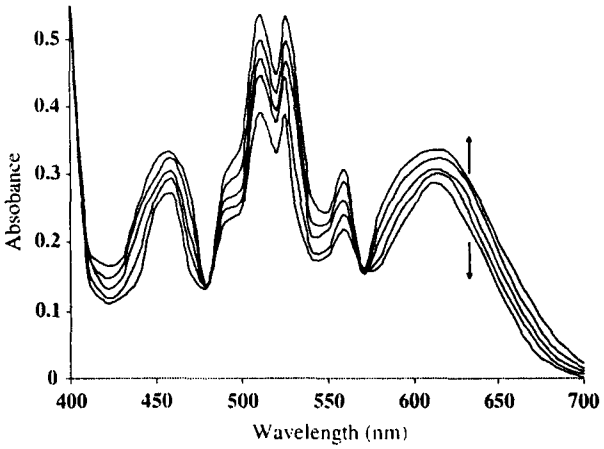

Fig. 3 Spectral changes during the oxidation of levofloxacin (LF) by MnO_4^- in alkaline medium at 25 °C: $[MnO_4^-] = 1 \times 10^{-4}$, $[LF] = 1 \times 10^{-3}$, $[OH^-] = 2 \times 10^{-3}$ and $I = 0.10$/mol dm^{-3}

Discussion

Under our experimental conditions at pH > 12, the reduction product of Mn(VII), i.e., Mn(VI), is stable, and no further reduction is initially observed [10]. However, on prolonged standing, the green Mn(VI) is reduced to Mn(IV) under our experimental conditions. Permanganate ion in alkaline medium exhibits various oxidation states, such as Mn(VII), Mn(V) and Mn(VI). During this reaction, color changes from violet Mn(VII) to dark green Mn(VI) through blue Mn(IV) were observed. It is clear from Fig. 3 that the concentration of MnO_4^- decreases at 526 nm, while increases at 610 and 460 nm are due to Mn(VI). As the reaction proceeds, a yellow turbidity slowly develops, and after keeping for a long time the solution decolourises and forms a brown precipitate. This suggests that the initial products might have undergone further oxidation resulting in a lower oxidation state of manganese. It appears that the alkali combines with permanganate to give $[MnO_4{\cdot}OH]^{2-}$ [32, 33]. In the second step, $[MnO_4{\cdot}OH]^{2-}$ combines with levofloxacin to form an intermediate complex. The variable order with respect to LF most probably results

from the complex formation between oxidant and LF prior to the slow step. A plot of $1/k_{obs}$ versus 1/[LF] (Fig. 1) shows an intercept in agreement with complex formation. Further evidence for complex formation was obtained from the UV–vis spectra of reaction mixtures. Two isosbestic points were observed for this reaction (Fig. 3), indicating the presence of an equilibrium before the slow step of the mechanism [34, 35]. In our proposed mechanism, in the complex one electron is transferred from levofloxacin to Mn(VII). The cleavage of this complex (C) is assigned as the slowest step, leading to the formation of an LF radical intermediate and Mn(VI). The radical intermediate reacts with another Mn(VII) species, $[MnO_4{\cdot}OH]^{2-}$, to give the final products, Mn(VI) and the alcohol (Scheme 2). The effect of the ionic strength and dielectric constant on the rate is consistent with the involvement of a neutral molecule in the reaction. The suggested structure of complex (C) is given in Scheme 2.

From Scheme 2, the rate law (Eq. 7) can be derived as follows:

$$\text{Rate} = \frac{-d[MnO^{4-}]}{dt} = kK_1K_2\,[MnO_4^-]_f[LF]_f[OH^-]_f \quad (1)$$

The total $[MnO_4^-]$ can be written as

$$[MnO_4^-]_t = [MnO_4^-]_f + [MnO4\cdot OH]^{2-} + [Complex]$$
$$= [MnO_4^-]_f + [MnO_4^-]\,[OH^-] + kK_1K_2[MnO_4^-]\,[LF]\,[OH^-]$$
$$[MnO_4^-]_t = [MnO_4^-]_f(1 + K_1[OH^-] + K_1K_2[LF]\,[OH^-])$$
$$[MnO_4^-]_f = \frac{[MnO_4^-]_t}{1 + K_1[OH^-] + K_1K_2[LF]\,[OH^-]} \quad (2)$$

where "t" and "f" stand for total and free. Similarly, total $[OH^-]$ can be calculated as

$$[OH^-]_t = [OH^-]_f + [MnO4\cdot OH]^{2-} + [Complex]$$
$$[OH^-]_f = \frac{[OH^-]t}{1 + K_1[MnO_4^-] + K_1K_2[LF]\,[MnO_4^-]} \quad (3)$$

In view of the low concentrations of MnO_4^- and levofloxacin used in the experiment, in Eq. 3, the terms $K_1[MnO_4^-]$ and $K_1K_2[MnO_4^-]$ [LF] are neglected. Thus,

$$[OH^-]_f = [OH^-]_t \quad (4)$$

Similarly,

$$[LF]_f = [LF]_t \quad (5)$$

Substituting Eq. 2, 4, and 5 in Eq. 1 we get

Scheme 2 Proposed mechanism for the oxidation of levofloxacin by alkaline MnO_4^-

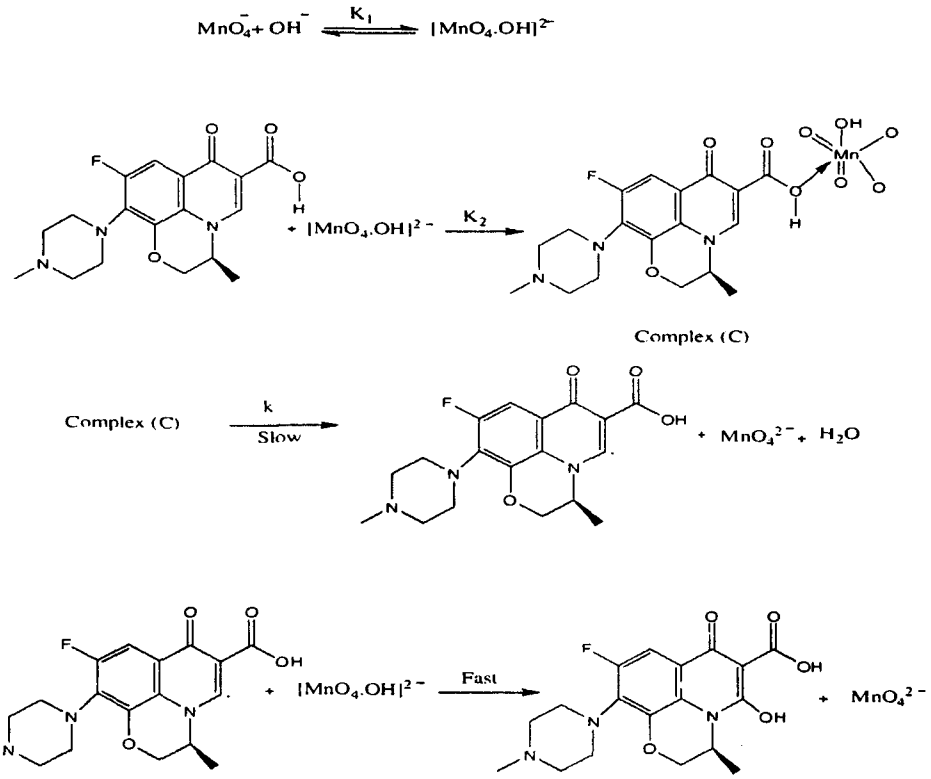

$$[MnO_4^-]_f = \frac{1 + K_1[OH^-] + K_1K_2[LF][OH^-]}{1 + K_1[OH^-] + K_1K_2[LF][OH^-]} \quad (6)$$

$$\frac{\text{Rate}}{[MnO_4^-]} = K_{obs} = \frac{kK_1K_2[LF][OH^-]}{1 + K_1[OH^-] + K^1K^2[LF][OH^-]} \quad (7)$$

Equation 7 is consistent with the observed orders with respect to different species, which can be verified by rearranging to Eq. 8.

$$\frac{1}{K_{obs}} = \frac{1}{k\,K_1K_2[LF][OH^-]} + \frac{1}{K_1K_2[LF]} + \frac{1}{K} \quad (8)$$

According to Eq. (8), other conditions being constant, plots of $1/k_{obs}$ versus 1/[LF] and $1/k_{obs}$ versus $1/[OH^-]$ should be linear (Figs. 4 and 5). The slopes and intercepts of such plots lead to the values of K_1, K_2 and k (Table 3). With these values, the rate constants were calculated under different experimental conditions, and there is a reasonable agreement between the calculated and experimental values [36] (Table 1). The thermodynamic quantities for the first and second equilibrium steps of Scheme 2 can be evaluated. The [LF] and $[OH^-]$ (as in Table 1) were varied at four different temperatures. Van't Hoff's plots of $\log K_1$ versus $1/T$ and $\log K_2$ versus 1/T gave the values of enthalpy of reaction $\Delta H^{\#}$, entropy of reaction $\Delta S^{\#}$ and free energy of reaction ΔG, calculated for the first, and second equilibrium steps (Table 3). A comparison of the latter values (from K_2) with those obtained for the slow step of the reaction shows that they mainly refer to the rate-limiting step, supporting the fact that the reaction before the rate determining step is fairly fast and involves low activation energy [37, 38]. The moderate values of $\Delta H^{\#}$ and $\Delta S^{\#}$ were both favorable for electron transfer processes. The value of $\Delta S^{\#}$ that is within the expected range for radical reactions has been ascribed to the nature of electron pairing and unpairing processes and the loss of degrees of freedom formerly available to the reactants upon the formation of a rigid transition state [39]. The negative value of $\Delta S^{\#}$ indicates that complex (C) is more ordered than the reactants [40, 41]. The enthalpy of activation and a relatively low value of the entropy and a higher rate constant of the slow step indicate that the oxidation most probably occurs via inner-sphere mechanism [42, 43].

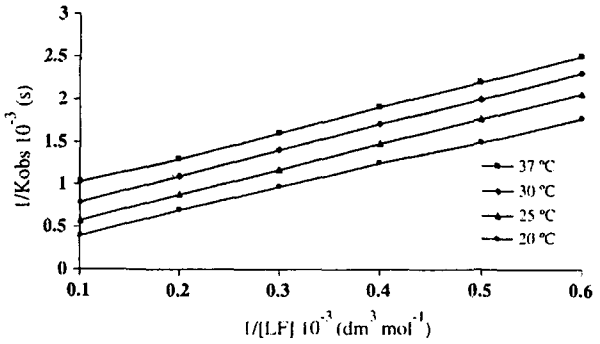

Fig. 4 Plots of $1/k_{obs}$ versus 1/[LF] at four different temperatures

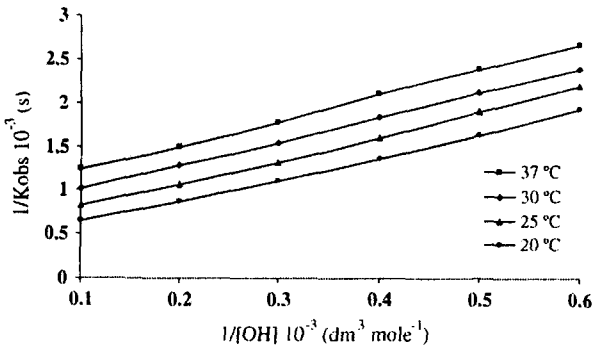

Fig. 5 Plots of $1/k_{obs}$ versus $1/[OH^-]$ at four different temperatures

Conclusion

It is noteworthy that the oxidant species $[MnO_4^-]$ required the pH 12, below which the system gets disturbed and the reaction proceeds further to give a more reduced of Mn(IV) product, which slowly develops yellow turbidity. In this reaction, the role of pH is crucial. The rate constant of the slowest step and other equilibrium constants involved in the mechanism were evaluated and activation parameters with respect to the slowest step were computed. The proposed mechanism is consistent with product, mechanistic and kinetic studies.

References

1. Shaabani A, Tavasoli-Rad F, Lee DG (2005) Synth Commun 35:571
2. Caron S, Dugger RW, Ruggeri SG, Ragan JA, Brown Ripin DH (2006) Chem Rev 106:2943
3. Lee DG (1982) In: Trahanovsky WS (ed) Oxidation in Organic Chemistry, Part D. Academic Press, New York, p 147
4. Simandi LI (1983) In: Patai S, Rappoport Z (eds) The Chemistry of Functional Groups. Wiley, Chichester Suppl. C
5. Lee DG, Lee EJ, Brown KC (1987) Phase Transfer Catalysis, New Chemistry, Catalysis and Applications, ACS Symposium Series, vol. 326. American Chemical Society, Washington
6. Fatiadi AJ (1987) Synthesis 106:85
7. Perez-Benito JF, Lee DG (1987) J Org Chem 52:3239
8. Stewart R, Gardner KA, Kuehnert LL, Mayer JM (1997) Inorg Chem 36:2069
9. Simandi LI, Jaky M, Savage CR, Schelly ZA (1985) J Am Chem Soc 107:4220
10. Timmanagoudar PL, Hiremath GA, Nandibewoor ST (1997) Transition Met Chem 22:193–196
11. Nadimpalli S, Rallabandi R, Dikshitulu LSA (1993) Transition Met Chem 18:510–514

12. Panari RG, Chougale RB, Nandibewoor ST (1998) Pol J Chem 72:99–107
13. Bohn A, Adam M, Mauermann H, Stein S, Mullen K (1992) Tetrahedron Lett 33:2795
14. Croisier D, Etienne M, Bergoin E, Charles PE, Lequeu C, Piroth L, Portier H, Chavanet P (2004) Antimicrob Agents Chemother 48:1699
15. Roblin PM, Hammerschlag MR (2003) Antimicrob Agents Chemother 47:1447
16. Owens RC Jr, Ambrose PG (2000) Med Clin North Am 84:1447
17. Shulgina MV, Fadeeva NI, Bolshakova TN, Levshin IB, Glushkov RG (1999) Parm Chem J 33:343
18. Waggoner TB, Bowman MC (1987) J Assoc Off Anal Chem 70:813
19. Veiopoulou CJ, Ioannou PC, Liaidou ES (1997) J Pharm Biomed Anal 15:1839
20. Turel I, Golobi PA, Klazar A, Pihlar B, Buglyo P, Tolib E, Rehder D, Sepiv K (2003) J Inorg Biochem 95:199
21. Kilic E, Koseoglu F, Akay MA (1994) J Pharm Biomed Anal 12:347
22. Mostafa S, Elsadek M, Awadalla E (2002) J Pharm Biomed Anal 27:133
23. Liu Z, Huang, Cai R (2000) Analyst 125:1477
24. Trindade MAG, Cunha PAC, de Araujo TA, dasilva GM, Ferreira VS (2006) vol 31. Ecl. Quim, Sao Paulo, p 31
25. Fierens C, Hillaert S, Bossche WV (2000) J Pharm Biomed Anal 76:220
26. Novakovic J, Nesmark K, Nova H, Filka K (2001) J Pharm Biomed Anal 25:957
27. Jeffery GH, Bassett J, Mendham J, Denny RC (1996) Vogel's Textbook of Quantitative Chemical Analysis, 5th edn. Longman, Essex, p 370
28. Carrington A, Symons MCR (1956) J Chem Soc 3373
29. Macias B, Villa MV, Rubio I, Castineiras A, Borras J (2001) J Inorg Biochem 84:163
30. Macias B, Villa MV, Saste M, Castineiras A, Borras J (2002) J Pharm Sci 91:2416
31. Bhattacharya S, Benerjee P (1996) Bull Chem Soc 69:3475
32. Panari RG, Chougale RB, Nandibewoor ST (1998) J Phys Org Chem 11:1
33. Thabaj KA, Kulkarni SD, Chimatadar SA, Nandibewoor ST (2007) Polyhedron 26:4877–4885
34. Chang R (1981) Physical Chemistry with Applications to Biological Systems. MacMillan Publishing Co. Inc, New York, p 536
35. Sathyanarayana DN (2001) Electronic Absorption Spectroscopy and Related Techniques. Universities Press (India) Ltd, Hyderabad, p 12
36. Bilehal DC, Kulkarni RM, Nandibewoor ST (2003) Z Phys Chem 1
37. Rangappa KS, Raghavendra MP, Mahadevappa DS, Channegouda D (1998) J Org Chem 63:531
38. Bilehal DC, Kulkarni RM, Nandibewoor ST (2001) Can J Chem 79:1926
39. Walling C (1957) Free Radicals in Solution. Academic Press, New York, p 38
40. Rangappa KS, Anitha N, Madegouda NM (2001) Synth React Inorg Met Org Chem 31:1499
41. Bugarcic ZD, Nandibewoor ST, Hamza MSA, Heimemann F, van Eldik R (2006) Dalton Trans 2984
42. Hicks KW (1976) J Inorg Nucl Chem 38:1381
43. Farokhi SA, Nandibewoor ST (2003) Tetrahedron 59:7595

JOURNAL OF DISPERSION SCIENCE AND TECHNOLOGY

From: johsj <johan.sjoblom@chemeng.ntnu.no>
Subject: Ms JDST 2011 / 87
To: aizi_pasha@yahoo.com, "VanSciver, Catherine" <catherine.VanSciver@taylorandfrancis.com>, camild@chemeng.ntnu.no, ks_siddiqi@yahoo.co.in
Date: Tuesday, 27 April, 2010, 4:58 PM

Dear Shaista Bano /K.S. Siddiqi

Your ms "Resonance Rayleigh Scattering and Non-linear Scattering Spectra of selected Cephalosporins-Cd(II) Chelate with Titan Yellow and their Analytical Application" is accepted for publication in **J Dispersion Science Technology**. Your ms will appear in JDST (2011).

You will be contacted by our Production Editor Catherine van Sciver if some stylistic corrections are needed in your ms.

Thank you for this most valuable contribution to JDST !!!

Before starting the editing process you should fill in the copyright transfer form (attached) and send it (properly signed) as a PDF file to Production Editor Catherine VanSciver. Please clearly indicate on the form the name of the journal (JDST/volume/issue/ms nr) as specified in this email of acceptance.

Email: catherine.VanSciver@taylorandfrancis.com

Thank you very much for your collaboration !

Johan Sjöblom
Editor-in-chief

CODEN : ECJHAO ISSN: 0973 4945

E-J.CHEM

http://www.e-journals.net

Volume 7, No. 1

January 2010

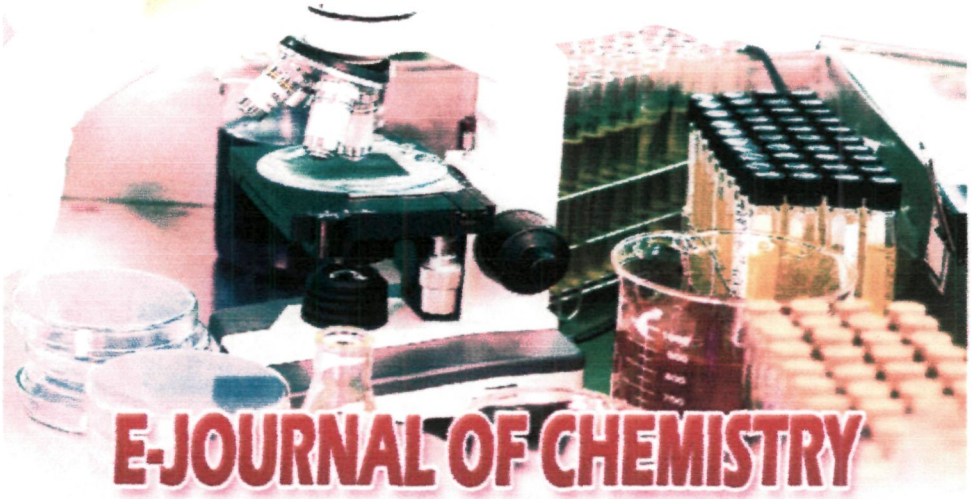

E-JOURNAL OF CHEMISTRY

(An International Quarterly Research Journal of Chemistry)

WWW PUBLICATIONS

INDIA

E-J.Chem
http://www.e-journals.net

ISSN: 0973-4945; CODEN ECJHAO
E-Journal of Chemistry
2009, 6(S1), S103-S110

Spectroscopic and Substitution Kinetic Studies of Hexacyanoferrate(II) Complexes by EDTA Catalysed with Mercury(II)

K.S. SIDDIQI*, AFTAB ASLAM PARWAZ KHAN,
AYAZ MOHD and SHAISTA BANO

Department of Chemistry,
Aligarh Muslim University, Aligarh- 20200, (U.P.), India.
ks_siddiqi@yahoo.co.in

Received 3 March 2009; Accepted 1 May 2009

Abstract: Kinetics and mechanism of substitution of cyanide ion in hexacyanoferrate(II) by EDTA catalysed by mercury(II) has been studied spectrophotometrically at 365 nm in potassium hydrogen phthalate buffer of pH = 5.0 and ionic strength, I = 0.1 M, maintained by (KNO_3) at 25 ^{0}C. Effect of the pH and concentration of the EDTA, [$Fe(CN)^{4-}_6$] on the rate of reaction has been studied. The kinetics and mechanism of the reaction has been shown through dissociative mechanism. The mechanism of ligand substitution in the complex together with the kinetic data has been shown. The catalytic activity of mercury(II) has also been studied as a function of its concentration. The maximum reaction product was detected at pH = 5 after which a decline in absorption occurs followed by precipitation. It is an inexpensive method to identify and remove the cyanide ion in solution even in very low concentration of the order of 10^{-4} M.

Keyword: Kinetics, Hexacyanoferrate(II), EDTA, Mercury(II), Thermodynamics, Mechanism.

Introduction

It has been demonstrated that of all the heavy metals mercury(II) easily forms bonds to cyanide and slowly removes it from hexacyanoferrate(II). Kinetics and mechanism of ligand replacement in low spin Fe(II) complex has been done, although it is limited to the study of pentacyano(L)ferrate(II) complex[1-7]. Few studies have been done in aqueous electrolyte and micellar media to acquire an in depth knowledge of the mechanistic scheme[8-9]. The oxidation kinetics of the hexacyanoferrate(II) complex by various reagents in acidic and basic media have been studied and all these investigation have been applied to specific analytical problems[10-12]. $K_4[Fe(CN)_6^{4-}]$ hardly undergoes exchange reaction as CN^- itself is a

very strong ligand although slow exchange of labelled CN^- group or aminopyridine has been demonstrated. Under UV light reversible aquation occurs leading to the formation[13] of $[Fe(CN)_5H_2O]^{3-}$. However, only mono substituted $[Fe(CN)_5L]^{3-}$ have been obtained either through photochemical or by dissociation reaction or by metal catalysed substitution reaction[14].

$$[Fe(CN)_6^{4-}] + H_2O \longrightarrow [Fe(CN)_5H_2O]^{3-} + CN^- \quad (1)$$

Hexacyanoferrate(II) reacts with EDTA according to the following equation

$$[Fe(CN)_5H_2O]^{3-} + EDTA \longrightarrow [Fe(CN)_5EDTA]^{3-} + H_2O \quad (2)$$

$$CN^- + H_2O \longrightarrow HCN + OH^- \quad (3)$$

Mercury(II) readily forms complex with cyanide ion but decomposition occurs in UV light.

$$Hg^{2+} + [Fe(CN)_6^{4-}] + H_2O \longrightarrow [Fe(CN)_5H_2O]^{3-} + HgCN^+ \quad (4)$$

$$HgCN^+ \; H^+ \longrightarrow HCN + Hg^{2+} \quad (5)$$

In the present work, we have studied the kinetics of substitution of CN^- by EDTA, catalysed by Hg^{2+}. A probable mechanism of the reaction has been proposed. Any attempt to study the substitution of CN^- by phenanthroline, pyridine, hydrazine and piperazine resulted in precipitation even in low concentration.

Experimental

Double distilled, de-ionized water was used throughout. The chemicals used were of analytical grade. Stock solutions of the compounds were wrapped with carbon paper to protect them from photodecomposition. The mercury(II) and hexacyanoferrate(II) solutions were diluted just before use. The desired pH= 5 of the reaction mixture was maintained by adding KHP-NaOH buffer[15]. The ionic strength was maintained at 0.1 M by adding appropriate amount of KNO_3.

Apparatus

The absorption spectra were obtained with double beam UV-vis spectrophotometer (Elico-SL-169). pH-metric measurements were done with Elico-LI 120 pH meter.

Procedure

All the solutions were thermally equilibrated for about 30 minutes at 25 ^{0}C and 2.0 mL of each EDTA, phthalate buffer of pH = 5.0 and mercury(II) chloride were mixed in a flask and left for 10 min to ensure complete reaction. Finally, 2.0 mL of $[Fe(CN)_6]^{4-}$ was added to this mixture and the wavelength of maximum absorption (365 nm) was determined (Figure 1).

Effect of pH

The reaction was studied first by fixed time kinetic method in the pH ranges 1-13. Figure 2 shows plots of absorbance (measured at t =5 and 10 minutes after mixing the reagents) *versus* pH of the reaction mixture. It was found that, with increasing pH the absorbance increases and attains a maximum between pH 5.0 to 5.5. However, above this pH the absorption decreases which is due to the deficiency of protons. The rate is reduced at low pH value due to the formation of various protonated forms of $[Fe(CN)_6]^{4-}$ which are less reactive than $[Fe(CN)_6^{4-}]$ itself[16].

Effect of EDTA

The complex formation with EDTA is influenced by a change in the pH of solution which is perhaps due to ionization of the metal complex at low pH and hydrolysis of the metal ion at higher pH. The effect of EDTA was examined as a function of its concentration at a fixed

pH 5. A plot of initial rate *versus* EDTA is shown in Figure 3. Almost constant rate was obtained in the concentration range 2×10^{-5} to 7×10^{-5} M and finally decrease at still higher concentrations. A fixed concentration 4×10^{-4} M was thus selected as optimum.

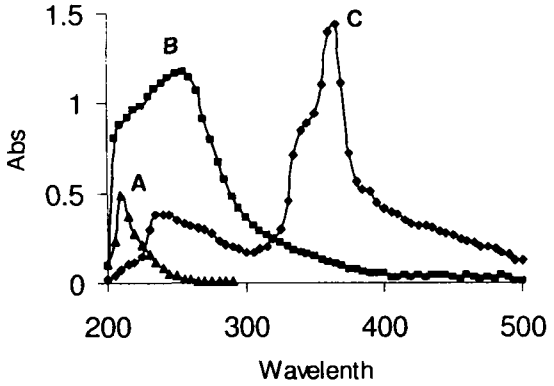

Figure 1. Absorption spectra of reactants and products: (A) [EDTA] = $1X10^{-3}$; (B) $[Fe(CN)_6]^{4-}$ = $5X10^{-4}$M (C) $[Fe(CN)_6]^{4}$ = $4X10^{-4}$M, [EDTA] = $4X10^{-3}$ M, $[Hg^{2+}] = 3X10^{-5}$ M and pH = 5.0

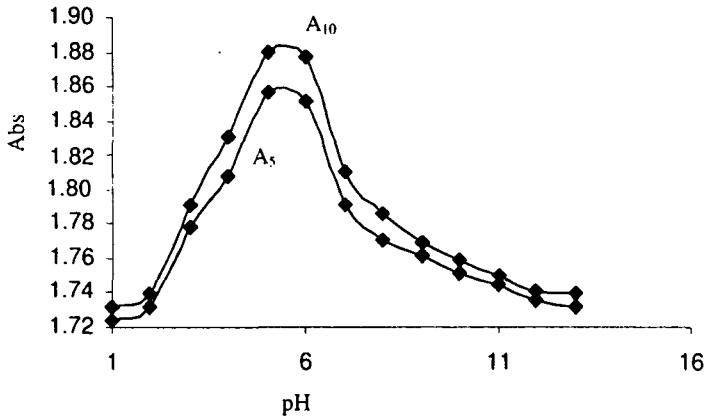

Figure 2. Effect of pH on Hg^{2+} catalysed substitution of CN^- in hexacyanoferrate(II) by EDTA ion at $[Fe(CN)_6^{4-}] = 5X10^{-3}$ M, EDTA = $5X10^{-5}$ M, $[Hg^{2+}] = 3X10^{-5}$ M, Temp = 25 ^{0}C and I = 0.1 M (KNO_3).

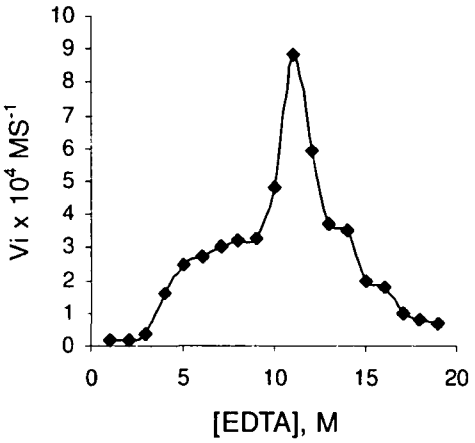

Figure 3. Effect of EDTA on initial rate at $[Fe(CN)_6^{4-}]$ = $3.5X10^{-2}$ M, $[Hg^{2+}] = 3x10^{-5}$ M, pH = 5, Temp =25 ^{0}C and I = 0.1 M (KNO_3)

Effect of $[Fe(CN)_6]^{4-}$ on the initial rate

Dependence in $[Fe(CN)_6^{4-}]$ was found, changing from first order at lower concentration to higher concentration not zeroth order, Keeping all parameters constant, effect of the concentration of $[Fe(CN)_6^{4-}]$ on the reaction rate was studied in the concentration range 5×10^{-4} to 2×10^{-2} M, Figure 4.A variable order .

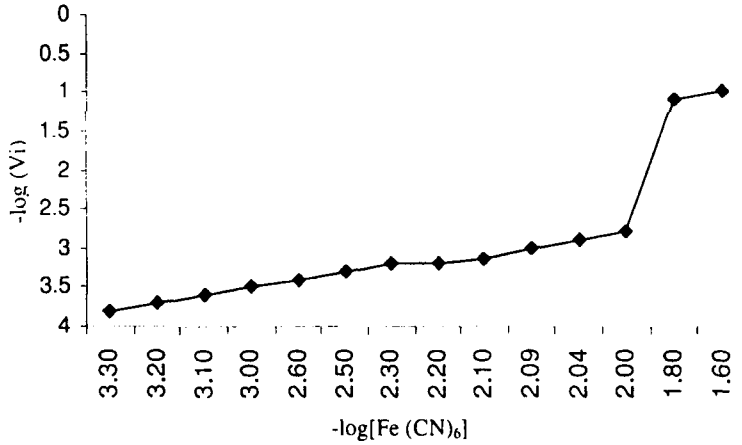

Figure 4. Dependence of the initial rate on $[Fe(CN)_6^{4-}]$ in presence of $[Hg^{2+}]$ at [EDTA] 3×10^{-4}M, $[Hg^{2+}] = 3\times10^{-5}$ M, pH 5.0, temp = 25 ^{0}C and 0.2 M (KNO_3).

Effect of $[Hg^{2+}]$ on initial rate

The concentration of mercury(II) was kept between 1×10^{-5} to 2×10^{-3}M and those of the $[Fe(CN)_6^{4-}]$ and EDTA were kept constant. The pH and temperature were maintained at 5 and 25 ^{0}C respectively. The results are shown in Figure 5. The large variation in $[Hg^{2+}]$ was selected in order to test the linearity between initial rate and $[Hg^{2+}]$ for its analytical application and also the changing role in $[Hg^{2+}]$ mixture. A plot of the absorbance measured after an interval of one min *versus* $[Hg^{2+}]$ as a function of pH is given in Figure 5.

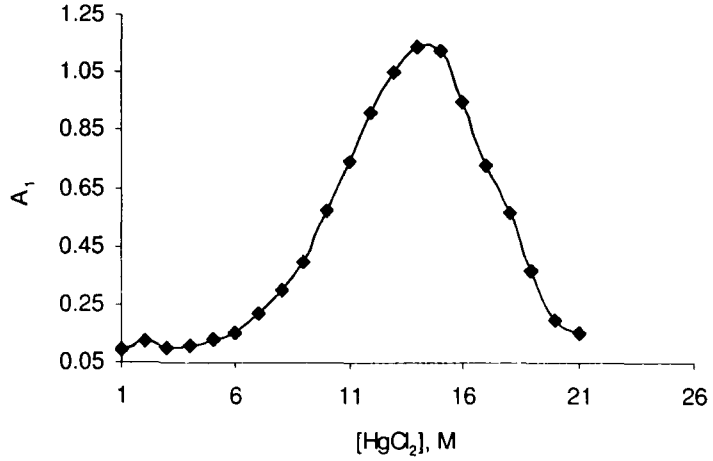

Figure 5. Dependence of the initial rate of substitution of CN^- in $[Fe(CN)_6^{4-}]$ by EDTA on $[HgCl_2]$ at $[Fe(CN)_6^{4-}] = 3.5\times10^{-3}$ M, [EDTA] = 3×10^{-4} M, pH = 5, temp = 25 ^{0}C and I = 0.1 M (KNO_3).

It clearly indicates that the rate increases linearly until the ratio of the $[Fe(CN)_6^{4-}]$ and $[Hg^{2+}]$ reaches 1:1.When the concentration of $[Hg^{2+}]$ exceeds that of $[Fe(CN)_6^{4-}]$ the absorption begins to

decrease and follows a non-linear pattern. The intercept computed from the initial linear portion of the Figure 5 provides the rate due to the uncatalyzed path. However, decline in the rate of reaction at higher $[Hg^{2+}]$ is probably due to the formation of a binary adduct, $[Fe(CN)_6^{4-}.\ HgCl_2]$. In a separate experiment it was observed that a white precipitate is formed immediately after mixing $[Fe(CN)_6^{4-}]$ with $[Hg^{2+}]$ in 1:2 molar ratio which rapidly turned blue, confirming the formation of a binuclear complex. A similar observation has also been made by Beck[17].

Effect of temperature and ionic strength

The rate of the $[Hg^{2+}]$ catalyzed ligand exchange between $[Fe(CN)_6^{4-}]$ and EDTA was studied as a function of temperature in range 20-30 ^{0}C. The higher temperature was avoided due to the possibility of decomposition of $[Fe(CN)_5EDTA]^{3-}$. The Arrhenius equation was used to determine the activation energy (Ea) for the catalyzed reaction and the other activation parameters, *viz.* enthalpy of activation ($\Delta H^{\neq}$) and entropy of activation ($\Delta S^{\neq}$) were calculated using Eyring equation. The values of activation parameters are found to be Ea = 78.2 kJ mol^{-1}, $\Delta S^{\neq}$ = -48.67 JK^{-1} mole^{-1} and $\Delta H^{\neq}$ = -52.5 kJ mole^{-1}.The effect of ionic strength on the initial rate of reaction was also studied employing (KNO_3) for maintaining ionic strength in the 0.015 to 0.2 M range. The higher ionic strength was avoided due to the limited solubility of (KNO_3). When KCl was used to maintain the ionic strength the rate was found to decrease considerably. This is probably due to a subsequent decrease in $[Hg^{2+}]$ or $[HgCl^+]$ along with the concentration of an ion-pair formation between $[Fe(CN)_6^{4-}]$ and $[Hg^{2+}]$[18].

Results and Discussion

The following Scheme for the mercury(II) catalyzed ligand exchange between $[Fe(CN)_6^{4-}]$ and EDTA has been proposed:

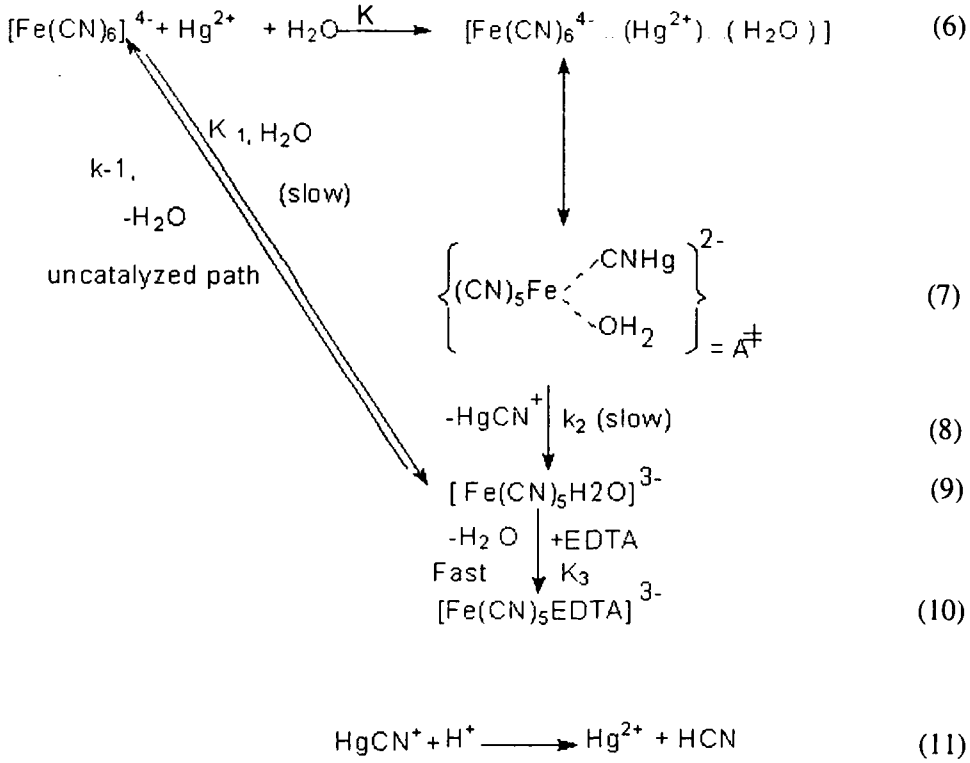

(6)

(7)

(8)

(9)

(10)

(11)

Formation of the complex, $[Fe(CN)_5EDTA]^{3-}$ through the catalyzed path can be written as:

$$\frac{d\,[Fe(CN)_5EDTA]^{3-}}{dt} = K_2\,[A^{\neq}] \qquad (12)$$

While, that for the uncatalyzed path the

$$\text{rate} = k'\,[Fe(CN)_6^{4-}] \qquad (13)$$

where, k' is a composite rate constant involving a concentration term. If the rate determining step is taken to be the composition of the activated complex ($A^{\neq}$), the activity of the mercury(II) at low concentration can be easily explained by the above mechanism. The overall rate for uncatalyzed reaction can be expressed through equation (13) using a non limiting concentration of EDTA.

$$\text{Rate} = \frac{d\,[Fe(CN)_5EDTA]^{3-}}{dt} = k'[Fe(CN)_6^{4-}] + \frac{k_2K\,[Fe(CN)_6^{4-}][Hg^{2+}][H_2O]}{1+K\,[Fe(CN)_6^{4-}]} \qquad (14)$$

The second term in the above equation refers to the rate of the catalyzed reaction and explains the variable order dependence in $[Fe(CN)_6^{4-}]$. K is defined as the equilibrium constant for the association of the mercury (II) with water and $[Fe(CN)_6^{4-}]$. Since water is in a large excess, the equation (14) is reduced to equation (15)

$$\text{Rate} = k'[Fe(CN)_6^{4-}] + k'_2K[Hg^{2+}][Fe(CN)_6^{4-}] \qquad (15)$$

Now equation (15) yields the observed rate constant (k_{obs}) as expressed by equation (16)

$$k_{obs} = k' + k'_2K[Hg^{2+}] \qquad (16)$$

where, $k'_2 = k_2 + [H_2O]$.

A plot of the initial rate *versus* $[Hg^{2+}]$ at low $[Fe(CN)_6^{4-}]$ is given in Figure 6. In case of higher $[Fe(CN)_6^{4-}]$, equation (14) takes the form of equation (17).

$$\text{Rate} = k'\,[Fe(CN)_6^{4-}] + k_2'[Hg^{2+}] \qquad (17)$$

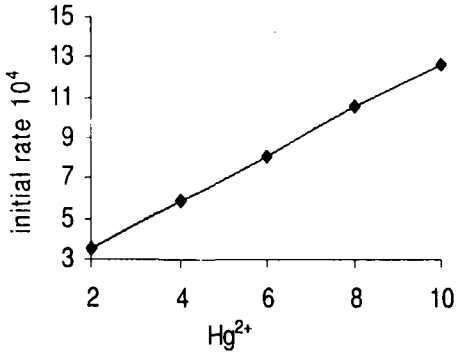

Figure 6. $[Fe(CN)_6^{4-}] = 8\times10^{-4}$ M, [EDTA] = 5×10^{-4} M, pH = 5, temp. = 25 ^{0}C, I = 0.1 M (KNO_3).

The value of the initial rate (V_i) as a function of $[Hg^{2+}]$ at low $[Fe(CN)_6^{4-}]$ is listed in Table 1. The value of the k' and k_2' have been calculated from the plot Figure 6 of initial rate *versus* $[Hg^{2+}]$ using equation (17) at specified experimental condition. The rate constant k' and k_2 are found to be 4.17×10^{-3} s^{-1} and 2.50 s^{-1} respectively, at I = 0.1 M, pH = 5, temp = 25 ^{0}C .The value of k_1' and k_2 so obtained are substituted in equation (17) to evaluate the equilibrium constant K at various $[Hg^{2+}]$ at low $[Fe(CN)_6^{4-}]$. The K (Table 1) and the average value of log K (2.80) in our case is comparable with that reported by Beck for $[Fe(CN)_6^{4-}$. $Hg(CN)_2]$ complex (logK = 2.38)[17]. Although the values of k_2 have been calculated employing high $[Fe(CN)_6^{4-}]$ using equation (17) it can be obtained even at low $[Fe(CN)_6^{4-}]$ using equation (18)

Table 1. Calculation of K by varying $[Hg^{2+}]$ at constant $[Fe(CN)_6^{4-}]$. $[Fe(CN)_6^{4-}] = 8x10^{-4}$ M, $[Hg^{2+}] = 5X10^{4-}$ M, pH = 5, temp= 25 ^{0}C and I = 0.1 M (KNO_3),

$[Hg^{2+}] \times 10^{-4}$, M	Vi x 10^4	K(calcd.)
2	3.5	709.07
4	5.9	660.02
6	7.9	610.60
8	10.6	625.80
10	12.6	601.80
Average log K = 2.80		

$$k_2 = \frac{\text{Rate} - k'[Fe(CN)_6^{4-}]}{K[Fe(CN)_6^{4-}][Hg^{2+}][H_2O]} \quad (18)$$

However, the values calculated from this equation are almost identical. The ionic behavior of $[Hg^{2+}]$ may be represented by the following reactions.

$$Hg^{2+} + Cl \rightleftharpoons HgCl^+ \quad (19)$$

$$HgCl^+ + Cl \rightleftharpoons HgCl_2 \quad (20)$$

It has been shown that when $Hg(NO_3)_2$ reacts with $[Fe(CN)_6^{4-}]$ in solution the resultant was $Hg_2[Fe(CN)_6^{4-}]$[19], which has also been verified from the absorption spectra of both the reacting components and the eventual product. This is quite obvious because the $[Hg^{2+}]$ is more electropositive than K^+ ion. The activation energy calculated for this reaction is a little less than the reported values in the literature[20,21] for the replacement of CN^- in nearly similar reaction systems. The entropy of activation is negative and is expected if the virtual solvations of the activated complex and its highly charged dissociation products are considered. Thus, the activation parameters provide further support to the proposed mechanism.

Conclusion

In the present work we have studied the kinetics of substitution of CN^- by EDTA catalyzed with $[Hg^{2+}]$. A probable mechanism of the reaction has been proposed. The results presented here clearly demonstrate work, EDTA as a chelating agent was used for the neutralization of CN^- in complex formation which is more effective and inexpensive. The values of thermodynamic parameters for complex formation are found to be Ea = 78.2 kJ mol^{-1}, $\Delta S^{\neq}$ = -48.67 JK^{-1} $mole^{-1}$ and $\Delta H^{\neq}$ = -52.5 kJ $mole^{-1}$. The negative value of shows the exothermic nature of reaction.

References

1. Abu-Gharib E A, Ali R, Blandamer M J, Burgess J, *Transition Met Chem.*, 1987, **12**, 371.
2. Stochel G, van Eldik R, *Inorg Chim Acta*, 1989, **155**, 95.
3. Borges S D S S, Coelho A L, Moreira I S and Araujo M A B D, *Polyhedron*, 1994, **13**, 1015
4. Alshehri S, *Transition Met Chem.*, 1997, **22**, 553.
5. Maciejowska I, Stasicka Z, Stochel G and van Eldik R, *J Chem Soc.*, 1999, 3643.

6. Fernandez G, Del M G M, Rodriguz A, Munoz M, Moya M L, *React Kinet Cat Lett.*, 2000, **70**, 389.
7. Sabo E M, Shepherd R E, Rau M S and Elliott M G, *Inorg Chem.*, 1987, **26**, 2897.
8. Fernando M D, Refael J, Carlos G H and Francisco S, *New J Chem.*, 1999, **23**, 1203.
9 Fernandez G, Del M G M, Rodriguz A, Munoz M and Moya M L, *J Colloid Interface Sci.*, 2000, **225**, 47.
10. He R and Wang J, *Xiyou Jinshu Cailiao Yu Gongcheng*, 1999, **28**, 60; *Chem Abstr.*, 1999, **130**, 275849g.
11. Zmikic A, Cvrtila D, Pavlovic D, Murati I, Reynolds W and Asperger S, *J Chem Soc., Dalton Trans.*, 1973, 1284.
12. Feng Y L, Narasaki H, Tian L C, Wu S M and Chen H.Y, *Anal Sci.*, 1999, **15**, 915.
13. Alam T and Kamaluddin, *Bull Chem Soc Jpn.*, 1999, **72**, 1697.
14. Sharpe A G, The Chemistry of Cyano Complexes of Transition Metals, Academic Press, London, 1976, p. 1081, 1262.
15. Weast R C, CRC Handbook of Chemistry and Physics, The Chemical Rubber Co., Ohio, 49th Ed., 1969, D-79
16 Eaton W A, George P and Hanaria G H, *J Phys Chem.*, 1967, **71**, 2016.
17. Beck M T, Fourteen: A Magic Number of Coordination Chemistry, Proc. XX ICCC, Calcutta, India, 1979, In Coordination Chemistry-20, Pergamon Press, Oxford, 1979, p. 31.
18. Masaru Kimura, Yuko Shiota, Shinobu Kishi and Keiichi Tsukahara, *Bull Chem Soc.*, 1999, **72**, 1293-1299
19 Athos Bellomo, Domenico De Marco and Agatino Casale, *Talanta*, 1975, **22**, 197-199
20. Reddy B R and Raman S, *Indian J Chem.*, 1984, **23A**, 616.
21. Raman S, *Indian J Chem.*, 1980, **19**, 907.

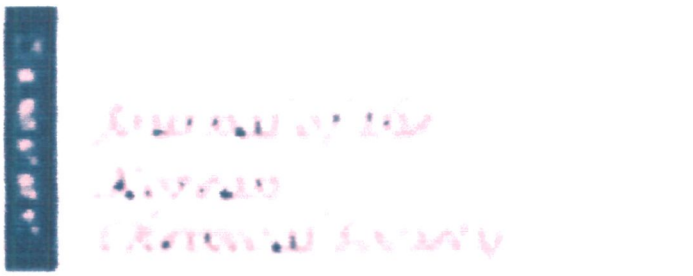

Journal of the Korean Chemical Society
2009, *Vol. 53, No. 2*
Printed in the Republic of Korea

속 이온과 CFP 상호작용: 흡수 형광 분광법에 의한 금속 이온과 CFP의 착물 형성

K. S. Siddiqi*, Ayaz Mohd, Aftab Aslam Parwaz Khan, and Shaista Bano
Department of Chemistry, Aligarh Muslim University, Aligarh-202001, India
(2008. 12. 24 접수)

Interaction of CFP with Metal ions: Complex Formation of CFP with Metal ion by Absorption and Fluorescence Spectrophotometery

K. S. Siddiqi*, Ayaz Mohd, Aftab Aslam Parwaz Khan, and Shaista Bano
Department of Chemistry, Aligarh Muslim University, Aligarh-202001, India
(Received December 24, 2008)

요 약. 산성 용액에서 Ca^{2+}, Mg^{2+}, Mn^{2+}, Fe^{3+}, Co^{2+}, Ni^{2+}, Cu^{2+} 및 Zn^{2+}와 Cefpodoxime proxetil (CFP)의 상호작용을 분광학적으로 조사한 결과 1:1 착물이 형성됨을 알 수 있다. 순수한 약품의 흡수스펙트럼은 270과 345 nm에서 두 개의 현저한 봉오리를 보였다. 여러 pH에서 스펙트럼은 두 개의 isosbestic 점(305과 330 nm)을 나타내었다. 이는 용액상에서 약품의 쯔비터 이온이 존재함을 의미한다. 다른 농도의 금속이온에서 CFP의 형광방출 스펙트럼은 chelating enhancement fluorescence(CHEF)효과에 의해 형광강도가 증가함을 알 수 있었다. 착체의 화학량론은 Job"s 와 Benesi-Hildebrand 방법에 의해 결정되었다. 착체의 안정도는 다음 순서와 같다. $Ca^{2+} < Mg^{2+} < Co^{2+} < Ni^{2+} < Zn^{2+} < Mn^{2+} < Cu^{2+} < Fe^{3+}$.

주제어: CFP; 형강증강; 안정도 상수; 착체형성; CHEF

ABSTRACT. Spectrophotometric investigation of the interaction of Cefpodoxime proxetil (CFP) with Ca^{2+}, Mg^{2+}, Mn^{2+}, Fe^{3+}, Co^{2+}, Ni^{2+}, Cu^{2+} and Zn^{2+} in acidic medium showed the formation of 1:1 complex. The absorption spectrum of pure drug exhibits two prominent peaks at 270 and 345 nm. Its spectra scanned at several pH exhibited two isosbestic points (305 and 330 nm) indicating the presence of zwitterionic condition of drug in solution phase. The fluorescence emission spectra of CFP in presence of different concentrations of metal ions showed enhancement in fluorescence intensity which is ascribed to chelating enhancement fluorescence effect (CHEF). The stoichiometry of the complexes was determined by Job's and Benesi-Hildebrand method. The stability of the complexes follow the order $Ca^{2+} < Mg^{2+} < Co^{2+} < Ni^{2+} < Zn^{2+} < Mn^{2+} < Cu^{2+} < Fe^{3+}$.

Keywords: CFP, Fluorescence enhancement, Stability constant, Complex formation, CHEF

INTRODUCTION

Cefpodoxime proxetil (CFP) is a semisynthetic β-lactum antibiotic known as (RS)-1(isopropoxycarbonyloxy) ethyl (+)-(6R, 7R)-7-[2-(2-amino-4-thiazolyl)-2-{(Z) methoxyimino} acetamido]-3-methoxymethyl-8-oxo-5-thia-1-azabicyclo [4.2.0] oct-2-ene-2-carboxylate. It is an ester prodrug of cefpodoxime acid where a proxetil radical is attached to cefpodoxime acid (*Fig.* 1). It is the third generation cephalosporin ester, used in the treatment of upper respiratory tract and urinary tract infection. In biological system cefpodoxime undergoes ester hydrolysis and converted into cefpodoxime acid to exhibit its antibiotic activity.[1,2] It has an asymmetric carbon at position 4 and is supplied as racemic mixture of R and S-enantiomers. Only a few methods are reported to quantify

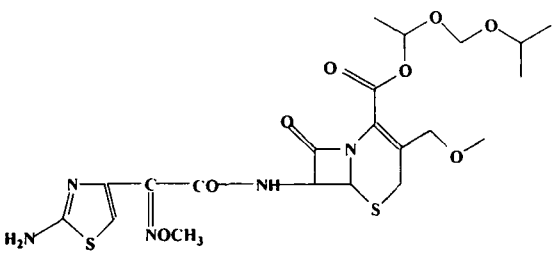

Fig. 1. Structure Cefpodoxime Proxetil (CFP).

CFP,[3,4] nevertheless the analytical methods of detection of CFP are handful, and they employ RP-HPLC. These methods are based on separation of the R- and S-isomers.[5] However, both the isomers are reported to exhibit similar biological activity,[1] the use of highly sophisticated and time-consuming methods is not always required for routine analysis of CFP from the different dosage forms.

The discovery of cephalosporin from *C.acremonium* culture by Brotzu[6] and demonstration of its remarkable stability towards aqueous solution even at pH 2 as well as its excellent *in vitro* activity against penicillin-resistant organisms by Abraham and Newton,[7] were major breakthroughs in the history of β-lactam antibiotics. The realization that fungi might be a good source for novel antibiotics spurred microbiologists to develop novel soil-screening programmes for the investigation of microbial culture leading to the discovery of several non-classical β-lactams like carbapenem[8] and oxacephems.[9] The reactivity of β-lactam antibiotics is fundamentally linked to antimicrobial activity, it led Woodward[10] to design and synthesize carbapenem group of compounds for evaluation of their antibacterial activity through systematic screening of the soil microorganism. Numerous of these compounds show broad-spectrum antimicrobial activity as predicted earlier and it was further substantiated by the subsequent discovery of thienamycin. It is unstable in its pure form and hence its derivatives are used which also led to the introduction of imipenem, which is regarded as one of the most effective drugs among the β-lactam antibiotics. Although several methods have been developed to determine the drug in biological fluids and pharmaceutical preparations[11] no effort seems to have been made to investigate the interaction of the drug with metal ions.

In the present work an earnest effort has been made to study the interaction of the CFP with metal ions by fluorescence emission and absorption spectrophotometric measurements. Since quenching or enhancement in fluorescence intensity of the drug in presence of metal ions occurs, the spectra of the drug in presence of different concentrations of metal ions such as Ca^{2+}, Mg^{2+}, Mn^{2+}, Fe^{3+}, Co^{2+}, Ni^{2+}, Cu^{2+}, and Zn^{2+} were scanned. The ratio of the drug to metal ions was determined by Job's method and Benesi-Hildebrand methods.[12,13] The absorption spectra of the drug in the pH range 2.32-11.50 were run to see the zwitterionic condition, apparent ionization constant and the isosbestic point which indicate the presence of different species in solution. The stability constant of the complexes formed between the drug and metal

Table 1. Stability constant and other thermodynamic parameters of CFP complexes (Job's method)

Metal	logK		Gibbs energy change	Enthalpy change	Entropy change
	25 °C	35 °C	($-\Delta G$)(kJ.mol^{-1})	(ΔH) (J.mol^{-1})	(ΔS) (J.mol^{-1} K^{-1})
Ca^{2+}	5.600	5.846	31.95	270.22	108.13
Mg^{2+}	5.915	6.044	33.75	164.93	113.82
Mn^{2+}	6.200	6.289	35.38	49.97	118.91
Fe^{3+}	6.287	6.356	35.87	260.34	121.22
Co^{3+}	5.983	6.122	34.13	244.95	115.38
Ni^{2+}	6.130	6.276	34.97	178.43	117.97
Cu^{2+}	6.211	6.315	35.44	240.25	119.93
Zn^{2+}	6.184	6.297	35.28	190.29	119.04

Table 2. Stability constant, Gibbs energy change of CFP complexes (Benesi-Hildebrand method) at 25 °C

Metal	logK	Gibbs energy change ($-\Delta G$) ($kJ.mol^{-1}$)	R^2
Ca^{2+}	6.854	39.11	0.9843
Mg^{2+}	6.869	39.19	0.9784
Mn^{2+}	6.886	39.29	0.9769
Fe^{3+}	6.919	39.48	0.9914
Co^{2+}	6.883	39.27	0.9807
Ni^{2+}	6.884	39.28	0.9845
Cu^{2+}	6.896	39.34	0.9668
Zn^{2+}	6.889	39.30	0.9706

ion was also evaluated.

EXPERIMENTAL

Instruments

The absorption spectra were obtained with Elico-SL-169 double beam UV-visible spectrophotometer. Fluorescence emission spectra were scanned with Hitachi-F-2500FL-spetrophotometer. All potentiometric measurements were done with Elico-LI-120 pH meter.

Methods and materials

Double distilled water was used throughout Cefpodoxime proxetil (Lupin pharmaceutical Ltd, India), sodium hydroxide and metal chloride (Merck Ltd, Mumbai, India) and HCl (Ranbaxy fine chem. Ltd, India) were used as received.

Preparation of solution

Stock solution of Cefpodoxime proxetil and metal salts of 1×10^{-3} M were prepared in 1×10^{-2} M HCl. Stock solution of drug was stored at 4 °C.

Spectrophotometric method

Solutions of equimolar concentration (1×10^{-4} M) of CFP and metal ions were prepared. The pH of the drug was adjusted between 2.32 to 11.50 by adding sodium hydroxide and hydrochloric acid (1×10^{-1} M and 1×10^{-2} M respectively). The absorption spectra were recorded in the range 250-380 nm. The ratio of metal to CFP was determined by Job's method. The linearity of CFP was found in the range 2×10^{-5} to 6×10^{-4} mg/ml and the correlation factor (R^2) 0.9236.

Fluorescence study

Solution of the CFP (7×10^{-6} M) and those of metal ions (1×10^{-6} to 7×10^{-6} M) were prepared. To prepare dilute solutions, an aliquot of stock solution was placed in a 10 ml volumetric flask and made up to the mark with distilled water. Spectra were recorded immediately after sample preparation in the optimum wavelength range 370-430 nm at optimum excitation wavelength of 335 nm. For calibration curve an aliquot of stock solution (1×10^{-6} to 3×10^{-5} mg/ml) was prepared which showed linearity with correlation factor (R^2) 0.9652

RESULTS AND DISCUSSION

Spectrophotometric study

The absorption spectrum of CFP (1×10^{-4} M) was run in the region 250-380 nm. It exhibited two peaks at 270 and 345 nm (*Fig.* 2). Since the first peak is very strong it was selected for further absorption studies.

When the spectra of the drug were run at varying pH in the region 250-380 nm two isosbestic points, one at 305 nm and another at 330 nm were observed which indicated the presence of zwitter ionic condition in solution (*Fig.* 3).[14] The appa-

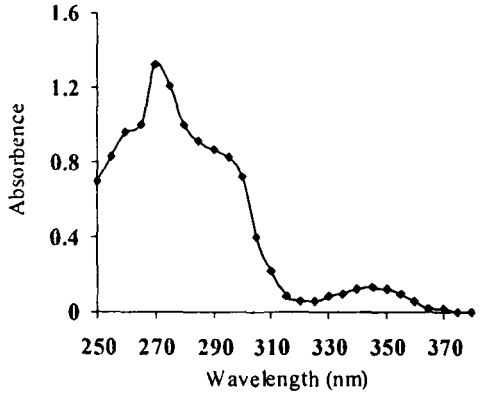

Fig. 2. Absorption spectrum of CFP (1×10^{-4} M) at pH 5.15.

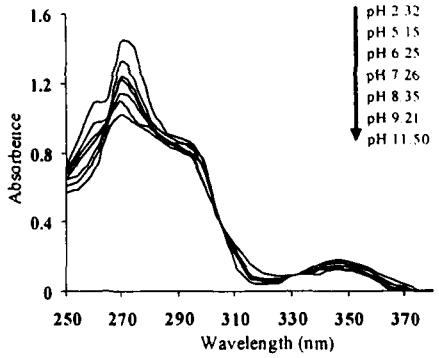

Fig. 3. Absorption Spectra of CFP (1×10^{-4} M) in (2.32-11.50) pH range.

rent ionization constant (pKa') of the drug was calculated (8.92) by the following equation.

$$pKa' = pH + \log \{(A_I - A_M)/(A - A_M)\} \quad (1)$$

where, A_I = absorbance of drug in basic medium, A_M = absorbance of drug in acidic medium, A= absorbance of drug in aqueous medium.

The absorption spectra corresponding to the metal, drug and complexes were obtained in acidic medium. The concentration of cations and drug (CFP) were 1×10^{-4} M. The stoichiometry of the complexes was obtained by Job's methods[12,15] a sample of resulting plots is shown in *Fig.* 4. The stability constant of chelate formed is calculated by following equation

$$K = \frac{A/A_{ex}\,C_X}{(C_M - A/A_{ex}\,C_X)(C_L - A/A_{ex}\,C_X)} \quad (2)$$

where, K is the stability constant of the metal chelate formed in the solution, M = metal, L = ligand, X = mole fraction of the ligand at maximum absorption. A/A_{ex} is the ratio of the absorbance to that indicated by the tangent for the same wavelength. C_X, C_M and C_L are the limiting concentration of complex, metal ion and the drug respectively.

The stability constant is related to the standard enthalpy changes ΔH and other thermodynamic function by the equation:

$$\Delta G = -2.303RT\log K = \Delta H - T\Delta S \quad (3)$$

where R is the gas constant T is the experimental

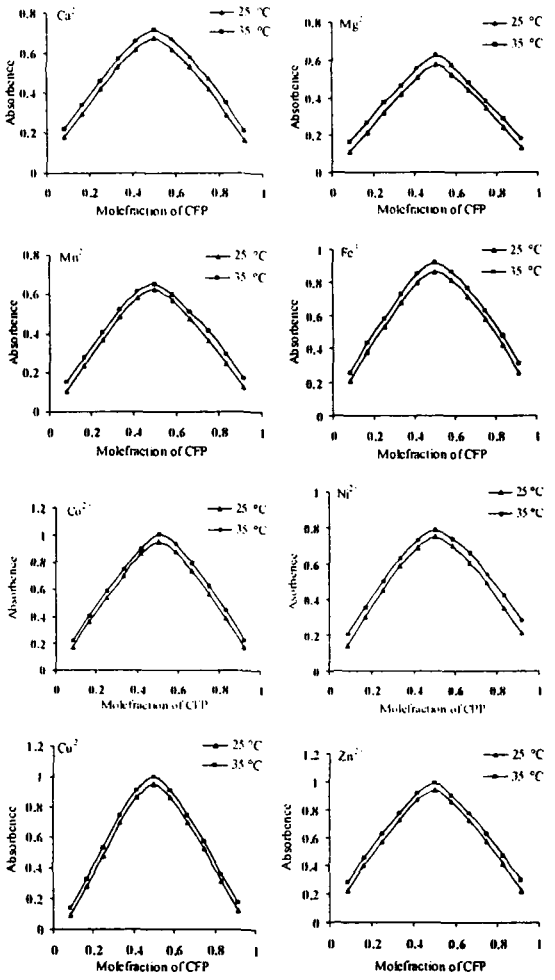

Fig. 4. Continuous variation curves of CFP and metal complexes.

temperature, K is the binding constant at the corresponding temperature.

From the value of stability constant at different temperature the enthalpy changes can be calculated by using the equation:

$$\text{Log}K_2/K_1 = [1/T_1 - 1/T2]\Delta H/2.303R \quad (4)$$

The negative value of ΔG for the complexation process suggests spontaneous nature of such process.[16,17] The positive value of ΔH suggests that these processes are endothermic and are favourable at higher temperature. Also it is entropically favourable. The positive value of H and S indicates that hydrophobic force may play a major

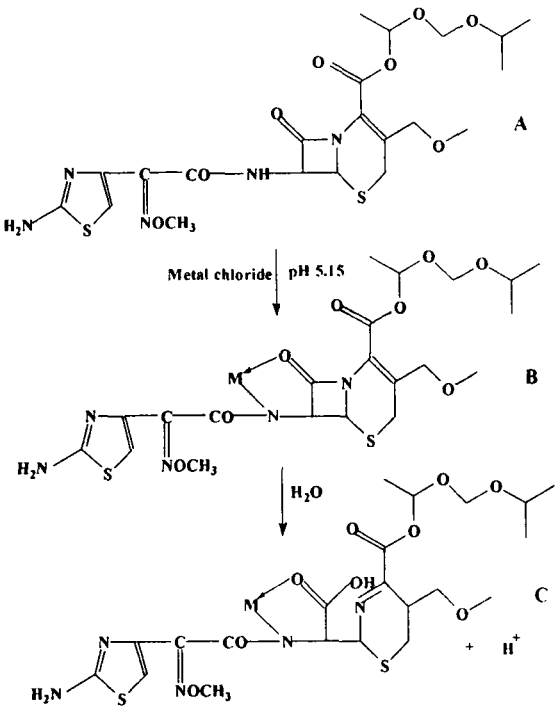

Fig. 5. Mechanism of binding of CFP with metal ions: A. CFP, B. CFP-metal complex, C hydrolyzed form of complex.

role in the interaction.[18] It is reasonable to think, on the basis of these results that the metal ions form a five membered chelate ring with CFP.

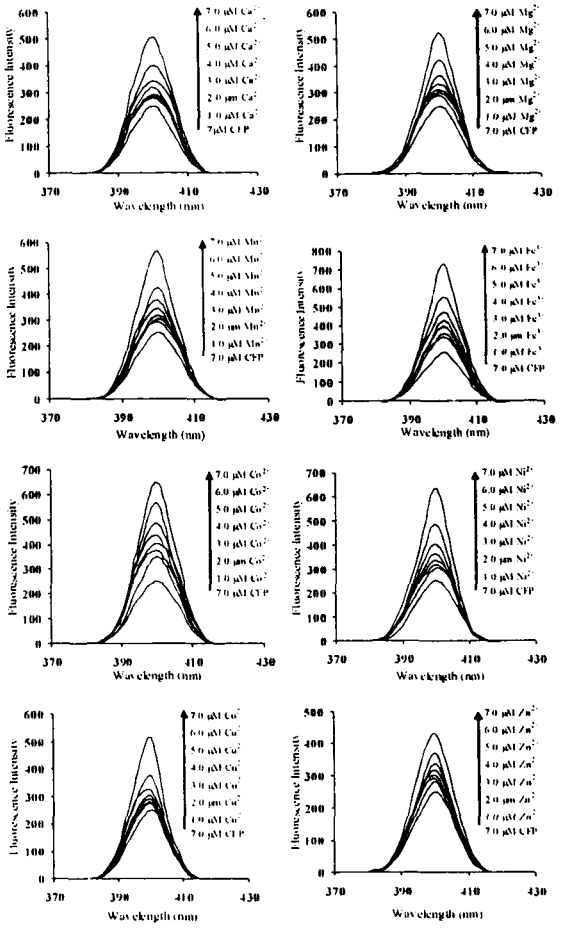

Fig. 6. Fluorescence enhancement (at λ_{ex} 335nm) of CFP in presence of metal ions.

Fluorescence study

The fluorescence emission spectrum of the pure drug is markedly different from its absorption spectrum in UV region. The emission spectrum run between 350-450 nm at excitation wavelength of 335 nm showed a peak at 400 nm. The addition of metal ions to the drug causes enhancement or quenching in the fluorescence spectrum. We have noted an enhancement in fluorescence intensity at 400 nm in each case (Ca^{2+}, Mg^{2+}, Mn^{2+}, Fe^{3+}, Co^{2+}, Ni^{2+}, Cu^{2+} and Zn^{2+}) (*Fig.* 6) although the shape and position of emission spectrum remains unchanged.

The stoichiometry and stability constant of the complexes was determined by Benesi-Hildbrand method.[13] The Benesi-Hildebrand plots were examine to further characterize the stoichiometry of the CFP-metal complexes. In case of a 1:1 complex, the following equation is applicable:

$$1/F\text{-}F_o = 1/(F_\infty\text{-}F_o)K\,[Me]_o + 1/(F_\infty\text{-}F_o) \quad (6)$$

In this approach, a graph of $1/(F - F_o)$ versus $1/[Me]_o$, was made where F is the observed fluorescence at each concentration tested, F_o is the fluorescence intensity of analyte in the absence of metal ion, F_x is the maximum fluorescence intensity in presence of metal ions and $[Me]_o$ is the concentration of metal ion. A linear plot is required for this double reciprocal plot in order to conclude 1:1 stoichiometry. In such cases, a linear relationship has to be obtained when $1/(F - F_o)$ versus $1/[Me]_o$ is plotted. The stability constant is determined by dividing the intercept by the slope

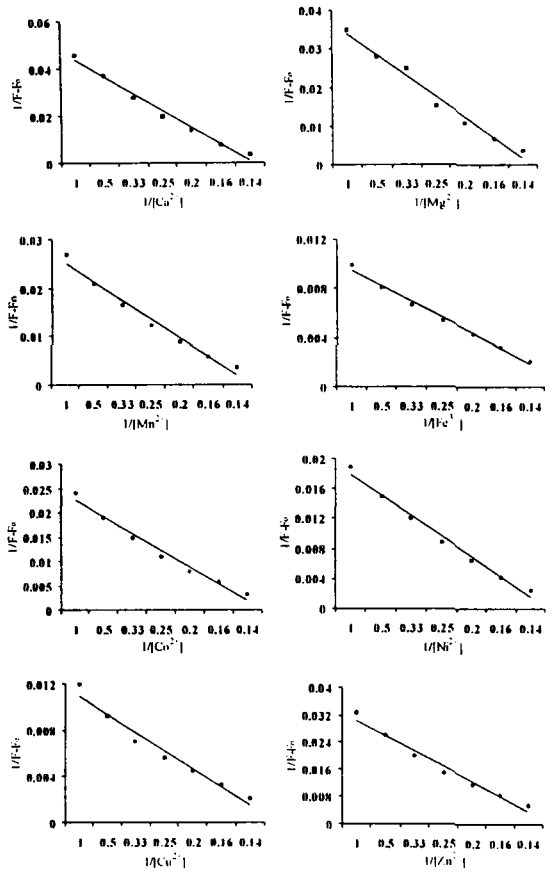

Fig. 7. Benesi-Hildebrand's plots for 1:1 (CFP: metal complexes)

of the straight line obtained in the double-reciprocal plot. (*Fig.* 7)

Influence of metal ion concentrations

The influence of metal ions concentration was studied in the range of 1×10^{-6}-10×10^{-6} M. The fluorescence study of interaction CFP with metal ions in acidic aqueous medium showed 1:1 stoichiometry. Both these study also support the formation of 1:1 CFP:Metal complex, with the possibility of metal ions chelating with CFP by β-actum carbonyl carbon and acidamide nitrogen.

In general, the phenomenon of enhancement is observed because the complexation by cations causes increase in the redox potential of the donor so that the relevant HOMO energy decreases to a level lower than that of fluorophore. Consequently the excited state energy of fluorophore is dumped as a visible emission.[19]

The reason of this enhancement lies in strong perturbation of the excited state upon coordination of the metal ion. A low lying internal charge transfer state due to the presence of electron donor and acceptor group in the CFP is the lowest excited state, this state is however, a less emitting state and in equilibrium with the π-π^* excited state of the molecule, upon coordination with metal cation the PCT interaction becomes weaker since the electron withdrawing group is now electron rich moiety due to the deprotonation of –NH group necessary for coordination of metal cation.

In the present work an attempt has been made to study the interaction of the CFP with metal ions by fluorescence emission, absorption spectrophotometric and measurements. Since enhancement in fluorescence intensity of the CFP in presence of the metal ions occurs, the spectra of the drug in presence of different concentrations of several metal ions were scanned. The ratio of the drug to metal ions was determined by Job's and Benesi-Hildbrand method. The absorption spectra of the CFP was run at different pH to see the zwitterionic condition, apparent ionization constant and the isosbestic point indicating the presence of different species in solution. The stability constant of the complex formed between the drug and metal ion was also evaluated.

CONCLUSION

In this paper the nature and magnitude of the interaction of CFP with biologically important metal ion was investigated by fluorescence spectra and UV spectra. The experimental result indicated the formation of 1:1 complex of CFP with metal ions in acidic medium by Job's and Benesi-Hildbrand method. The absorption spectra at different pH showed the presence of two isosbestic point indicating the existence of zwitterionic condition. The thermodynamic parameters showed that the interaction between CFP and metal ion was spontaneous, and that the hydrophobic force was a major factor in the interaction.

REFERENCE

1. Borin, M. T. Drugs **1991**, *42*, 13.
2. Rodriguez, J. C.; Hernandez, R.; Gonzalez, M.; Rodriguez, Z.; Tolon, B; Velez, H.; Valdes, B.; Lopez, M. A.; Fini, A. Il Farmaco. **2003**, *58*, 363.
3. Camus, F.; Deslandes, A.; Harcouet, L.; Farinotti, R. *J. Chromatogr B.* **1994**, *656*, 383.
4. Steenwyk, R. C.; Brewer, J. E.; Royer, M. E.; Cathcart, K. S. *J. Liq. Chromatogr.* **1991**, *14*, 3641.
5. Fakutsu N.; Kawasaki T.; Saito K.; Nakazawa H. *J. Chromatogr. A.* **2006**, *1129*, 153.
6. Abraham, E. P. *Drugs*, **1987**, *34*, 1.
7. Abraham, E. F; Newton, G. G. H. *Biochem. J.* **1961**, *79*, 377.
8. Nagahara, T.; Kametani, T. *Heterocycles.* **1987**, *25*, 729.
9. Nagata, W. *Pure Appl. Chem.* **1989**, *61*, 325.
10. Mitsuhashi, S.; Franseschi, G. *Penem Antibiotics*; Japan Scientific Societies Press: Springer Verlag, Berlin, 1991, p. 26.
11. Antonio, L.; Doadrio, A. M.; and Regina, O. *J. Braz. Chem. Soc.* **2002**, *13*, 95.
12. P. Job. *Ann. Chim. Phys.* **1928**, *9*, 113.
13. Benesi, H.; and Hildebrand, J. H. *J. Am. Chem. Soc.* **1949**, *71*, 2703.
14. Park, H. R.; Chung, K. Y.; Lee, H. C.; Lee, J. K.; Bark, K. M. *Bull. Chem. Soc.* **2000**, *21*, 849.
15. Vosburgh, W. C.; Copper, G. R. *J. Am. Chem. Soc.* **1941**, *63*, 437.
16. El-Sonbati, A. Z.; El-Bindary, A. A.; Ahmad, R. M. *J. Solution Chem.* **2003**, *32*, 617.
17. Bebot-Brigaud, A.; Dange, C.; Fauconnier, N.; Gérard, C. *J. Inorg. Biochem.* **1999**, *75*, 71.
18. Ross, P. D; Subramanium, S. *Biochemistry.* **1981**, *20*, 3096.
19. Quang, D. T.; Jung, H. S.; Yoon, J. H.; Lee, S. Y.; Kim, J. S. *J. Bull. Korean Chem.* **2007**, *28*, 682.

Journal of the Korean Chemical Society
2009, *Vol. 53, No. 6*
Printed in the Republic of Korea

알칼리성 용매에서 과망간에 의한 세프포독심 프록세틸의 산화의 분광광도법적 조사: 속도론적 연구

Aftab Aslam Parwaz Khan, Ayaz Mohd, Shaista Bano, and K. S. Siddiqi*
Department of Chemistry, Aligarh Muslim University, Aligarh, 202002, (U. P.) India
(접수 2009. 5. 13; 수정 2009. 11. 9; 게재확정 2009. 11. 16)

Spectrophotometric Investigation of Oxidation of Cefpodoxime Proxetil by Permanganate in Alkaline Medium: A Kinetic Study

Aftab Aslam Parwaz Khan, Ayaz Mohd, Shaista Bano, and K. S. Siddiqi*
Department of Chemistry, Aligarh Muslim University, Aligarh, 202002, (U. P.) India
(Received May 13, 2009; Revised November 9, 2009; Accepted November 16, 2009)

요약. 일정한 이온 세기의 알칼리 용액에서 과망간산에 의한 프포독심 프록세틸(Cefpodoxime Proxetil)의 산화의 속도론적 경로가 분광광도법적으로 연구되었다. 그 반응은 과망간산 이온 농도에서 일차 속도론적으로 나타났으며, 프포독심 산과 알칼리 농도에서 단일 이하의 차수를 나타내었다. 용매의 이온 세기가 증가함에 따라 속도도 증가하였다. 산화 반응은 프포독심 산과 함께 복합체를 형성하는 알칼리-과망간산 종들을 통하여 진행된다. 반응물을 만들기 위해서 프포독심 산의 자유 라디칼과 과망간산의 다른 분자 사이의 빠른 반응에 이어서 다음 분해가 천천히 진행된다. 다양한 온도에서 반응의 조사는 제안하는 메커니즘의 느린 단계를 고려한 활성화 변수들의 결정할 수 있게 하고 일차 속도론을 따른다. 제안하는 메커니즘과 유도된 속도 법칙들은 관찰된 속도들과 일치하였다.

주제어: 프포독심 프록세틸, 과망간산, 속도론, 열역학

ABSTRACT. A Kinetics pathway of oxidation of Cefpodoxime Proxetil by permanganate in alkaline medium at a constant ionic strength has been studied spectrophotometrically. The reaction showed first order kinetics in permanganate ion concentration and an order less than unity in cefpodoxime acid and alkali concentrations. Increasing ionic strength of the medium increase the rate. The oxidation reaction proceeds via an alkali-permanganate species which forms a complex with cefpodoxime acid. The latter decomposes slowly, followed by a fast reaction between a free radical of cefpodoxime acid and another molecule of permanganate to give the products. Investigations of the reaction at different temperatures allowed the determination of activation parameters with respect to the slow step of proposed mechanism and fallows first order kinetics. The proposed mechanism and the derived rate laws are consistent with the observed kinetics.

Keywords: Cepfodoxime proxetil, Permanganate, Kinetics, Themodynamics

INTRODUCTION

Cefpodoxime proxetil (CFP) is one of the several new cephems administered orally as inactive esters of the antibiotic Cefpodoxime. It is (1-[isopropoxy-carbonyl) oxy] ethyl ester of (z)-7-[2-(2-amino-1,3-thiazol-4-yl)-2-methoxyiminoacetamido]-3-meth oxymethyl-3-cephem-4-carboxylic acid) (*Fig.* 1). CFP is an ester prodrug of Cefpodoxime acid (CFA), where a proxetil radical is attached to CFA. It is an orally absorbed, broad spectrum, third generation cephalosporin ester implicated in the treatment of

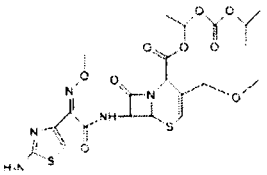

Fig. 1. Structure of Cefpodoxime Proxetil (CFP).

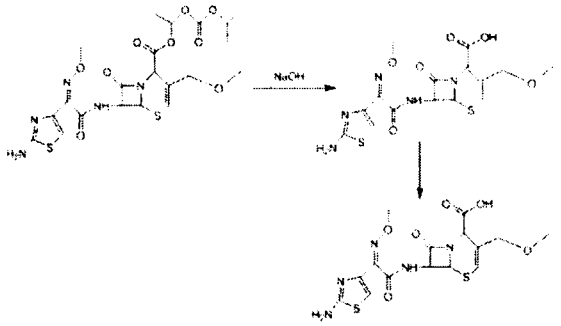

Fig. 2. Degradation Pathway of Cefpodoxime Proxetil to Cefpodoxime acid.

upper respiratory tract and urinary tract infections. In the biological system, CFP undergoes ester hydrolysis and is converted into CFA to exhibit its antibiotic activity.[1-2] CFP has an asymmetric carbon at position 4 and is supplied as racemic mixture of R- and S-enantiomers. Few methods are reported to quantify CFA.[3-4] The β-lactum antibiotic is known to degrade by hydrolysis in alkaline solution (*Fig.* 2).[5] Hydrogen peroxide is used for degradation study in the development of pharmaceuticals. The HCl, NaOH, NH_2OH and H_2O_2 at appropriate concentration were evaluated as degradation agents for cleaning or decontamination.[6] Permanganate ion oxidizes a larger variety of substrate and finds extensive application in organic synthesis.[7-12] During oxidation permanganate is reduced to various oxidation states in acidic, alkaline and neutral media. The mechanism of oxidation depends on the substrate and medium.[13] The process Mn(VII) to Mn(IV) can be divided into a number of partial steps and examined discretely. The MnO_2 appears only a after the complete consumption of MnO_4^-. No mechanistic information is available to distinguish between a direct one-electron reduction of Mn(VII) to Mn(VI) or a hypopermanganate ion is formed in a two-electron reduction followed by a quick reaction.[14-15] In this paper a simple and sensitive kinetic spectrophotometric method has been developed to establish the thermodynamic parameters of Cepfodoxime acid. The method is based on the oxidation of the drug by permanganate in alkaline medium. The present studies is aimed at checking the reactivity of CFA toward permanganate, at determining the redox chemistry of the Mn(VII) in such media, and at arriving at a plausible mechanism.

EXPERIMENTAL

Apparatus

A Shimadzu UV-visible 1601 spectrophotometer was used for all spectral measurements, pH-metric measurements were done with Elico-LI 120 pH meter and a water bath shaker NSW 133, India was used to control the temperature.

Materials

The Cepfodoxime Proxetil was obtained from (Lupin pharmaceutical Ltd, India). Pharmaceutical preparations containing the studied compounds were purchased from commercial sources in the local market. The permanganate solution was prepared and standardized against oxalic acid.[16] Potassium permanganate solution was prepared as described by Carrington and Symons.[17] NaOH (Merck Ltd, Mumbai, India) and $NaClO_4$ (Ranbaxy fine chem. Ltd, India) were employed to maintain the required alkalinity and ionic strength, respectively.

Reagents

Double distilled, de-ionized water was used throughout. The chemicals used were of analytical grade. Stock solutions of the compounds were wrapped with carbon paper to protect them from photodecomposition.

Kinetic procedure

The oxidation of (CFA) by permanganate ion was followed under pseudo- first order conditions where CFA concentration was greater than manganese (VII) at 25 °C. The reaction was initiated by mixing

previously thermostated solutions of MnO_4^- and (CFA), which also contained required quantities of NaOH and $NaClO_4$ to maintain alkaline medium and ionic strength, respectively. The temperature was maintained at 25 °C: The reaction was monitored by a the decrease in absorbance of MnO_4^-, at its absorption maximum of 525 nm. Earlier it was verified that there is no interference from other reagents at this wavelength. Application of Beer's Law for permanganate at 525 nm had earlier been verified, giving ε, was found to be 2083 ± 50 dm^3 mol^{-1} cm^{-1}. The reaction was followed more than three half lives The first order rate constants k_{obs} were evaluated by plots of log [MnO_4] *vs.* time. The first order plots in almost all cases were linear up to 85% of the reaction and k_{obs} were reproducible at 525 nm and an increasing absorbance of Mn(VI) at 610 nm during the course of the reaction (*Fig.* 5). The effect of dissolved oxygen on the rate of reaction was checked by preparing the reaction mixture and following the reaction in nitrogen atmosphere. No significant difference between the results obtained under nitrogen and in the presence of air was observed. Added carbonate had also no effect on the reaction rate. Regression analysis of experimental data to obtain the regression coefficient r and the standard deviation S of points from the regression line was performed using a Microsoft excel-2007 program.

RESULTS

The absorption spectrum of CFP was exhibited two peaks at 270 and 345 nm (*Fig.* 3).[18] After addition of potassium permanganate in the same medium is oxidized the (CFA) and exhibits a green colour of manganate ion, appears which absorbs at 610 nm. It was empirically found that the blue colour originated from a mixture of violet MnO_4^- and green

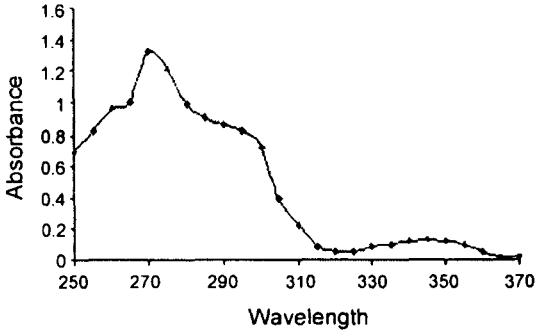

Fig. 3. Absorption spectrum of CFP.

colour MnO_4^{2-} rather than form the formation of hypopermanganate. The formation of Mn (VII) was also evidence by the decrease of the absorbance of Mn(VII) at 525 nm and the increase of that of Mn(VI) at 610 nm during the course of reaction (*Fig.* 5).The intensity of the colour increases with time and hence a kinetic method based on the spectrophotometric measurement was developed.

Stoichiometry of the reaction

The reaction mixture containing an excess of permanganate over (CFA) were mixed in the presence of 5.0×10^{-2} mol dm^{-3} NaOH and at constant ionic strength I = 0.10 mol dm^{-3} were kept in a closed container under a nitrogen atmosphere at 25 °C. After 1 h the manganese (VII) concentration was assayed by measuring the absorbance at 610 nm. The results indicated that 2 mols of manganese (VII) consumed 1 mol of (CFA). Therefore, the reaction mechanism is proposed on the basis of the literature background[19] and our experimental study as shown in eq 1.

Reaction order

The reaction order were evaluated from the slope of log k_{obs} *versus* log concentration plots by the varying concentration of (CFA) and alkali keeping other factors constant.

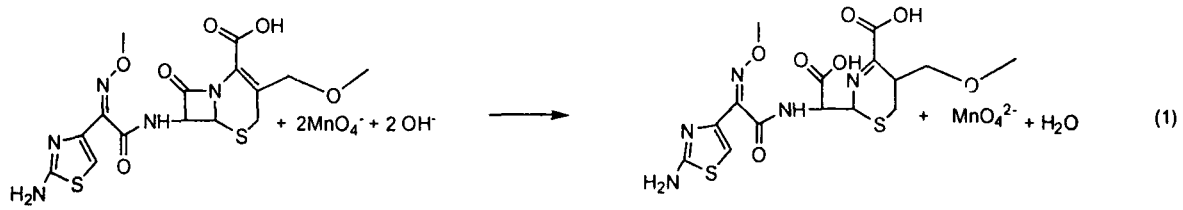

(1)

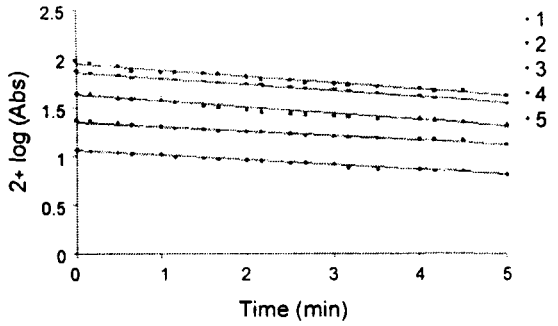

Fig. 4. First order plots for the oxidation of CFA by alkaline MnO^{4-} at 25 °C; [CFA] = 1.0 × 10^{-3}; [OH-] = 2 × 10^{-3}; I = 0.10/mol dm^{-3}. [Mn(VII)] × 10^{4} mol dm^{-3}: (1) 0.6, (2) 0.8, (3) 1.0, (4) 2.0, and (5) 3.0.

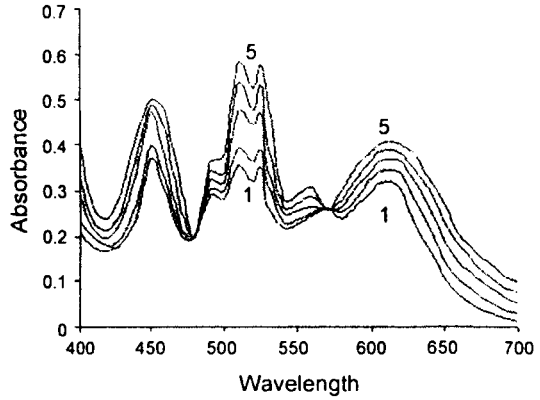

Fig. 5. Spectral changes during the oxidation of [CFA] by alkalineMnO^{4-} at 25 °C; [Mn(VII)] = 1.0 × 10^{-4}, [CFA] = 1.0 × 10^{-3} [OH^-] = 2 × 10^{-2}, I = 0.10/mol dm^{-3}.

Effect of Concentration of Manganese (VII)

At constant concentration of (CFA), 1.0 × 10^{-3} mol dm^{-3}, and alkali, 5.0 × 10^{-2} mol dm^{-3}, and at constant ionic strength, 0.10 mol dm^{-3}, The oxidant $KMnO_4$ concentration was varied in the range of 6 × 10^{-5} – 6 × 10^{-4} mol dm^{-3}. All kinetic runs exhibited identical characteristics. The linearity of plots of log (absorbance) *vs* time, for different concentrations of permanganate, indicates order in manganese(VII) concentration as unity (*Fig.* 4). This was also confirmed by the constant values of pseudo first order rate constants, k_{obs}, for different manganese(VII) concentrations (*Table* 1).

Effect of NaOH Concentration

The effect of increasing conc of alkali on the reaction was examined at constant concentration of drug and permanaganate ion at 25 °C. The alkali concentration was varied in the range of 0.6 × 10^{-2} to 1.0 × 10^{-1} mol dm^{-3}. The k_{obs} values increased with increase in concentration of alkali.

Table 1. Effect of variation of [$KMnO_4$] ,[CFA] and [OH^-] on the oxidation of cefpodoxime acid by alkaline [$KMnO_4$] at 25°C and ionic strength I = 0.10/mol dm^{-3}

10^4× [$KMnO_4$] mol dm^{-3}	10^3× [CFA] mol dm^{-3}	10^2× [OH^-] mol dm^{-3}	10^3 k_{obs} (S^{-1})	10^3 kcal (S^{-1})
0.6	3.0	2.0	1.08	1.09
0.8	3.0	2.0	1.09	1.09
1.0	3.0	2.0	1.08	1.09
2.0	3.0	2.0	1.07	1.09
3.0	3.0	2.0	1.10	1.09
4.0	3.0	2.0	1.08	1.09
6.0	3.0	2.0	1.09	1.09
3.0	0.6	2.0	0.984	0.983
3.0	0.8	2.0	1.05	1.06
3.0	1.0	2.0	1.06	1.07
3.0	1.2	2.0	1.37	1.36
3.0	1.4	2.0	1.60	1.58
3.0	1.6	2.0	1.72	1.73
3.0	1.8	2.0	1.99	1.98
3.0	3.0	0.6	0.984	0.985
3.0	3.0	0.8	1.03	1.04
3.0	3.0	1.0	1.07	1.06
3.0	3.0	1.2	1.06	1.07
3.0	3.0	1.4	1.60	1.59
3.0	3.0	1.6	1.75	1.76
3.0	3.0	1.8	2.02	2.01

Effect of [CFA]

The effect of (CFA) concentration on the reaction was studied at constant concentrations of alkali and permanganate and at a constant ionic strength of 0.10 mol dm^{-3} at 25 °C. The substrate, (CFA) was varied in the range of 5.0 × 10^{-4} – 5.0 × 10^{-3} mol dm^{-3}. The k_{obs} values increased with increase in concentration of (CFA) (*Table* 1).

Effect of Ionic Strength

The effect of ionic strength was studied by varying the $NaClO_4$ concentration from 0.01 to 0.10 mol dm^{-3} at constant concentrations of permanganate,

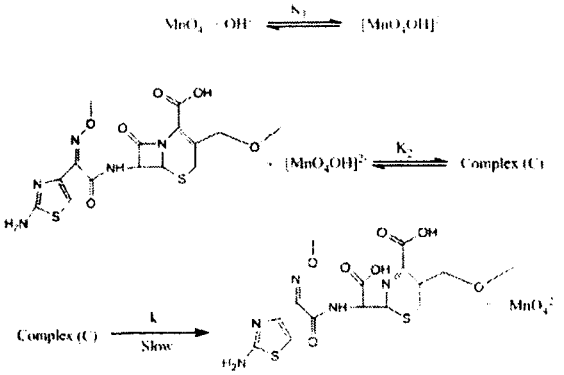

Scheme 1

(CFA), and alkali. It was found that increasing ionic strength had no effect on the rate of reaction.

Effect of temperature

The kinetics was studied at four different temperatures under varying concentrations of (CFA), and alkali, keeping other conditions constant. The rate constants were found to increase with increase in temperature. The rate constant (k) of the slow step of *Scheme* 1 were obtained from the slopes and intercepts of $1/k_{obs}$ *versus* 1/[CFA] and $1/k_{obs}$ *versus* $1/[OH^-]$ plots at four different temperatures. The energy of activation corresponding to these rate constants was evaluated from the Arrhenius plot of log k *versus* 1/T and from which other activation parameters were obtained (*Table* 2).

Polymerization Study

The possibility of free radicals was examined as follows: the reaction mixture, to which a the reaction mixture with methanol, precipitate resulted, suggesting that the there was participation of free radicals in the reaction.

DISCUSSION

At the observe experimental condition at pH > 12 the reductant product of Mn(VII) might be stopped.[20-21] Although During our study the colour of the solution undergoes a series of change from blue to green. It is probable that green color originated from the permanganate ion. The spectrum of green solution was identical to that of MnO_4^{2-}. It is probable that the blue color originated from the violet of permanganate and the green from manganate, excluding the accumulation of hypomanganate. It is evident from the (*Fig.* 5) that the concentration of MnO^{4-} decreases at 525 nm due to Mn(VII) and increases at 610 nm due to Mn(VI). As the reaction proceeds, slowly yellow turbidity develops, and after keeping for a long time the solution decolorizes and forms a brown precipitate. This suggests that the products formed might have undergone further oxidation resulting in a lower oxidation state of manganese. The results imply that first the alkali combines with permanganate to give an alkali-permanganate species $[MnO4 \cdot OH]^{2-}$ in a prior equilibrium step, which is in accordance with literature[22-23] and also experimentally observed order

Table 2. Activation and Thermodynamic parameters for the oxidation of cefpodoxime acid by $KMnO_4$ in alkaline medium and I = 0.10/mol dm^{-3} with respect to slow step of *Scheme* 1

Temperature (K)		$10^2 k (S^{-1})$
(a) Effect of Temperature		
293		2.7
298		2.9
303		4.8
308		5.1
(b) Activation Prameter		values
Ea (kj $mole^{-1}$)		65.4
ΔH (kj $mole^{-1}$)		61.7
$\Delta S^{\pm}$ ($jk^{-1}mole^{-1}$)		-120.4
$\Delta G^{\pm}$ (kj $mole^{-1}$)		19.11
Temperature (K)	K_1 ($dm^3 mol^{-1}$)	$10^{-2} K_2$ ($dm^3 mol^{-1}$)
(c) Effect of Temperature		
293	15.41	30.14
298	17.74	26.69
303	19.55	20.54
308	21.71	18.76
Thermodynamic Parameters	using K_1 values	using K_2 values
ΔH (kj $mole^{-1}$)	76.5	-61.7
$\Delta S^{\pm}$ ($jk^{-1}mole^{-1}$)	128	-63.2
$\Delta G^{\pm}$ (kj $mole^{-1}$)	-5.6	-6.71

in OH^- ion concentration. In the second step $[MnO4 \cdot OH]^{2-}$ combines with CFA to form an intermediate complex. The fractional order with respect to CFA presumably results from the complex formation between oxidant and substrate prior to the slow step. The reaction between permanganate and CFA is supported by Michaelis-Menten plot which is linear with positive intercept which is in agreement with complex formation. Within the complex one-electron is transferred from CFA to Mn(VII). Then this complex (C) decomposes in a slow step to form a species derived from CFA. All the results indicate a mechanism as given in *Scheme* 1.

$$\text{Rate} = \frac{-d[MnO_4^-]}{dt} = kK_1K_2[MnO_4^-]_f[CFA]_f[OH^-]_f \quad (2)$$

The total $[MnO^{4-}]$ can be written as

$$[MnO_4^-]_t = [MnO_4^-]_f + [MnO_4.OH]^{2-} + [\text{Complex}]$$

$$= [MnO_4^-]_f + [MnO_4^-][OH^-] + K_1K_2[MnO_4^-][CFA][OH^-]$$

$$= [MnO_4^-]_f (1 + K_1[OH^-] + K_1K_2[CFA][OH^-])$$

$$[MnO_4^-]_f = \frac{[MnO_4^-]_t}{1 + K_1[OH^-] + K_1K_2[CFA][OH^-]} \quad (3)$$

where "t" and "f" stand for total and free. Similarly, total $[OH^-]$ can be calculated as

$$[OH^-]_t = [OH^-]_f + [MnO_4.OH]^{2-} + [\text{Complex}]$$

$$[OH^-]_f = \frac{[OH^-]_t}{1 + K_1[MnO_4^-] + K_1K_2[CFA][MnO_4^-]} \quad (4)$$

In view of the low concentrations of MnO_4^- and CFA used in the experiment, in eq 4 the terms $K_1[MnO_4^-]$ and $K_1K_2[MnO_4^-][CFA]$ can be neglected in comparison with unity.

Thus,

$$[OH^-]_f = [OH^-]_t \quad (5)$$

Similarly,

$$[CFA]_f = [LFA]_t \quad (6)$$

Substituting equation 3, 5, and 6 in equation 2 and omitting the subscripts, we get

$$\text{Rate} = \frac{kK_1K_2[MnO_4^-][CFA][OH^-]}{1 + K_1[OH^-] + K_1K_2[CFA][OH^-]} \quad (7)$$

Equation 7 confirms all the observed orders with respect to different species, which can be verified by rearranging to eq 8.

$$\frac{1}{k_{obs}} = \frac{1}{kK_1K_2[CFA][OH^-]} + \frac{1}{kK_2[CFA]} + \frac{1}{k} \quad (8)$$

According to eq 8, other conditions being constant, plots of $1/k$obs *versus* $1/[CFA]$ and $1/k$obs *versus* $1/[OH^-]$ should be linear and are found to be so (*Figs* 6a and 6b). The slopes and intercepts of such plots lead to the values of K_1, K_2, and k (*Table* 2). The value of K_1 is in good agreement with the literature[24] Using these constants, the rate constants were calculated over different experimental conditions, and there is a reasonable agreement between the calculated and the experimental values, which for the proposed mechanism (*Table* 1). The thermodynamic quantities for the first and second equilibrium step of *Scheme* 1 can be evaluated as follows: The [CFA] and $[OH^-]$ as in *Table* 1 were varied at four different temperature. The spectral evidence of the complex formation was obtained from UV-Vis spectral study.[25] It is also proved kinetically by the non zero intercept of the plots of $1/k_{obs}$ *versus* $1/[CFA]$ ($r > 0.9997$, $S < 0.0148$) (*Fig.* 6b). According to the rate law the plots of 1/kobs *versus* $1/[OH^-]$ ($r > 0.9987$, $S < 0.0124$) and $1/k_{obs}$ *versus* $1/[CFA]$ ($r > 0.9998$, $S < 0.0151$) should be linear (*Figs* 6a and b) from the slope and intercept, the value of k, K_1 and K_2 could be derived as 2.87×10^{-4}, 13.8 dm^3 $mole^{-1}$, and 22.36 dm^3 $mole^{-1}$ respectively. The rate constant were calculated from these values (*Table* 1) which supports the proposed mechanism. The reaction rate of CFA increased with increasing intensity of the complex. The kinetics was studied at four different temperature and concentration of CFA and NaOH keeping all other conditions constant. The rate constant was found to increase with increasing

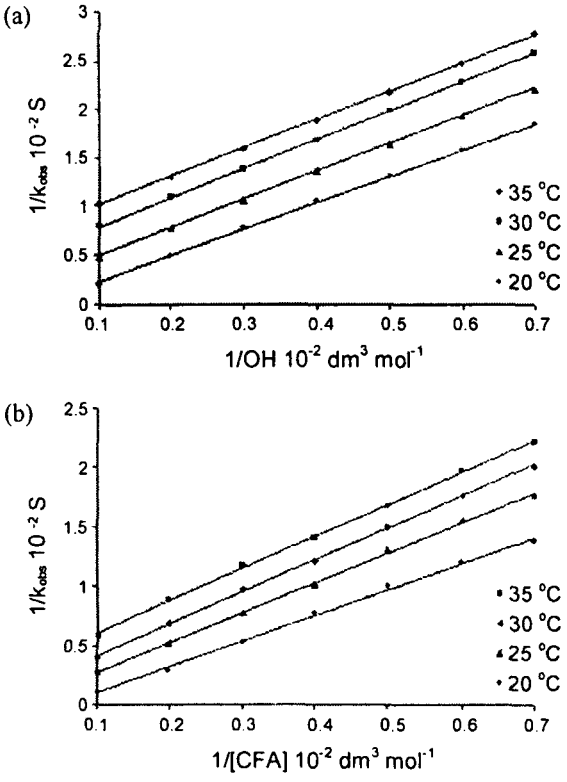

Fig. 6. (a) Rate law plots 1/kobs *versus* 1/ [OH^-] of oxidation of cefpodoxime acid by $KMnO_4$ in alkaline medium at different temperatures (circumstance as in *Table* 1). (b) Rate law plots 1/kobs *versus* 1/ [CPP] of oxidation of cefpodoxime acid by $KMnO_4$ in alkaline medium at different temperatures (circumstance as in *Table* 1).

temperature. The rate constant k of the slow step of *Scheme* 1 were obtained from the slope and intercept of $1/k_{obs}$ *versus* 1/[CFA] and $1/k_{obs}$ *versus* 1/ [OH^-] plots at four different temperatures. The activation parameters corresponding to these constant were evaluated from the Arrhenius plot of log k *versus* 1/T and are listed in *Table* 2. The experimental value of $\Delta H^{\pm}$ and $\Delta S^{\pm}$ were both favorable for electron transfer process. The high negative value of $\Delta S^{\pm}$ indicate that interaction of the reaction ions of similar charges form an activated complex and is more ordered than the reactants due to loss of degree of freedom.[26] The hydroxyl ion concentration i.e. *Table* 1 was verified at four different temperature and the K_1 value were determined from a (*Fig.* 6a) as shown in *Table* 2. Similarly CFA concentration as in *Table* 1 was varied at four different temp and K_2 values were determined at each temp (*Fig.* 6b) as listed in *Table* 2. The effect of temp on reaction rate is well known and important in the various activation parameters of the reaction product. A Arrehenius plot was made for the variation of K_1 with temperature (i.e. log K_1 *versus* 1/T). The values of the enthalpy change of the first equilibrium step K_1 of the reaction (ΔH), enthalpy of the reaction (ΔS) and free energy of raction (ΔG) were calculated as listed in *Table* 2. Similarly thermodynamic parameters for second step K_2 are calculated such as enthalpy; entropy and free energy of activation of the reaction product were calculated using Eyring equation.

$$\text{Log } K/T = [\log kb/h + S/2.302R] - \Delta H/2.303R\,1/T$$

The plot of log K_2/T *versus* 1/T was linear with correlation coefficient of -0.9996 $\Delta H^{\neq}$ was evaluated from the slope (- ΔH/ 2.303R 1/T) and $\Delta S^{\neq}$ from the intercept [log kb/h + S/2.302R] of the compiled Eyring plot. The Gibbs free energy of activation was determined by $\Delta G^{\neq} = -2.303$ RT log K at room temperature. These values are given in *Table* 2.The proposed mechanism supported by the above thermodynamic parameter. A comparison of the later values (from K_2) with those obtained for the slow step of the reaction shows that these values mainly refer to the rate-limiting step, supporting the fact that the reaction before rate determining step is fairly fast and involves low activation energy.[27] The negative value of indicate that the complex (C) is more ordered than the reactant.[28] A detailed mechanistic explanation is given in *Scheme* 2.

CONCLUSION

It is interesting to note that the oxidant species [MnO^{4-}] required a pH > 12 below which the system becomes anxious and the reaction proceeds to Mn(IV) which slowly develops yellow turbidity. The oxidant, manganese(VII), exists in alkali media as alkali-permanganate species $[MnO4{\cdot}OH]^{2-}$, which takes part in the chemical reaction. The role of hydroxyl ions is essential to the chemical reaction.

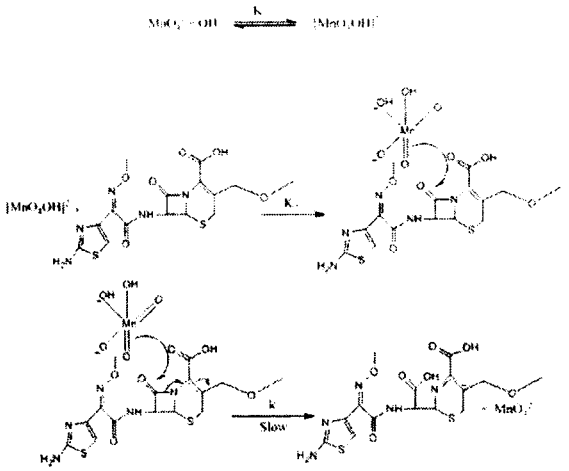

Scheme 2. Mechanistic Interpretation for the Oxidation of CFA by Alkaline Permanganate

The given mechanism is consistent with all the experimental evidence. The rate constant of slowest step involved in the mechanism are evaluated and activation parameters with respect to slowest step of reaction were computed. The overall mechanistic sequence described here is consistent with the final product, mechanistic and kinetic studies.

REFERENCES

1. Borin, *M. T. Drugs* **1991**, *42*, 13.
2. Rodriguez, J. C.; Hernandez, R.; Gonzalez, M.; Rodriguez, Z.; Tolon, B; Velez, H.; Valdes, B.; Lopez, M. A.; Fini, A. *Il Farmaco*. **2003**, *58*, 363.
3. Camus, F.; Deslandes, A.; Harcouet, L.; Farinotti, R. *J. Chromatogr B.* **1994**, *656*, 383.
4. Lovdahl, M. J.; Recher, K. E.; Russlie, H. Q.; Canafax, D. M. *J. Chromatogr B.* **1994**, *653*, 227.
5. Yamana, T.; Tsuji, A. *J. Pharm. Sci.* **1976**, *65*, 1563.
6. Hovorka, S. W.; Schoneich, C. *J. Pharm. Sci.* **2001**, *90*, 254.
7. Shaabani, A.; Tavasoli-Rad, F.; Lee, D. G. *Synth. Commun.* **2005**, *35*, 571.
8. Caron, S.; Dugger, R. W.; Ruggeri, S. G.; Ragan, J. A.; Brown, D. H.; Ripin, *Chem.Rev.* **2006**, *106*, 2943.
9. Lee, D. G.; Trahanovsky, W. S., "Oxidation in Organic Chemistry Part D", Ed.; Academic Press: New York, U. S. A., 1982, 147.
10. Simandi, L. I.; Patai, S.; Rappoport, Z., "The Chemistry of Functional Groups", Ed.; Wiley: Chichester, 1983, Suppl. C.
11. Lee, D. G.; Lee, E. J.; Brown, K. C., "Phase Transfer Catalysis, New Chemistry, Catalysis and Applications" ACS Symposium Series, American Chemical Society: Washington, DC, 1987, vol. 326.
12. Fatiadi, A. J. *Synthesis* **1987**, *106*, 85.
13. Stewart, R.; Gardner, K. A.; Kuehnert, L. L.; Mayer, J. M. *Inorg. Chem.* **1997**, *36*, 2069.
14. Panari, R. G.; Chougale, R. B.; Nandibewoor, S. T. *Pol. J. Chem.* **1998**, *72*, 99, 107.
15. Bohn, A.; Adam, M.; Mauermann, H.; Stein, S.; Mullen, K. *Tetrahedron Lett* **1992**, *33*, 2795.
16. Jeffery, G. H.; Bassett, J.; Mendham, J.; Denny, R. C. "*Vogel's Text Book of* Quantitative Chemical Analysis" 5th ed.; ELBS Longman: Essex, U. K, 1996, 370.
17. Carrington, A.; Symons, M. C. R. "Structure and Reactivity of Oxyanions of Transition Metals. Part I. The Manganese Oxy-anions." *J. Chem. Soc.* **1956**, *337*, 3.
18. Siddiqi, K. S.; Mohd, A.; Parwaz Khan, A. A.; Bano, S. *J. Korean. Chem. Soc.* **2009**, 53, 152.
19. Darwish, I. A. *Analytica Chimica Acta*, **2005**, *551*, 222.
20. Timmanagoudar, P. L.; Hiremath, G. A.; Nandibewoor, S. T. *Transition. Met. Chem.* **1997**, *22*, 193.
21. Nadimpalli, S.; Rallabandi, R. A.; Dikshitulu, L. S. A. *Transition Met. Chem.* **1993**, *18*, 510.
22. Thabaj, K. A.; Kulkarni, S. D.; Chimatadar, S. A.; Nandibewoor, S. T. *Polyhedron* **2007**, *26*, 4877.
23. Panari, R. G.; Chougale, R. B.; Nandibewoor, S. T. *J. Phys. Org. Chem.* **1998**, *11*, 448.
24. Kini, A. K.; Farokhi, S. A.; Nandibewoor, S. T. *Transition. Met. Chem.* **2002**, *27*, 532.
25. Devi, J.; Kothari, S.; Banerjee, K .K. *Indian J. Chem.* **1995**, *34A*, 116.
26. Weissberger, A.; Lewis, E. S. Ed, "Investigation of rate and Mechanism of reaction In Techniques of Chemistry", Ed.; Willey: Interscience Publication, New York 1974, 421.
27. Rangappa, K. S.; Raghavendra, M. P.; Mahadevappa, D. S.; Channegouda, D. *J.Org. Chem.* **1998**, *63*, 531.
28. Bugarcic, Z. D.; Nandibewoor, S. T.; Hamza, M. S. A.; Heimemann, F.; Rudi, Van, Eldik, *Dalton Trans.* **2006**, 2984.

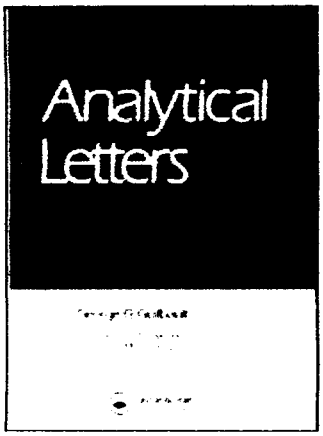

Analytical Letters
Publication details, including instructions for authors and subscription information:
http://www.informaworld.com/smpp/title~content=t713597227

Fluorescence Enhancement of Levosulpiride Upon Coordination with Transition Metal Ions and Spectrophotometric Determination of Complex Formation

K. S. Siddiqi [a]; Shaista Bano [a]; Ayaz Mohd [a]; Aftab Aslam Parwaz Khan [a]
[a] Department of Chemistry, Aligarh Muslim University, Aligarh, India

Online Publication Date: 01 January 2009

To cite this Article Siddiqi, K. S., Bano, Shaista, Mohd, Ayaz and Parwaz Khan, Aftab Aslam(2009)'Fluorescence Enhancement of Levosulpiride Upon Coordination with Transition Metal Ions and Spectrophotometric Determination of Complex Formation',Analytical Letters,42:14,2192 — 2205
To link to this Article: DOI: 10.1080/00032710903137350
URL: http://dx.doi.org/10.1080/00032710903137350

Analytical Letters, 42: 2192–2205, 2009

ISSN: 0003-2719 print/1532-236X online
DOI: 10.1080/00032710903137350

Taylor & Francis
Taylor & Francis Group

SPECTROSCOPY

Fluorescence Enhancement of Levosulpiride Upon Coordination with Transition Metal Ions and Spectrophotometric Determination of Complex Formation

K. S. Siddiqi, Shaista Bano, Ayaz Mohd, and Aftab Aslam Parwaz Khan
Department of Chemistry, Aligarh Muslim University, Aligarh, India

Abstract: Absorbance and fluorescence spectral pattern of levosulpiride in absence and presence of first row transition metal ions (Mn-Zn) has been studied at room temperature under physiological condition. The fluorescence spectra of the drug in presence of different concentrations of transition metal ions showed enhancement in fluorescence intensity of levosulpiride. The photophysical changes owing to the direct interaction between metal ion and the amide nitrogen of levosulpiride has been described in terms of CHEF (chelating enhancement fluorescence) effect. The absorption spectra of the drug at different pH exhibited two isosbestic points at 255 and 275 nm respectively, indicating the presence of three chemical species in solution. The ratio of the drug to metal ions is found to be 2:1 and the log K of the resulting complex was determined spectrophotometrically and potentiometrically. The apparent ionization constant of levosulpiride is found to be 8.98. The low value of stability constant suggests that complexes may dissolve and the drug can be absorbed.

Keywords: Absorption study and stability constant, fluorescence enhancement, levosulpiride

Received 11 November 2008; accepted 12 June 2009.
Address correspondence to K. S. Siddiqi, Department of Chemistry, Aligarh Muslim University, Aligarh-202001, India. E-mail: ks_siddiqi@yahoo.co.in

1. INTRODUCTION

Levosulpiride, a levo enantiomer of sulpiride, chemically known as 5-(amino sulfonyl)-N-[(1-ethyl-2-pyrrolidinyl)methyl]-2-methoxy benzamide is used as antipsychotic, antidyspeptic and antiemetic medicine (Fig. 1). This drug has also been used for the treatment of male sexual disorder and a dose of 25 mg/day for 60 days resulted in complete recovery. The studies are mainly concerned with the validation and determination of levosulpiride in human beings. The drug is fairly stable in human serum and urine which has been tested in different patients. It has been found that the drug can be detected in a concentration range of 0.25–200 ng/ml in human serum and 0.2–20 μg/ml in urine by HPLC (Cho and Lee 2003; Geo, Balbi, and Speranza 2002). The bioavailability of the drug at a dose of 100–200 mg/day is approximately 20–30% only (Jin et al. 2004). Levosulpiride has both antiemetic and prokinetic properties because it antagonizes dopamine receptor in the central nervous system and gastro-intestinal tract (Mansi et al. 2000; Nagahata et al. 1995). Recently, it has been shown that levosulpiride has moderate agonistic effect on 5HT4 receptors in the nervous system and is useful in the treatment of depression or Schizophrenia (Tonini et al. 1999). Patients treated for functional dyspepsia over a period of one month did not show any adverse effect. The doses of levosulpiride range between 50–75 mg/day over a period of 30 days and showed no adverse effect except for fatigue, headache, and drowsiness (Lozano et al. 2007). It is, therefore, considered an effective and safe drug in the treatment of dyspepsia. It has been shown that the levosulpiride does not interfere with most of the drugs, but drinking during this period should be avoided. As a precaution, the drug should be avoided in pregnancy and during lactation period.

The major work done on the sulpiride thus far, concerns its identification, determination, and efficacy against dyspepsia, psychosis, and male sexual disorder. However, absorption and fluorescence emission spectrophotometric behavior of the drug under physiological condition and its interaction with several cations has not been studied so far.

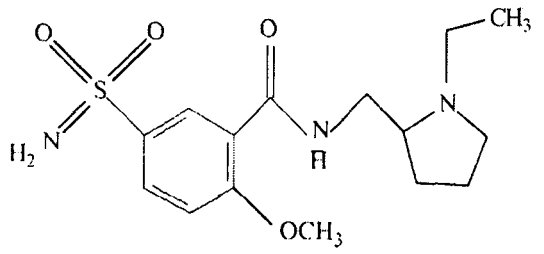

Figure 1. Structure of levosulpiride.

In this communication, we are, therefore, reporting the electronic and fluorescence emission spectra of the drug in the presence and absence of transition metal ions at different pH, ranging from 2.38 to 10.6 in order to find the effect of pH on the absorption of drug in aqueous medium. Fluorescence emission spectra of the drug in presence and absence of metal ion has been recorded to examine if quenching or enhancement in fluorescence intensity occurs. Stability constant and other physical parameters of the complexes formed in solution have also been calculated.

2. EXPERIMENTAL

2.1. Instruments

The absorption spectra were obtained with Elico-SL-169 double beam UV-visible spectrophotometer. Fluorescence emission spectra were scanned with Hitachi-F-2500FL-spectrophotometer. All potentiometric measurements were done with Elico-LI-120 pH meter.

2.2. Methods and Materials

Double distilled water was used throughout. Levosulpiride (Sun Pharmaceutical Industries, Jammu, India), sodium hydroxide (Merck Ltd, Mumbai, India) anhydrous zinc chloride (SDH Pvt. Ltd India), and HCl (Ranbaxy Fine Chem. Ltd, India) were used as received.

2.3. Preparation of Solution

Stock solution of levosulpiride and metal salts of 1×10^{-2} M were prepared in double distilled water. Stock solution of drug was stored at 4°C.

2.4. Spectrophotometric Method

Solution of equimolar concentration (1×10^{-4} M) of levosulpiride and metal ions was prepared. The pH of the drug was adjusted between 2.31 to 10.6 by the use of only sodium hydroxide and hydrochloric acid (1×10^{-1} M to 1×10^{-2} M) to avoid interactions with buffer solution. The absorption spectra were recorded in the range 200–330 nm. The ratio of metal to levosulpiride was determined by Job's method.

2.5. Potentiometric Method

For potentiometric study the following solutions were titrated against standard NaOH. The ionic strength was maintained at 0.1 M by NaCl and the total volume was kept at 50 ml by adding appropriate amount of water.

(a) 5 ml (1×10^{-1} M) HCl + 5 ml (1×10^{-1} M) NaCl + 40 ml water.
(b) 5 ml (1×10^{-1} M) HCl + 5 ml (1×10^{-1} M) NaCl + 10 ml (5×10^{-3} M) drug + 30 ml water.
(c) 5 ml (1×10^{-1} M) HCl + 5 ml (1×10^{-1} M) NaCl + 10 ml (5×10^{-3} M) drug + 20 ml (5×10^{-4} M) metal ions + 10 ml water.

2.6. Fluorescence Spectrophotometric Method

Solution of the levosulpiride (7×10^{-6} M) and those of metal ions (1.2×10^{-6} M to 8.4×10^{-6} M) were prepared. The steady state fluorescence spectra of the drug were recorded in the $\lambda_{em} = 270$–430 nm with excitation at the maximum centered on $\lambda_{exc} = 275$ nm. This wavelength was chosen in order to avoid the inner-filter effect and to obtain the most complete as possible emission spectrum.

3. RESULTS AND DISCUSSION

3.1. Spectrophotometric Study

The levosulpiride solution (1×10^{-4} M) was prepared in double distilled, demineralized water, and its absorption spectrum was run in the region 200–330 nm. It exhibited two peaks at 216 and 295 nm (Fig. 2). Since the first peak is very strong, it was selected for further absorption studies.

When the spectra of the drug were run at varying pH in the region 200–330 nm, two isosbestic points, one at 255 nm and another at 275 nm, were observed which indicated the presence of three chemical species in solution in equilibrium with each other (Fig. 3) (Park et al. 2000).

The apparent ionization constant (pKa′) of the drug was calculated (Table 1) by the following equation:

$$pKa' = pH + \log\{(A_I - A_M)/(A - A_M)\} \quad (1)$$

where A_I = Absorbance of drug in basic medium, A_M = Absorbance of drug in acidic medium, and A = Absorbance of drug in aqueous medium.

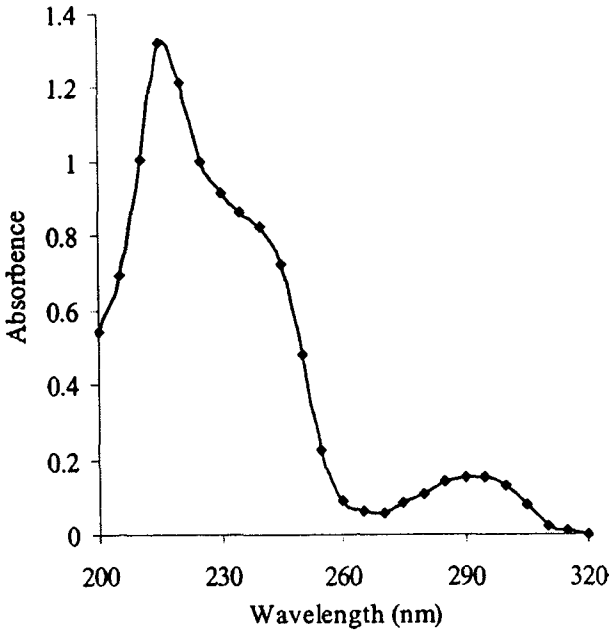

Figure 2. Absorption spectrum of levosulpiride (1×10^{-4} M) at room temperature (pH 5.6).

The metal to levosulpiride ratio was determined by continuous variation method (Fig. 4) at their respective λmax (Table 1). It was found, in each case, that two moles of the drug are bonded to one mole of the metal ion which seems quite reasonable because, of all the donor groups,

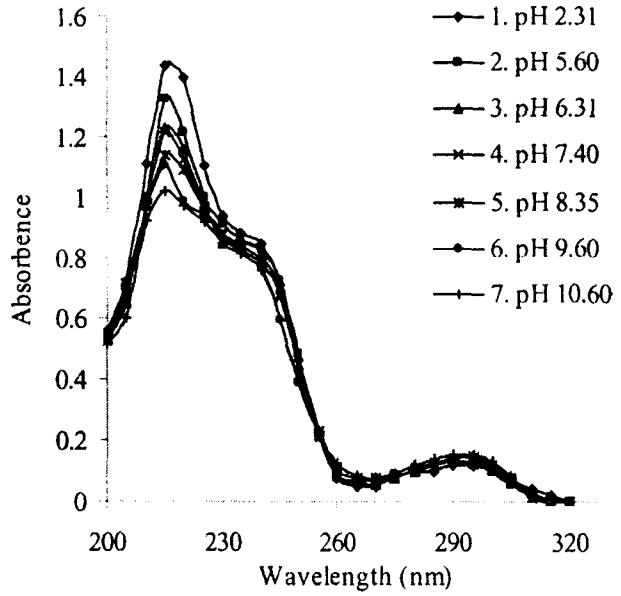

Figure 3. Absorption Spectra of levosulpiride (1×10^{-4} M) at different pH (room temperature).

Table 1. Apparent ionization constant (pKa′) of the drug

Potentiometrically	Spectrophotometrically
8.753	8.98

the amide nitrogen appears to be the most plausible site for coordination as it is the proper combination of hard acid and hard base.

The stability constant of the complexes were calculated by the following equation:

$$K = \frac{A/A_{ex}C_X}{(C_M - A/A_{ex}C_X)(C_L - nA/A_{ex}C_X)^n} \quad (2)$$

where K is the stability constant of the metal chelate formed in solution, M = metal, L = drug, n = X/(1 − X), and X is the mole fraction of the ligand at maximum absorption. A/A_{ex} is the ratio of the observed absorbance indicated by the tangent for the same wavelength. C_X, C_M, and C_L are the limiting concentrations of the complex, metal ion, and the ligand, respectively (Salem 2005; El-Kommas et al. 2007). The value of log K is shown in Table 2.

3.2. Potentiometric Study

To calculate the stability constant of metal chelates, the acid dissociation constant of the drug was first determined from the titration curve for HCl

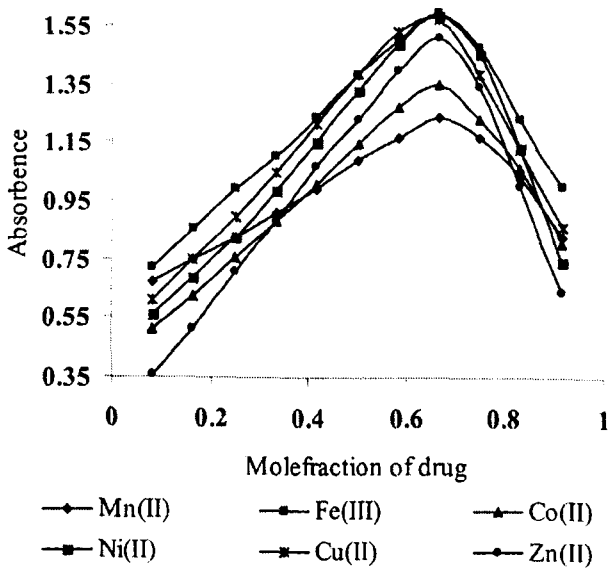

Figure 4. Continuous variation curve of levosulpiride with metal ions.

Table 2. The stability constant potentiometrically and spectrophotometrically

	Potentiometrically		Spectrophotometrically	
Metal ions	log K	$-\Delta G$ (KJ/mol)	log K	$-\Delta G$ (KJ/mol)
Mn(II)	8.82	50325.57	9.3965	53615.00
Fe(III)	8.907	50821.39	9.3981	53652.32
Co(II)	9.028	51512.39	9.4328	53822.12
Ni(II)	8.895	50753.51	9.4000	53634.90
Cu(II)	9.174	52345.44	9.5413	54441.20
Zn(II)	9.045	51609.39	9.4396	53860.92

in the presence and absence of the drug. The average number of proton, n_A associated with levosulpiride at different pH was calculated and maximum value of $\overline{n_A}$ is 1 which suggests that it has one dissociable proton. The formation curve was obtained by plotting the average number of ligand attached per metal ion ($\bar{n}$) versus free ligand exponent (pL) (Jeragh et al. 2007; Irving and Rassotti 1953). The apparent ionization constant and the average value of stability constant are shown in Tables 1 and 2, respectively. According to average value in Table 2, the following general remarks can be made:

1. The maximum value of n was about 2, so it is presumed that complex is formed in a 2:1 (Drug: Metal) ratio.
2. The very low concentration of metal ion solution used in the present study was 5×10^{-4} M and precludes the possibility of formation of polynuclear complexes (Sanyal and Sengupta 1990).
3. The metal titration curve is displaced to the right hand side of the ligand titration Curves along the volume axis (Fig. 5), indicating a proton release upon complex formation.
4. All calculation of stability constant has been successful for the low pH region. Therefore the formation of hydroxo species (e.g. [ML (OH)], $[MS_{x-1}\ (OH)]^+$ where L is ligand, S is the solvent molecule, and x is the number of solvent molecule bound) could be neglected.

The value of ΔG is $-$ve indicating that chelation process proceeds spontaneously. This is evaluated by both method potentiometrically and spectrophotometrically.

3.3. Fluorescence Study

The fluorescence emission spectrum of the pure drug is markedly different from its absorption spectrum in the UV region, which is

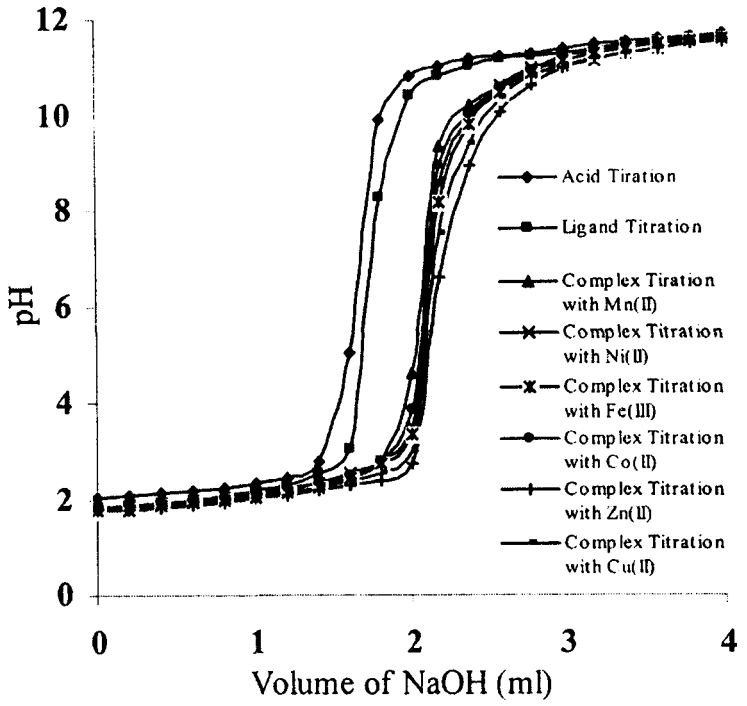

Figure 5. Potentiometric titration curve of levosulpiride with metal ions.

attributed to its different geometry in the ground and excited states (Fig. 6). When the emission spectrum of the pure drug is run between 270–430 nm at an excitation wavelength of 275 nm, a strong peak at 300 nm and two weak emission peak at 342 and 406 nm were observed (Fig. 7). The 5-aminosulfonyl 2-methoxy benzamide group of levosulpiride acts as an electron acceptor where as the pyrrolidinyl group acts as electron donor. The peak in absorption spectra is due to the intramolecular charge transfer between the acceptor and donor groups. The addition of the metal ion to the drug can cause either enhancement or quenching in the fluorescence emission spectrum (Quang et al. 2007). We have noted an enhancement of fluorescence intensity at 300 nm in each case (Mn-Zn). The shape and position of emission spectrum of levosulpiride in presence and absence of transition metal ions remains unchanged, which suggests no significant change in the overall electronic structure of drug upon addition of metal ions (Fig. 8). The relative enhancement in the fluorescence intensity I/I_o is shown in Table 3.

The enhancement in emission intensity of levosulpiride in the presence of various metal ions follows the order $Fe^{3+} > Ni^{2+} > Cu^{2+} > Zn^{2+} > Co^{2+} > Mn^{2+}$ (Fig. 9). The enhancement in emission intensity does not follow any trend from Mn-Zn, although it is minimum in the case of Mn, probably due to its half filled 'd' orbital. Although the transition metal ions are known to effectively quench fluorescence (Ghosh and

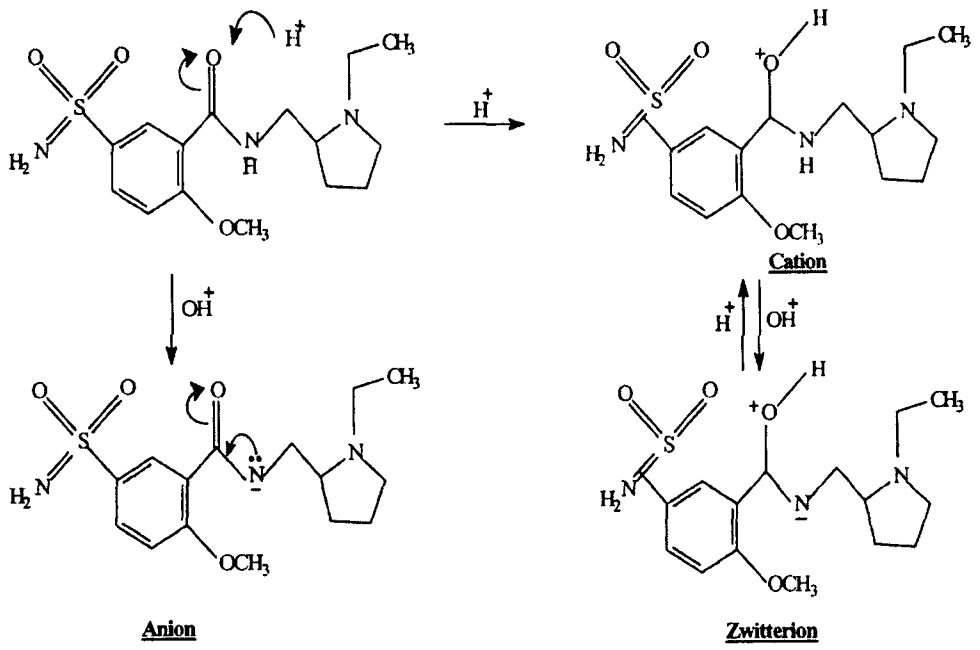

Figure 6. Showing different ionic species in the solution at different pH.

Bharadwaj 1996; Varnes, Dodson, and Wehry 1972; Rurack et al. 1993; Kemlo and Shepherd 1977), we observed over two fold increase in intensity as a consequence of photo induced charge transfer besides the chelation of the amide nitrogen resulting in CHEF (Chelating enhancement fluorescence) effect (Choi et al. 2006; Kim et al. 2007; Kim et al. 2003).

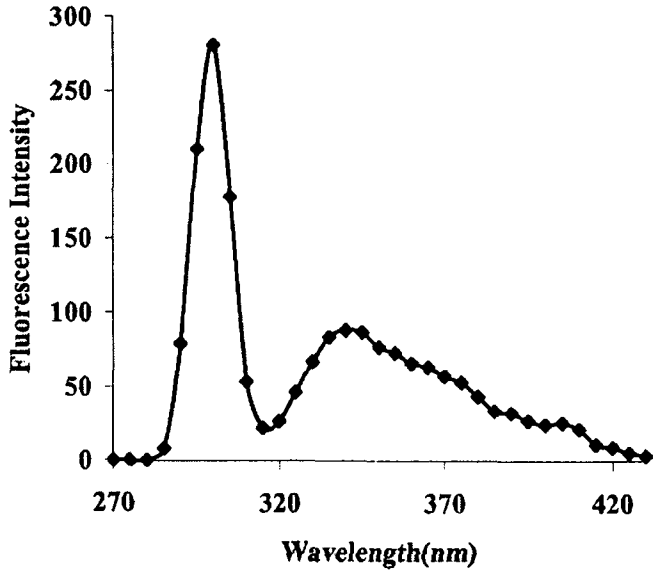

Figure 7. Fluorescence Emission spectra of levosulpiride (7×10^{-6} M) at room temperature.

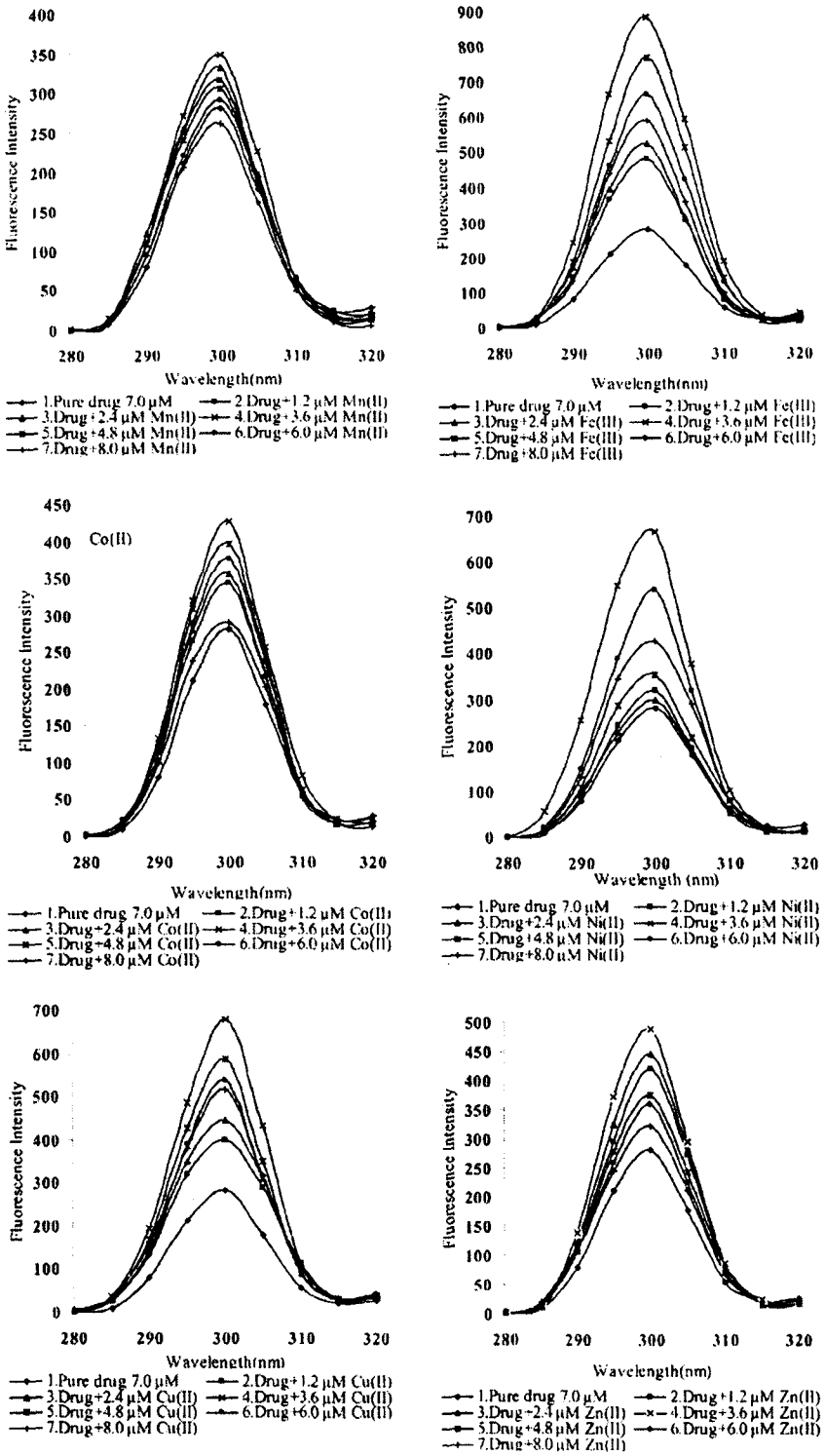

Figure 8. Fluorescence enhancement (at 300 nm) of levosulpiride with Mn(II), Fe(III), Co(II), Ni(II), Cu(II), and Zn(II) at room temperature.

Table 3. The relative intensity and limiting concentration

Metal ions	I/I_o	Limiting concentration
Mn(II)	1.24	3.6 μm
Fe(III)	3.13	3.6 μm
Co(II)	1.52	3.6 μm
Ni(II)	2.41	3.6 μm
Cu(II)	2.37	3.6 μm
Zn(II)	1.53	3.6 μm

It is accepted that aromatic compounds having amide groups are strongly quenched by intersystem crossing to a triplet state and/or by the rotational relaxation linked to excited state rotation around the CO-NH and N-alkyl bonds. This may explain why, when complexed by cations, these rotors are less available for relaxation (Kawakami et al. 2002). An increase of rigidity of the system by metal cation complexation may therefore be an explanation for the fluorescence enhancement. In general, the phenomenon of enhancement is observed because the complexation by cations causes increase in the redox potential of the donor so that

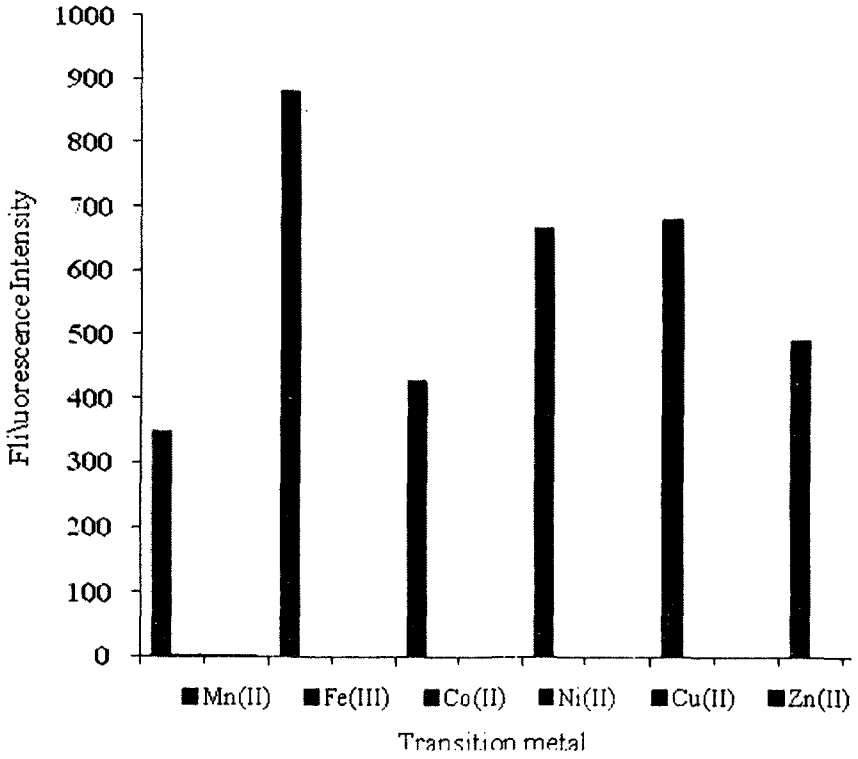

Figure 9. The enhancement in emission intensity of levosulpiride in presence of various metal ions follows the order $Fe^{3+} > Ni^{2+} > Cu^{2+} > Zn^{2+} > Co^{2+} > Mn^{2+}$.

the relevant HOMO energy decreases to a level lower than that of fluorophore. Consequently the excited state energy of fluorophore is dumped as a visible emission (Quang et al. 2007). The reason for this enhancement lies in strong perturbation of the excited state upon coordination of the metal ion. A low-lying internal charge transfer state, due to the presence of electron donor and acceptor group in the levosulpiride, is the lowest excited state. This state is, however, a less emitting state. And, in equilibrium with the $\pi - \pi^*$ excited state of the molecule, upon coordination with metal cation, the PCT interaction becomes weaker since the electron withdrawing group is now an electron rich moiety due to the deprotonation of –NH group necessary for coordination of metal cation.

In the present work, an attempt has been made to study the interaction of the drug with metal ions by fluorescence emission, absorption spectrophotometric, and potentiometric measurements. Since quenching or enhancing in fluorescence intensity of the drug in presence of the metal ions occurs, the spectra of the drug in presence of different concentrations of several metal ions were scanned. The ratio of the drug to metal ions was determined by Jobs method. The absorption spectra of the drug was run at different pH to see the zwitterionic condition, apparent ionization constant, and the isosbestic point indicating the presence of different species in solution. The stability constant of the complex formed between the drug and metal ion was also evaluated.

4. CONCLUSION

The effect of cation binding on the photophysical properties of levosulpiride was studied. A dramatic fluorescence enhancement was observed upon binding of transition metal ions. This was interpreted in term of the control of photoinduced charge transfer (PCT) and CHEF. The stability constants, which is calculated by spectrophotometrically and potentiometrically, suggest that the complexes are fairly stable in solution.

REFERENCES

Cho, H.Y., and Y. B. Lee. 2003. Improvement and validation of a liquid chromatographic method for the determination of levosulpiride in human serum and urine. *J. Chromatogr.* 796: 243–251.

Choi, J. K., S. H. Kim, J. Yoon, K. H. Lee, R. A. Bartsch, and J. S. Kim. 2006. A PCT-Based, Pyrene-Armed calyx[4] crown fluoroionophore. *J. Org. Chem.* 71: 8011–8015.

El-Kommas, M. E., G. A. Saleh, S. M. El-Gizawi, and M. A. Abou-Elwafa. 2003. Spectrofluorometric determination of certain quinolone antibacterials using metal chelation. *Talanta* 60: 1033–1050.

Ghosh, P., and K. Bharadwaj. 1996. Ni(II), Cu(II), and Zn(II) cryptate-enhanced fluorescence of a trianthrylcryptand: A potential moleculer photonic OR operator. *J. Am. Chem. Soc.* 118: 1553–1554.

Geo, E., P. P. Balbi, and J. C. Speranza. 2002. Levosulpiride: A new solution for premature ejaculation. *Int. J. importance research* 14: 308–309.

Irving, H., and H. S. Rassotti. 1953. Methods for computing successive stability constants from experimental formation curves. *J. Chem. Soc.* P: 3397–3405.

Jeragh, B., D. Al-wahaib, A. A. El- Sherif, and A. El- Dissouky. 2007. Potentiometric and thermodynamic studies of dissociation and metal complexation of 4-(3-Hydroxypyridin-2-ylimino)-4-phenylbutan-2-one. *J. Chem. Eng. Data* 52: 1609–1614.

Jin, S. E., E. Ban, Y. B. Kim, and C. K. Kim. 2004. Development of HPLC method for the determination of levosulpiride in human plasma. *J. Pharm. Biomed. Anal.* 35: 929–936.

Kawakami, J., R. Miyamoto, A. Fukushi, K. Shimozaki, and S. Ito. 2002. *J. Photoch. Photobio. A*: 146–163.

Kemlo, J. A., and T. M. Shepherd. 1977. Quenching of excited singlet states by metal ions. *Chem. Phys. Lett.* 47: 158–162.

Kim, J. S., K. H. Noh, S. H. Lee, S. K. Kim, and J. Yoon. 2003. A New Calix [4 azacrown bearing two different binding sites as a new fluorescent ionophore. *J. Org. Chem.* 68: 597–600.

Kim, J. S., O. J. Shon, J. A. Rim, S. K. Kim, and J. Yoon. 2002. Pyrene-Armed calix[4]azacrowns as new fluorescent lonophores: "Molecular Taekowndo" process via fluorescent change. *J. Org. Chem.* 67: 2348–2351.

Lozano, R., M. G. P. Concha, A. Montealegre, L. de Leon, J. O. Villalba, H. O. L. Esteban, M. Cromeyer et al. 2007. Effectiveness and safety of levosulpiride in the treatment of dysmotility like functional dyspepsia. *Therapeutics and Clinical Risk Management* 3: 49.

Mansi, C., P. Borro, R. Biagini, M. R. Mele, and N. Pandolfo. 2000. Comparative effects of levosulpiride and cisapride on gastric emptying and symptoms in patients with functional dyspepsia and gastroparesis, Aliment. *Pharmacol. Ther.* 14: 561–569.

Nagahata, Y., Y. Azumi, N. Kawakita, T. Wada, and Y. Saitoh. 1995. Inhibitory effect of dopamine on gastric motility in rats. *Scand J Gastroenterol.* 30: 880–885.

Park, H. R., K. Y. Chung, H. C. Lee, J. K. Lee, and K. M. Bark. 2000. Ionization and divalent cation complexation of quinolone antibiotics in aqueous solution. *Bull. Chem. Soc.* 21: 849–854.

Quang, D. T., H. S. Jung, J. H. Yoon, S. Y. Lee, and J. S. Kim. 2007. Coumarin appended calix[4]arene as a selective fluorometric sensor for Cu^{+2} ion in aqueous solution. *J. Bull. Korean Chem. Soc.* 28: 682–684.

Rurack, K., U. Resch, M. Senoner, and S. Dachne. 1993. A new fluorescence probe for trace metal ions: Cation-dependent spectroscopic properties. *J. Fluorescence* 3: 141–143.

Salem, H. 2005. Spectrofluoremetric, atomic absorption spectrometric and spectro photo metric determination of some fluoroquinolones. *Am. J. App. Sci.* 3: 719–729.

Sanyal, P., and G. P. Sengupta. 1990. Potentiometric studies of some trivalent rare earth complexes with p-sulphono-2-hydroxy-1-naphtalidene anil. *J. Ind. Chem. Soc.* 67: 342

Tonini, M., V. Spelta, and R. De Giorgio et al. 1999. A re-assessment of the pharmacodynamics of levosulpiride in the guineapig gastrointestinal tract. *Gastroenterology* 116: A1093 (Abstract).

Varnes, A. W., R. B. Dodson, and E. L. Wehry. 1972. Transition Metal Ion Complexes of 2,2′-Bipyridyl-3,3′-diol and 2,2′-Bipyridyl-3-ol: Spectroscopic properties and solvent-dependent binding modes. *J. Am. Chem. Soc.* 94: 946–950.

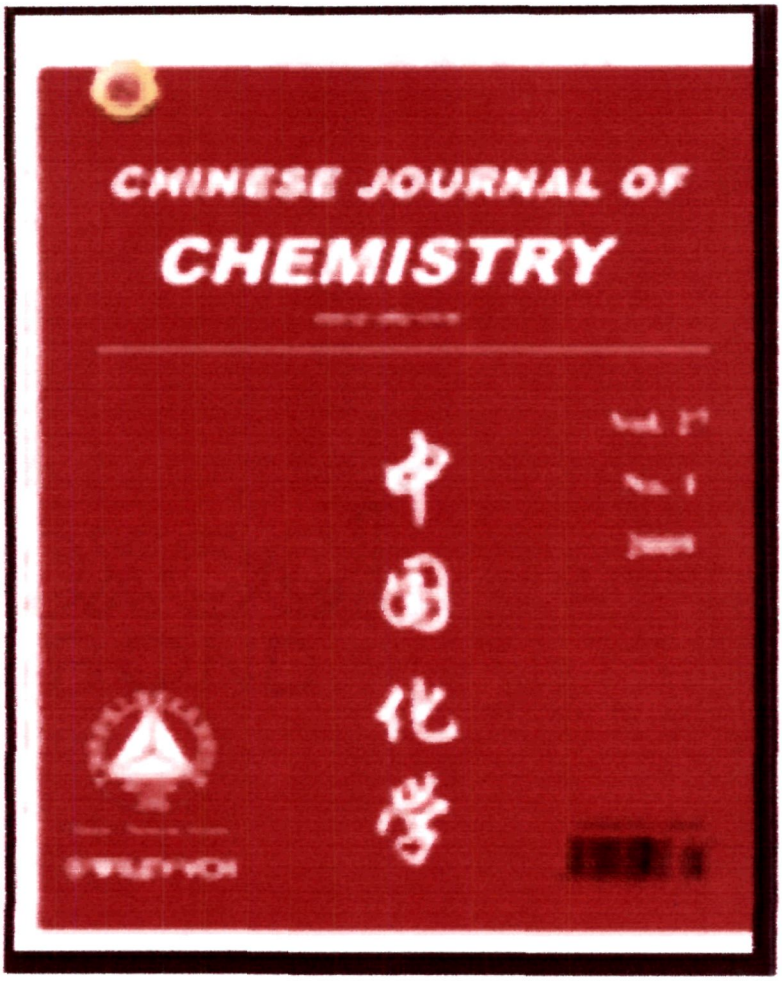
CHINESE JOURNAL OF
CHEMISTRY
中国化学

Chinese Journal of Chemistry, 2009, 27, 1755—1761 **Full Paper**

Binding Interaction of Captopril with Metal Ions: A Fluorescence Quenching Study

SIDDIQI, K. S.* BANO, Shaista MOHD, Ayaz KHAN, Aslam Aftab Parwaz

Department of Chemistry, Aligarh Muslim University, Aligarh-202001, India

The binding interaction of captopril (CPL) with biologically active metal ions Mg^{2+}, Ca^{2+}, Mn^{2+}, Co^{2+}, Ni^{2+}, Cu^{2+} and Zn^{2+} was investigated in an aqueous acidic medium by fluorescence spectroscopy. The experimental results showed that the metal ions quenched the intrinsic fluorescence of CPL by forming CPL-metal complexes. It was found that static quenching was the main reason for the fluorescence quenching. The quenching constant in the case of Cu^{2+} was highest among all quenchers, perhaps due to its high nuclear charge and small size. Quenching of CPL by metal ions follows the order $Cu^{2+}>Ni^{2+}>Co^{2+}>Ca^{2+}>Zn^{2+}>Mn^{2+}>Mg^{2+}$. The quenching constant K_{sv}, bimolecular quenching constant K_q, binding constant K and the binding sites "n" were determined together with their thermodynamic parameters at 27 and 37 ℃. The positive entropy change indicated the gain in configurational entropy as a result of chelation. The process of interaction was spontaneous and mainly ΔS-driven.

Keywords captopril (CPL), fluorescence quenching, metal-drug complex, stability constant

Introduction

Captopril, 1-[2(*S*)-3-mercapto-2-methyl-1-oxopropyl]-*L*-proline (Figure 1), is an angiotensin converting enzyme inhibitor drug for the treatment of hypertension, heart failure following myocardial infarction and diabetic nephrotherapy.[1] It inhibits the active sites of a zinc glycoprotein, the angiotensin converting enzyme (ACE), blocking the conversion of angiotensin(I) to angiotensin(II), the level of which is elevated in patients with hypertensions. CPL has three different potential donor groups (S_{thiol}, O_{acid} and O_{amide}) which may bind with metal ions to form 1 : 1 complexes in acidic medium and 1 : 2 complexes[2] in nearly basic medium (pH 6—8.2). The key functional group in the metabolism of CPL is the sulfhydryl group.[3] CPL is oxidized at its sulfhydryl group after dissolution in water to form its disulfide and is found in human urine after CPL administration. It has an equilibrium conformation between *cis* and *trans* isomers, however, the *trans* isomer is the active form when bound to the enzyme.[4] It also acts as a free radical scavenger.[5]

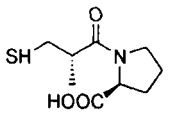

Figure 1 Structure of CPL.

Over the last decade, close attention has been paid to the interaction of CPL with various metal ions[6] as drug metal interaction may result in the formation of a stable metal-drug complex, which may deplete the blood with trace element. On the other hand the side effect that can arise during CPL treatment[7] may well be caused by the interaction of CPL with other metal ions present in the plasma.[8] Therefore, to gain a deeper insight into the mechanism of the inhibition and side effect of CPL, equilibrium and structural studies were earlier performed with several metal ions.[9] Studies have also been done on the use of transition metal ions for quantitative spectrophotometric determination of CPL in pharmaceutical formulations.[10] CPL has also been assayed spectrofluorimetrically after reacting with fluorogenic reagents[11] or reducing Ce(IV) to fluorescent Ce(III).[12]

The fluorescence spectroscopy has been widely used to monitor the molecular interaction because of its high sensitivity, reproducibility and relatively easy use. Since no detailed fluorescence study on the binding interaction of CPL with Mg^{2+}, Ca^{2+}, Mn^{2+}, Co^{2+}, Ni^{2+}, Cu^{2+} and Zn^{2+} has been done so for, a thorough investigation was therefore made using this technique. Such interactions between CPL and these metal ions can cause fluorescence quenching. Therefore, valuable information such as binding mechanism, binding constant, and binding sites can be obtained using fluorescence quenching study of CPL by these metal cations. In addition the thermodynamic parameters of the process were also proposed in this work.

Experimental

Instruments, methods and materials

The fluorescence emission spectra were scanned with a Hitachi-F-2500FL spectrophotometer. The phase modulation method was used to obtain fluorescence

* E-mail: ks_siddiqi@yahoo.co.in; Tel.: 0091-0571-2401664
Received January 12, 2009; revised March 9, 2009; accepted May 16, 2009.

lifetime by an SLM48000S spectrofluorometer (SLM Aminco, Rochester, NY). The procedure for lifetime measurement was described in reference.[15] Doubly distilled water was used throughout. CPL (Across organics), sodium hydroxide, metal chloride (Merck Ltd, Mumbai, India), and HCl (Ranbaxy Fine Chem. Ltd, India) were used as received.

Preparation of solution

The stock solution of CPL in aqueous acidic medium (1×10^{-3} mol•L^{-1}) was stored at 4 ℃ and metal salts of 1×10^{-2} mol•L^{-1} were prepared in doubly distilled water.

The working solution of the CPL (8×10^{-6} mol•L^{-1}) and those of metal ions (1×10^{-6} to 18×10^{-6} mol•L^{-1}) were prepared. The steady state fluorescence spectra of the drug were recorded in the λ_{em} of 320—360 nm with excitation at the maximum centered at $\lambda_{ex}=305$ nm. The excitation wavelength was chosen such that absorbance at this excitation wavelength was less then 0.02 to minimize the inner-filter effect and to obtain the most complete emission spectrum as possible.

Results and discussion

Figure 2 shows the emission spectra of CPL in the presence of metal ions of various concentrations. It was observed that the fluorescence intensity of captopril decreased regularly with the increasing concentration of metal ions without any change in emission maxima and shape of peaks. As there was no significant λ_{em} shift with the addition of metal ions, it was indicated that metal ion could quench intrinsic fluorescence of CPL and that the interaction between CPL and metal ion indeed existed without inducing any conformational change in it under the condition studied here.

Quenching can occur by a variety of molecular interactions, *viz.* excited-state reactions, molecular rearrangement, energy transfer, ground state complex formation (static quenching) and collisional or dynamic quenching. Static and dynamic quenching can be distinguished by their different dependence on temperature and excited state life time. Dynamic quenching is diffusion controlled because the quencher must diffuse to the fluorophore during the life time of excited state. Since high temperature will result in large diffusion coefficient, the bimolecular quenching constants are expected to increase with temperature. If the K_{sv} decreased with increased temperature, it could be concluded that the quenching process was static rather than dynamic.[13,14] Static quenching implies either the existence of a sphere of effective quenching or the formation of a ground state non-fluorescent complex, whereas collisional or dynamic quenching involves the collision and subsequent formation of a transient complex between an excited state fluorophore and a ground state quencher. The excited state complex dissociates upon radiative and non-radiative deactivation. In order to confirm the quenching mechanism the procedure of fluorescence quenching was first assumed to be dynamic. For dynamic quenching the mechanism can be described by the Stern-Volmer equation.[15]

$$F_o/F=1+K_q\tau_o[Q]=1+K_{sv}[Q] \quad (1)$$

where, F_o and F are the fluorescence intensities in the absence and presence of the quencher, respectively, K_q is the bimolecular quenching rate constant, K_{sv} is the dynamic quenching constant and τ_o is the average life time of the molecule without quencher. Figure 3 displays the Stern-Volmer plots of quenching of CPL by different metal ions and at different temperatures.

Based on the experimental data in Figure 3, the dynamic quenching constants and bimolecular quenching constants at different temperatures are shown in Table 1. It is evident from the table that the K_q values in each case are considerably larger than those possible for diffusion controlled quenching in solution (about 10 L•mol^{-1}•ns^{-1}). Usually, large K_q beyond the diffusion-controlled limit indicates that some type of binding interaction exists between fluorophore and quencher.[16] It was observed that K_{sv} decreased with increasing temperature for all metal ions. It can be therefore, concluded that the quenching is not initiated by a dynamic, but probably by a static process. Among all the metal quenchers, Cu^{2+} quenches CPL the most effectively. The quenching constant by Cu^{2+} is larger than those by other metal quenchers and that of Mg^{2+} is the minimal, which follows the order $Cu^{2+}>Ni^{2+}>Co^{2+}>Ca^{2+}>Zn^{2+}>Mn^{2+}>Mg^{2+}$. Cu^{2+} is well known as a strong quencher because of its electronic structure (d^9). Quenching by this type of substance most likely involves the donation of an electron from the fluorophore to the quencher, and the ion dipole interaction between Cu^{2+} and the molecule will also be strong due to the large nuclear charge and the relatively small size compared with other metals. Cu^{2+} usually introduces easily accessible low energy levels, which can give rise to energy and electron transfer processes and is capable of quenching the fluorescent excited state of the mole-

Table 1 Stern-Volmer and bimolecular quenching constant at 27 and 37 ℃

Metal	K_{sv}/(L•mol^{-1})		K_q/(L•mol^{-1}•s^{-1})	
	27 ℃	37 ℃	27 ℃	37 ℃
Ca	2.82×10^4	2.57×10^4	8.47×10^{12}	7.71×10^{12}
Mg	1.36×10^4	1.21×10^4	4.08×10^{12}	3.63×10^{12}
Mn	1.89×10^4	1.83×10^4	5.67×10^{12}	5.49×10^{12}
Co	3.05×10^4	2.73×10^4	9.16×10^{12}	8.19×10^{12}
Ni	4.11×10^4	3.66×10^4	12.34×10^{12}	10.99×10^{12}
Cu	6.42×10^4	5.09×10^4	19.3×10^{12}	15.28×10^{12}
Zn	2.66×10^4	2.32×10^4	7.98×10^{12}	6.96×10^{12}

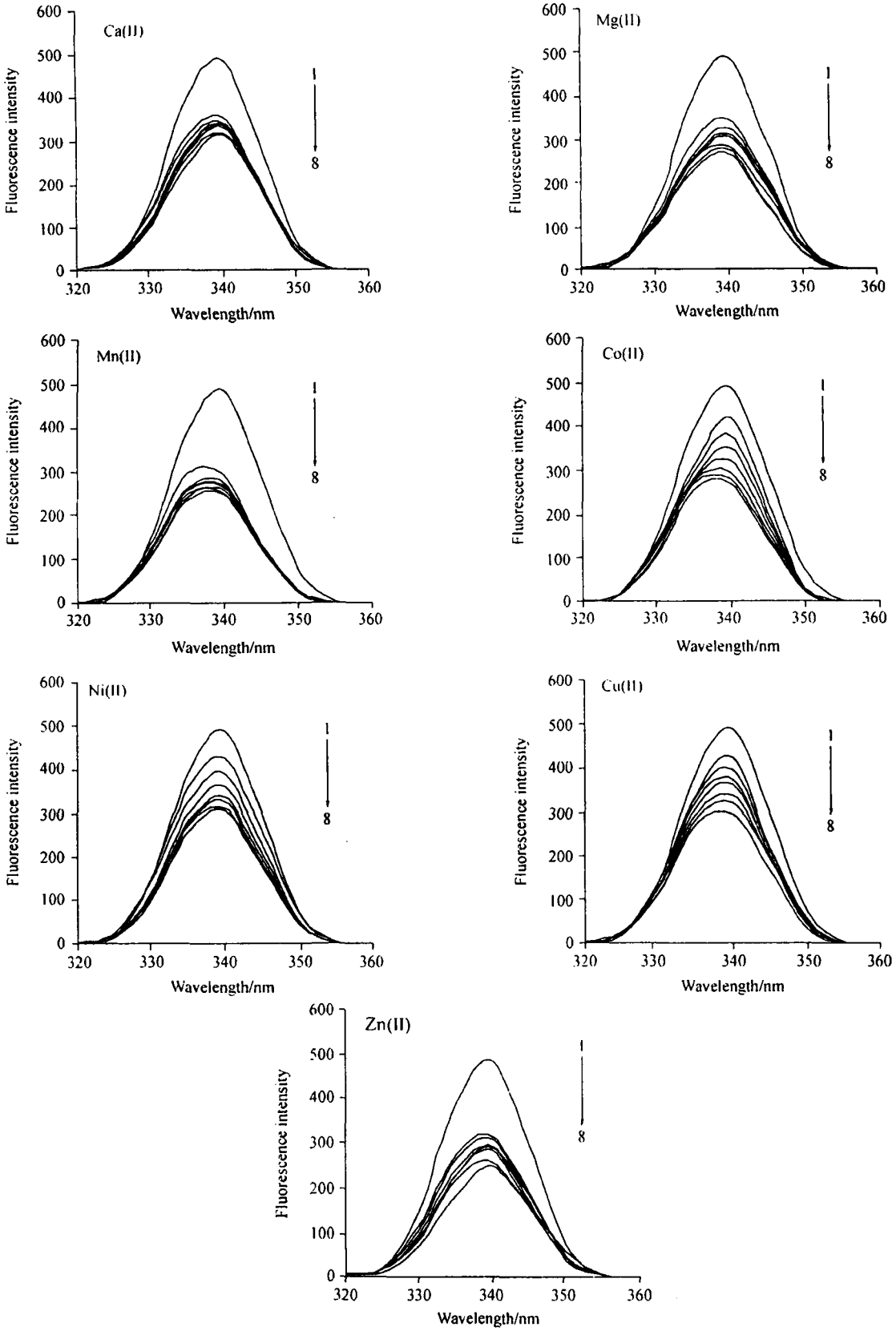

Figure 2 Fluorescence enhancement (at λ_{ex} 305 nm) of CPL with Ca(II), Mg(II), Mn(II), Co(II), Ni(II), Cu(II) and Zn(II) at room temperature. 1: 7.0 μmol•L^{-1} CPL, from 2 to 8: 2, 3, 6, 8, 10, 12, 18 μmol•L^{-1} of metal ions.

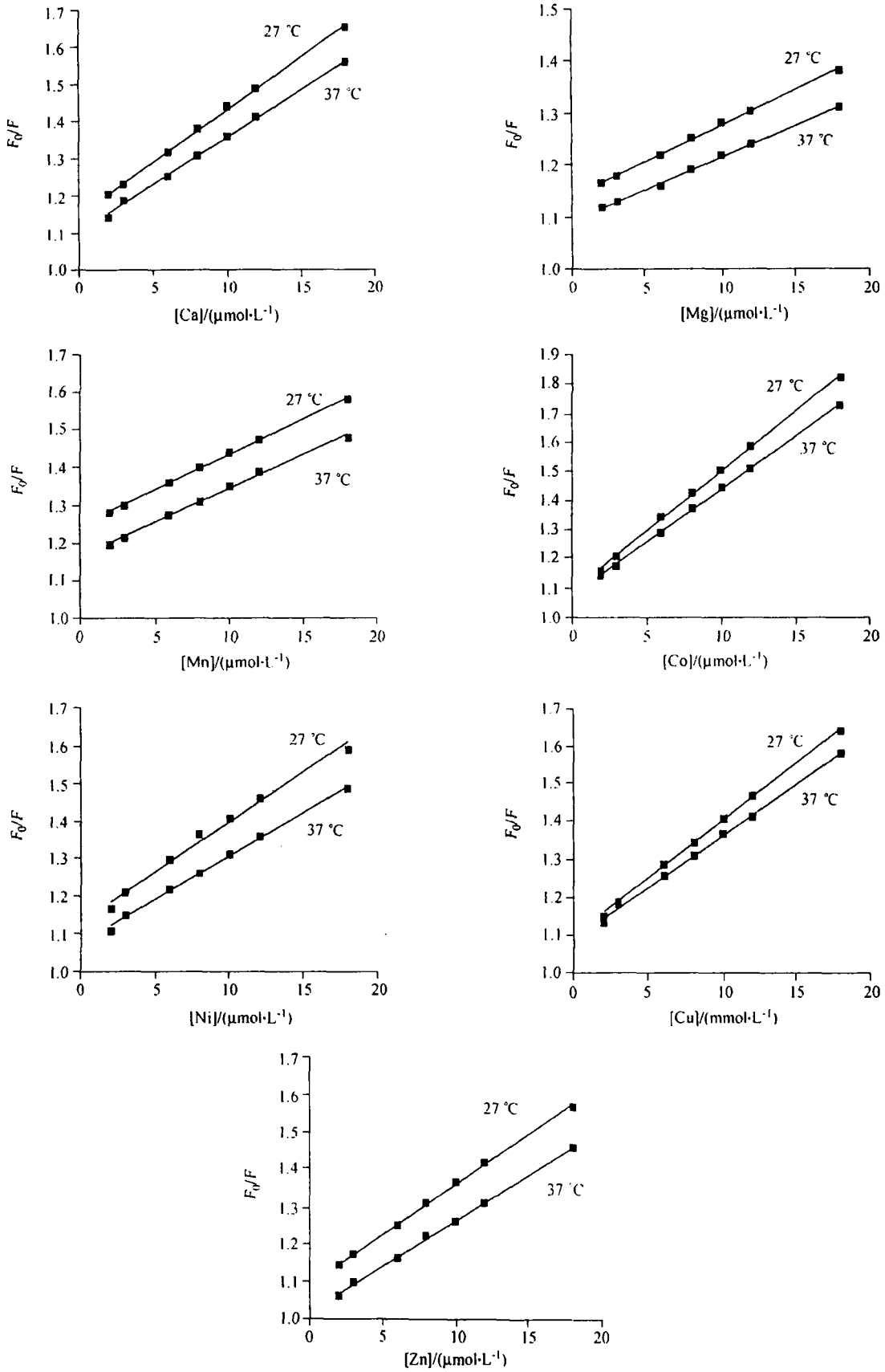

Figure 3 Stern-Volmer plots of CPL with Ca(II), Mg(II), Mn(II), Co(II), Ni(II), Cu(II) and Zn(II) at 27 and 37 ℃.

cule.[17] The larger K_{sv} and K_q values of Ni^{2+} in comparison to Co^{2+}, Mn^{2+} and Zn^{2+}can be explained in terms of its smaller ionic radius and larger nuclear charge. In cases of Mn^{2+} and Zn^{2+} the K_{sv} and K_q are quite small due to their half filled and completely filled "d" orbitals, respectively. The K_{sv} and K_q values for Ca^{2+} are larger than those of Mg^{2+} probably because of its higher reactivity and lower ionization potential.

Binding constant and binding sites

For static quenching, the relationship between intensity and the concentration of quencher can be described by the binding constant formula.[18,19]

$$\lg(F_0-F)/F=\lg K+n\lg[Q] \quad (2)$$

where K is the binding constant, and n is the number of binding sites per CPL. After the fluorescence quenching intensities of CPL at 340 nm were measured, the double-logarithm algorithm was assessed by Eq. (2). Figure 4 shows double-logarithm curve and Table 2 gives the corresponding calculated results. The linear correlation coefficients for all the curves are larger than 0.970, indicating that the interaction between the metal ions and CPL agrees well with the site-binding model underlying Eq. (2). The value of binding constant for these CPL-metal complexes follows the same order as mentioned in cases of K_{sv} and K_q values and is in agreement with the Irving-Williams series in cases of transition metal series.

Table 2 Binding constant, binding site and regression coefficient at 27 and 37 ℃

Metal	lg K		n		R	
	27 ℃	37 ℃	27 ℃	37 ℃	27 ℃	37 ℃
Ca	2.319	2.580	0.58	0.61	0.996	0.997
Mg	1.359	1.492	0.39	0.43	0.998	0.960
Mn	1.285	1.710	0.35	0.44	0.985	0.993
Co	2.887	2.828	0.65	0.66	0.998	0.997
Ni	3.416	3.450	0.74	0.76	0.999	0.998
Cu	4.811	5.049	1.00	1.07	0.999	0.998
Zn	2.535	2.922	0.58	0.68	0.999	0.997

Thermodynamic parameters and nature of binding forces

Considering the dependence of the binding constant on the temperature a thermodynamic process was considered to be responsible for this interaction. Therefore, the thermodynamic parameters dependent on temperature were analyzed in order to further characterize the forces acting between CPL and metal ions. The thermodynamic parameters enthalpy changes (ΔH), entropy changes (ΔS), and free energy changes (ΔG) are the main evidences to determine the binding mode. If the temperature does not vary significantly, the enthalpy changes (ΔH) can be regarded as constant. The free energy change (ΔG) can be estimated from the following equation, based on the binding constant at different temperatures.

$$\Delta G=-2.303RT\lg K \quad (3)$$

where R is the gas constant, T is the experimental temperature, and K is the binding constant at the corresponding temperature.

From the values of stability constant at different temperatures the enthalpy changes can be calculated by using equation:

$$\lg(K_2/K_1)=(1/T_1-1/T_2)\Delta H/2.303R \quad (4)$$

The entropy changes can be calculated by using equation:

$$\Delta G=\Delta H-T\Delta S \quad (5)$$

The thermodynamics parameters for the interaction of metal ions and CPL are shown in Table 3. The negative value of ΔG means that the interaction process is spontaneous. The positive ΔS value obtained for all investigated complex is characteristic of chelation, which occurs because the water molecules that are normally arranged in an orderly fashion around the CPL and metal ions have acquired a random configuration as a result of chelation. This is referred as gain in configurational entropy.[20] The positive value of ΔH indicate that the processes are endothermic and binding between the metal ions and CPL is mainly ΔS-driven, with little contribution from the enthalpy factor.

Table 3 Thermodynamics parameters at 27 and 37 ℃

Metal	ΔG/(kJ•mol^{-1})		ΔH/(kJ•mol^{-1})	ΔS/(kJ•mol^{-1}•K^{-1})	
	27 ℃	37 ℃		27 ℃	37 ℃
Ca	−13.32	−14.82	46.59	0.199	0.1981
Mg	−7.808	−8.575	23.76	0.105	0.1043
Mn	−7.386	−9.828	75.50	0.276	0.2752
Co	−16.58	−16.24	67.59	0.280	0.2704
Ni	−19.62	−19.82	6.160	0.085	0.0838
Cu	−27.63	−29.00	42.32	0.233	0.3371
Zn	−14.56	−16.78	68.93	0.261	0.2604

Conclusion

In this paper we have investigated the nature and magnitude of the interaction of CPL with biologically important metal ions Mg^{2+}, Ca^{2+}, Mn^{2+}, Co^{2+}, Ni^{2+}, Cu^{2+} and Zn^{2+} by fluorescence spectroscopy. Since the Stern-Volmer quenching constants, K_{sv} in all cases are inversely proportional to temperature, it indicates that probable quenching mechanism is initiated by static quenching. Cu^{2+} is the best quencher among all the metal ions. The thermodynamic parameters showed that the interaction between CPL and metal ions was spon-

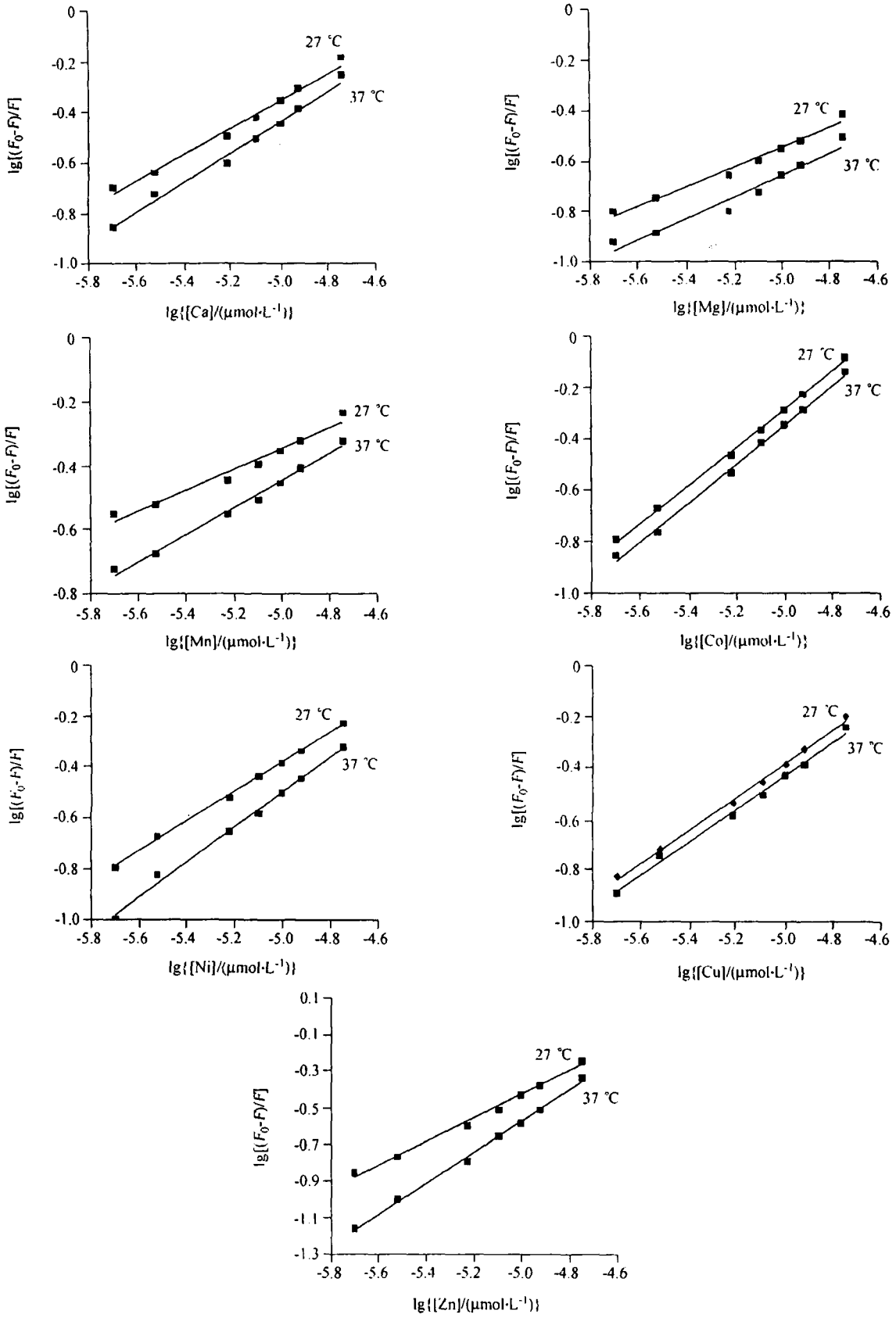

Figure 4 Double logarithm plots of CPL with Ca(II), Mg(II), Mn(II), Co(II), Ni(II), Cu(II) and Zn(II) at 27 and 37 ℃.

taneous and entropically favored in which entropy increased and Gibbs free energy decreased. The positive value of ΔS indicates the gain in configurational entropy.

References

1 El-Enany, N.; Belal, F.; Rizk, M. *Int. J. Biomed. Sci.* **2008**, *4*, 147.
2 Hughes, M. A.; Smith, G. L.; Williams, D. R. *Inorg. Chim. Acta* **1985**, *107*, 247.
3 Cushman, D. W.; Cheung, H. S.; Sabo, E. F.; Ondetti, M. A. In *Angiotensin Converting Enzyme Inhibitors*, Ed.: Horovitz; Zolap, U., Schwarzenberg, Munich, **1981**.
4 Cavalu, S.; Pinzaru, S. C.; Chis, V. *Romanian J. Biophys.* **2007**, *17*, 195.
5 Nakagawa, K.; Ueno, A.; Nishikawa, Y.; Zasshi, Y. *Pharm. Soc. Jpn.* **2006**, *126*, 37.
6 Joshaghani, M.; Gholivand, M. B.; Mosavat, A. R. *Am. J. Biochem. Biotechnol.* **2008**, *4*, 245.
7 Heel, R. C.; Brodgen, R. N.; Spieght, T. M.; Avery, G. S. *Drugs* **1980**, *20*, 409.
8 Catalanotto, F. A. *Am. J. Clin. Nutr.* **1978**, *31*, 1098.
9 Jankovics, H.; Nagy, L.; kele, Z.; Pettinari, C. Agati, P. D.; Mansueto, C.; Pellerito, C.; Pellerito, L. *J. Organomet. Chem.* **2003**, *668*, 129.
10 Jovanovic, T.; Stanovic, B.; Korcanak, Z. *J. Pharm. Biomed. Anal.* **1995**, *13*, 213.
11 Cavrini, V.; Gatti, R.; Roveri, P.; Cesaroni, M. R. *Analyst* **1988**, *113*, 1447.
12 Segarra, G. R.; Sagrado, V. S.; Martinez, C. J. *Microchim. J.* **1991**, *43*, 176.
13 Guo, M.; Zou, J. W.; Yi, P. G.; Shang, Z. C.; Hu, G. X.; Yu, Q. S. *Anal. Sci.* **2004**, *20*, 465.
14 Wang, C.; Wu, Q. H.; Li, C. R.; Wang, Z.; Ma, J. J.; Zang, X. H.; Qin, N. X. *Anal. Sci.* **2007**, *23*, 429.
15 Lakowicz, J. R. *Principles of Fluorescence Spectroscopy*, Plenum Press, New York, **1999**.
16 Park, H. R.; Oh, C. H.; Lee, H. C.; Choi, J. G.; Jung, B. I.; Bark, K. M. *Bull. Korean Chem. Soc.* **2006**, *27*, 2002.
17 Posokhov, Y.; Kus, M.; Biner, H.; Gumus, M. K.; Tugcu, F. T.; Aydemir, E.; Kaban, S.; Icli, S. *J. Photochem. Photobiol.* **2004**, *161*, 247.
18 Feng, X. Z.; Jin, R. X.; Qu, Y.; He, X. W. *Chem. J. Chin. Univ.* **1996**, *17*, 866 (in Chinese).
19 Xu, Y.; Shen, H. X.; Huan, H. G. *Anal. Chem.* **1997**, *25*, 419.
20 Calvin, M.; Melchior, N. C. *J. Am. Chem. Soc.* **1948**, *70*, 3270.

(E0901125 Zhao, C.; Dong, H.)

ISSN 0970-7077
Asian J. Chem.
Supplementary Issue 2009
CODEN: AJCHE9
Vol. 21, No. 10
pp. 9001-9147

Asian Journal of Chemistry

(An International Peer Reviewed Research Journal of Chemistry)

Proceedings of National Conference on
Advanced Materials and Radiation Physics
(AMRP-2009) (March 9-10, 2009)

Guest Editor
Dr. M.M. Sinha

Organized by
Department of Physics
Sant Longowal Institute of Engineering and Technology
Deemed University
Longowal-148106 (Punjab) India

Asian Journal of Chemistry Vol. 22, No. 3 (2010), 1957-1965

Binding Constant: Fluorescence Quenching of Ciprofloxacin with Fe(III) and Zn(II)

K.S. SIDDIQI*, AYAZ MOHD, AFTAB ASLAM, PARWAZ KHAN and SHAISTA BANO
Department of Chemistry, Aligarh Muslim University, Aligarh-202 002, India
Tel: (91)(571)2401664; E-mail: ks_siddiqi@yahoo.co.in; aizi_pasha@yahoo.co.in

Absorbance and fluorescence spectral pattern of ciprofloxacin in absence and presence of Fe(III) and Zn(II) has been studied at room temperature and under physiological condition. The fluorescence spectra of the drug in presence of the different quantities and different concentrations of the Fe(III) and Zn(II) showed the quenching of ciprofloxacin. It was observed that with increasing quantity of the quencher the emission intensity decreases with negligible variation in the peak position. The absorption spectra of the drug at different pH exhibits two isosbestic points at 320 and 350 nm indicating the presence of three chemical species in solution. The ratio of the two reacting components, the drug and the metal ions was determined by absorption and fluorescence spectrophotometrically.

Key Words: Ciprofloxacin, HCl, Fluorescence quenching, Binding constant, Stability constant.

INTRODUCTION

Ciprofloxacin is [1-cyclopropyl-6-fluoro-1,4-dihydro-4-oxo-7-(piperazinyl)-quinolone-3-carboxylic acid] one of the fluoroquinolones used as broad spectrum drug against gram positive and gram negative bacteria. It has been found that the activity of quinolone drugs is completely lost if consumed with antacids containing aluminum or magnesium because the drug is neutralized. At higher pH precipitation occurs and the drug is made unavailable for absorption[1-4]. The mechanism of interaction of quinolone with metal ions is based on the chelation of the metal with the carbonyl and carboxyl groups of the drug (Fig. 1). The antibacterial activity of the drug has also been found to be reduced manifold after chelation[5] of the metal ions *via* these groups.

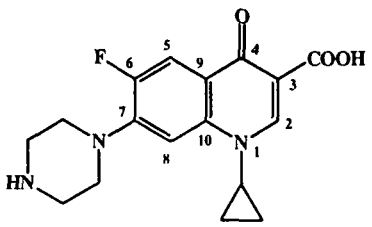

Fig. 1. Structure of ciprofloxacin

The interaction of fluoroquinolones with metal ions has attracted considerable interest not only for the development of analytical techniques but also to provide information about the mechanism of action of the pharmaceutical preparation[6]. Since the metal ions cause fluorescence quenching of the drug, spectrofluorimetric method for quantitative determination of the quinolone type drugs has been developed[7,8] besides titrimetric[9] spectrophotometeric[10], electrochemical[11], electrophoretic[12] and chromatographic[13] techniques.

The maximum solubility of the ciprofloxacin has been reported at 37 °C, which also happens to be the normal temperature of human body although the interaction of drug with metal ions has been studied in a wide range of temperature between 25 -60 °C[14,15]. Since we have to *mimic* the biological system under physiological condition we have studied, the interaction of Fe(III) and Zn(II) with ciprofloxacin at room temperature using absorption and fluorescence emission spectrophotometry at pH 3.98. The stability of the Fe(III) and Zn(II) complexes has been calculated by spectrophotometric and fluorescence emission spectrophotometric techniques. The fluorescence spectroscopy has been widely used to monitor the molecular interaction because of its high sensitivity, reproducibility and relatively easy use. Since no detailed fluorescence study on the binding interaction of ciprofloxacin with Fe(III) and Zn(II) has been done so for, a through investigation was therefore made using this technique. Such interactions between ciprofloxacin and these metal ions can cause fluorescence quenching. Therefore, valuable information's such as binding mechanism, binding constant and binding sites can be obtained using fluorescence quenching study of ciprofloxacin by these metal cations. In addition the thermodynamic parameters of the process were also proposed in this work.

EXPERIMENTAL

Fluorescence emission spectra were scanned using a Hitachi-F-2500 FL-spectrophotometer. The absorption spectra were obtained with Elico-SL-169 double beam UV-Vis spectrophotometer. All potentiometric measurements were carried out with Elico-LI-120 pH meter.

Ciprofloxacin was purchased from Windlas Biotech. Ltd.(India). All solvents and chemicals were of analytical grade. Double distilled water was used throughout. Sodium hydroxide, $Fe(NO_3)_3.9H_2O$ (Merck Ltd., Mumbai, India) $ZnCl_2$ (anhydrous) (SDH Pvt. Ltd. India) and hydrochloric acid (Ranbaxy fine chem. Ltd., India) were used as received.

Preparation of solutions: The stock solution of ciprofloxacin HCl (5×10^{-2} M) prepared in 1×10^{-2} M HCl was stored at 4 °C and those of the metal salts (1×10^{-2} M) were prepared in double distilled water, respectively. All working solutions were prepared by dilution with double distilled water.

Spectrophotometeric methods: Solutions of equimolar concentration (1×10^{-4} M) of ciprofloxacin HCl and metal ions were prepared. The pH of the drug was adjusted between 2.12 to 10.50 by adding sodium hydroxide and hydrochloric acid

(1×10^{-1} M to 1×10^{-2} M). The absorption spectra were recorded in the range 230-360 nm. The ratio of metal to ciprofloxacin.HCl was determined by Job's method. The linearity of ciprofloxacin HCl was found in the range 3.5×10^{-5}-7.5×10^{-4} mg/mL and the correlation factor (R^2) 0.9629.

Fluorescence spectrophotometeric methods: Solution of the ciprofloxacin (5×10^{-6} M) and those of metal ions (1×10^{-6} M to 10.5×10^{-6} M) were prepared. To prepare dilute solutions, an aliquot of stock solution was placed in a 10 mL volumetric flask and made up to the mark with distilled water. Spectra were recorded immediately after sample preparation in the optimum wavelength range 300-600 nm at optimum excitation wavelength of 315 nm. For calibration curve an aliquot of stock solution (5×10^{-7}-1×10^{-5} mg/mL) was prepared which showed linearity with correlation factor (R^2) 0.9739.

RESULTS AND DISCUSSION

Absorption studies: The absorption spectrum of ciprofloxacin run at room temperature and at constant pH 3.98 displayed a strong peak at 272 nm and a weak absorption at 315 nm (Fig. 2). When the UV spectra of the drug were run at varying pH, at room temperature and, under physiological condition, the strong peak was shifted to lower wavelength while the broad peak was shifted to higher wavelength. The decrease in the position and intensity of the first peak is attributed to the extent of ionization of the carboxylic group while the increase in the intensity and height of the peak at 315 nm occurs as a consequence of protonation of the piperazinyl nitrogen on 7-carbon atom. Two isosbestic points appearing at 320 and 350 nm indicated the presence of three chemical species in solution (Fig. 3) similar to those observed by Bark and Barrell[14].

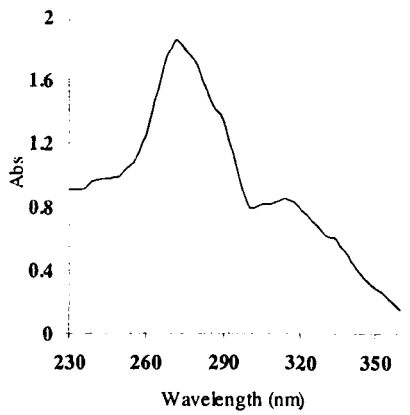

Fig .2. Absorption spectrum of ciprofloxacin (1×10^{-4} M) at pH 3.98

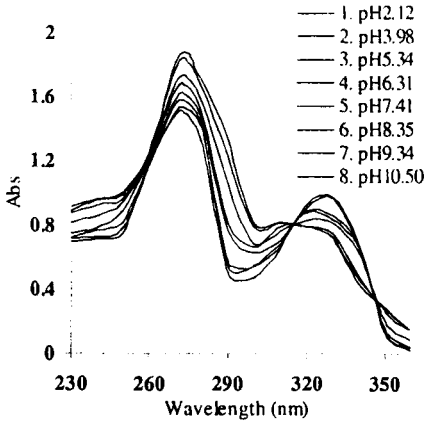

Fig. 3. Absorption spectra of ciprofloxacin (1×10^{-4} M) at different pH (2.12-10.50) at 25 °C

The apparent ionization constant (pKa') of the drug was calculated (6.871) by the following equation.

$$pKa' = pH + \log \{(A_I - A_M)/(A - A_M)\} \quad (1)$$

where, A_I = Absorbance of drug in basic medium, A_M = Absorbance of drug in acidic medium, A = Absorbance of drug in aqueous medium. The pure drug has maximum solubility at pH 5 although it increases in the presence of Fe(II) and Fe(III) ions[16].

The stability constant of the complexes were calculated by the continuous variation method using the following equation:

$$K = \frac{A/A_{ex}C_X}{(C_M - A/A_{ex}C_X)(C_L - nA/A_{ex}C_X)^n} \quad (2)$$

where, K is the stability constant of the metal chelate formed in solution, M = metal, L = ligand, n = X/(1-X) where X is the mole fraction of the ligand at maximum absorption. A/A_{ex} is the ratio of the observed absorbance to that indicated by the tangent for the same wavelength. C_X, C_M and C_L are the limiting concentration, metal ion concentration and the ligand concentrations, respectively.

The continuous variation curves are shown in Fig. 4. The ratio of ciprofloxacin: metal, is 2:1, which is quite obvious. The fairly large value of log k of the two complexes (Table-1) suggests that they are pretty stable in acidic medium only. The drug under this condition must be acting as ionophore since the solubility of the drug is maximum in presence of Fe(III). However, precipitation occurs when the solution becomes alkaline[17,18].

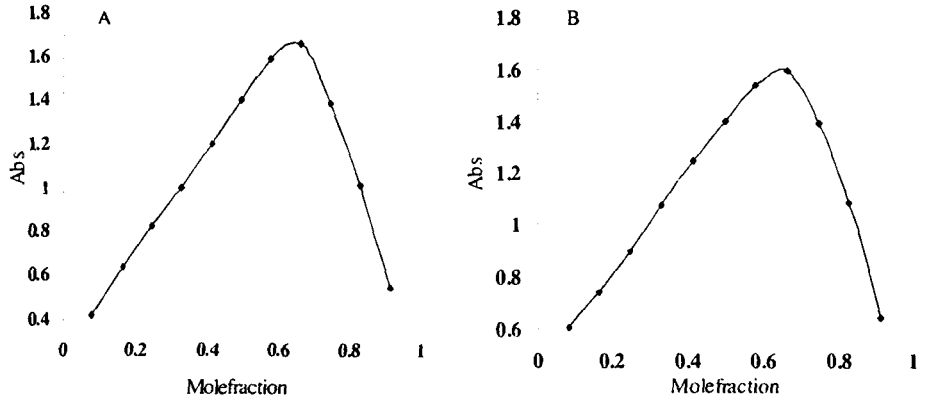

Fig. 4. Continuous variation curves of equimolar solutions of ciprofloxacin and (A) Fe(III) and (B) Zn(II) at 25 °C

Fluorescence study: The absorption spectrum of the drug is markedly different from its emission spectrum, which is attributed to different molecular geometries (Fig. 5) in ground and excited states. The piperazinyl group of ciprofloxacin acts as

TABLE-1
STABILITY CONSTANT (log K AND -ΔG OF THE FORMED CHELATES AT 25 °C BY ABSORPTION STUDY

Metal	log K	ΔG (kJ mol^{-1})
Fe(III)	9.378	-53.509
Zn(II)	9.381	-53.526

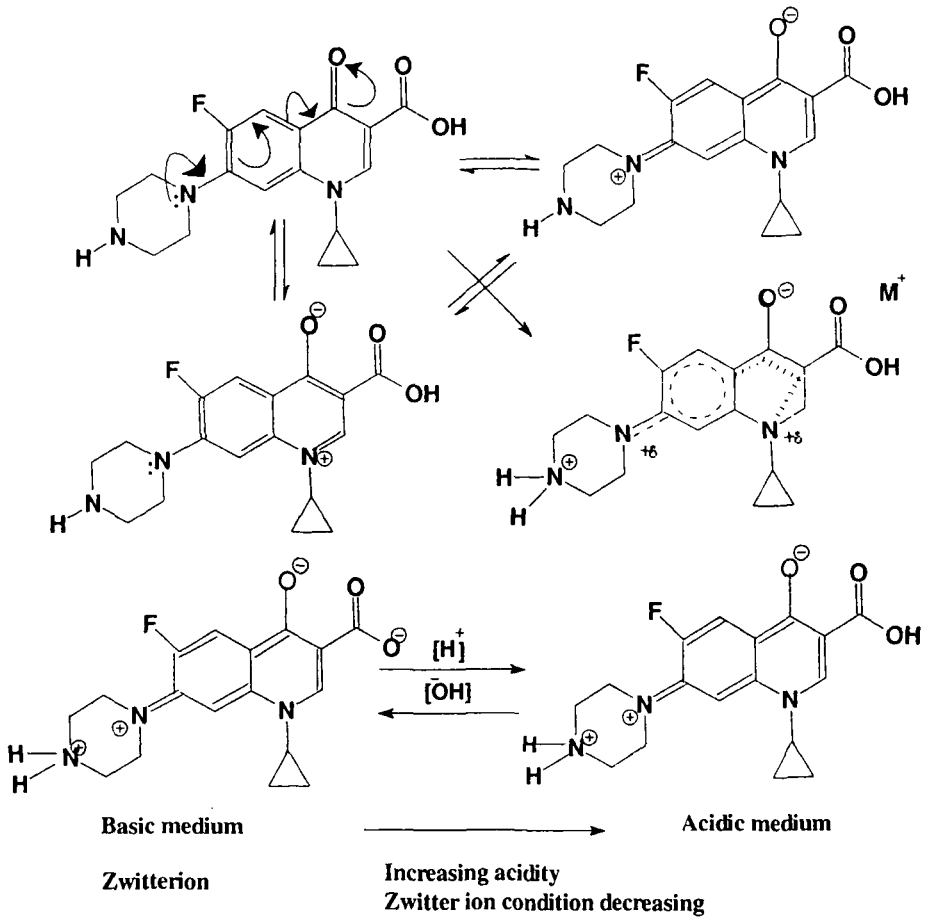

Fig. 5. Zwitterion formation and intramolecular charge transfer of drug in solution phase at varying pH

electron donor while the keto group acts as electron acceptor. Since all investigations were done in acidic medium, ciprofloxacin exists in zwitter ionic form. The peaks in the absorption spectra are due to intramolecular charge transfer, the greater the number of resonating structures the stronger the fluorescence emission.

The fluorescence spectra are very sensitive to the nature of the metal quencher, which is reflected from the emission spectra of the drug in presence of the Fe(III) and Zn(II) quencher. They showed a consistent decrease in the intensity of fluorescence with increasing concentration of the metal ion until it was nearly completely quenched (Fig. 6) as a consequence of the complex formation between the metal ions and ciprofloxacin.

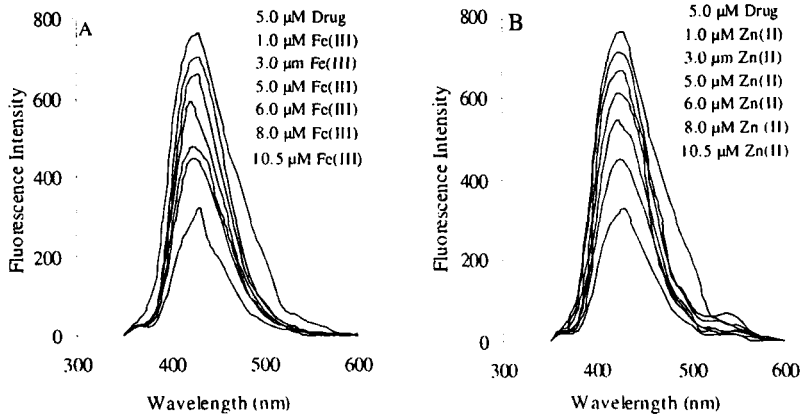

Fig. 6. The fluorescence emission spectra of drug quenched (A) Fe(III) and (B) Zn(II)

Many workers[19,20] have studied the interaction of drug with metal ions at temperature exceeding 37 °C in order to show the Stern-Volmer plot although such experiments above body temperature do not *mimic* the biological system. We, therefore, did all the experiments at room temperature. The fluorescence intensity increases rapidly with decrease in temperature. The lower stability at higher temperature also supports lowering in quenching. The fluorophore is quenched both by collision and complex formation with the metal ions. The complex formation is mainly due to ion dipole interaction.

Fluorescence quenching refers to any process in which the fluorescence intensity of a given fluorophore decreases upon adding a quencher. Assuming that the fluorescence intensity of a fluorophore-quencher complex is negligible as compared to an unquenched fluorophore, the intensity in the absence (F_o) and presence (F) of the quencher is expressed by Stern-Volmer equation

$$F_o / F = 1 + Ksv\,[Q] \qquad (3)$$

where [Q] is the concentration of quencher, Ksv is the Stern-Volmer constant which is the equilibrium constant of the complex formed in the static quenching process. If a system obeys the Stern-Volmer equation, a plot of F_o/F-1 *vs.* [Q] will give straight line with a slope of Ksv and y-axis intercept. Fig. 8 represents the quenching of ciprofloxacin by Fe(III) and Zn(II), respectively. The linearity of Stern-Volmer plot (Fig. 7) increases with increasing concentration of quencher. The values of Ksv and correlation coefficient are shown in Table-2.

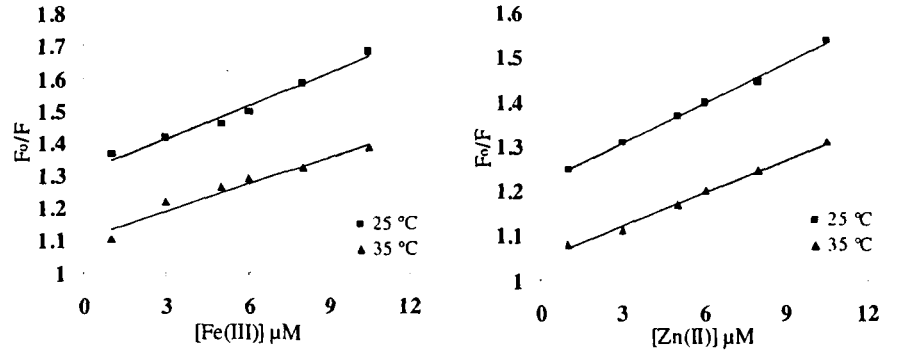

Fig. 7. Stern-Volmer plot for the quenching of drug with Fe(III) and Zn(II)

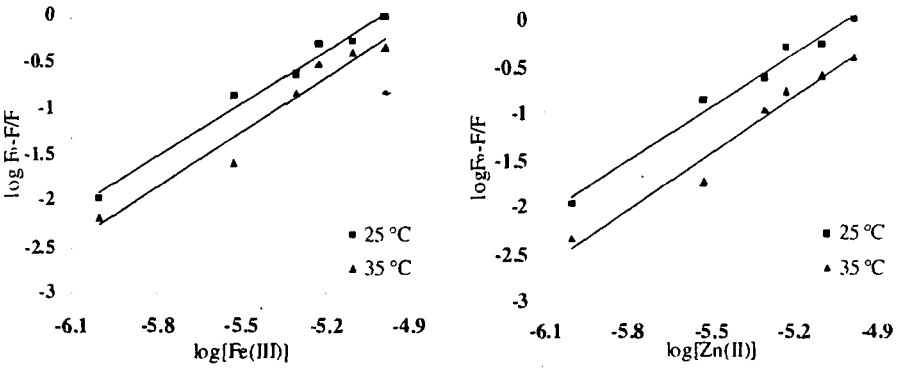

Fig. 8. Double reciprocal plot of drug with Fe(III) and Zn(II)

TABLE-2
STERN-VOLMER CONSTANT (Ksv, BINDING CONSTANT (log k), BINDING SITE AND REGRESSION COEFFICIENT AT 25 and 35 °C

Metal	Ksv/mol^{-1}		log K		n		R^2	
	25 °C	35 °C	25 °C	35 °C	25 °C	35 °C	25 °C	35 °C
Fe(III)	3.36×10^{4}	2.77×10^{4}	9.42	9.58	1.88	1.97	0.982	0.950
Zn(II)	2.97×10^{4}	2.48×10^{4}	9.46	9.60	1.89	2.01	0.981	0.965

The metal ions with large nuclear charge and small size will experience greater ion-dipole interaction and hence the emission intensity in the case of Zn(II) should be less than that for Fe(III) although Fe(III) has greater nuclear charge and smaller ionic radius.

The large value of stability constant of the complexes formed in solution reflects strong interaction between ciprofloxacin and the metal ions.

Binding constant and binding sites: For static quenching, the relationship between intensity and the concentration of quencher can be described by the binding constant formula[21,22]:

$$\log(F_o\text{-}F)/F = \log K + n \log [Q] \quad (4)$$

where K is the binding constant (Table-3), n is the number of binding sites per ciprofloxacin. After the fluorescence quenching intensities on ciprofloxacin at 315 nm were measured, the double-logarithm algorithm was assessed by eqn. 4. Fig. 8 shows double-logarithm curve and Table-2 gives the corresponding calculated results. The linear correlation coefficient for all the curves are larger than 0.945, indicating that the interaction between metal ions and ciprofloxacin agrees well with the site-binding model underlying eqn. 4. The results illustrate that there is a strong binding force between ciprofloxacin and metal ions and approximately two binding site would be formed in each case which is consistent with the previous studies that in acidic medium ciprofloxacin and metal ions form 2:1 complex.

TABLE-3
THERMODYNAMICS PARAMETERS AT 25 AND 35 °C

Metal	ΔG (kJ mol^{-1})		ΔH (kJ mol^{-1})	ΔS (kJ mol^{-1} K^{-1})	
	25 °C	35 °C		25 °C	35 °C
Fe(III)	-53.77	-56.54	118.59	180.85	183.96
Zn(II)	-54.01	-56.62	98.94	181.57	184.16

Thermodynamic parameters and nature of binding forces: Considering the dependence of the binding constant on the temperature a thermodynamic process was considered to be responsible for this interaction. Therefore, the thermodynamic parameters dependent on temperature were analyzed in order to further characterize the forces acting between drug and metal ions. The thermodynamic parameters enthalpy changes (ΔH), entropy changes (ΔS) and free energy changes (ΔG) are the main evidences to determine the binding mode. If the temperature does not vary significantly, the enthalpy changes (ΔH) can be regarded as constant. The free energy change (ΔG) can be estimated from the following equation, based on the binding constant at different temperatures.

$$\Delta G = - 2.303 RT \log K \quad (3)$$

where R is the gas constant, T is the experimental temperature and K is the binding constant at the corresponding temperature.

From the value of stability constant at different temperature the enthalpy changes can be calculated by using equation:

$$\log K_2/K_1 = [1/T_1\text{-}1/T_2]\Delta H/2.303R \quad (4)$$

The entropy changes can be calculated by using equation:

$$\Delta G = \Delta H\text{-}T\Delta S \quad (5)$$

Thermodynamics parameters for the interaction of metal ions and ciprofloxacin are shown in Table-3. The negative value of ΔG means that the interaction process is spontaneous. The +ve ΔS value obtained for all investigated complex is characteristic of chelation. It occurs because the water molecules that are normally arranged

in an orderly fashion around the ciprofloxacin and metal ions have acquired a random configuration as a result of chelation. This is referred as gain in configurational entropy[23]. The +ve value of ΔH indicate that the processes are endothermic and binding between metal ions and ciprofloxacin is mainly ΔS-driven, with little contribution from the enthalpy factor.

Conclusion

It is concluded that the drug stays as zwitter ions. Ionization of carboxylic group and protonation of piperazinyl group occurs. The two isosbestic points indicate the presence of three chemical species in solution. The result shows that the complex of ciprofloxacin with Fe(III) and Zn(II) are fairly stable. The thermodynamic parameters showed that the interaction between ciprofloxacin and metal ion was spontaneous and that the hydrophobic force was a major factor in the interaction.

REFERENCES

1. G.K. Haffken, R. Borner, P.D. Glatzal, P. Kaeppe and H. Lode, *Eur. J. Clin. Microbiol.*, **4**, 845 (1985).
2. T.E. Spratt, S.S. Schultz, D.E. Levy, D. Chen, G. Schluter and G.M. Williams, *Chem. Res. Toxicol.*, **12**, 809 (1999).
3. H. Stass and D. Kubitza, *Clin. Pharmacokin.*, **40**, 57 (2001).
4. M. Cordoba-Diaz, M. Cordoba-Borrego and D. Cardoba Diaz, *J. Pharm. Biomed. Anal.*, **18**, 565 (1998).
5. J.T. Smith, *J. Chemother.*, **4**, 134 (1989).
6. I. Turel, P.A. Golobi A. Klazar, B. Pihlar, P. Buglyo, E. Tolib, D. Rehder and K. Sepiv, *J. Inorg. Biochem.*, **95**, 199 (2003).
7. H.R. Park, T.H. Kim and K.M. Bark, *Bull. Korean Chem. Soc.*, **37**, 443 (2002).
8. E. Kilic, F. Koseoglu and M.A. Akay, *J. Pharm. Biomed. Anal.*, **12**, 347 (1994).
9. S. Mostafa, M. Elsadek and E. Awadalla, *J. Pharm. Biomed. Anal.*, **27**, 133 (2002).
10. Z. Liu and C.R. Huang, *Analyst*, **125**, 1477 (2000).
11. M.A.G. Trindade, P.A.C. Cunha, T.A. de Arauja, G.M. dasilva and V.S. Ferreira, *Ecl. Quim. Sao Paulo.*, **31**, 31 (2006).
12. C. Fierens, S. Hillaert and W.V. Bossche, *J. Pharm. Biomed. Anal.*, **220**, 763 (2000).
13. J. Novakovic, K. Nesmark, H. Nova and K. Filka, *J. Pharm. Biomed. Anal.*, **25**, 957 (2001).
14. H.R. Park, K.Y. Chung, H.C. Lee, J.K. Lee and K.M. Bark, *Bull. Korean Chem. Soc.*, **21**, 849 (2000).
15. J. Hernadez-Borrell and M.T. Monterro, *J. Chem. Educ.*, **47**, 1311 (1997).
16. C.J. Etoba and H.N. Okeri, *Tropic. J. Pharm. Res.*, 349 (2005).
17. H. Salem, *Am. J. Appl. Sci.*, **3**, 719 (2005).
18. M.E. El-Kommas, G.A. Saleh, S.M. El-Gizawi and M.A. Abou-Elwafa, *Talanta*, **60**, 1033 (2003).
19. H.R. Park, C.H. Oh, H.C. Lee, J.G. Choi, B.I. Jung and K.M. Bark, *Bull. Korean Chem. Soc.*, **27**, 2002 (2006).
20. H.R. Park, J.J. Seo, S.C. Shin, H.S. Lee and K.M. Bark, *Bull. Korean Chem. Soc.*, **28**, 1573 (2007).
21. X.Z.F. Eng, R.X. Jin, Y. Qu and X. Whe, *Chem. J. Chin. Univ.*, **17**, 866 (1996).
22. Y. Xu, H.X. Shen and H.G. Huan, *Anal. Chem.*, **25**, 419 (1997).
23. M. Calvin and N.C. Melchior, *J. Am. Chem. Soc.*, **70**, 3270 (1948).

(*Received*: 29 April 2009; *Accepted*: 25 November 2009) AJC-8081